Application of the Transformation of 1,2,4-Trimethylbenzene to monitor the Chemical Vapour Deposition of Tetraethoxysilane over ZSM-5

By

Hans Peter Röger Dipl. Ing. (Chem. Eng.)

Submitted to the University of Cape Town in fulfillment of the requirements for the degree of

DOCTOR OF PHILOSOPHY

Department of Chemical Engineering
University of Cape Town
Rondebosch
Cape Town

April 1998

Acknowledgements

This thesis was done between January 1993 and April 1998 at the Department of Chemical Engineering at the University of Cape Town. The project was funded by the Catalysis Research Unit, the FRD and the University of Cape Town for which I express my appreciation.

I would like to thank my supervisors *Dr. Klaus Möller* and *Prof. Dr. Cyril O'Connor* for their help and guidance without which this thesis would not have been possible. Many thanks to *Walter Böhringer* for his valuable contributions. My thanks also go to *Dr.-Ing. Eric van Steen, Prof. Dr. Mark Dry* and especially to *Dr. Koos Jansen* and *Prof. Dr.-Ing. habil. Jens Weitkamp* for their constructive commenting on this project.

Special thanks to *Prof. Dr. rer. nat. habil. Hans Schulz* for the support when suggesting me as a PhD student to Prof. Cyril O'Connor.

I especially want to state my appreciation to *Ansgar, Rob, Gary, Sarah, James, Erna, Frank* and *Paul* for their friendship, help, motivation and solidarity especially in times when I was navigating through the doldrums in the ocean of research.

I also want to thank *Jeanny Pearse, Linda Callanan, Thabiso Manne, Matthias Unger* and *Michael Krämer*, who contributed in their projects, Diplom- and Seminararbeiten to this work.

Many thanks to all the members of the staff for their help throughout my stay in the department, especially *Pam, Leslie, Peter, Joachim, Bill, Granville, James, Martin* and *Charlie*.

Last but not least to my parents, *Diethelm* and *Monika*, my sisters *Anja* and *Natascha*, and my brothers *Bastian* and *Axel*, thank you for being the best friends I could ever wish for.

Publications which have resulted from this thesis:

A. Journal Publications

A1. H.P. Röger, K.P. Möller, and C.T. O'Connor; "The Transformation of 1,2,4-Trimethylbenzene - A Test Reaction to monitor External Surface Modifications of ZSM-5?"; *Microporous Materials* **8** (1997) 151-157

A2. H.P. Röger, K.P. Möller, and C.T. O'Connor; "The Reaction Network in the Transformation of 1,2,4-Trimethylbenzene over ZSM-5"; *J. Catal. (In press)*

A3. H.P. Röger, M. Krämer, K.P. Möller, and C.T. O'Connor; "Effects of in-situ Chemical Vapour Deposition using Tetraethoxysilane on the Catalytic and Sorption Properties of ZSM-5"; *Microporous and Mesoporous Materials (In press)*

B. Conference Proceedings

B1. H.P. Röger, K.P. Möller, and C.T. O'Connor; "The Transalkylation of 1,2,4-Trimethylbenzene - A Test Reaction to probe the External Surface Activity of HZSM-5" ,Conference of the South African Catalysis Society, Rustenberg, South Africa, July, 1995

B2. H.P. Röger, K.P. Möller, and C.T. O'Connor; "Probing Catalyst Structure and Activity using Catalyst Specific Reactant Molecules", Conference of the South African Catalysis Society, Midrand, South Africa, November, 1996

B3. H.P. Röger, M. Krämer, K.P. Möller, and C.T. O'Connor; "The Reaction Network in the Transformation of 1,2,4-Trimethylbenzene over ZSM-5"; 11th IZC, Korea, 1996

B4. R.W. Weber, H.P. Röger, M. Unger, K.P. Möller, and C.T. O'Connor; "Chemical Vapour Deposition of Tetraethoxysilane onto ZSM-5"; 11th IZC, Korea, 1996

B5. H.P. Röger, M. Krämer, K.P. Möller, and C.T. O'Connor; "Effects of in-situ Chemical Vapour Deposition using Tetraethoxysilane on the Properties of ZSM-5"; AICHE, Annual Meeting, Los Angeles, 1997

B6. H.P. Röger, M. Krämer, K.P. Möller, and C.T. O'Connor; "Effects of in-situ Chemical Vapour Deposition using Tetraethoxysilane on the Catalytic and Sorption Properties of ZSM-5"; ZMPC'97, Tokyo, Japan, 1997

B7. H.P. Röger, R.W. Weber, K.P. Möller, and C.T. O'Connor; "Chemical Vapour Deposition using Tetraethoxysilane over ZSM-5"; IPCAT'98, Cape Town, South Africa, 1998

Synopsis

The present work reports an improved chemical vapour deposition (CVD) technique using low temperature, tetraethoxysilane (TEOS) and repeated CVD-calcination cycles. This results in a better control of the external surface activity and the pore mouth size of ZSM-5. In search for effective characterisation tools and a model reaction which involves molecules which are critical in size relative to the size of the ZSM-5 channels, the transformation of 1,2,4-trimethylbenzene (1,2,4-TMB) was investigated with respect to the reaction network, the role of the micropore space and the response to CVD treatments and Silicalite I coating. A generalised interpretation of the effect of modifications of the external surface activity and the pore mouth size on activity and shape selectivity of zeolites is proposed.

CVD treatments at 100°C, 270°C and 450°C showed that at the unusually low temperature of 100°C the CVD of TEOS is subject to a saturation effect resulting in a self-regulating deposition which is uniform throughout the catalyst bed. The intrinsic limitation with respect to the degree of modification can be overcome by calcination steps between CVD treatments. The repeated application of CVD-calcination cycles makes it possible to adjust the degree of modification, viz. the external surface inactivation and the reduction of the pore mouth size, with a high controllability without affecting intrinsic properties of the micropore space. The CVD treatments were characterised using sorption studies and the conversion of 1,3,5-triisopropylbenzene, n-hexane and toluene as probe reactions. The shape selectivity during toluene disproportionation was incrementally enhanced from the equilibrium distribution of xylenes, viz. 25% p-xylene over the parent ZSM-5, up to 98.5% p-xylene after 15 CVD-calcination cycles at an activity loss of less than 10%.

The transformation of 1,2,4-TMB was investigated regarding its application as a probe and model reaction. The reaction network was studied by an analysis of product concentrations versus space time behaviour over ZSM-5 and amorphous silica-alumina. 1,2,3-TMB, 1,3,5-TMB, ethyl-methyl-benzenes, propyl-benzenes and tetramethylbenzenes

(TeMBs) are primary products while benzene, toluene, C_2-C_4-aliphatics, methane and coke are secondary products. Xylenes are both primary and secondary products. Methane, the lower aromatics, and olefins, in particular toluene and ethene, however, are pseudo-primary products. Rapid 1,2-methyl-shift-isomerisation, slow transalkylation and a slow isomerisation reaction involving the rearrangement of methylgroups to form ethyl- and higher alkylgroups appear as primary and as secondary reactions.

The isomerisation via methylgroup rearrangement is followed by fast dealkylation of the higher alkylgroups. This acid catalysed reaction path was described first by Sullivan *et al.* [1961] and is known as "paring reaction". It explains the behaviour of toluene and ethene as pseudo-primary products and of TeMBs as less stable intermediates. The paring reaction is promoted by high temperatures and the microporous structure of ZSM-5 as compared to silica-alumina.

A comparative study using silica-alumina, unmodified, Silicalite I coated, and CVD treated ZSM-5 showed that the 1,2-methyl-shift-isomerisation of 1,2,4-TMB takes place almost completely on the external surface whereas the transalkylation and paring reaction occur primarily in the micropores of unmodified and moderately modified ZSM-5.

Based on a study of the 1,2,4-TMB transalkylation over these catalysts a generalised behaviour of reactions in response to a continuous inactivation of the external surface and reduction of the pore mouth size is proposed. Stepwise modification at first increases the shape selectivity. At low modification degrees transport between the micropore space and the gas phase is still possible for reactants and products of the shape selective reaction. With increasing degree of modification the micropore space accessibility decreases thus increasingly restricting the reaction to the modified external surface. This effect decreases the shape selectivity until selectivity and activity are totally determined by the intrinsic kinetics of the modified external surface.

The transformation of 1,2,4-TMB is proposed as a probe reaction to monitor the external surface activity, equivalent to 1,3,5-triisopropylbenzene cracking, and to optimise the

shape selectivity in the range of bulky molecules at low and medium degrees of CVD modification of ZSM-5 where the toluene disproportionation is not as sensitive.

TABLE OF CONTENTS

LIST OF FIGURES

LIST OF TABLES

LIST OF SYMBOLS

A	Area counts in a GC-trace	
AAS	Atomic absorption spectroscopy	
BET	Brunauer Emmet Teller	
BuB	Butyl-benzene	
C	Carbon	
CVD	Chemical vapour deposition	
D_m	Mean diffusivity	m^2/s
DEB	Di-ethyl-benzene	
EB	Ethyl-benzene	
EDMB	Ethyl-di-methyl-benzene	
EMB	Ethyl-methyl-benzene	
EXAFS	X-ray adsorption fine structure	
F	Molar flow rate	mmol/min
FID	Flame ionisation detector	
GC	Gas chromatograph	
IR	Infra-red	
IStd	Internal standard	
L	Catalyst bed length	cm
M	Molar mass	g/mol
N_C	Number of carbon atoms in a molecule	
Pa	Paring reaction	
Pe	Peclett number	
PrB	Propyl-benzene	
PrMB	Propyl-methyl-benzene	
R	Universal gas constant	J/mol K
Re	Reynolds number	
RF	Relative response factor on molar carbon basis	
Sc	Schmidt number	
SEM	Scanning electron microscopy	

Sh	Sherwood number	
SIMS	Secondary ion mass spectroscopy	
ST	Modified space time	min
T	Temperature	K, °C
TEM	Transmission electron microscopy	
TeMB	Tetramethylbenzene	
TEOS	Tetraethoxysilane, Tetraethylorthosilicate	
TG-DTA	Thermo gravimetric differential temperature analysis	
TiPB	Triisopropylbenzene	
TMB	Trimethylbenzene	
TPD	Temperature programmed desorption	
V	Volume	m^3
WHSV	Weight hourly space velocity	h^{-1}
X	Conversion	%
XPS	X-ray photoelectron spectroscopy	
XRD	X-ray diffraction	
ZSM-5	Zeolite Socony Mobil	

a_m	Specific surface area	m^2/kg
c	Molar concentration	mol/m^3
d	Diameter	cm, mm, μm, Å
k	Rate constant	$cm^3/s\ g$
k_f	Gas film mass transfer coefficient	m/s
m	Mass	mg, g, kg
n	Number of moles	mol
p	Pressure	kPa
r	Specific rate	mmol/min g
u	Linear gas velocity in empty reactor	cm/s

μ	Dynamic viscosity	g/s m
ρ	Specific density	kg/m^3

Indices

C	Carbon
cat	Catalyst
De	Dealkylation
Dis	Disproportionation
i	Compound
in	Reactor inlet
Is	Isomerisation
IStd	Internal standard
m	Mean
out	Reactor outlet
p	Particle

Chapter 1

Introduction

1.1 ZEOLITES

Zeolites were first recognised as a new class of minerals by the Swedish mineralogist Cronstedt in 1756, who derived the name from the Greek words "zeo" and "lithos" meaning "to boil" and "stone" due to the observed intumescence of the mineral when it was heated [Flanigen, 1991]. The uniform pore dimensions, ionexchange properties, the ability to possess acidity and high thermal stability make zeolites suitable for a wide range of commercial applications, which can be divided into four main areas:

Adsorbents:	Drying, purification and separation processes.
Catalysts:	Mainly in petroleum refining, synfuels production and petrochemicals production
Detergents:	as substitute for phosphates (mainly Zeolite A)
Natural Zeolites:	animal feed supplements, fertiliser

Even though some zeolites are available in the form of huge natural deposits, mostly synthetic zeolites are used, which possess well defined characteristics due to their homogeneous and unpolluted appearance. The combined estimated usage of the industrialised countries of Western Europe, North America and Japan was approximately 550 thousand metric tons in 1988 [Moscou, 1991] with the following distribution of application areas:

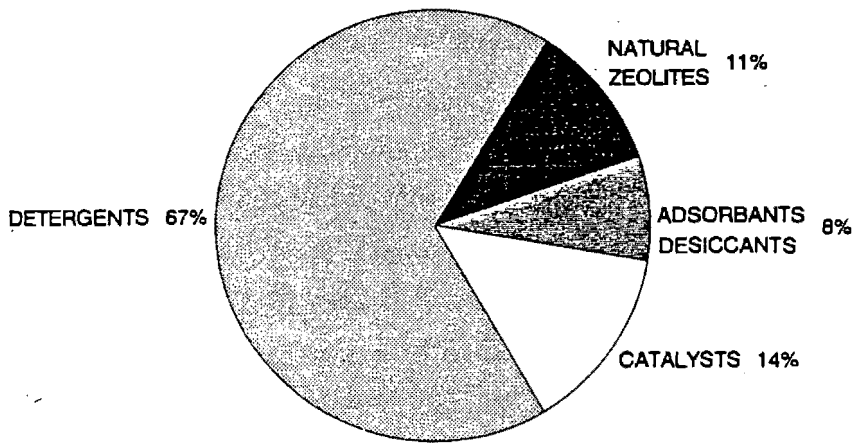

Figure 1.1: Estimated consumption of zeolite in 1988 for various applications in North America, Western Europe and Japan

1.1.1 Structure of zeolites

Table 1.1: Properties of the channel system for selected zeolites [Venuto, 1994; Breck, 1974]

Structure type	Ring size[a] of channels	Pore size largest channel[b] (Å)	Channel system dimensionality[c]	Largest molecule adsorbed at 25 °C
Very small pore				
Analcime	6	2.6	1	NH_3
Sodalite	6-6-6	2.6	3	H_2O
Small pore				
Linde type A	8-8-8	4.1	3	C_2H_4
Erionite	8-8-8	3.6 x 5.1	3	-
Chabazite	8-8-8	3.8 x 3.8	3	n-paraffins
ZK-5	8-8-8	3.9	3	-
Rho	8-8-8	3.6	3	-
Medium pore				
ZSM-5	10-10-10	5.3 x 5.6	3	-
ZSM-11	10-10-10	5.3 x 5.4	3	-
Ferrierite	10-8	4.2 x 5.4	2	C_2H_4
ZSM-48	10	5.3 x 5.6	1	-
ZSM-23	10	4.5 x 5.2	1	-
ZSM-22/Theta-1	10	4.4 x 5.5	1	-
Large pore				
Faujasite (X/Y)	12-12-12	7.4	3	$(C_2F_5)_3N$
Beta	12-12	7.6 x 6.4	3	-
Mordenite	12-8	6.5 x 7.0	2	C_6H_6
Offretite	12-8-8	6.7	3	-
Mazzite/Omega/ZSM-4	12-8	7.4	1	-
Linde type L	12	7.1	1	-
ZSM-12	12	5.5 x 5.9	1	-

[a] Number of T or O atoms comprising smallest rings in channels
[b] Mainly crystallographic free diameters as given in [Meier and Olson, 1992]
[c] Based on criteria given in [Meier and Olson, 1992, pp. 8-11]; infers interconnecting channel systems, but not necessarily accessibility to organic molecules

Zeolites are crystalline aluminosilicates with the unit cell formula given by

$$M_pD_q(Al_{p+2q}Si_rO_{2p+4q+2r})\cdot sH_2O \qquad \text{[Smith, 1979]}$$

where M and D represent monovalent and divalent cations respectively which are typically

H^+, Na^+, K^+, Mg^{2+}, Ca^{2+} and Ba^{2+}. Sometimes zeolites contain heteroatoms such as Ga, Be, Ti, B, Fe, V and P as T atoms. Their framework structures are based on an infinitely extending three-dimensional network of SiO_4 and AlO_4 tetrahedra (primary building unit) sharing all the oxygen atoms. These networks result in a well defined regular pore structure of molecular dimensions. The silicon and aluminium atoms are often referred to as T atoms and zeolites are frequently classified according to the number of T atoms in the rings that form the pore structure. These may range from very small- (6 atoms, 2-3 Å pore diameter) to large-pore zeolites (12 atoms, 5.5-8 Å pore diameter) as shown in Table 1.1. The pore systems of zeolites may be one dimensional (non-interconnecting parallel pores, e.g. Linde type L), two dimensional (Ferrierite) or three dimensional (Faujasite, ZSM-5). In recent years systems with more than 12-membered oxygen rings have been discovered such as $AlPO_4$-8 (MCM37) which contains 14-membered oxygen rings [Dessau *et al.*, 1990], the 18-membered oxygen ring crystalline aluminophosphate VPI-5 [Davis *et al.*, 1988] and Cloverite, a gallophosphate, which has a 20- and 8-membered oxygen rings dual pore structure [Estermann *et al.*, 1991].

Channel dimensions are important in that they determine which molecules may enter the intracrystalline pore space of the zeolite. This property classifies zeolites as molecular sieves. This sieving property is a function of both temperature and the cation content of the zeolite. Higher temperatures increase the flexibility of the zeolite structure and guest molecules while cations of different size and locations offer different steric constraints.

1.1.1.1 ZSM-5

The secondary building unit of ZSM-5 is the five membered ring (5-1) (Figure 1.2) which, when linked together, forms chains. The chains lead to the formation of a framework with a three-dimensional channel system. The channel system consists of two intersecting, ellipsoidal channels of similar size with 10 membered rings, one sinusoidal and the other straight. ZSM-5 is a medium pore zeolite with free apertures of 5.2x5.7 Å for the straight channel and 5.3x5.6 Å for the sinusoidal channel. The intersection cavity has a free diameter of ~9 Å [Meier and Olson, 1996]. The crystal structure is

orthorhombic, with a unit cell of the dimensions: a=20.1 Å, b=19.9 Å, c=13.4 Å [Szostak, 1992]. The chemical composition of the sodium form is given by $Na_x[Si_{96-x}Al_xO_{192}]\cdot 16H_2O$ ($x \leq 8$) and the framework density is 17.9 T-atoms per 1000 Å^3.

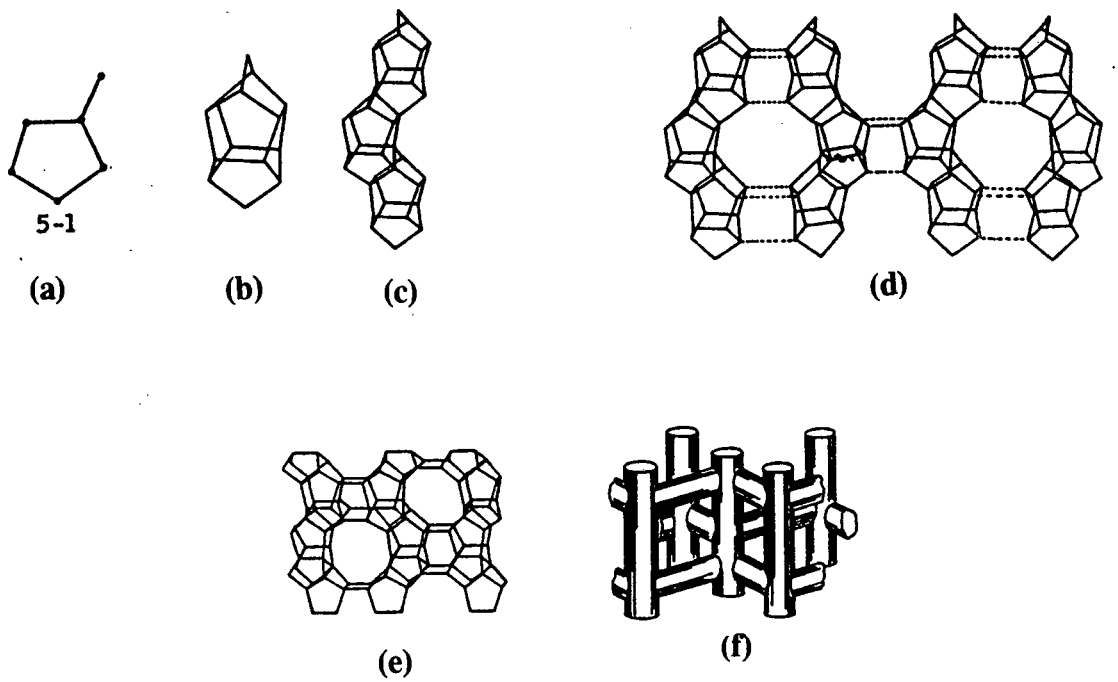

Figure 1.2: **Structure of ZSM-5: (a) Secondary building unit, (b) building block, (c) Linear chain obtained by the linkage of building blocks, (d) Linear-chain combination, (e) Skeletal diagram of the [010] face of the ZSM-5 unit cell, the x-axis is horizontal and the y-axis is vertical, (f) Channel network [Derouane, 1982]**

1.1.2 Acidity and activity of zeolites

The acidity of zeolites is determined by the nature, strength and density of acid sites. Regarding their nature, acid sites in zeolites can be divided into two categories, namely Lewis and Brønsted sites.

Lewis acids are electronically unsaturated atoms, molecules and ions [Schmidt, 1988]. In zeolites Lewis acidity may generally emanate from extra-framework cations, such as extra-framework aluminium [Karge and Dondur, 1990] and charge compensating alkali

metal ions, or from tricoordinated aluminium and silicon occurring at defect sites in the catalyst [Kustov *et al.*, 1984; Karge, 1993]. While the early theory of tricoordinated aluminium and silicon as the cause of Lewis acidity [Uytterhoeven *et al.*, 1965] has been frequently contested, the association of Lewis acidity with extra-framework alumina has become a feature of recent literature. Stronger Lewis acidity appears with extra-framework alumina, however, there is no clarity on the catalytic activity of these acid sites. Weak Lewis acidity from charge compensating alkali metal ions (particularly sodium) do not appear to contribute to activity in the catalysis of hydrocarbon reactions [Rabo and Poutsma, 1971].

The charge imbalance of a tetrahedrally coordinated, trivalent aluminium atom results in a net negative charge on the zeolite framework. This is compensated for by the presence of charge balancing cations. If the cation is a proton the zeolite possesses hydroxyl groups which act as Brønsted acid sites. While it has been widely accepted that the number of aluminium atoms in the framework determines the number of Brønsted acid sites [Stach *et al.*, 1992], an important factor which controls the acid site strength is the lattice composition. As the Si/Al ratio changes, the deprotonation energy, and thus the strength of Brønsted acid sites, is seen to vary. The strongest acid site is that associated with no aluminium atoms in its second coordination sphere (Next-Nearest-Neighbour Theory) [Mikovsky and Marshall, 1976]. This condition is met for virtually all Brønsted sites for Mordenite with a Si/Al ratio larger than 9.4 [Stach and Jänchen, 1992a] and for Zeolite-Y with a Si/Al ratio larger than 5.6 [Stach *et al.*, 1992b].

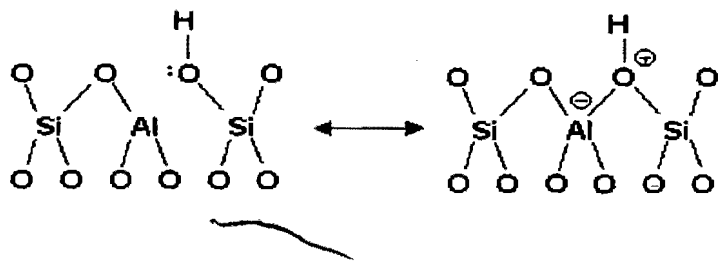

Figure 1.3: The structure of the Brønsted acid site in zeolites [Haag and Chen, 1987]

The detailed understanding of the relationship between acid sites and catalytic activity in zeolites, such as HY has remained controversial, due to the instability of HY and the complexity of the system. The catalytic significance of Lewis acid sites, if any, has remained poorly understood. Brønsted acid sites have been recognised early on to play a key role in acid catalysed reactions over zeolites. When the hydrogen form of ZSM-5 is prepared in the absence of steam, it contains only one type of catalytic site. Each framework Al atom gives rise to one Brønsted acid site. In several reactions the catalytic activity has been found to be strictly proportional to the aluminium concentration and hence to the content of active sites, for SiO_2/Al_2O_3 ratios ranging from about 17 to 10^5 [Haag and Chen, 1987]. The correlation line for the n-hexane cracking activity (α-value) and the aluminium concentration went through the origin [Haag *et al.*, 1984b]. Thus if an aluminium free zeolite could be made, it would have no acid activity. This linear correlation was found for the cracking of n-hexane, toluene disproportionation, hexene cracking [Haag *et al.*, 1984b], methanol conversion [Chen and Reagan, 1979], ethylbenzene dealkylation and cyclopropane isomerisation [Chu and Chang, 1985]. Similar relationships between activity and framework Al content were reported for dealuminated zeolite Y [Haag and Chen, 1987].

1.1.3 Shape selectivity

Shape selective catalysis in zeolites has its original cause in the majority of active sites being located in the steric restrictive environment of the intracrystalline micropores with exactly defined dimensions similar to those of many molecules.

Examples of shape selective catalysis in zeolites were first described more than 30 years ago by Weisz and coworkers [Weisz and Frilette, 1960; Weisz *et al.*, 1962; Chen and Weisz, 1967]. Csicsery [1976] categorised shape selectivity as follows (Figure 1.4):

(i) Reactant selectivity occurs when only a fraction of reactant molecules have a minimum molecular diameter which is small enough to allow diffusion through the catalyst pores.

(ii) Product selectivity occurs when some of the product formed within the pores are

too bulky to diffuse out.

(iii) Restricted transition state selectivity occurs when certain reactions are prevented because the corresponding transition state would require more space than is available in the cavities. Neither reactant nor potential product molecules are prevented from diffusing through the pores. Reactions requiring smaller transition states proceed unhindered.

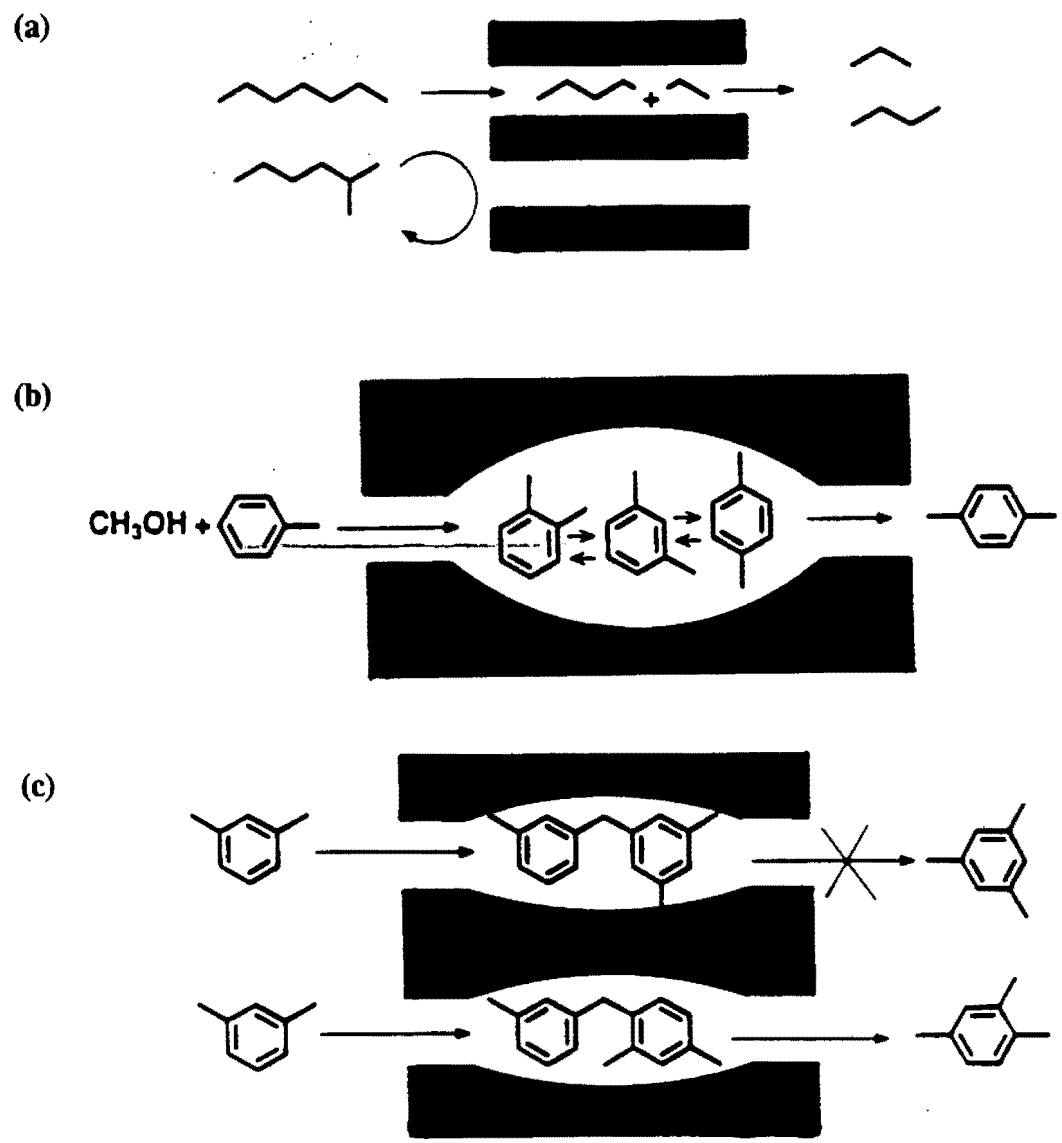

Figure 1.4: **Examples of shape selectivity, a) Reactant selectivity, b) Product selectivity, c) Restricted transition state selectivity [Csicsery, 1976]**

Two different mechanisms operate to cause shape selectivity. In one, shape selectivity results from a large difference in the diffusivity of the participating molecules in the zeolite channels (mass transport selectivity in reactant and product selectivity). In the other, selectivity is caused by steric constraints in the transition state of the catalytic transformation step (transition state selectivity).

In the case of mass transport selectivity, the observed net rates of conversion or production of different molecular species is governed by the classical relationships for diffusion-reaction inhibition [Thiele, 1939; Weisz and Prater, 1954; Satterfield, 1970]. For example, for two parallel reactions with an intrinsic selectivity $S = k_A/k_B$,

$$\begin{aligned} A &\rightarrow P_1 \\ B &\rightarrow P_2 \end{aligned}$$

the observed selectivity is

$$S_{obs} = \frac{k_A \eta_A}{k_B \eta_B} = S \frac{\eta_A}{\eta_B} \qquad (1.1)$$

A completely shape selective conversion of A occurs when $D_B \sim 0$, that is when the B molecules are essentially completely excluded from the zeolite interior (molecular sieving). With medium and large pore zeolites, both D_A and D_B are often finite. The observed selectivity in this case depends on the degree of diffusion limitation $\phi^2 = R^2k/D$ (Thiele modulus), of the bulkier non-selective species. For a given zeolite, the selectivity may be adjusted by varying the crystal size (R) and the catalytic activity (k) via synthesis and / or dealumination. A more recent development is the post-synthesis engineering of the pore size which allows to adjust the diffusivity (D) (Section 1.2). Under conditions of severe diffusion limitation, the effectiveness factor is described by $\eta = 1/\phi$ and Eq. (1.1) becomes:

$$S_{obs} = \frac{k_A \phi_B}{k_B \phi_A} = \sqrt{\frac{k_A D_A}{k_B D_B}} \qquad (1.2)$$

It is apparent that the degree of selectivity can be controlled by choosing the appropriate zeolite, which determines the individual diffusivities and their ratio. A change in crystal size or activity does not change the observed selectivity as long as the reaction remains severely diffusion limited.

1.1.4 The influence of external active sites on the catalytic behaviour

Generally it can be stated, that external acid sites have no significant, catalytic effect, if the rates of reactions catalysed by external acid sites are negligible in relation to the rates of reactions catalysed by internal acid sites. The catalytic significance of the external surface relative to the intracrystalline surface depends on the surface areas, adsorption effects and diffusion effects.

1.1.4.1 Effect on activity

For a simple reaction A→B a general kinetic expression was suggested, which considers external surface activity of zeolites [Farcasiu and Degnan, 1988]:

$$k_{obs} = (1-f)\eta k_{int} + fk_s \qquad (1.3)$$

where f is the fraction of acid sites on the external surface and k_{int} and k_s are the intrinsic rate constants for internal and external sites, respectively. The effectiveness factor η takes into account that the external acid sites are more accessible than internal sites. It is apparent that for small effectiveness factors η the external active sites can significantly affect the rate constant and thus the catalytic activity, although the percentage of external sites f might be very low. An example for such a case is the cracking of 1,3,5-triisopropylbenzene over ZSM-5 [Namba *et al.*, 1986]. The catalytic effect of external sites may also be emphasised by a relatively large fraction of external acid sites f, while the possibility, that the intrinsic rate constant of external sites is higher than for internal sites $k_s > k_{int}$, is rather unlikely to have a significant effect.

1.1.4.2 Effect on shape selectivity

Several authors [Farcasiu and Degnan, 1988; Paparatto *et al.*, 1988; Wang and Ay, 1989; Fraenkel, 1990; Uguina, 1993] have pointed out the role of external surface sites of ZSM-5 as the cause of nonselective transformations. It also has been shown that the removal, deactivation or coating of external acid sites can improve shape selective properties of ZSM-5 [Wang and Ay, 1989; Rollmann, 1991].

Despite the percentage of acid sites located on the external surface being very low, their effect on shape selectivity has to be taken into account when comparing reactions with largely differing rates. In the case of toluene disproportionation over ZSM-5, Olson and Haag [1984a] have reported that the ratio between the intrinsic rate constants of the secondary xylene isomerisation and the desired main reaction is over 7000. For that, the rate of both reactions would be comparable, even if the toluene disproportionation utilises the intracrystalline pore space with an effectiveness factor $\eta = 1$ and the subsequent xylene isomerisation would take place only on the external surface. The other possibility for a catalytically significant external surface is a high fraction of external acid sites or a low effectiveness factor of the desired shape selective reaction.

1.1.4.3 Effect on catalyst lifetime

The formation of coke during hydrocarbon conversion on zeolite catalysts can be considered as a nucleation-growth process. Nucleation is due to the retention of coke precursors (heavy secondary reaction products) in the zeolite micropores. As with other catalysts, deactivation of zeolite catalysts occurs either through site coverage or through pore blockage. Pore blockage is the only mode of deactivation of monodimensional zeolites and of zeolites with trap like cavities (large cavities with small apertures), both types deactivating very rapidly. With the other types of zeolites at low coke contents deactivation is due to site coverage, while at high coke contents it is due to a blockage of the pores by coke deposits on the outer surface of the crystallites [Guisnet *et al.*, 1996].

It is this coverage of the external surface which is the main cause of the deactivation of HZSM-5 [Magnoux *et al.*, 1987; Schulz *et al.*, 1987; Anderson *et al.*, 1989; Bibby *et al.*, 1986; Bülow *et al.*, 1987]. It was therefore apparent that the external surface activity may have some bearing on the deactivation characteristics of the zeolite [Suzuki *et al.*, 1983].

The effect of the external surface activity on catalyst lifetime has been poorly studied. Namba *et al.* [1986] and Suzuki *et al.* [1988] selectively dealuminated the external surface of ZSM-5 using $SiCl_4$ and studied the effect on the deactivation behaviour in the conversion of cumene and methanol respectively. The Si/Al ratio of the external surface was monitored by means of XPS.

Namba *et al.* [1986] compared deactivation data obtained during cumene cracking at 275°C at similar conversion levels (15%-20%). A decrease in the deactivation rate, viz. Δconversion/time, from approximately $1\%h^{-1}$ to $0.5\%h^{-1}$ was observed as the aluminium content and therefore the number of acid sites at the external surface decreased. In order to compare ZSM-5 and the dealuminated ZSM-5 at a similar conversion level, however, the ratio W/F had to be increased from $3.1ghmol^{-1}$ to $4.2ghmol^{-1}$ respectively. This means that the apparently faster deactivating parent has converted approximately 30% more cumene per gram of catalyst in total after the same time on stream than the dealuminated ZSM-5, which may explain the apparently faster deactivation with respect to time on stream. The deactivation rate, however, has been halved and therefore it can be concluded that the dealuminated ZSM-5 shows less deactivation when the same absolute amounts of feed were converted. Thus catalyst lifetime actually has been improved.

In the conversion of methanol at high temperature (540°C) [Suzuki *et al.*, 1988] the lifetime of the parent ZSM-5 and the dealuminated sample were compared at equal WHSVs. The lifetime was determined by the time on stream during which the methanol conversion was above 97%. The lifetime increased from 45h to 56h when the Si/Al ratio of the external surface increased from 148 to 190. The bulk Si/Al ratio increased less drastically from 224 to 243.

1.1.4.4. Proportion of external acid sites

The fraction of external acid sites *f* has an important bearing on the catalytic effect of the external surface activity (Equation 1.3). The share of the external surface is indicative for the fraction of external acid sites and depends on the morphology and the size of the zeolite crystals. Well crystallised zeolites are strictly microporous and therefore have very low external surface areas that may be approximated by their apparent geometrical areas as measured by scanning electron microscopy [Suzuki *et al.*, 1983, 1986; Inomata *et al.*, 1986]. However, more often than not zeolite samples are less than perfectly crystalline and may exhibit mesopores and consequently external surface areas much higher than their apparent geometrical areas. This was supported by non-contact atomic force microscopy (AFM) and nitrogen adsorption measurements on beta zeolites, which revealed the extreme irregularity of the external crystal surface [Harvey *et al.*, 1995].

Inomata *et al.* [1986], who proposed the benzene-filled pore method, reported fractions of external surface area to the total BET-surface area between 1 and 3 % for zeolite Y, 3 and 5 % for mordenite and 0.4 and 5 % for ZSM-5. The external surface areas obtained by the benzene-filled pore method were in agreement with geometrical values obtained from electron micrographs. Y zeolite exhibited sphere-like crystals of 0.55 to 0.75 μm in diameter. Mordenite was represented by a sample consisting of cubic crystals of 0.2 μm in height as well as a sample which contained bundles of rod like crystals. ZSM-5 crystals were cube- or plate-shaped with crystal sizes between 0.5 and 2 μm. The largest ZSM-5 crystals were flat plates of 7 x 4.5 x 2.5 μm^3 and showed the lowest external surface area.

Evaluating nitrogen adsorption isotherms in combination with methylene blue adsorption, Handreck and Smith [1989] reported external surface areas from 85 to 120 m^2/g and 15-25% of exchange sites being located on the external surface of ZSM-5. The crystal morphologies ranged from intergrown monolithic particles (1-3.5μm) to highly intergrown crystallites which formed secondary aggregates (0.5-1.5μm). Recently, Remy and Poncelet [1995] proposed a new approach to the determination of the external surface and

micropore volume of zeolites from the nitrogen adsorption isotherm at 77K using the t-plot method. The fractions of external surface area to total BET-surface area ranged from 3 to 20 % for zeolite Y, 2 to 20 % for mordenite and from 26 to 40 % for ZSM-5.

It may be suspected that the wide range of reported external surface areas is due to the different measuring methods. However, Remy and Poncelet [1995] showed that different crystal morphologies cause the external surface area to vary in a wide range as measured by one method. The fraction of the external surface being as high as 40% of the BET-surface area indicated that external acid sites may significantly affect catalytic properties, putting the widely made assumption that the external surface area is negligible into a new light. Studies by von Ballmoos and Meier [1981] showed that aluminium zoning occurs during the synthesis of ZSM-5 with the aluminium concentration increasing towards the rim of the zeolite crystal. This is another aspect which emphasises the catalytic significance of external acid sites. Qin *et al.* [1985] suggested that approximately 35% of the strong acid sites are located at the external surface or near the pore mouths for small ZSM-5 crystals ($\leq 0.1 \mu m$).

1.1.4.5. Summary

The catalytic significance of the external surface activity and how it affects selectivity and catalyst lifetime clearly depends on the catalyst morphology (f, Equation 1.3) and the catalytic system, viz. the combination of reaction and catalyst (η, reaction kinetics, reaction network).

1.1.5 Catalysis using zeolites

While the unique ion exchange and sorptive properties of zeolites have been recognised and utilised for some time, the use of zeolites as catalysts is a rather recent development. Two centuries passed between the discovery of natural zeolites by Cronstedt (1756) and their first commercial catalytic application as cracking catalysts (1959) [Rabo *et al.*, 1960; Weisz and Frilette, 1960]. Synthetic faujasites, known as Linde *X* and *Y*, constituted the

first and still most widely used zeolitic catalysts.

The development of synthetic routes for manufacturing zeolites led to the discovery of many new synthetic zeolites over the past 30 years. Their commercial application in catalytic processes has expanded well beyond the boundaries of traditional petroleum refining. Presently, a substantial amount of effort by petroleum and chemical companies is directed towards the discovery and use of unique zeolites for petroleum refining, synfuel production, petrochemical manufacture, fine chemical manufacture and NO_x abatement.

As far as catalysis is concerned, zeolites share the following six properties that make them attractive as heterogeneous, shape selective catalysts [Chen and Degnan, 1988]:

1. Well-defined crystalline structure
2. High internal surface areas ($> 600\ m^2/g$)
3. Uniform pores with one or more discrete sizes
4. Good thermal stability
5. Ability to sorb and concentrate hydrocarbons
6. Highly acidic sites when ion exchanged with protons

Out of approximately 150 synthetic and natural zeolites mainly Faujasite (Linde type *X* and Linde type *Y*), Mordenite, zeolite L, ZSM-5, synthetic Ferrierite and Erionite are of industrial catalytic importance [Chen and Degnan, 1988]. While the application of zeolites in the synthesis of organic fine chemicals is still underdeveloped [Hölderich and van Bekkum, 1991], the main industrial applications are in petroleum refining, synfuels production and petrochemicals production [Moscou, 1991].

In petroleum refining the largest application is catalytic cracking (Y, ZSM-5) followed by hydrocracking (Y, Mordenite). Other applications are in hydro-isomerisation and catalytic dewaxing (i.e. the removal of long chain hydrocarbons from the linear paraffin products) using mostly ZSM-5 and Mordenite [Moscou, 1991].

Synthetic fuels production includes processes such as the production of high quality

gasoline and distillates fuels from natural gas via the well known methanol to gasoline process, which employs primarily zeolite ZSM-5 as catalyst [Tabak and Yurchak, 1990].

Important petrochemical processes, such as aromatic isomerisation, disproportionation and alkylation, employ zeolites to produce valuable petro-chemicals. Xylene isomerisation and toluene disproportionation or transalkylation to form p-xylene are examples were the shape selective properties of ZSM-5 are used [Pujado *et al.*, 1992]. An example for aromatic alkylation is the Mobil-Badger process which uses HZSM-5 as a catalyst for the alkylation of benzene to produce ethylbenzene [O'Connor *et al.* 1995].

Table 1.2: Processes utilising zeolite catalysts [Haag and Chen, 1987]

Process	Description	Zeolite catalyst
Cracking	Gas oil to gasoline and distillates	REY, US-Y, ZSM-5
Hydrocracking	Heavy fractions to naphtha and distillates	Me+REX, REY, US-Y
Hysomer	Isomerisation of pentane and hexane	Pt/Mordenite
Selectoforming	Post-reforming process	Erionite
M-forming	Upgrading of reformate	ZSM-5
MDDW, MLDW	Dewaxing of distillates and lube oil	ZSM-5
MLPI, MVPI, MHTI	Xylene isomerisation	ZSM-5
MTDP	Toluene disproportionation	ZSM-5
MEB	Ethylbenzene synthesis	ZSM-5
MOGD	Conversion of olefins to gasoline and distillate	ZSM-5
MTG	Methanol conversion to gasoline	ZSM-5
MTO	Methanol conversion to olefins	ZSM-5
M2-forming	Formation of aromatics from paraffins and olefins	ZSM-5
Para-selective	Synthesis of p-ethyltoluene	ZSM-5
reactions	Synthesis of p-xylene from toluene	

1.2 SILICALITE SHELLS

A US patent by Rollmann [1980] reported on the Silicalite-I coating of ZSM-5 by reintroduction of the ZSM-5 crystals into an aluminium-free synthesis mixture. This treatment was reported to yield ZSM-5 crystals with an Al-rich core and an Al-free shell with an isostructural configuration. Weber [1993] suggested that the synthesis mixture used in the modification procedure may extract small amounts aluminium out of the framework and replace it with silicon when detemplated ZSM-5 seeds are used (i.e. the channels are not filled with template). The freed aluminium could thus be included in the formation of the shell, or in the formation of acidic amorphous material. The formation of amorphous material appears to be possible [Handreck and Smith, 1990] especially when detemplated ZSM-5 seeds were used [Weber, 1993]. Amorphous material has the potential to catalyse reactions in a non-shape-selective manner and may thus place a limit on the overall effectiveness of this method.

Rather thick shells of Silicalite-I were required to coat the ZSM-5 crystals completely as the TPD of 4-methyl-quinoline showed [Weber, 1993]. Compared to the silica-to-parent weight ratios reported for the CVD of alkoxysilanes which were generally smaller than 1.3:10 (Section 1.4.1) , the shell-to-core weight ratios were generally greater than 1:1 [Rollmann, 1980; Lee *et al.*, 1993; Weber, 1993] thus being more likely to cause diffusion resistances.

The adsorption capacity of n-hexane [Weber, 1993] and the ion exchange capacity [Handreck and Smith, 1990] were reported to remain constant and thus showed that this method retains the micropore volume, the access to the channels of the Al-rich ZSM-5 core and also indicates that the material formed had a high crystallinity. However, these data do not rule out that the Silicalite-I coating has introduced diffusion resistances, such as partial pore blockage, pore mouth narrowing or a prolongation of the intracrystalline diffusion path.

Lee *et al.* [1993] used Na-ZSM-5 as seed material and reported that the inertisation of the

acid sites on the external surface by coating the ZSM-5 crystals increased the p-selectivity during toluene alkylation, without narrowing the channels. The activity, as measured by toluene conversion, however, decreased from 30% to 20%. Crystal sizes could not be compared quantitatively by SEM micrographs, as the catalyst with a shell-to-core weight ratio of 1:1 is expected to be only 1.26 times larger than the seed. The introduction of diffusion resistances by the Silicalite coating, however, has not been experimentally ruled out. Therefore the enhanced p-selectivity and the decreased activity may not necessarily be due to the inertisation of the external surface.

1.3 CHEMICAL VAPOUR DEPOSITION OF ALKOXYSILANES

Economic and environmental factors are the driving force for research and catalyst manufacturers to provide customised catalysts. Post-synthesis modification of zeolites can be considered a tool to tailor the materials properties for catalytic application and are often unavoidable to obtain competitive catalysts. There are a variety of post-synthesis modification methods to further control the activity, shape selectivity or catalytic stability of zeolites. They are either aimed at changing the density, strength or nature of the active sites or the porous structure of the catalyst.

Chemical Vapour Deposition (CVD) is a method of film formation on solid substrates that relies upon the transport of the agent in the gas phase, followed by deposition on the substrate to form the film. CVD is known for excellent conformal coverage of complex structures and simple deposition equipment. In order for a chemical compound to serve as a useful CVD-precursor, it must be sufficiently volatile, so that it can be transported in the gas phase in high enough concentrations to allow reasonable film deposition rates. The affinity towards the zeolite surface should be higher than towards deposited surface species to promote epitaxial growth rather than the formation of bulky islands or towers.

1.3.1 Deposition of silanes and organo-silanes

The silylation of zeolites can be done at water free conditions by exposure to silanes or organo-silanes in the liquid or vapour phase. The Si-H bond in the silanes has a hydridic reactivity due to the charge separation Si^{+}-H^{-} which results from the greater electronegativity of H compared with Si. Therefore silane can be hydrolysed by the silanol groups in zeolites. Studies about the use of silanation precursors were carried out for SiH_4, Si_2H_6 [Vansant, 1990], $(CH_3)_3SiH$ and $(CH_3)_2SiH$ [Von Ballmoos and Kerr, 1985]. The treatment can be carried out at temperatures ranging from 20°C to 500°C. The deposited silane may be stabilised by subsequent calcination in air or hydrolysis with water.

A modification of the pore size can be the result of an internal and an external modification. If the pore dimensions are large enough to allow the silanation precursor to diffuse into the micropore system the internal and the external surface are modified [Cody, 1984] and the pore diameter throughout the intracrystalline space is reduced. If the pore size is too small the deposition is restricted to the external surface of the zeolite crystal and a pore size modification only takes place at the pore entrance as in the case of alkoxysilanes (Section 1.4.1.3).

In contrast to tetraalkoxysilane, organo-silanes and silanes cannot form a polymer like structure without repeated hydrolysis-deposition cycles [Vansant, 1990]. Therefore one deposition treatment only yields monoatomic Si fragments.

1.3.2 Alkoxysilanes used

A particularly promising class of CVD precursors are alkoxysilanes. Tetramethoxysilane (TMOS) was the first alkoxysilane which was employed in the CVD treatment of a zeolite [Niwa *et al.*, 1982]. Since then the CVD alkoxysilanes has drawn considerable attention as a potential method to tailor the shape selective properties of zeolites. Table 1.3 summarises alkoxysilane / zeolite systems which have been reported in literature. For

Table 1.3: Overview over alkoxysilane / zeolite systems reported in literature

Alkoxysilane	Zeolite	T_{CVD} (°C)	Apparatus	Reference
$SiOCH_3(CH_3)_3$	H-ZSM-5	320	vacuum	Kim *et al.*, 1996
$Si(OCH_3)_2(CH_3)_2$	H-ZSM-5	320	vacuum	Kim *et al.*, 1996
$Si(OCH_3)_3(CH_3)$	H-ZSM-5	320	vacuum	Kim *et al.*, 1996
$Si(OCH_3)_4$	H-ZSM-5	320	vacuum	Niwa *et al.*, 1986
= TMOS	H-ZK-5	350	-	Fetting *et al.*, 1990
	H-Mord	320	vacuum	Niwa *et al.*, 1982
	Na-Mord	20 and 320	vacuum	Hibino *et al.*, 1988
	H-Ba-Mord	320	vacuum	Sawa *et al.*, 1990
	Zeolite Na-A	400	vacuum	Niwa *et al.*, 1991
$Si(OC_2H_5)_4$	H-ZSM-5	180-230	flow	Wang *et al.*, 1988
= TEOS	MFI-Metallosilicates	240	flow	Halgeri *et al.*, 1995
	H-β	21-250	vacuum	Chun *et al.*, 1994
	K-X	20	vacuum	Chun *et al.*, 1997
	H-Y	0-200	flow	Murakami *et al.*, 1988
$SiOCH_3(C_3H_7)_3$	H-ZSM-5	70	vacuum	Kim *et al.*, 1996
$Si(OC_4H_9)_4$	H-ZSM-5	180-230	flow	Wang *et al.*, 1988

each alkoxysilane / zeolite system only the earliest reference found is listed. More recently CVD of alkoxysilanes has also been applied to metallosilicates with MFI structure [Halgeri *et al.*, 1995; Bhat *et al.*, 1996a].

Each of the alkoxysilanes listed in Table 1.3 has been applied to ZSM-5. However, only TMOS and TEOS were applied to a broader range of zeolites, including 8-, 10- and 12-membered ring zeolites and zeolites with different cations. The deposition of a silica layer is possible in the absence of Brønsted acidity as the successful deposition of TMOS over Na-mordenite [Hibino *et al.*, 1988] and zeolite Na-A [Niwa *et al.*, 1991] has shown.

However, zeolites are mostly modified in their proton form, since they are more reactive. While the deposition of TMOS, TEOS, $SiOCH_3(C_3H_7)_3$ and $Si(OC_4H_9)_4$ was restricted to the external surface of the zeolite crystals Kim *et al.* [1996] showed that $SiOCH_3(CH_3)_3$, $Si(OCH_3)_2(CH_3)_2$ and $Si(OCH_3)_3(CH_3)$ were also deposited inside the micropores at a deposition temperature of 320°C.

1.3.3 Methods using tetraethoxysilane

More recently TEOS has found interest as CVD precursor alternative to TMOS. Both agents can be hydrolysed and are thus moisture sensitive. Being classified as flammable, corrosive and possibly blindness causing liquid, the safety hazard of TMOS is clearly greater than for TEOS which is classified as irritant only [Aldrich catalogue, 1996-1997]. TEOS is also less reactive than TMOS [Niwa *et al.*, 1989] and should therefore show different deposition characteristics, which might lead to a silica layer with different qualities. Due to its larger molecular diameter TEOS appears to have a broader applicability than TMOS with respect to the pore size of zeolites. Thus TEOS has been applied successfully to selectively deposit a silica layer on the external surface of the large pore zeolite Y [Murakami *et al.*, 1988a]. A number of CVD techniques employing TEOS have been reported for the modification of various zeolites (Table 1.4).

1.3.3.1 Vacuum- or flow-conditions

CVD techniques using a vacuum system are mainly of academic interest. A microbalance accommodated in a vacuum line enables in-situ monitoring of the mass deposited, while the zeolite is in contact with the alkoxysilane vapour [Chun *et al.*, 1994]. Weber *et al.* [1996] used a vacuum system, which can be used for TPD studies subsequently to the CVD treatment. At the first glance it might appear that CVD in a vacuum line takes place in a well defined, waterfree atmosphere, on a clean catalyst surface and without competitive adsorption of molecules other than the alkoxysilane. However, gaseous deposition products and / or the formation of coke may interfere with the primary deposition reaction [Niwa *et al.*, 1986; Weber, 1998].

Table 1.4: Overview over CVD techniques using TEOS and references where the respective method was first published

Reference[a]	Zeolite	Apparatus	Pre-CVD	CVD-atmosphere	T_{CVD} (°C)	Post-CVD
Chun *et al.*, 1994, 1997	Hβ, KX, NaY	Vacuum, gravimetric apparatus	Evacuation	TEOS	20-250	Calcination in flowing O_2
Dong Fei *et al.*, 1995	HZSM-5	Flow system	-	TEOS carrier gas: N_2	180-400	Coke burning
Itoh *et al.*, 1989	HY	Flow reactor	-	TEOS, ether	-	-
Murakami *et al.*, 1988a	HY	Flow reactor, glass tube	Calcination in He	TEOS carrier gas: He	0-200 (70)	Calcination in He, repeated silanisation cycles
Murakami *et al.*, 1988b	HY	Flow reactor, glass tube	Calcination in He	TEOS, ethanol carrier gas: He	100	Calcination in He, repeated silanisation cycles
Wang *et al.*, 1988 Halgeri *et al.*, 1991	HZSM-5 Pentasil-gallosilicate	Flow integral reactor,	Calcination,	TEOS, toluene, methanol, carrier gas: -	180-230	Not mentioned
Das *et al.*, 1993a, 1994a Bhat *et al.*, 1993, 1996a	HZSM-5 HGaMFI	glass tube, glass tube	in air, in N_2	carrier gas: H_2 carrier gas: H_2	230 240	Calcination in air
Weber *et al.*, 1996	HZSM-5	Vacuum line	Calcination in flowing air, followed by evacuation	TEOS	320 and 400	Calcination in flowing air

[a] Reference where the respective method was reported first

A more frequently studied method than the CVD in an evacuated static system is the CVD in conventional flow reactors, which are easy to use and more practical for large scale application [Niwa *et al.*, 1989]. Concentration gradients over the catalyst bed are avoidable by operating the reactor differentially, thus facilitating a homogeneous silica deposition throughout the catalyst bed. Gaseous deposition products are removed to a greater extent than in a vacuum system and are thus prevented from interfering with the deposition by consecutive reactions or the formation of carbonaceous deposits. The deposited mass, however, can only be monitored indirectly, via mass balance using gas chromatography. Wang *et al.* [1988] successfully modified HZSM-5 by CVD of TEOS in a 100kg/h (ethylbenzene feed) pilot plant for the selective synthesis of p-diethylbenzene. A continuous flow method for the preparation of zeolites modified by CVD of alkoxysilanes, which can be applied to modify large amounts of zeolites sufficient for industrial use, has been patented by Murakami (JGC Corp.) [1987a-e].

1.3.3.2 Pre-CVD, CVD and post-CVD treatment

The CVD of TEOS in a flow system was generally preceded by calcination of the zeolite in a flowing gas, such as air, oxygen, nitrogen or helium (Table 1.4). The CVD in vacuum system was preceded by an evacuation step [Chun *et al.*, 1994] or by a calcination-evacuation sequence [Weber *et al.*, 1996]. The temperatures at which CVD of TEOS were carried out range from 0°C to 400°C (Table 1.4). The CVD techniques which use vacuum conditions admitted only pure TEOS to the zeolite. In flow reactors the CVD of TEOS was carried out in the presence of other gases, such as toluene, methanol, ethanol, ether and hydrogen or helium as carrier gas. The co-feeding of alcohols was suggested to promote a uniform deposition of the silica layer due to competitive adsorption and hydrolysation of the alkoxysilane by water, which is formed by dehydration of the alcohol [Wang *et al.*, 1988]. However, the CVD temperature has to be high enough (200°C) to facilitate the dehydration of methanol [Ono *et al.*, 1979]. The modification of zeolite Y at 70°C [Murakami *et al.*, 1988a] using pure TEOS and an inert carrier gas showed that additional compounds are not necessary for a successful CVD of TEOS at low temperatures. Generally, the rate and amount of silica deposition

can be regulated mainly by co-feeding of alcohols or ether [Murakami *et al.*, 1988b; Niwa *et al.*, 1989] the CVD temperature [Wang *et al.*, 1988; Chun *et al.*, 1994], CVD time [Chun *et al.*, 1994] and the number of CVD treatments [Murakami *et al.*, 1988a,b]. The CVD treatment is usually followed by a post-CVD calcination step in air, oxygen or helium (Table 1.4).

1.3.4 Effect of crystal morphology

Bhat *et al.* [1996b] reported that the extent of modification required to achieve a particular *para*-selectivity in the alkylation of toluene with ethanol was higher for zeolite samples with a smaller crystal size, while it was lower for twinned, elongated, prismatic crystals as compared to spherical crystals. The CVD of TEOS is restricted to the external surface, therefore the external surface area has a direct bearing on the catalytic effect of the CVD. This area depends on the morphology and crystal size of the zeolite (Section 1.1.4.4).

1.3.5 Effect of pelletisation and extrusion

All zeolites employed in the methods listed in Table 1.4 were modified in their proton form. CVD of TEOS was successfully carried out over ZSM-5 powder [Bhat *et al.*, 1995c; Weber *et al.*, 1996], granulated pellets [Wang *et al.*, 1988; Bhat *et al.*, 1996b] and extrudates [Bhat *et al.*, 1995a]; and over extruded or pelletised Y-zeolite [Itoh *et al.*, 1989]. Extrusion and pelletisation may not only affect the catalytic properties but also the effectiveness of a CVD treatment. Bhat *et al.* [1995a] found that extrudates required a higher amount of silica deposition than the pure zeolite to enhance the selectivity to the para-isomer in the alkylation of ethylbenzene with ethanol. This may be attributed to catalytic effects of the respective binder, an increased diffusional path length or a different exposure of the zeolite's external surface. Wang *et al.* [1988] published that TEOS decomposes over HZSM-5, SiO_2-Al_2O_3, γ-Al_2O_3 and Kieselguhr with the decomposition rate decreasing in this sequence, thus showing that typical binder materials (alumina, silica or clays) clearly have an effect on the CVD of TEOS. Extra-framework alumina and tiny crystals on the external surface of zeolite crystals were observed to cause a higher

required amount of silica concentration for inertisation of the external surface [Hibino *et al.*, 1993; Bhat *et al.*, 1996b].

1.3.6 Reaction scheme

Based on an investigation of saturated surface concentrations of silicon, the products evolved, and IR spectroscopy Niwa *et al.* [1988] proposed a reaction scheme for the CVD of TMOS over H-mordenite as illustrated by Equation 1.4 to 1.7 and Figure 1.5. The molecular size of tetra-alkoxysilanes is larger than the pore size of mordenite. Therefore, the primary deposition reaction is restricted to the external surface. As initial step, one of the functional methoxide groups of TMOS reacts with a surface hydroxyl and is anchored on the zeolite's external surface as tri-alkoxy-derivative (Figure 1.5.a(I) and Equation 1.4) or di-alkoxy-derivative (Equation 1.5), accompanied by the formation of methanol. In a subsequent reaction neighbouring surface tri-alkoxide-derivatives may form siloxane bonds accompanied by the formation of dimethylether (Figure 1.5.a(II)). This poly-condensation process may continue and thus lead to a covering monolayer (Figure 1.5.a(III)). In the presence of water, methanol may be formed instead of dimethylether.

There are two possibilities for subsequent reactions between gaseous alkoxide and surface alkoxy derivatives:

i) hydrolysis of the surface methoxides by water to generate silanol groups (Equation 1.7) on which the chemisorption of TMOS continues, and

ii) direct condensation of TMOS (Equation 1.8).

Methanol and dimethylether, respectively, will be produced in these secondary deposition reactions. Reaction path (i) can only be followed in the presence of water, which may be present as adsorbed water on the zeolite or it may be formed as secondary product in a dehydration reaction of methanol to water and dimethylether (Equation 1.6.a). In the absence of adsorbed water, all subsequent reactions discussed above, are accompanied by the formation of dimethylether. Interestingly, during the CVD of TMOS over H-mordenite, dimethylether was observed only at temperatures above 100°C [Niwa *et al.*, 1988]. Thus, at temperatures lower than 100°C and in the absence of water, chemisorbed

derivatives of TMOS neither react with each other nor with gaseous alkoxide subsequent to the primary deposition reaction. Therefore, these conditions are expected to favour the formation of monoatomic Si-fragments. At temperatures above 100°C subsequent reactions become significant and the CVD of TMOS becomes more complex. Between 150°C and 250°C methanol, dimethylether and hydrocarbons were observed in the gaseous product [Niwa *et al.*, 1988]. In an earlier paper the mordenite sample was reported to be brownish black after the CVD of TMOS at 320°C [Niwa *et al.*, 1984]. This suggests that methanol is converted in consecutive reactions into hydrocarbons and coke or carbonaceous material at high temperatures. Dimethylether appearing in the gaseous product is an intermediate in the consecutive transformation of methanol but may also be formed in condensation reactions of the deposited surface alkoxides. Therefore, at temperatures above 100°C, a network structure consisting of siloxane bonds may be formed owing to the occurrence of the discussed subsequent reactions (Figure 1.5 and Equations 1.4 to 1.8).

$$Z\text{-}OH + Si(OMe)_4 \rightarrow Z\text{-}O\text{-}Si(OMe)_3 + MeOH \quad \textbf{(T > 0°C)} \qquad (1.4)$$

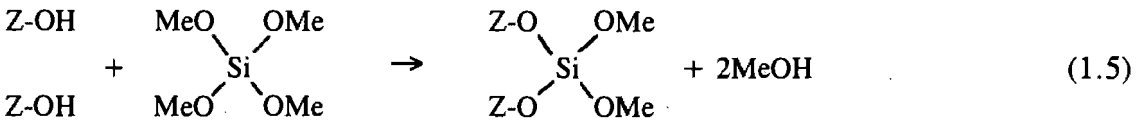

$$2MeOH \rightarrow MeOMe + H_2O \quad \textbf{(T > 100°C)} \qquad (1.6.a)$$

$$m\text{MeOH} \rightarrow \text{hydrocarbons} + mH_2O \quad \textbf{(T > 100°C)} \qquad (1.6.b)$$

$$Z\text{-}O\text{-}Si(OMe)_3 + 3H_2O \rightarrow Z\text{-}O\text{-}Si(OH)_3 + 3MeOH \qquad (1.7)$$

The proposed reaction system may be extended by the following equation:

$$Z\text{-}O\text{-}Si(OMe)_3 + Si(OMe)_4 \rightarrow Z\text{-}O\text{-}Si(OMe)_2\text{-}Si(OMe)_3 + MeOMe \qquad (1.8)$$

In summary, Hibino *et al.* [1988] suggested that the formation of the deposited phase may be divided into primary formation of a monoatomic silicon fragment (Figure 1.5.a), followed by the formation of covering monolayer (Figure 1.5.c), and subsequent build up of silica multilayers (Figure 1.5.d). The CVD of TMOS onto a zeolite can be regarded as a poly-condensation reaction which is catalysed by surface hydroxyls.

Alkoxide → Monoatomic Si fragment → Silica Monolayer → Silica Multilayer

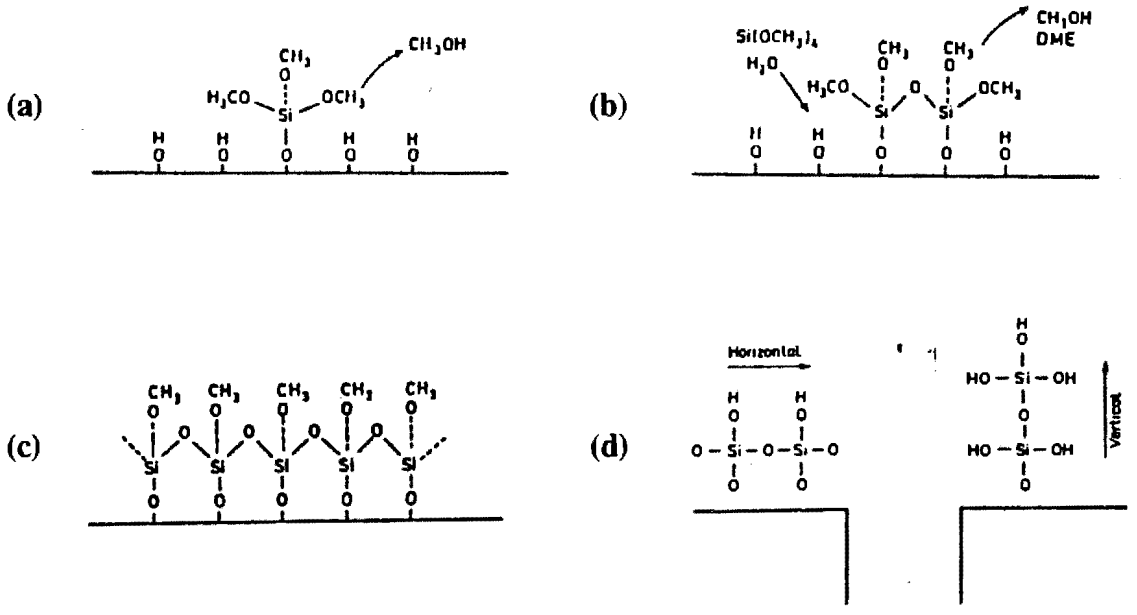

Figure 1.5: Reactions during the CVD of TMOS over Mordenite [Niwa et al., 1988]

Surface hydroxyls of zeolites are external Brønsted acid sites and terminal hydroxyl (silanol) groups. IR-spectroscopy allows a tentative discrimination of two OH-stretch vibrational band ranges. The bands in the range of 3600 cm^{-1} are generally assigned to acid OH-groups. Bands being detected around 3740 cm^{-1} represent weak acidic OH-groups. These terminal OH-groups, which are not in the immediate vicinity of an aluminium atom, occur mainly at the external surface of the crystal [Nunan *et al.*, 1984]. In special cases they may also occur in the interior of the zeolite [Dessau *et al.*, 1987; Kraushaar *et al.*, 1988]. In the example of mordenite there are six terminal hydroxyls at

each pore mouth [Niwa *et al.*, 1989]. For ZSM-5 total numbers of external hydroxyls between 1 and 5.5 OH/nm^2 were reported [Vankelecom *et al.*, 1996].

The irreversible deposition of TMOS on mordenite and the non-zeolitic oxides SiO_2, Al_2O_3 and SiO_2-Al_2O_3 at 320°C showed that any kind of surface hydroxyl may be available for the deposition reaction [Niwa *et al.*, 1984]. Later IR studies suggested that non-acidic silanol groups are available for the deposition of TMOS over HZSM-5 as chemisorption sites [Niwa *et al.*, 1986]. CVD studies over amorphous SiO_2 (silica) in combination with IR studies showed that the terminal silanol groups are already reactive at 18°C and that deposition is possible without Brønsted acid sites [Niwa *et al.*, 1988]. Hibino *et al.* [1993] observed that the silica concentration on the external surface of mordenite crystals required for the inertisation neither depends upon the included cation nor on the Si/Al ratio. This shows that TMOS reacted equivalently with non acidic, terminal silanol groups and acidic hydroxyls.

When TEOS was used as CVD precursor only physisorption but no decomposition products were observed over silica at 50°C thus indicating that no reaction with the surface occurred. However, ethanol was observed when Silicalite-I (Si/Al > 500) was exposed to TEOS, thus indicating that TEOS reacted with the surface [Weber, 1998].

The reaction of TMOS with a surface hydroxyl group is accompanied by the formation of methanol, while the reaction with a methoxide group of a deposited alkoxide species is accompanied by the formation of dimethylether. Since methanol was observed at lower deposition temperatures rather than dimethylether [Niwa *et al.*, 1984] it is concluded that surface hydroxyl groups are more reactive and are therefore the preferred deposition site.

Silicon compounds and carbonaceous material were the final products adsorbed on the zeolite upon deposition of TMOS. IR-spectra showed that organic material was removed by calcination in oxygen at 400°C. The deposited silicon compounds were completely oxidised by the final calcination and was stabilised on the external surface of H-mordenite [Niwa *et al.*, 1984]. This suggests the calcination to be an important step which may

facilitate surface reactions between deposited species to form a two-dimensional SiO_2 compound possessing siloxane bonds.

No investigations were found on the reaction scheme of CVD using TEOS. Chun *et al.* [1994] proposed a reaction system in the CVD of TEOS over zeolite Hβ (Equations 1.9-1.12) by deduction from the reaction system proposed for TMOS [Niwa *et al.*, 1984].

$$Z\text{-}OH + Si(OEt)_4 \rightarrow Z\text{-}O\text{-}Si(OEt)_3 + EtOH \quad (1.9)$$

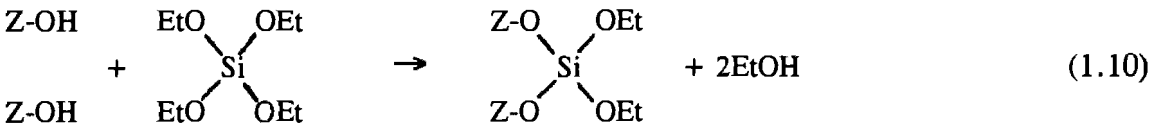

(1.10)

$$2EtOH \rightarrow EtOEt + H_2O \quad \textbf{(T < 200°C)} \quad (1.11.a)$$

$$EtOH \rightarrow CH_2{=}CH_2 + H_2O \quad \textbf{(T > 200°C)} \quad (1.11.b)$$

This reaction system may be extended by the following two equations:

$$Z\text{-}O\text{-}Si(OEt)_3 + 3H_2O \rightarrow Z\text{-}O\text{-}Si(OH)_3 + 3EtOH \quad (1.12.a)$$

$$Z\text{-}O\text{-}Si(OEt)_3 + Si(OEt)_4 \rightarrow Z\text{-}O\text{-}Si(OEt)_2\text{-}Si(OEt)_3 + EtOEt \quad (1.12.b)$$

Ethoxy groups of chemisorbed ethoxysilanes may be hydrolysed to silanol groups by reaction with product water accompanied by the formation of ethanol (1.12.a). Yet, it is not clear how readily reactions 1.11.a and 1.11.b occur and how available the water is. The formation of water depends on the CVD temperature and may affect the structure of the final silica layer. A direct chemisorption at a deposited alkoxysilane derivative accompanied by the formation of diethylether may also be possible, but has not been reported in literature to date (Equation 1.12.b).

Wang *et al.* [1988] deposited TEOS at temperatures between 180°C and 230°C on HZSM-5. The deposition rate decreased with deposition time and thus with increasing coverage, to finally reach a constant value. This shows that either physisorption is initially superimposed on chemisoprtion or the chemisorbed phase is less reactive towards the CVD agent than the original zeolite surface. This condition is ideal to promote the complete coverage of the external surface with a monolayer before the build up of multilayers. The measurable final deposition rate, indicates that the formation of multilayers does occur in the studied temperature range when methanol is co-fed. The decomposition of methanol to water and diethylether is thought to hydrolyse the ethoxy groups on the deposited phase, forming silanol groups. These hydroxyl groups are the sites for further deposition. Kieselguhr (SiO_2xH_2O) was shown to be less reactive than HZSM-5, supporting the discussed hypothesis [Wang *et al.*, 1988].

1.3.7 Proposed CVD conditions

The silanation of zeolites reduces the pore mouth size and simultaneously inertises the external surface by deposition of an inert, ultrathin, permeable and epitaxially grown silica phase, without affecting the properties of the intracrystalline pore space. This has been shown for Mordenite and ZSM-5 using TMOS as CVD agent [Niwa and Murakami, 1989]. For other zeolites and CVD agents (TEOS) these findings were transferred without supporting them experimentally. The possibility of inhomogeneous deposition due to vertical growth to form pillars or bulky islands of silica has thus not been clearly ruled out (Section 1.4).

A controlled and well defined modification of the pore mouth size and the external surface activity is obtained rather by a homogeneous, layered structure of deposited silica than by a silica polymerised in the form of bulky islands [Hibino *et al.*, 1989a]. Therefore the CVD conditions and the agent should be chosen in order to promote epitaxial growth, even though the CVD of alkoxysilanes yielded successful results over a wide range of conditions. Once the alkoxysilane is anchored to the zeolite surface the remaining three functional groups compete with the surface hydroxyls in the reaction with gaseous

alkoxysilanes. The extent to which horizontal or vertical growth occurs is determined by the reactivity of the zeolitic surface hydroxyls as compared to the reactivity of the functional groups for further deposition of alkoxysilane from the gas phase.

Temperature

The deposition temperature may have a significant influence on the quality of the final silica layer, if the activation energies in the reaction of an alkoxysilane with a surface hydroxyl and the reaction with an alkoxy group of a deposited species are different. The saturation effect at room temperature and at 320°C during the CVD of TMOS over Na- and H-mordenite shows that the surface hydroxyls of zeolites are more reactive than methoxy groups in a wide temperature range [Hibino *et al.*, 1988; Niwa *et al.*, 1988].

Role of water

It was shown that water activates the deposited species for further deposition [Hibino *et al.*, 1988] by converting the alkoxy groups into alcohol and silanol groups in a hydrolysis reaction. Thus the silanol group is more reactive towards gaseous alkoxides than the previous alkoxy group, and it is concluded that CVD conditions at which the surface alkoxides are stable prevent vertical growth. Therefore the presence of water and high temperature promote vertical growth. In the presence of Brønsted acidity and at temperatures above 300°C [Hibino *et al.*, 1988], water can be a secondary product of the CVD reaction of TMOS and TEOS due to dehydration of methanol or ethanol respectively. This suggests that deposition temperatures below 300°C are favourable for a homogeneous deposition. Water may also be adsorbed on the zeolite, thus suggesting a calcination step prior to the CVD treatment in order to promote water free CVD conditions.

In contrast Wang *et al.* [1988] co-fed methanol and claimed that the water, formed by dehydration of methanol, results in a more uniform deposition throughout the catalyst bed. However, they also report that TEOS was not only deposited on the original zeolite surface but also on the deposited silica layer. Interestingly, the rate of deposition decreased as the amount of deposited material increased which shows that TEOS reacts

faster with the original zeolite surface than with surface species' methoxy or silanol group. Therefore, epitaxial growth is still ensured even in the presence of reaction water.

Co-feeding of organic compounds

The reasons for co-feeding compounds such as toluene [Wang *et al.*, 1988; Das *et al.*, 1994a] or ether [Itoh *et al.*, 1989] have not been stated. A possible reason may be that the competitive adsorption of toluene with the alkoxysilane slows down the deposition rate and thus increases the control over the amount of silica deposited. Ether may be co-fed during the CVD of TEOS to minimise the formation of water which occurs when the deposition by-product ethanol dimerises to dimethylether, which is an equilibrium reaction.

CVD-agent

It appears that the reactivity of silicon alkoxide decreases with increasing numbers of carbon atoms. For example it has been confirmed that silicon methoxide is more reactive than silicon ethoxide [Niwa and Murakami, 1989]. The ethoxy groups of deposited TEOS derivatives are therefore likely to be less reactive. Thus TEOS may deposit more selectively on surface hydroxyls than TMOS, forming more homogeneous monolayers.

Ideal CVD-conditions

The conditions which promote the controlled and homogeneous deposition of well defined silica layers employ low temperatures, a water free CVD environment, a flow system and possibly TEOS instead of TMOS. Since these conditions promote the conservation of rather inactive surface alkoxy groups, a sequence of deposition and activation steps has to be applied in order to form multilayers. The activation of the deposited phase can be achieved by decomposition of alkoxy groups in a calcination step or in a hydrolysis treatment using steam at high temperatures. Calcination has the advantage of removing coke simultaneously to the activation process. The high temperature used during a calcination step may additionally stimulate polymerisation reactions between deposited silica species to form a layered silica compound. Due to the saturation effects which occur at the suggested conditions, the deposition is expected to be self regulating with

respect to vertical growth and a homogeneous deposition throughout the catalyst bed is expected to be achieved, even if the CVD is carried out in an integral flow reactor or a static system.

CVD carried out in a system with concentration gradients may lead especially at higher deposition temperatures to a non-homogeneous deposition throughout the catalyst bed and therefore to a non-uniform reduction of the pore mouth size (Section 1.4.1.1). If concentration gradients have to be avoided the CVD should be carried out in a differentially operated flow reactor.

1.4 CHARACTERISTICS OF SILANISED ZEOLITES

The present work focuses at the CVD of tetra-alkoxysilanes onto zeolites. The CVD treatment with tetra-alkoxysilanes results in changes to the structural and catalytic nature of the zeolite. This is caused by the deposition of a silica layer on the external surface of the zeolite crystals.

1.4.1 Structure and Acidity

1.4.1.1 Micropore space

Fetting and Dingerdissen [1990], studied the depth profile of the elemental composition of zeolite ZK5 modified by CVD of TMOS, applying secondary ion mass spectroscopy (SIMS) in order to investigate to what extent the deposition is limited to acid sites on the external surface. The TMOS-molecule (8.9 Å) is larger than the pore size of the ZK-5 zeolite (4Å). However, it cannot be simply concluded that no preceding reaction at the pore mouth may occur, thus forming a slimmer reactive molecule which diffuses into the micropores and there undergoes the actual silanisation reaction. The Si/Al-ratio depth profile showed that the Si/Al-ratio of the crystal interior remained constant with increasing degree of coating proving that the walls of the micropores remain unmodified. The Si/Al ratio of the external surface clearly increased with the degree of coating. The thickness of the silicon enriched layer for a sample with 8 wt% was found to be 100 to 150 Å. The total average crystal size was 1.5 μm. From the weight increase during CVD a thickness of 100 Å was estimated which is consistent with the SIMS result, thus indicating that the deposition was limited to the external surface.

NH_3-TPD and IR spectroscopy showed no changes in strength or amount of acid sites, when TMOS or $SiOCH_3(C_3H_7)_3$ was deposited onto ZSM-5, thus indicating the conservation of acidity in the micropore space [Kim *et al.*, 1996]. Recent NH_3- and pyridine-TPD studies showed that the number of acid sites per gram of catalyst was not affected by CVD of TEOS either [Bhat *et al.*, 1995c; Weber *et al.*, 1996]. Handreck and

Smith [1990], however, reported the decline of ion exchange capacity for cesium chloride to be three times as high as the decline experienced by the methylene blue adsorption capacity. While the adsorption of methylene blue is restricted to the external surface, the cesium ion has access to the micropore space. The different declines indicated that the CVD of TMOS affected exchange sites inaccessible to the methylene blue molecule, i.e. within the channels or channel mouths.

Adsorption of molecules such as water, nitrogen and p-xylene showed that the adsorption capacity and therefore the micropore volume remained unaffected by the CVD of TMOS even for high amounts of deposited silica (11.3 wt% or 12 theoretical monolayers) [Niwa *et al.*, 1986; Hibino *et al.*, 1991; Kim *et al.*, 1996]. The data reported for the adsorption of o-xylene, however, were in contrast to each other. Niwa *et al.* [1986] and Hibino *et al.* [1991] reported that the adsorption capacity for o-xylene was retained, whereas Kim *et al.* [1996] observed a decrease of the adsorption capacity as the amount of deposited silica increased. The latter either contradicts the conservation of the micropore volume or it shows that the pore mouth size was not reduced uniformly. The adsorption capacity of a single crystal with a 3 dimensional pore system, however, cannot be reduced by a non-uniform reduction of the pore mouth size. As long as there are pore entrances which are large enough to allow the diffusion of the adsorbate into the micropore space the same equilibrium adsorption capacity as for the parent crystal should be obtained. The adsorption capacity of a single crystal with a 3 dimensional pore system will thus be either unaffected or reduced to zero when all pore entrances are too narrow. An intermediate reduction of the average adsorption capacity for more than one zeolite crystal is, however, possible if the reduction of the pore mouth size is non-uniform from crystal to crystal. This means that some crystals were modified to a higher degree than others. A non-uniform deposition of TMOS may be caused by a concentration gradient within the catalyst bed which is more likely for a CVD method operating at static conditions than at flow conditions. Of interest is that both authors used a vacuum system and a deposition temperature of 320°C. It may be concluded that a reduction of the adsorption capacity to a value larger than zero as reported by Kim *et al.* [1996] indicates a non-uniform deposition.

When TMOS was deposited onto Mordenite, the silica to alumina ratio in the external surface layer as measured by XPS increased with the amount of deposited TMOS while the average bulk silica to alumina ratio changed very little. It was thus concluded that the silicon compound is not deposited uniformly in the zeolite bulk but is enriched near the external surface. This is supported by a good agreement between the calculated thickness, assuming the formation of complete layers, and the thickness as measured by XPS [Niwa *et al.*, 1984; Handreck and Smith, 1990]. NH_3-TPD and an unaffected adsorption capacity for water showed the conservation of the internal acid sites and the internal surface respectively [Niwa *et al.*, 1982, 1984]. It can be concluded that the intracrystalline pore space remained unmodified. In contrast to the adsorption capacity of water, the adsorption capacity of larger adsorbates such as m- and p-xylene was reduced, indicating a non-uniform reduction of the pore mouth size rather than a loss of micropore volume.

Chun *et al.* [1994] deposited TEOS onto Zeolite Hβ. The modified samples showed no change of n-hexane sorption capacity, which indicated that the micropore volume was not affected. When 1,3,5-TMB and m-xylene were adsorbed the adsorption capacity, however, decreased by approximately a third of the original sorption capacity when 5 wt% of silica were deposited on the zeolite. Similar to ZSM-5, Zeolite β also has a 3 dimensional pore structure. A reduction of an adsorption capacity which is not total thus indicates that the pore mouth size was reduced non-uniformly rather than a decrease of the micropore volume. A similar observation for the adsorption capacity of CVD treated ZSM-5 for o-xylene was already discussed above. As in the above case, the gravimetric apparatus used by Chun *et al.* [1994] did not facilitate a flow through the catalyst bed during the CVD treatment, which may lead to concentration gradients and a non-uniform deposition throughout the catalyst bed.

The general trend of the above results indicates that the micropore space remains in its original state, provided the diameter of the alkoxysilane is too large to enter the micropores of the respective zeolite.

1.4.1.2 *Morphology of the deposited phase*

Since tetra-alkoxysilanes possess four functional groups, growth of the deposited material is generally possible horizontally or vertically to yield a layered or whisker-like compound respectively. To which extent horizontal or vertical growth occurs is determined by the reactivity of the zeolitic surface hydroxyls and the functional groups for further deposition of alkoxysilane from the gas phase. This has consequences for the morphology of the deposited silica which may be spread as a tetrahedral monomeric species, polymerised in the form of bulky islands, or as mono- or multi-layered structure. It also would be desirable to identify the structure of the deposited material as crystalline or amorphous and to determine the elemental composition and thickness of the deposited phase.

The repeatedly observed reduction of the pore mouth size (Section 1.4.4) clearly shows that the deposited silica phase is not isostructural to the zeolite. However, it has been reported that the higher the SiO_2 content of the zeolite, the more similar the basal plane and the deposited SiO_2 layer are [Hibino *et al.*, 1991a].

Direct observations to analyse the structure and composition of the silica deposited on the external surface of zeolites are difficult due to the small amounts deposited and the similarity of the deposited phase and the zeolite. To overcome that problem Hibino *et al.* [1989a] used germanium-methoxide as a model reagent in the CVD over H-Mordenite at 60°C. Since it can be distinguished between the deposited GeO_2 and the zeolite, it is possible to analyse composition and structure of the deposited GeO_2 with various spectroscopic techniques [Hibino *et al.*, 1989b]. Coordination numbers (number of next nearest neighbours) for Ge-O and Ge-Ge as determined by EXAFS spectroscopy showed that the structure of the deposited GeO_2 has a short-range order of GeO_4 units and is therefore different from α-quartz type GeO_2 with a long-range order. Structure types of GeO_2 with short-range order are amorphous GeO_2 and thin layers of GeO_2 [Hibino *et al.*, 1989b]. TEM measurements showed that germanium-methoxide is deposited not as particles but as an ultrathin GeO_2 layer which covers uniformly the external surface of Mordenite [Hibino *et al.*, 1989a]. These findings and the proposed reaction scheme

(Section 1.3.6) suggest that in the CVD of alkoxysilanes the final stabilised deposit also consists of tetrahedral SiO_4 units which are interlinked by siloxane bonds and / or terminated by silanol groups. The presence of silanol groups in the silica phase which was deposited onto the external surface of zeolite ZK5 by means of CVD at 350°C using TMOS as agent was indicated by IR spectroscopy measurements [Fetting and Dingerdissen, 1990].

Applying EXAFS, XPS and TEM measurements it could be shown that the deposited GeO_2 layer was transformed into bulky particles when the modified Mordenite was stored at humid conditions and subsequently treated at 500°C for 1 hour [Hibino *et al.*, 1989a]. The shape selectivity in cracking of octane isomers was enhanced when the catalyst was modified by deposition of an ultrathin, uniform GeO_2 layer and deteriorated when the deposited GeO_2 was transformed into bulky particles. This shows that the deposited GeO_2 needs to be uniform to enhance shape selectivity (Figure 1.6). Since the enhancement in shape selectivity by the deposition of TMOS is analogous [Hibino *et al.*, 1989b], it was suggested that the CVD of silicon alkoxides also yields a uniformly distributed ultrathin layer [Hibino *et al.*, 1989a]. According to the frequently observed enhancements of shape selectivity (Section 1.4.4.2), it seems that CVD of TMOS and TEOS generally yield homogeneous, ultrathin silica layers on the external surface of zeolites. Since it also appears that surface hydroxyl groups are more reactive than the methoxide and ethoxide group of a deposited alkoxide derivative (Section 1.3.6), the CVD of TMOS and TEOS should cover the external zeolite surface with a homogeneously distributed, deposited phase rather than forming silica pillars.

Assuming that silica is deposited as a uniform layer only on the external surface the surface concentration of silicon atoms can be calculated from the amount of deposited material and the external surface area of the zeolite. Niwa and co-workers [1989] assumed the site density to be the same as the cation site density of the zeolite (8.6 nm^{-2} for Mordenite [Barrer, 1978] and 8.9 nm^{-2} for ZSM-5 [Olson *et al.*, 1981]), and were thus able to obtain the theoretical number of silica layers by dividing the silicon concentration by the cation site density. The theoretical thickness of the deposited layers

was determined using an estimated thickness of SiO_2-monolayer of approximately 3Å.

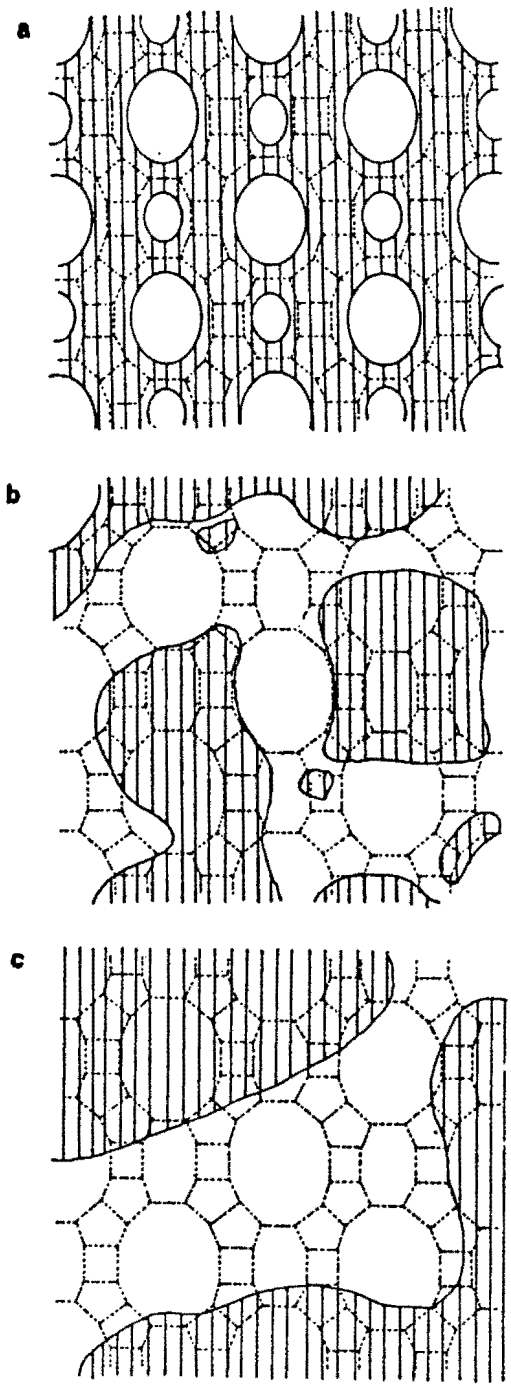

Figure 1.6: Schemes for the control of the pore mouth size by the deposited GeO_2: (a) ultrathin layer, (b) particles at an early stage of growing, and (c) particles fully grown. Shaded parts indicate the deposited GeO_2 [Hibino *et al.*, J. Phys. Chem. (1989a)]

Using TMOS, Niwa *et al.* [1986] and later Hibino *et al.* [1991] deposited between 2 and 14 silica layers on the external surface of HZSM-5. The theoretical thickness of the deposited phase would thus range from 6Å to 42Å. More detailed experiments with Mordenite showed that the concentration to saturate the external surface was independent of temperature from 0°C to 100°C and corresponded to single to double layers of silica [Niwa *et al.*, 1988]. The saturated surface concentration for a sylilated Mordenite sample corresponded only to half a layer. At high temperatures (320°C) the external surface approached saturation at higher surface concentrations [Niwa *et al.*, 1984]. The highest surface concentration corresponded to 6.9 silica layers. The thickness of the deposited layers ranged between 3Å and 21Å, which was in good agreement with XPS measurements where a thickness of the deposited layer between 4 and 8 Å was estimated [Murakami *et al.*, 1989].

SIMS measurements [Fetting and Dingerdissen, 1990] of the Si/Al-ratio depth profile of zeolite ZK5 modified by CVD of TMOS, showed that the Si/Al-ratio of the external surface increased with the degree of coating. The thickness of the silicon enriched layer for a sample with 8 wt% and an average crystal size of 1.5 μm, was found to be 100 to 150 Å. The thickness of this layer is one order of magnitude higher than the thicknesses reviewed above.

It seems that the CVD of tetra-alkoxysilanes results in ultrathin silica deposits. The form (tetrahedral monomers, mono- or multi-layered oxides) and the thickness of the deposited phase depends on the surface concentration which again can be controlled via the CVD conditions, i.e. mainly deposition time, temperature, and number of CVD-cycles.

1.4.1.3 Pore mouth size

Generally it has to be distinguished between CVD-agents which modify the internal surface and CVD-agents which modify the external surface only. CVD-agents which can enter the micropores reduce the pore diameter throughout the crystal interior [Vansant, 1990]. In contrast to that the CVD of tetra-alkoxysilanes is restricted to the external surface and only the size of the pore entrance is reduced. CVD of TMOS was proposed first by Niwa *et al.* [1982] as a method to tailor the pore mouth size of Mordenite. The introduction of this post synthesis modification method thus expands the range of pore sizes naturally available. The pore size can be controlled by adjusting the extent of deposition to achieve desired shape selective sorption or catalytic properties.

When ZSM-5 was modified by CVD of TMOS, the adsorption rate of o-xylene decreased gradually with increasing amount of silica deposited [Niwa *et al.*, 1986]. The ratio of the sorption rate constants $k_{p\text{-xylene}}$ to $k_{o\text{-xylene}}$ increased from 84 over the parent to 22340 over a modified ZSM-5 with 13.3 wt% silica deposited [Hibino *et al.*, 1991]. The estimated increase in the average crystal size from 0.250 μm to 0.258 μm due to deposited silica was considered to be too small to alter the diffusion rate of o-xylene by a factor of 1000. Since the micropore volume was shown to remain unaffected, it was concluded that the

pore mouth size is gradually reduced. Kim *et al.* [1996] suggested that the pore mouth size of ZSM-5 is reduced to a similar extent by silica deposited from any silicon compound.

In the same manner the CVD of TMOS was shown to reduce the pore mouth size of Mordenite using n-hexane, m- and p-xylene as adsorbates [Niwa et al, 1984, 1984a]. The pore mouth size was reported to decrease with increasing extent of deposition. Supported by cracking experiments of various paraffins it was proposed that the pore mouth size can be controlled to an accuracy of an angstrom with a uniform size of the pore mouth or at least a sharp distribution. The pore size is effectively reduced by ca. 0.1 and 0.2 nm upon formation of 1-2 and 3 molecular layers of silicon oxide, respectively. Later Niwa *et al.* [1986] stated that a thinner layer is required to narrow the pore entrance as compared to ZSM-5.

Itoh *et al.* [1989] deposited TEOS onto zeolite HY and evaluated the pore size by adsorption of hydrocarbons with different molecular sizes (i.e. hexane, 2,2-trimethyl-pentane, 1,3,5-TMB and 1,3,5-TiPB). They reported that the pore size was gradually reduced with increasing number of CVD procedures reaching 4.3Å after five cycles.

As discussed in Section 1.4.1.1 CVD carried out at non-flow conditions may lead to an inhomogeneous deposition throughout the catalyst bed and therefore to a non-uniform reduction of the pore mouth size.

Independent of the tetra-alkoxysilane and the zeolite used, sorption studies have repeatedly shown a reduction of the pore mouth size. A hypothesis for the relationship between the structure of deposited silica and the narrowing of the pore mouth has been derived from the following observation [Hibino *et al.*, 1993]. At equal amounts of deposited material, the pore mouth size of Mordenite was more readily reduced as the Si/Al ratio decreased [Hibino *et al.*, 1991a]. As shown earlier, silica is deposited on the external surface as a thin layer (Section 1.4.1.2) [Hibino *et al.*, 1989a]. The deposited silica layer is composed of siloxane bonds, whereas the zeolite is comprised of siloxane and Si-O-Al bonds.

Hibino *et al.* [1989a] suggested that this results in a difference in bond lengths and / or bond angles between silica layer and zeolite framework and concluded that this difference and thus the extent of pore mouth narrowing becomes larger as the Al content of the zeolite increases (Figure 1.7). The model suggests that terminal silanol groups of the silica layer protrude into the free section of the pore entrance, thus causing a reduction of the pore mouth size.

(1)

(2)

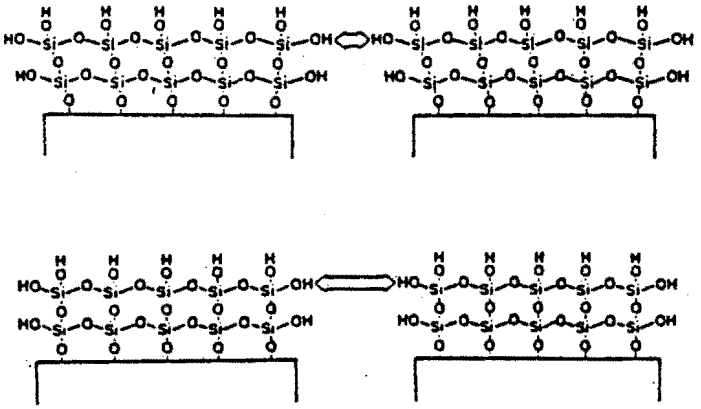

Figure 1.7: **Schematic illustration of narrowing the pore mouth size by silica layers on Mordenite. *Scheme 1:* low Si/Al ratio, *Scheme 2:* high Si/Al ratio**

1.4.1.4 Acidity / activity of the external surface

The CVD using $SiOCH_3(CH_3)_3$ [Mono], $Si(OCH_3)_2(CH_3)_2$ [Di], $Si(OCH_3)_3(CH_3)$ [Tri], $Si(OCH_3)_4$ [Tetra=TMOS] and $SiOCH_3(C_3H_7)_3$ [MTPS] at 320°C has been shown to inertise HZSM-5 in the conversion of 1,3,5-TiPB [Hibino *et al.*, 1991, 1993; Kim *et al.*, 1996]. This suggests that the inertisation of the external surface of zeolites takes place independently of the type of alkoxysilane.

Kim *et al.* [1996] reported that the amount of deposited silica required to fully inertise the external surface of ZSM-5 as measured by 1,3,5-TiPB cracking, was less for MTPS than for TMOS. The deposition of both alkoxides is restricted to the external surface. Since TMOS has four functional methoxide groups, it is easily polymerised into the siloxane

network structure. On the other hand, MTPS has only one methoxide; thereby it may be stabilised as an isolated species. Due to the attached alkyl groups, the anion property of the Si-O-species could be enhanced. To explain the more effective inertisation of the external surface when MTPS was used, Kim *et al.* [1996] suggested that MTPS may selectively be deposited on external acid sites, while TMOS is also deposited on non-acidic hydroxyl groups of the external surface [Hibino *et al.*, 1993].

Handreck and Smith [1990] reported a rapid drop of methylene blue adsorption capacity during the first 5 wt% of deposited material using the CVD technique as reported by Niwa *et al.*, 1986] followed by a slight decrease as the weight increase reached 17%. The adsorption capacity of the latter sample was 15 % of the original value for the parent. Previous studies [Handreck and Smith, 1988] have shown that adsorption of the cationic dye, methylene blue, from aqueous solution by ZSM-5 is sensitive to the aluminium content. Since the adsorption of the dye is restricted to the external surface of the zeolite crystals, its uptake has been used as a measure of the population of acid sites on the external surface. Optical microscope observations showed that the residual methylene blue adsorption capacity was restricted to 1 % of particles while the remainder were free of dye. No explanation is given why some particles escaped the modification by the silylation process.

On the other hand, four to five silica layers were required for the complete inertisation of the external surface of H-Mordenite and HZSM-5 using CVD of TMOS at 320° [Hibino *et al.*, 1993]. These findings indicate that the external surfaces of zeolites are not completely inertised by covering them fully with the silica monolayer. Niwa *et al.* [1990] reported that the silica deposited on alumina is not entirely inert but exhibits a weak acidity, where the isomerisation of 1-butene and the dehydration of tert-butyl alcohol occur. Thus, the following explanation for the above behaviour was offered: The silica attached to the acid site on the external surface possesses weak acidity. The acidity becomes weaker as the number of silica layers increases and is inert at a quadruple layer of silica [Hibino *et al.*, 1989a]. When Mordenite was modified by CVD of TMOS the Si/Al ratio did not influence the silicon concentration required for the inertisation of the

external surface [Hibino *et al.*, 1993].

1.4.2 Catalytic properties of silanised ZSM-5

Section 1.4.1 dealt with physicochemical properties and indicated that the CVD of tetra-alkoxysilanes generally covers the external surface of ZSM-5 crystals with a uniform, ultrathin, inert silica layer. This modification technique inertises the external surface and simultaneously reduces the pore mouth size with the accuracy of 1Å, while the micropore space remains in its original state. This section gives an overview of catalytic systems, where the ZSM-5 catalysts have been modified by CVD of TEOS. Of special interest is the effect of the CVD treatment on the catalyst performance and how this effect is related to the inertisation of the external surface and the reduction of the pore mouth size. Since the CVD method simultaneously reduces the pore mouth size and inertises the external surface, their effects on catalytic properties cannot be decoupled in a straightforward manner. It is emphasized that the significance of each effect depends very much on the catalytic system.

1.4.2.1 Activity

Both pore mouth narrowing and the inertisation of the external surface are expected to reduce catalytic activity. The extent to which either factor contributes to the loss of activity depends on the fraction of external surface area of the total surface area and on the degree to which the reaction takes place in the intracrystalline pore space, i.e. the pore effectiveness factor. While the former is a property of the catalyst the latter depends on the catalytic system.

Catalyst activity is reported to decrease with the amount of deposited silica. The activity loss in the cracking of 1,3,5-TiPB over ZSM-5 and Mordenite [Hibino *et al.*, 1993] is completely ascribed to the inertisation of the external surface, since the reactant is too large to enter the micropores. Whereas activity losses in reactions which easily take place

Table 1.5: Overview over catalytic reactions studied over ZSM-5 / MFI catalysts modified by CVD of TEOS

Reaction	Selectivity	Activity	Deactivation	Reference
n-Pentane aromatisation over MFI	enhanced selectivity to p-xylene	decreased	Cycle life of 3 months	Bhat *et al.*, 1995b
Toluene disproportionation	enhanced selectivity to p-xylene	-	-	Wang *et al.*, 1988
Toluene disproportionation	enhanced selectivity to p-xylene	decreased	-	Das *et al.*, 1994a
Ethylbenzene disproportionation	enhanced p-selectivity	decreased	-	Das *et al.*, 1993b
Alkylation of toluene with MeOH	enhanced selectivity to p-xylene	decreased	increased	Wang *et al.*, 1988 Bhat *et al.*, 1996a
Alkylation of toluene with EtOH	enhanced p-selectivity	decreased	-	Bhat *et al.*, 1996b
Alkylation of EB with EtOH	enhanced p-selectivity	decreased	-	Bhat *et al.*, 1994b
Alkylation of EB and toluene with ethylene	enhanced p-selectivity	decreased	Good regenerability	Wang *et al.*, 1988, 1989
m-Xylene conversion	-	decreased	-	Bhat *et al.*, 1994b

inside the micropores were mostly ascribed to pore mouth narrowing which retards the diffusion of reactant into, or products out of the zeolite channels. Examples are the activity losses observed in the methanol conversion [Niwa *et al.*, 1986], the disproportionation and alkylation of toluene and the conversion of o-xylene [Hibino *et al.*, 1991] when HZSM-5 was modified using TMOS. Table 1.5 lists examples when TEOS was used as CVD precursor. However, there is no reaction study to estimate the effect of the external surface inactivation on the activity. This is complicated by the fact that the area of the external surface depends on the crystallinity/morphology of the zeolite sample and is still a matter of debate (Section 1.3.3.1).

1.4.2.2 Selectivity

Since external acid sites were proposed to be responsible for non-shape-selective reactions [Gilson and Derouane, 1984], shape selectivity may not only be enhanced by the reduction of the pore mouth size, but also by the inertisation of the external surface. The diffusional resistance as introduced by the reduction of the pore mouth size may enhance reactant and / or product shape selectivity (Figure 1.7.a), but not restricted transition state shape selectivity.

P-xylene is a valuable compound because of its demand for production of polyester fibres via terephthalic acid and can be selectively formed over ZSM-5. Thus reactions such as xylene isomerisation, toluene alkylation and toluene disproportionation were mostly used to test the modified catalysts for improved shape selectivity. Table 1.5 gives an overview of reactions where the selectivity to the p-isomer could be enhanced by CVD of TEOS. The p-selectivity usually increased with silica loading.

Only a few studies shed light on the effect of external surface activity and pore mouth narrowing on shape selectivity. Kim *et al.* [1996] deposited various silicon-alkoxides onto HZSM-5 and showed that the inertisation of the external surface, as measured by 1,3,5-TiPB cracking, had only a minor effect on the para-selectivity in the methylation of toluene, while pore mouth narrowing, as measured by sorption studies, and increasing p-

selectivity were clearly correlated (Figure 1.8).

For several reactions there seems to be evidence that the inertisation of the external surface contributes to an enhanced shape selectivity. Wang *et al.* [1989] reported that poisoning of the external acid sites using β-naphthoquinoline enhanced p-selectivity in the alkylation of toluene with ethylene over HZSM-5. It was concluded that non-shape-selective reactions to other isomers are mainly catalysed on external surface sites of the zeolite crystal. This, however, implies the assumption that poisoning by β-naphthoquinoline causes no reduction of the pore mouth size. Using the same catalytic system, Cejka *et al.* [1995] observed enhanced formation of p-ethyltoluene after loading heteropolyacid (12-tungstosilicic acid) on the external surface of ZSM-5. The improved p-selectivity is shown to correlate qualitatively with the passivation of external active sites as shown by the decomposition of 1,3,5-TiPB.

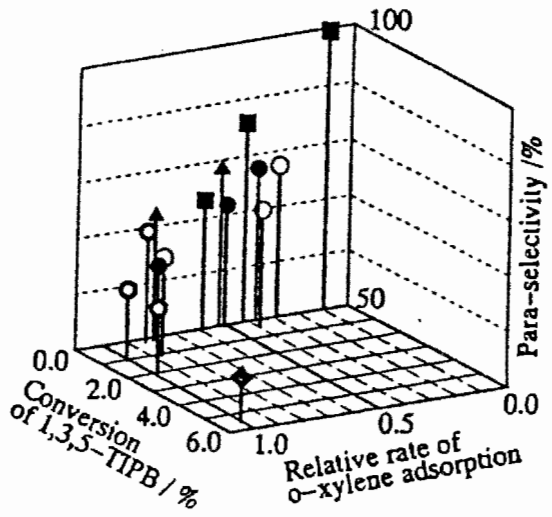

Figure 1.8: Effect of the modification with silica on the para-selectivity of ZSM-5 during the methylation of toluene [Kim *et al.*, 1996]

Kim *et al.* [1995] impregnated Mordenite with cerium. They reported an enhanced shape selective isopropylation of naphthalene to 2,6-DIPN and ascribed it to the selective deactivation of acid sites on the external surface since adsorption measurements indicated no reduction of the effective pore radius.

During the alkylation of methylnaphthalene over ZSM5 modified by CVD using TMOS the enhancement of the shape selectivity to beta-isomers of dimethylnaphthalenes (=sum of 2,3-, 2,6- and 2,7-dimethylnaphthalenes) was ascribed to the inertisation of the external surface as well as to the reduction of the pore mouth size [Niwa *et al.*, 1995].

The above examples have shown that the effect of pore mouth narrowing and inertisation of the external surface on shape selectivity clearly depend on the catalytic system and that both effects can be significant.

1.4.2.3 Lifetime

So far only a few studies have considered the effect of the CVD treatment using alkoxysilanes on lifetime. Niwa *et al.* [1986] reported that the CVD of TMOS had no significant effect on the deactivation rate during the conversion of methanol to hydrocarbons over HZSM-5. In contrast Sawa *et al.* [1990] showed that the deactivation rate increased rapidly with increasing amount of deposited silica when dealuminated H-Mordenite was used.

Hibino *et al.* [1991] observed deactivation in the alkylation of toluene with methanol when more than 11.1 wt% of silica were deposited onto ZSM-5 using TMOS as CVD agent. Below 8.44 wt% of deposited silica no deactivation was observed. Later Bhat *et al.* [1996a] observed an increased deactivation rate over a Ga-MFI-zeolite modified by CVD of TEOS. Cejka and co-workers [Wichterlova and Cejka, 1992; Mirth *et al.*, 1994] modified ZSM-5 by silylation in the liquid phase using a TEOS/n-hexane solution. In accordance with the effects of the CVD method on catalyst life, increased coking was found with surface silylated zeolites in the alkylation of toluene and ethylbenzene.

It is well known that coke leads to deactivation and is formed from heavy aromatics as coke precursors. It was suggested [Sawa *et al.*, 1990; Wichterlova and Cejka, 1992; Mirth *et al.*, 1994] that the reduced pore mouth size of silanised zeolites, retards the diffusion of heavy aromatics from the intracrystalline voids to the external surface. The accumulation of heavy aromatics in the micropore system may increase the rate of coke formation and therefore the deactivation rates as observed for ZSM-5 and Mordenite. However, the hypothesis that external surface acidity stimulates coke formation and that subsequent pore blocking significantly contributes to the deactivation of zeolites [Suzuki *et al.*, 1983] would predict an increase in life time when the external surface is inertised.

The observed decrease in lifetime over silanised zeolites is in contrast to that prediction, and therefore indicates that the reduction of pore mouth size dominates the effect on the deactivation behaviour. A positive effect of the inertisation of the external surface on the lifetime may thus be disguised by the negative effect of pore mouth narrowing. It is thus not possible to draw conclusions on the role of the external surface acidity in the deactivation behaviour of zeolites.

Despite the reduction of the pore mouth size it is possible to obtain long lifetimes. A cycle life of 3 months in the alkylation of ethylbenzene with ethanol over a CVD treated zeolite was shown by Bhat *et al.* [1994a]. How strongly the silanisation affects the deactivation rate depends on the zeolite, the reaction, the deposited amount of silica and the reaction temperature. High temperatures are feasible, since the deposited silica layer was reported to show a good durability and regenerability [Wang and Ay, 1988].

1.4.3 Summary

The CVD of an ultrathin silica layer on the external surface, using tetra-alkoxysilanes as silica source, proves to be a promising tool to adjust the shape selectivity of zeolites for a specific application as catalyst or adsorbent. This is achieved by the controlled reduction of the pore mouth size, which allows the design of zeolites with pore mouth sizes different from the naturally available pore sizes, and the simultaneous inertisation of the external surface. This approach of "precise pore mouth size control" has opened up a new area in zeolite post-synthesis modification research.

The gain in selectivity, however, is often accompanied by a loss in catalytic activity and in some cases a more rapid deactivation. The effect of pore mouth narrowing and the inertisation of the external surface on activity, selectivity and deactivation behaviour is specific for each catalytic system and depends on the specific external surface area, the kinetics of the reaction and the size of the micropores, reactants, transition states and products. These relationships are often not understood.

Altered shape selectivity, the reduction of the pore mouth size, inertisation of the external surface and the conservation of the intracrystalline pore space have been shown for ZSM-5 and Mordenite which were silanised by CVD of tetra-alkoxysilanes. It may be anticipated that any modified zeolite shows the same characteristic features provided the tetra-alkoxysilane has a larger diameter than the micropores of the respective zeolite. Several other zeolites such as Y, A, ZK5 and β have been studied with respect to the above mentioned aspects. This method also seems to work in a wide range of deposition conditions, methods and materials. So far no study to optimise the CVD method with respect to these parameters has been reported.

1.5 PROBE REACTIONS

Monitoring the deposition of a silica layer on the external surface of zeolites using physicochemical characterisation tools is difficult , since the silica layer may be ultrathin, the percentage of the external surface area very small and thus the silica concentrations to be detected very low [Vankelecom *et al.*, 1996]. Probe reactions test catalysts under catalytically relevant conditions and are the most direct and possibly more sensitive characterisation tool.

Generally it is possible to distinguish between probe (model) reactions which are suited to monitor catalytic properties, viz. activity, selectivity and lifetime, and probe reactions where physicochemical properties could be related to activity or selectivity. Reactions which are used to test catalytic properties have ideally a commercial background and may employ a model reactant which represents a complicated feed mixture of an industrial process. For reactions which are used to probe physicochemical properties it is desirable that catalyst deactivation is absent or very slow, and that their mechanism is well understood, so that effects on activity or selectivity can be quantified.

The probe reactions discussed here, were chosen considering the relevant properties which are expected to be affected by post-synthesis modifications of the external zeolite surface, which are the number of acid sites (n-hexane cracking), the activity of the external surface (1,3,5-TiPB cracking) and shape selective effects (toluene disproportionation).

Comparing the effects of the external surface modifications on the overall activity for the mentioned reactions will enhance the understanding of the catalytic role of the external acid sites.

1.5.1 N-hexane cracking

Hexane cracking is a popular test reaction where the catalytic activity of an acid catalyst can be evaluated as a measure of the number (concentration, Figure 1.9) and strength of

acid sites [Olson *et al.*, 1980; Haag *et al.*, 1984, 1990]. The reaction is also useful to measure relative activities of cracking catalysts in the so called α-test [Weisz and Miale, 1965, 1966]. Over HZSM-5 and at α-conditions, viz. high temperatures, such as 538°C, and at low partial pressure, the reaction follows simple first order kinetics and catalyst deactivation is eliminated [Haag *et al.*, 1990]. It has been found that even for ZSM-5, of high activity, diffusion limitations are negligible for crystal sizes smaller than 40 μm even at this relatively high temperature [Haag *et al.*, 1981; Post *et al.*, 1983; Voogd and Van Bekkum, 1990]. Thus hexane cracking represents a reaction which fully utilises the intracrystalline pore space and the rate constant provides a direct measure of the intrinsic acid activity of ZSM-5.

The classical mechanism [Thomas, 1949; Greensfelder *et al.*, 1949; Voge, 1958; Pines, 1981] occurs according to a carbenium ion chain reaction, illustrated with n-hexane as a feed:

$$\text{C-C-C-C-C-C} + \text{C-C-C}^{+} \xrightarrow{\text{HT}} \text{C-C-C-C-C-C}^{+} + \text{C-C-C} \qquad (1)$$

$$\text{C-C-C-C-C-C}^{+} \rightarrow\rightarrow \text{C-C(C)-C-C-C}^{+} \xrightarrow{\beta\text{-scission}} \text{C-C-C} + \text{C=C-C}^{+} \qquad (2)$$

Since hexene, which involves the same intermediate hexyl cation, cracks about 260 time faster than hexane [Haag *et al.*, 1981], step (2) is very rapid, and the rate determining step is the hydrogen transfer reaction (1). For this reason the cracking pathway is referred to as bimolecular cracking. The origin of the first chain initiating carbenium ion in step (1) has not been clearly been identified so far. While olefins can undergo facile secondary reactions, the saturated products are relatively unreactive and are diagnostically significant; they consist predominantly of propane and butanes rich in isobutane, independent of the structure of the feed paraffin. The conditions where the bimolecular mechanism predominates are low temperatures and high olefin concentration, i.e. high conversions.

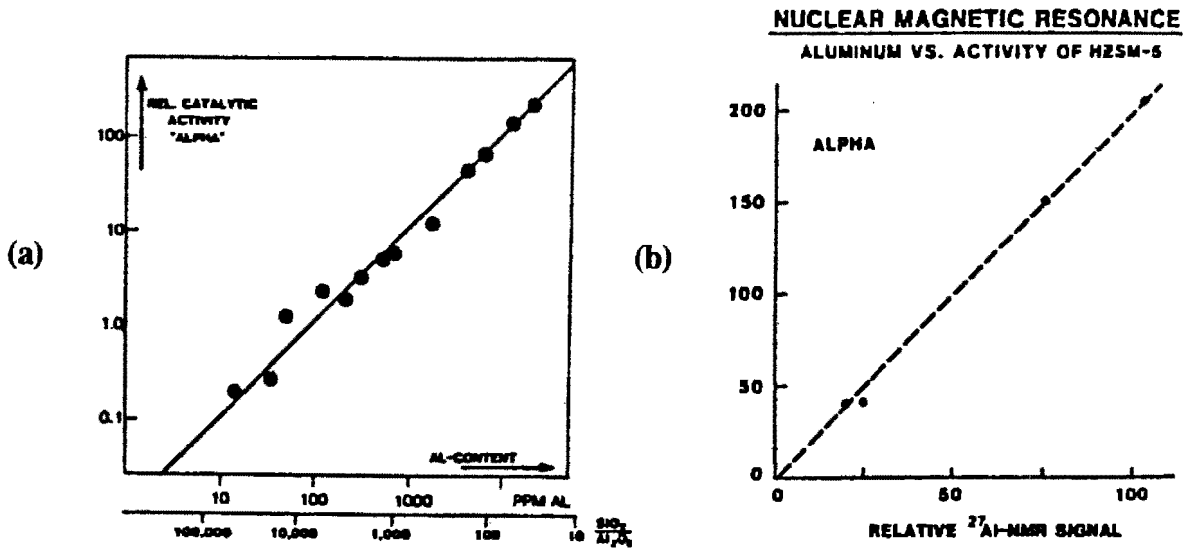

Figure 1.9: **a) Correlation of hexane cracking activity α with total aluminium content of HZSM-5; Slope = 1 indicates linear relationship [Haag, 1984]**
b) Hexane cracking activity α is proportional to tetrahedral aluminium content (by NMR) in HZSM-5 [Haag, 1984]

At high temperature, low partial pressure and low conversion, acid catalysed cracking of simple paraffins does not occur by the classical bimolecular carbenium chain reaction, but by protonation of the paraffins to produce penta-coordinated carbonium ions with the solid catalyst acting as a superacid (Figure 1.10) [Haag and Dessau, 1984a]. The protonated paraffin can be envisioned as a mixture of sigma-protonated species containing three-centre two-electron bonds that can be conveniently represented as a penta-coordinated carbonium ion [Olah, 1972, 1974]. Products are formed by the collapse of the latter (Figure 1.10). Since the rate determining step involves the interaction of a single paraffin molecule with the active site, cracking via this reaction path is called monomolecular cracking. The nature of saturated products varies greatly with the feed. For n-hexane cracking over ZSM-5 at 538°C the observed saturated products (methane, ethane, propane, n-butane and little iso-butane) were shown to be formed in strictly parallel reactions. Noteworthy is the formation of hydrogen.

Conditions where the reaction is limited to either the monomolecular or the bimolecular reaction path can be realised to a good approximation. In these regimes the kinetics of both reaction paths follow a first order rate law, although with very different activation

energies (approximately 125kJ/mol for the monomolecular mechanism and 25kJ/mol for the bimolecular mechanism). In the intermediate regime, where both mechanisms contribute, the kinetics are quite complex [Haag *et al.*, 1990].

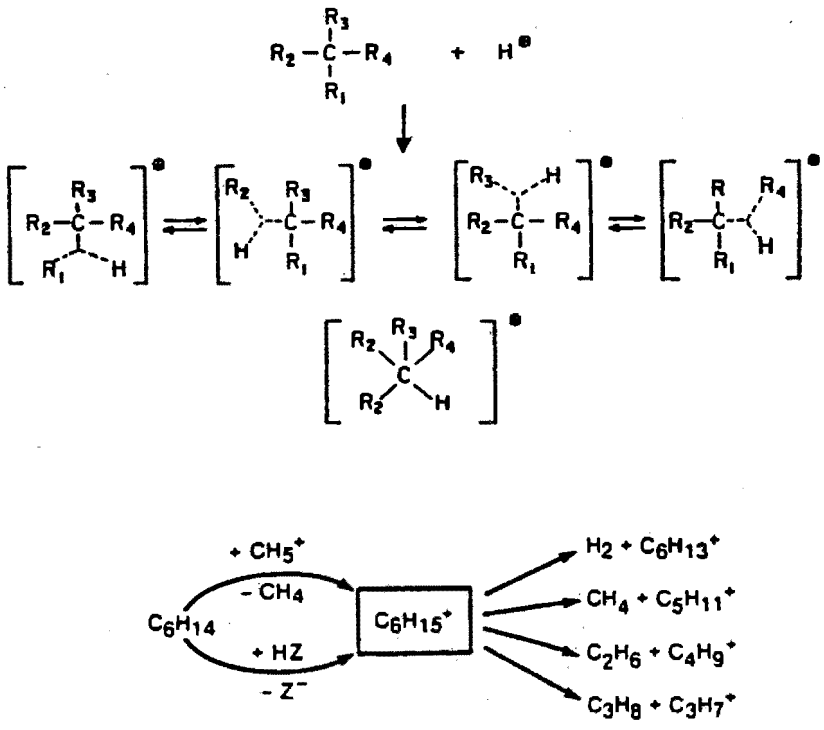

Figure 1.10: Monomolecular cracking mechanism [Haag *et al.*, 1990, p. 256]

1.5.2 Toluene disproportionation

The primary products in the disproportionation of toluene are mainly benzene, p-, m- and o-xylene. Only small amounts of methane, ethane, ethene, propane, ethylbenzene and trimethylbenzene were observed as by-products over HZSM-5 [Kaeding *et al.*, 1981; Uguina *et al.*, 1993]. P-xylene is a valuable compound because of its demand for production of polyester fibres via terephthalic acid. Shape selective formation of p-xylene minimises post-reaction separation costs and is thus of great commercial interest.

Below 1% toluene conversion the fraction of p-xylene in total xylenes increases with

decreasing conversion over ZSM-5 [Hibino *et al.*, 1991]. For conversions higher than 1% and crystal sizes up to 7.5μm only near equilibrium mixtures of xylene isomers (T=527-600°C; roughly 23% o-xylene, 53% m-xylene, 24% p-xylene) have been observed [Kaeding *et al.*, 1981; Beltrame *et al.*, 1985; Hibino *et al.*, 1991]. The selectivity to p-xylene in the disproportionation of toluene over ZSM-5, however, could be enhanced by post-synthesis modification [Kaeding *et al.*, 1981] such as CVD of TMOS [Hibino *et al.*, 1991] or TEOS [Wang *et al.*, 1989; Das *et al.*, 1994a]. Since activity losses caused by CVD treatment are small, compared to e.g. o-xylene isomerisation [Hibino *et al.*, 1991], the disproportionation of toluene is a convenient test reaction to monitor shape selective properties without difficulties to keep the conversion constant.

The model in Figure 1.11 is used to illustrate the relation between p-selectivity in the disproportionation of toluene and structural effects. The effect of the modifier agent on p-selectivity was initially explained by an increase in the diffusional constraints. Thus p-xylene is separated from o- and m-xylene while travelling through the channels to the crystal surface due to their difference in diffusivities ($D_{o\text{-}xyl/ZSM\text{-}5}=10^{-10}cm^2/s$, $D_{p\text{-}xyl,\ ZSM\text{-}5} \geq 10^{-7}cm^2/s$ at T=350°C [Haag, 1984]) yielding a product with a high proportion of p-xylene at low space times [Kaeding *et al.*, 1981]. The observed decline in p-selectivity with space time (Figure 1.12) was explained by subsequent isomerisation of the primary

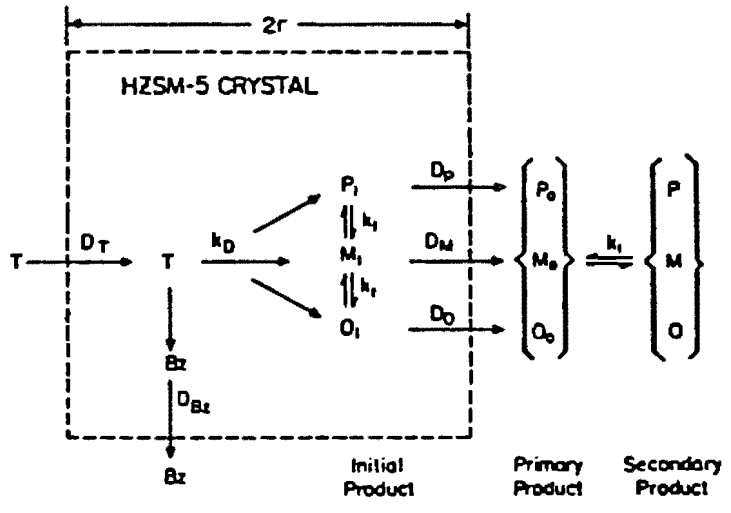

Figure 1.11: Model for selective toluene disproportionation [Haag and Chen, 1987]

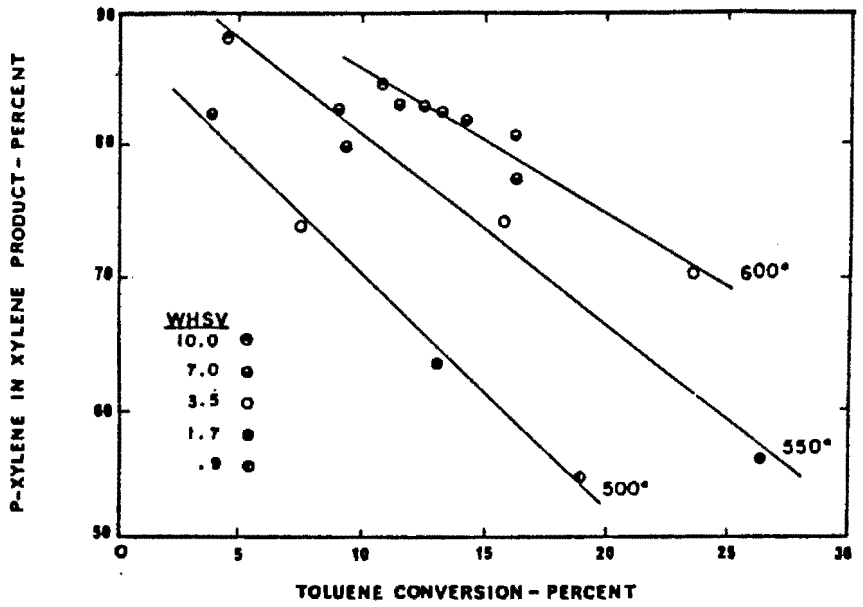

Figure 1.12: Toluene disproportionation over ZSM-5 modified with magnesium oxide (Mg=11wt%) [Kaeding *et al.*, 1981]

product by re-entry into the micropore structure. This approach appears to be complemented by a mathematical theory which has shown a good fit with experimental data [Wei, 1982].

The other approach simply states that p-selective events (restricted transition state shape selectivity or product shape selectivity) occur inside the zeolite channels while catalytic sites on the external surface are responsible for non-para-selective transformations [Derouane, 1980; Fraenkel, 1984; Nayak and Riekert, 1986]. Thus the high p-selectivity of modified samples may also be related to the inertisation of the external surface. In the case of toluene disproportionation over ZSM-5, Olson and Haag [1984] have reported that the ratio between the intrinsic rate constants of the secondary xylene isomerisation and the main reaction is approximately 7000. Then the rate of both reactions is comparable, even if xylene isomerisation as secondary reaction takes place only on external acid sites. This shows that the catalytic effect of the external acid sites has to be taken into account despite of their low percentage. Uguina *et al.* [1993] have developed a kinetic model for toluene disproportionation over unmodified and modified ZSM-5, which includes the effects of

the diffusional limitations, of external acid sites and the reversibility of the reaction.

Hibino *et al.* [1991] modified ZSM-5 by CVD of TMOS and found that the increase in p-selectivity was rather related to a reduction of the pore mouth size than to the inertisation of non-shape-selective acid sites on the external surface. The estimated increase in the average crystal size from 0.250 μm to 0.258 μm due to deposited silica was considered to be too small to alter diffusion rates and thus shape selectivity. This conclusion is supported by Yashima *et al.* [1981], who found that high p-selectivity is not achieved only by poisoning selectively the external surface with 2,4-dimethylquinoline. In contrast Beltrame *et al.* [1985] reported an increased selectivity to p-xylene at low toluene conversion when the external surface was poisoned by 4-methylquinoline. At high toluene conversions, however, the external surface activity may play a role.

The mechanism of toluene disproportionation over modified and unmodified ZSM-5 zeolites and even the terminology is still a matter of disagreement. Three different mechanisms have been proposed to account for this reaction [Poutsma, 1976; Gnep and Guisnet, 1981; Kaeding *et al.*, 1981; Dooley *et al.*, 1990; Fraenkel, 1990], which may be termed as dissociative, alkyl transfer and diphenylalkane mechanisms (Figure 1.13).

The dissociative mechanism consists of a dealkylation followed by an alkylation step. This mechanism may occur at high temperatures since the intermediate methyl carbenium cation is well known to be highly unstable and thus requires a high activation energy.

The alkyl transfer and the diphenylalkane mechanism are bimolecular and both involve a biphenylic transition state. In the alkyl transfer mechanism the proton attacks the aromatic ring attracted by the dislocated electron cloud, thus generating a pentavalent, adsorbed carbonium ion. For the alkyl transfer a second toluene molecule has to be close enough to contact the primary carbonium ion, thus creating the diphenyl-methane-type carbonium ion as transition state as proposed by Csicsery [1970, 1971]. This transition state decomposes into benzene, xylene and a proton.

(M1)

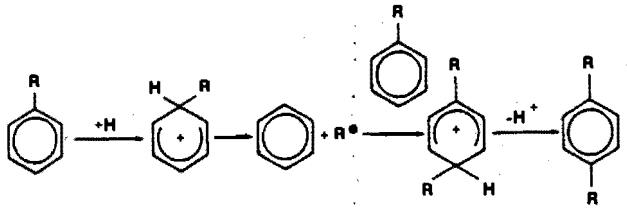

(M2)

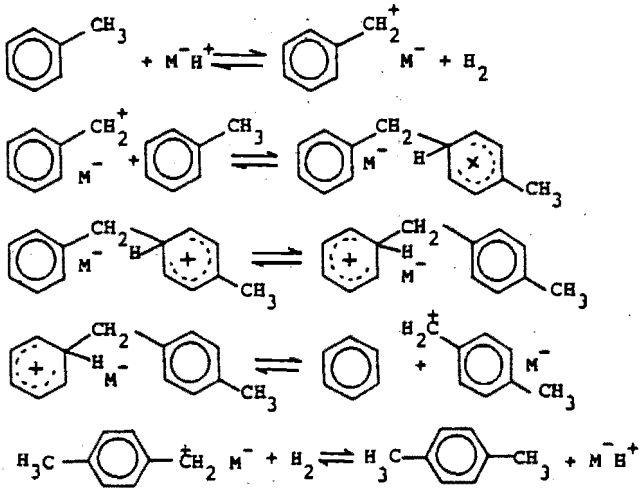

(M3)

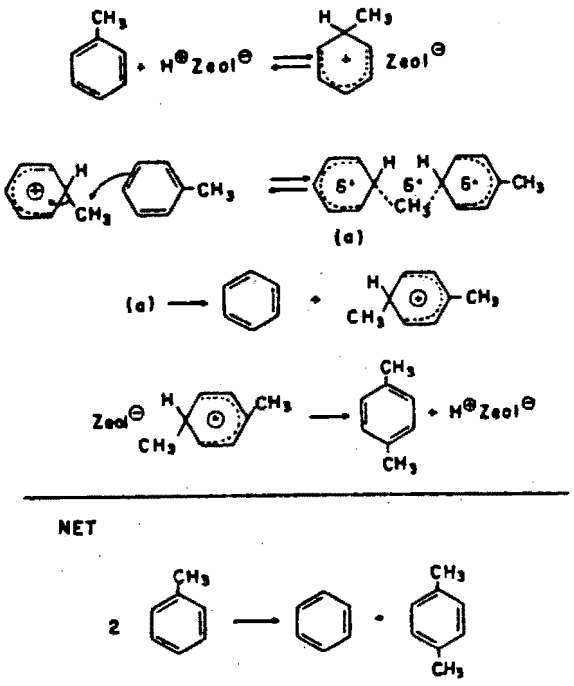

Figure 1.13: **Mechanism of toluene disproportionation over zeolites: (M1) dissociative [Santilli, 1986], (M2) diphenylalkane [Gnep and Guisnet, 1981] and (M3) alkyl transfer mechanisms [Kaeding, 1981]**

In the diphenylalkane mechanism the methyl group releases a hydride anion to form hydrogen and a tri-valent carbenium ion which is stabilised by dislocation of the aromatic electron cloud. The existence of this carbocation has been clearly demonstrated in a superacid medium [Hogeveen, 1969, 1970]. The decomposition of the diphenylmethane transition state requires a hydrogen shift reaction as well as the dissociation of molecular hydrogen and seems to be mechanistically more complicated than the two other mechanisms. The inhibiting effect of hydrogen on the disproportionation of toluene, however, can be explained quite well with this mechanism. If the first step in which toluene adsorbs as carbocation onto an acid site is at equilibrium, the presence of hydrogen decreases the concentration of carbocations and thus the rate of further reactions [Gnep and Guisnet, 1981].

Likewise the kinetics over unmodified ZSM-5 are not univocally clarified. While Nayak and Riekert [1986] found a first order dependence of the reaction rate on the toluene partial pressure, Dooley *et al.* [1990] collected data from different authors and zeolites, and concluded that most of the results can be adequately described by a second order rate expression.

1.5.3 The conversion of 1,3,5-triisopropylbenzene

Sorption experiments have shown that 1,3,5-triisopropylbenzene (1,3,5-TiPB), with a kinetic diameter of 8.5 Å, does not enter the micropore system of both ZSM-5, Mordenite [Hibino *et al.*, 1993] and NaY [Kim *et al.*, 1993]. Hence reactions of 1,3,5-TiPB are restricted to the external surface of the zeolite crystal. Consequently the rate of 1,3,5-TiPB conversion is a direct measure of the external surface activity and acidity as suggested by Namba *et al.* [1986]. No detailed studies of this reaction have been found. However, the most important reactions of 1,3,5-TiPB should be dealkylation and isomerisation [Kim *et al.*, 1993].

1.6 THE TRANSFORMATION OF 1,2,4-TRIMETHYLBENZENE

The use of reactant- and product-alkylaromatics to probe the effective pore width of molecular sieves has been extensively reviewed [Weitkamp and Ernst, 1994] suggesting that the exploration of reactions, which involve these molecules, might yield new powerful characterisation tools. Apart from the commercial production of 1,2,4,5-tetramethylbenzene (1,2,4,5-TeMB) the transformation of 1,2,4-trimethylbenzene (1,2,4-TMB) has scarcely been studied with respect to its application as a probe reaction. The reaction may involve products and transition states which are critically sized for the channels of ZSM-5. Their potential to probe various catalyst properties needs to be explored.

Reactions of 1,2,4-TMB appear to be highly inhibited inside the micropore system of ZSM-5 due to the critical dimensions of the reactant, transition states and products. Thus the transformation of 1,2,4-TMB is more likely to occur mainly at acid sites near or on the external surface of the zeolite crystal and is expected to be very sensitive to effects of external surface modifications on particular properties of ZSM-5, such as the external surface activity, pore mouth size, shape selectivity and lifetime.

1.6.1 Products and reactions

Over acid catalysts the reactions of 1,2,4-TMB are generally isomerisation, disproportionation and dealkylation [Kikuchi *et al.*, 1984; Beltrame *et al.*, 1985; Chao and Leu, 1989; Ko and Kuo, 1994]. Products observed at 300°C over zeolite HY where mainly xylene, 1,2,3-TMB, 1,3,5-TMB and TeMBs and small amounts of methane, ethane, ethene, propane, propene, iso-butane, n-butane, iso-pentane, n-pentane, benzene and toluene [Ko and Kuo, 1994]. Das *et al.* [1994b] observed small amounts of ethyltoluene over zeolite β. Over ZSM-5 at 350°C mainly toluene, xylenes with smaller amounts of benzene, 1,2,3-TMB and C_{10} hydrocarbons but no ethyltoluene were observed [Beltrame *et al.*, 1985]. The product composition of the disproportionation and isomerisation equilibrium for a TMB feed is shown in Table 1.6.

Table 1.6: Trimethylbenzene disproportionation equilibrium[a] in mol-% [Stull *et al.*, 1969, p.164]

T (°C)	227	327	427	527
Benzene	0.3	0.4	0.5	0.6
Toluene	4.5	5.2	5.4	5.6
o-Xylene	4.9	5.5	5.9	6.3
m-Xylene	13.4	13.6	13.2	13.2
p-Xylene	5.8	6.0	6.0	5.9
1,2,3-Trimethylbenzene	2.5	2.9	3.4	3.6
1,2,4-Trimethylbenzene	26.9	25.5	24.2	23.2
1,3,5-Trimethylbenzene	10.7	9.2	8.1	7.4
1,2,3,4-Tetramethylbenzene	3.7	4.3	5.1	5.5
1,2,3,5-Tetramethylbenzene	14.4	14.3	14.8	14.8
1,2,4,5-Tetramethylbenzene	9.9	9.7	9.3	9.4
Pentamethylbenzene	3.0	3.4	4.1	4.4
Hexamethylbenzene	0.0	0.0	0.0	0.1

[a] assuming ideal gas state

Ko and Kuo [1994] studied the reaction network of 1,2,4-TMB over zeolite HY between 200°C and 300°C (Figure 1.14) and found the xylenes, 1,2,3-TMB, 1,3,5-TMB and the TeMB isomers to be primary products. The primary reactions are isomerisation, leading to the parallel formation of 1,2,3-TMB and 1,3,5-TMB and disproportionation yielding all isomers of xylene and tetramethylbenzene while dealkylation was considered negligible at these conditions. Toluene and pentamethylbenzene were reported to be secondary products which form via disproportionation of xylene and TeMB respectively.

The primary products (xylenes, TMBs and TeMBs) were suggested to be consumed but also formed in secondary reactions such as disproportionation and transalkylation. The role of secondary isomerisation reactions, however, was only discussed for the TMB fraction. Based on reaction data which showed that 1,2,3-TMB isomerized consecutively into 1,2,4-TMB and 1,3,5-TMB it was found that the direct secondary isomerisation of 1,2,3-TMB to 1,3,5-TMB is negligibly slow. These findings are consistent with the work

of Collins *et al.* [1986] who used zeolite LaY at 350°C. They reported the relative rate constants for the isomerization between 1,2,3-TMB and 1,3,5-TMB to be an order of magnitude smaller than the rate constants for the isomerization between 1,2,4-TMB and 1,2,3-TMB or 1,2,4-TMB and 1,3,5-TMB indicating that the isomerisation mechanism occurs via 1,2-methylshifts.

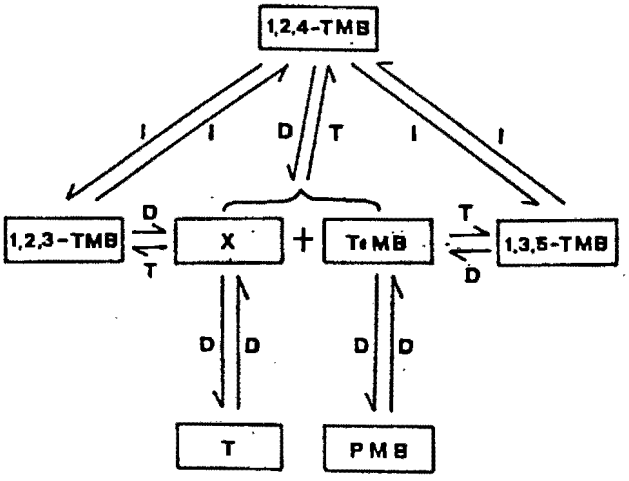

Figure 1.14: The reaction network of 1,2,4-TMB over HY zeolite. D, Disproportionation; I, Isomerisation; T, Transalkylation [Ko and Kuo, 1994]

While isomerisation and disproportionation of 1,2,4-TMB were reported as the main reactions over acid catalysts, dealkylation was often considered negligible. Alkyl-substituted aromatics, however, may undergo thermal and catalytic dealkylation [Pines *et al.*, 1953; 1955]. Dealkylation is facilitated by the crowding of the alkyl groups and high temperatures. Relief of strain depends also on the position of the alkyl groups in polyalkylbenzenes. When dealkylation of such compounds is thermally induced, some ring cleavage occurs. Dealkylation was reported to be the main reaction when 1,2,4-TMB was converted over ZSM-5 in hydrogen at 350°C [Beltrame *et al.*, 1985]. Demethylation was evidenced by the sum of side-chain carbons in the product falling short the theoretical value. They did not, however, report a direct observation of methane.

The conversion of 1,2,4-TMB is generally accompanied by fast deactivation of the acid catalyst due to coke formation [Ahn and Hakze, 1981; Cartraud *et al.*, 1986; Collins *et al.*, 1986; Bourdillon *et al.*, 1990; Ko and Kuo, 1994, Matsuda *et al.*, 1995]. It was found for zeolite Y that the ratio of disproportionation to isomerisation was not affected by catalyst regeneration or deactivation [Collins *et al.*, 1986].

1.6.2 Reaction mechanisms

The transalkylation of methylaromatics in sufficiently spacious pores is nowadays envisaged to proceed via carbocations with a diphenylmethane backbone [Weitkamp and Ernst, 1994] as discussed for the disproportionation of toluene (Section 1.5.2). The diphenyl-methane-type transition states for the alkyltransfer and the diphenylalkane mechanism in the disproportionation of 1,2,4-TMB have been formulated by Kikuchi *et al.* [1984] and Guisnet and co-workers [Cartraud *et al.*, 1986] respectively. The possible transition states as shown in Figure 1.15 apply to the alkyltransfer mechanism. The geometry of the transition states occurring in the diphenylalkane mechanism is more or less the same.

From the selective formation of o-xylene and 1,2,4,5-TeMB it was concluded that the disproportionation of 1,2,4-TMB follows one of these bimolecular mechanisms over alumina pillared montmorillonite [Kikuchi *et al.*, 1984; Ko and Chang, 1992], zeolite HY [Ko and Kuo, 1994] and mordenite [Cartraud *et al.*, 1986]. In zeolites, where the micropore system is incapable of accommodating large diphenylmethane transition states (possibly medium pore zeolites) bimolecular reactions are highly inhibited. At high reaction temperatures the disproportionation of 1,2,4-TMB may then rather follow the monomolecular dissociative mechanism as has been shown for example for the disproportionation of ethylbenzene [Amelse, 1988]. Otherwise the disproportionation may be restricted to the external crystal surface.

The isomerisation mechanism of methylbenzenes was primarily studied for the conversion of xylenes. The proposed mechanisms may, however, also apply to the isomerisation of TMBs. Csicsery [1969], Lanelwala *et al.* [1969] and later Corma and Sastre [1991] showed that the isomerisation of dialkylbenzenes proceeds via a monomolecular and a bimolecular pathway over zeolite Y. The bimolecular pathway, or intermolecular isomerisation, is nothing other than a consecutive disproportionation-transalkylation reaction, viz. a secondary reaction of the disproportionation product with the reactant. This reaction path occurs obviously via a disproportionation mechanism. At high

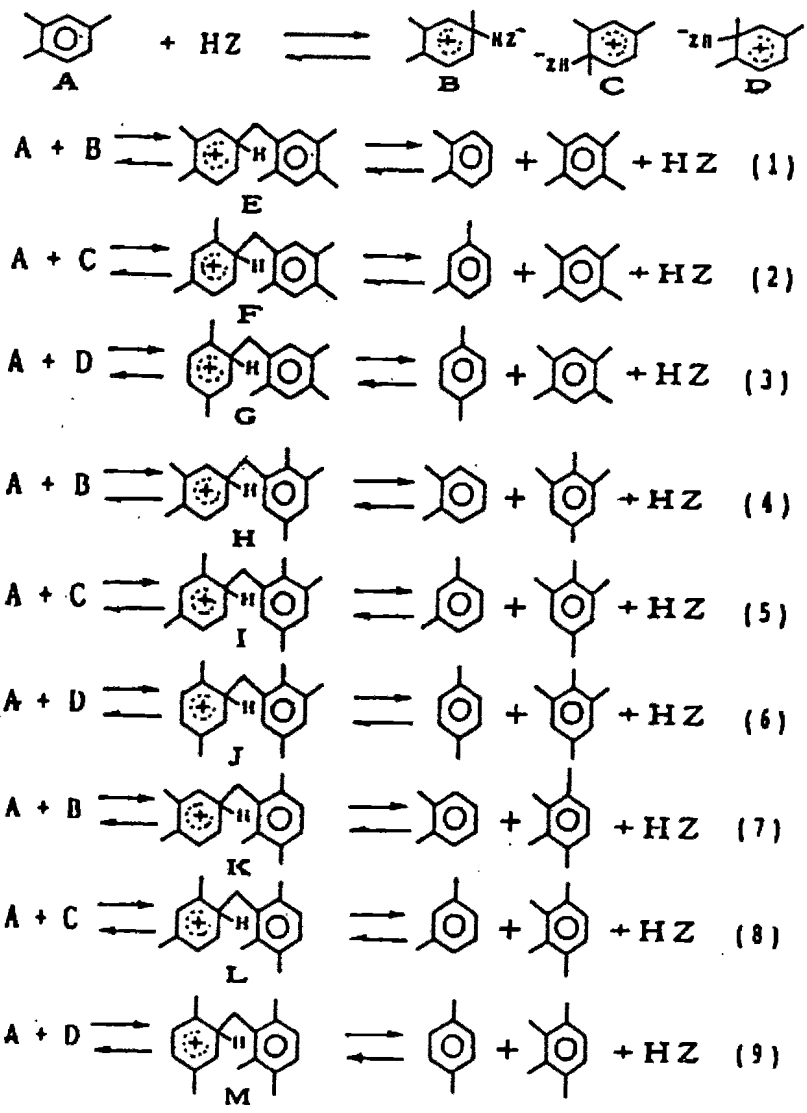

Figure 1.15: Transition states in the diphenylalkane disproportionation mechanism of 1,2,4-TMB [Kikuchi *et al.*, 1984; Ko and Kuo, 1994]

temperatures and over zeolites with narrower pores, such as Mordenite and ZSM-5, the contribution of the spatially more demanding bimolecular mechanism is significantly lower or zero [Corma and Sastre, 1991].

The monomolecular mechanism, as illustrated for the isomerisation of m- to o-xylene in Figure 1.16, occurs via an intramolecular 1,2-shift of the methyl group as the rate limiting step [Poutsma, 1976]. Initially a xylene molecule is adsorbed on an acid site to give the

corresponding, intermediate carbonium (benzenium) ions. The next step is the transformation of such a protonated species to an activated transition state. According to Corma *et al.* [1979], the activated transition state is a bicyclo-hexenyl complex, the formation of which proceeds in a concerted fashion with a high energetic barrier and is considered to be the rate determining step. Once the bicyclic complex is attained, the next step will be the methyl group migration which should have a lower activation energy (Figure 1.16.b), and then transformation into the corresponding isomers accompanied by the release of a proton. Selectivity plots clearly showed that the isomerisation of 1,2,4-TMB over zeolite Y at 350°C is dominated by the 1,2-methyl shift mechanism [Collins *et al.*, 1986].

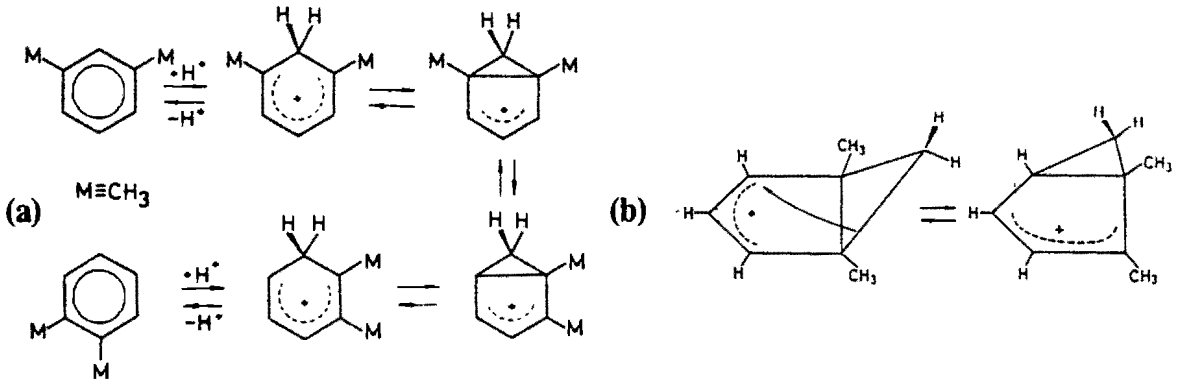

Figure 1.16: **(a) Monomolecular mechanism for the reversible isomerisation of *m*- to o-xylenes on acid catalysts;**
(b) Transition state: Isomerisation of the bicyclic hexenyl species [Corma *et al.* 1979]

1.6.3 Kinetics

The isomerisation and disproportionation of 1,2,4-TMB over Al-montmorillonite at 200°C were found to obey first and second order kinetics respectively [Kikuchi *et al.*, 1984]. However, no kinetic studies exist for the transformation of 1,2,4-TMB over ZSM-5.

1.6.4 Effect of the zeolite pore structure

The transformation of 1,2,4-TMB was studied over zeolite HY [Ahn and Hakze, 1981; Gnep *et al.*, 1982; Bourdillon *et al.*, 1990; Wang *et al.*, 1990; Ko and Kuo, 1994], β [Wang *et al.*, 1990; Das *et al.*, 1994b], H-Mordenite [Gnep *et al.*, 1982; Cartraud *et al.*, 1986] and ZSM-5 [Gnep *et al.*, 1982; Beltrame *et al.*, 1985]. The disproportionation to isomerization ratio of 1,2,4-TMB is sensitive to the pore structure [Gnep *et al.*, 1982]. For zeolite Y, Mordenite and ZSM-5, ratios of 1.3, 0.5 [Gnep *et al.*, 1982] and 0.1 [Beltrame *et al.*, 1985] respectively were reported. This ratio may, however, also depend on the reaction conditions, crystal size and the Si/Al ratio.

Over zeolite Y [Collins *et al.*, 1986; Bourdillon *et al.*, 1990; Ko and Kuo, 1994] and Mordenite [Ahn and Hakze, 1981] the disproportionation of 1,2,4-TMB led approximately to equimolar amounts of xylene and TeMB. The xylenes were only slightly favoured. This indicates that dealkylation and secondary transalkylation reactions are negligible at these conditions. Whereas over ZSM-5, where demethylation was evidenced by the sum of side-chain carbons in the product falling short the theoretical value, the ratio of xylenes to TeMBs was greater than one [Beltrame *et al.*, 1985].

The composition of the xylene and TeMB fraction was not at equilibrium; in particular o-, m-xylene and 1,2,4,5-TeMB were favoured over Mordenite [Ahn and Hakze, 1981; Gnep *et al.*, 1982; Cartraud *et al.*, 1986] and zeolite β [Wang *et al.*, 1990]. Bourdillon *et al.* [1990], Wang *et al.* [1990] and Matsuda *et al.* [1995] reported 1,2,4,5-TeMB, whereas Gnep *et al.* [1982] reported 1,2,3,5-TeMB to form with the highest selectivity amongst the TeMB isomers over zeolite HY. For ZSM-5 the TeMB distribution was not analysed while the xylene composition was at equilibrium [Beltrame *et al.*, 1985].

During the isomerisation of 1,2,4-TMB over LaY, 1,3,5-TMB was slightly favoured against 1,2,3-TMB [Collins *et al.*, 1986]. Gnep *et al.* [1982] reported 1,2,3-TMB to 1,3,5-TMB ratios of 0.4 and 1.0 for zeolite HY and H-Mordenite respectively.

1.6.5 1,2,4-TMB conversion over ZSM-5

Gnep *et al.* [1982] reported that 1,2,4-TMB was not converted over ZSM-5 at 350°C and a WHSV of 0.1 h^{-1} in a hydrogen atmosphere. It was suggested that 1,2,4-TMB is too bulky to access the active sites inside the ZSM-5 micropores or alternatively the reaction products are too bulky to leave the micropore system. Unfortunately neither crystal size nor the Si/Al ratio was given. In contrast, Beltrame *et al.* [1985] reported that 1,2,4-TMB dealkylates and to a smaller extent isomerises and disproportionates over ZSM-5 of 4μm crystal size, a Si/Al ratio of approximately 30, at 350°C in hydrogen.

Poisoning of the external surface of ZSM-5 with 4-methylquinoline enhanced the proportion of p-xylene in the xylene fraction from 28% to 39%. At the same time the isomerisation was completely suppressed while the disproportionation activity was only reduced to half and demethylation activity to a third of the original values. This indicates that the latter reactions partially take place in the ZSM-5 channels, whereas the isomerisation is restricted to the external surface [Beltrame *et al.*, 1985].

The transformation of m-xylene, the alkykation of 1,2,4-TMB with methanol and transalkylation reactions between TMBs and toluene over ZSM-5 may show similar features as the transformation of 1,2,4-TMB. The transfer of certain analogies of these reactions to understand the limiting factors in the transformation of 1,2,4-TMB will thus be discussed in the following sections. Reactant or product diffusion or the formation of transition states may limit or even completely inhibit reactions of 1,2,4-TMB inside the ZSM-5 channels.

1.6.6 Reactant diffusion

1,2,4-TMB and m-xylene have the same kinetic diameter as well as activation energy for diffusion in Na-ZSM-5 [Gorring, 1973]. 1,2,4-TMB should thus be able to enter the channels of ZSM-5 and penetrate the intracrystalline pore space when used as reactant. If the diffusion of 1,2,4-TMB is the rate determining step, the proportion with which

1,2,4-TMB is converted on the external surface depends on the ratio of the intrinsic rate of consumption to the rate of intracrystalline diffusion. The conversion of 1,2,4-TMB would thus be restricted to the external surface to a high degree, if the intrinsic reaction rate is much greater than the rate of intracrystalline diffusion.

However, the shape selective formation of 1,2,4,5-TeMB in the alkykation of 1,2,4-TMB with methanol [Yashima *et al.*, 1985; Namba *et al.*, 1986], the shape selective formation of 1,2,4-TMB during the alkylation of toluene [Hibino *et al.*, 1991] and the disproportionation of m-xylene [Martens *et al.*, 1988] over ZSM-5, strongly indicate that the intrinsic reaction rate of 1,2,4-TMB can be low enough relative to the rate of intracrystalline diffusion, so that a reaction which consumes or forms 1,2,4-TMB can occur to a significant extent inside the micropores of ZSM-5.

In the transformation of 1,2,4-TMB, however, transition states (Figure 1.15) and / or products (Table 1.7) are larger than the reactant and thus the intracrystalline diffusion of 1,2,4-TMB is unlikely to be the rate determining step. It is not clear to what extent restricted transition state or product shape selectivity limit or even prevent the various reactions of 1,2,4-TMB inside the zeolite channels.

1.6.7 Product diffusion

Apart from reactant diffusion or the formation of transition states, product diffusion may possibly be the rate limiting step. Although the minimum kinetic diameters of TMB isomers are clearly larger than the pore diameter of ZSM-5, the diffusion of trimethylbenzenes is not totally prevented inside the intracrystalline pore space of ZSM-5, since the diffusion coefficient for the largest TMB-isomer, viz. 1,3,5-TMB, is about $D_{135\text{-}TMB}(315°C)=10^{-12}$ cm^2/sec [Olson *et al.*, 1981; Weisz, 1980]. This would also be expected for TeMB isomers, since their critical diameters are the same as for the TMBs (Table 1.7). The intracrystalline diffusivity of these molecules even increases with temperature due to an increasing flexibility of the zeolite framework. Figure 1.17, however, shows that the diffusion of these molecules is highly restricted compared to p-

xylene (i.e. 5 orders of magnitude). Since the reaction rate at the external surface also increases with temperature, the intracrystalline diffusion may still be relatively slow, so that the rate with which 1,2,3-TMB, 1,3,5-TMB and TeMBs elute from the micropores is negligible as compared to the rate of product formation on the external surface even at high temperatures. In accordance with that, Gilson and Derouane [1984] suggested the conversion of 1,3,5-TMB at 450°C to probe the catalytic activity of the external surface of ZSM-5. Meshram *et al.* [1984] reported that 1,2,4-TMB and 1,2,3-TMB undergo transalkylation with toluene over ZSM-5 more readily than 1,3,5-TMB, revealing that 1,2,4-TMB and 1,2,3-TMB react partially inside the pores due to their smaller diameters.

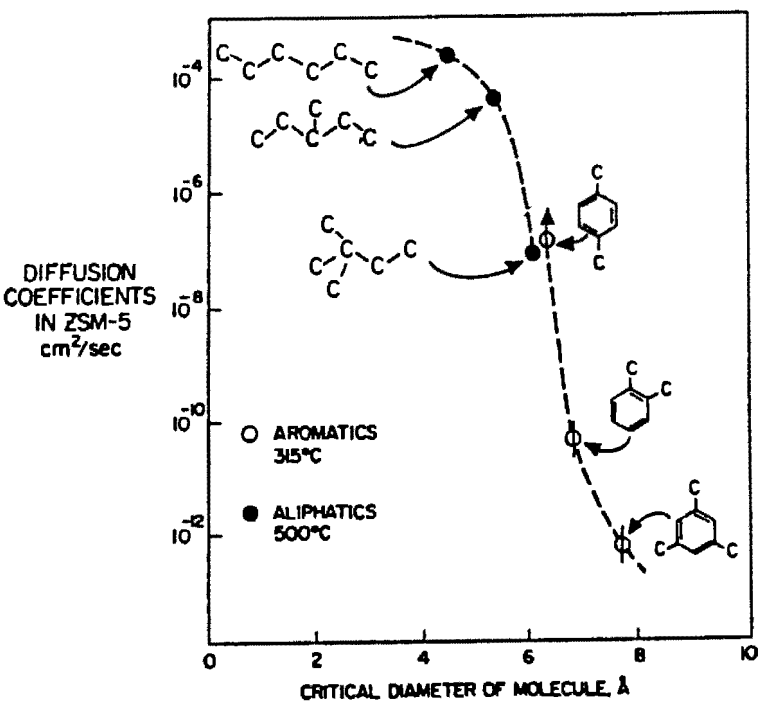

Figure 1.17: Diffusion coefficients in HZSM-5 for hexane isomers (at 500°C) and aromatics (at 315°C) [Haag and Chen, 1987]

NMR studies showed that during the conversion of methanol all xylene-, TMB- and TeMB-isomers were present in the adsorbed phase whereas 1,2,3-TMB, 1,3,5-TMB and TeMB were not observed in the product at 300°C [Anderson and Klinowski, 1989]. This proves that these molecules, which are also expected products in the transformation

Table 1.7: Minimum molecular diameters of alkyl aromatics and pore diameters of ZSM-5

Alkyl Aromatic	$D_{Eff/ZSM-5}$ (cm^2/s)	σ (Å)[a]	d_{min} (Å)[b]
n-Hexane	-	4.3[c]	4.9[c]
Benzene	-	5.85[c]	6.6[c]
Toluene	-	5.85[d]	6.6[d]
p-Xylene	350°C/$\geq 10^{-7}$ [g]	5.85[d]	6.6[d]
m-Xylene	-	6.6	7.4[e]
o-Xylene	350°C/10^{-10} [g]	6.6	7.4[e]
1,2,3-Trimethylbenzene (Hemimellitene)	-	7.0	7.9[e]
1,2,4-Trimethylbenzene (Pseudocumene)	-	6.6	7.4[e]
1,3,5-Trimethylbenzene (Mesitylene)	350°C/10^{-12} [g]	7.7	8.6[e]
1,2,3,4-Tetramethylbenzene	-	7.0	7.9[e]
1,2,3,5-Tetramethylbenzene	-	7.7	8.6[e]
1,2,4,5-Tetramethylbenzene (Durene)	-	6.6	7.4[e]
1,3,5-Triisopropylbenzene	-	8.5[f]	9.5
ZSM-5, straight			5.2 x 5.7
sinusoidal			5.3 x 5.6
intersection cavities			~9

[a] minimum kinetic diameter calculated from the minimum equilibrium cross-sectional diameter (minimum Van der Waals diameter) using the equation $\sigma = 2^{-1/6}\,\mathbf{d}_{min}$, where $\mathbf{d}_{min}$ is the minimum Van der Waals diameter [Breck, 1974]

[b] minimum Van der Waals diameter

[c] Breck, 1974, pp. 634-636.

[d] Taken as the same value as for benzene [Breck, 1974], assuming a molecular orientation with the methyl group on the channel axis

[e] Gnep *et al.*, Bulletin de la societe Chimique de France N^0 1-2 (1982) 5

[f] Hibino *et al.*, J. Catal., 128 (1991) 551

[g] Olson *et al.*, 1981; Weisz, 1980

of 1,2,4-TMB, can be accommodated by the micropore system of ZSM-5. Since the molecular diameter of these products is larger than the zeolite channels, it was argued that they were trapped in the more spacious channel intersections (Table 1.7) at this temperature. At 370°C all possible methyl-substituted benzenes up to C_{11} have been observed in the methanol conversion product [Chang and Silvestri, 1977]. It was

concluded that the larger species are now able to leave the crystallite because of the increased channel diameter [Anderson and Klinowski, 1989]. An increased rate of product formation at the external crystal surface due to increasing the temperature from 300°C to 370°C , however, was not taken into consideration.

HZSM-5 showed a higher selectivity towards the formation of 1,2,4,5-TeMB in the alkylation of 1,2,4-TMB with methanol than zeolite Y and Mordenite [Yashima *et al.*, 1985]. The TeMB-fraction obtained over ZSM-5 consisted of between 80 and 100% of 1,2,4,5-TeMB. The selectivity to 1,2,4,5-TeMB was reported to increase when the external surface of ZSM-5 was dealuminated [Namba *et al.*, 1986]. This may be interpreted as a shape selective effect and indicates that 1,2,4,5-TeMB is formed inside the pores. It was further suggested, that 1,2,3-TMB and 1,3,5-TMB (isomerisation products) and 1,2,3,4-TeMB and 1,2,3,5-TeMB (alkylation products) and pentamethylbenzene (polyalkylation product) are produced only by reaction on the external surface of HZSM-5 crystallites [Yashima *et al.*, 1985]. This would most probably be due to product shape selectivity, since eventual transition states in the methylation of toluene are not likely to be larger than the products. Interestingly, the cut off in the product distribution in the Mobil methanol to gasoline reaction over small ZSM-5 crystals is at 1,2,4,5-TeMB [Fraenkel, 1990].

This indicates that 1,2,4,5-TeMB may also be formed via disproportionation of 1,2,4-TMB provided the transition state can be accommodated by the ZSM-5 micropore system.

1.6.8 Restricted transition state shape selectivity

Restricted transition state selectivity can be ruled out as the rate determining step for the monomolecular isomerisation of 1,2,4-TMB in the intracrystalline pore space, because NMR studies showed that 1,2,3-TMB and 1,3,5-TMB can be accommodated by the micropore system [Anderson and Klinowski, 1989] and the transition states do not exceed the size of reactant or products. Thus the isomerisation of 1,2,4-TMB in the micropores of ZSM-5 is most likely mass transfer limited.

Although the bimolecular disproportionation mechanisms involve rather bulky transition states, it is not clear that restricted transition state selectivity is the limiting factor in the disproportionation inside the ZSM-5 channels. It may be suggested that one of the aromatic rings of the transition state is situated in the more spacious channel intersection (9Å) where the freedom of molecule orientation is rather high, while the other aromatic ring sticks into the channel in its most linear orientation. This flexibility may even be enhanced if one considers that the phenyl groups may be free to rotate around the two axes of the methane bridge bonds. For example the right phenyl group of the transition state "H" (Figure 1.15) would be located in the channel intersection while the left phenyl group sticks into the channel. This transition state could not be accommodated in a cylindrical pore. A similar concept was suggested to explain the accommodation of transition states during the formation of 1,2,3-TMB and 1,3,5-TMB in the disproportionation of m-xylene over the medium pore zeolite ZSM-50 which possesses spacious side pockets running perpendicular to the ten-membered ring channels [Martens *et al.*, 1988]. An illustration of the problem by Martens *et al.* [1988] (Figure 1.18) for the disproportionation of m-xylene strongly suggests that the accommodation of the analogous transition states in the disproportionation of 1,2,4-TMB (Figure 1.15) is hardly possible.

When m-xylene was converted over ZSM-5 the disproportionation was reported to be [Gnep *et al.*, 1982] suppressed due to transition state selectivity, whereas monomolecular isomerisation did not experience significant hindrance. Martens *et al.* [1988] reported an isomerisation to disproportionation ratio of 33. The disproportionation of m-xylene led to 1,2,4-TMB exclusively. The latter was attributed to transition state selectivity. Based on kinetic diameters of the TMB isomers, pressure effects and the deactivation behaviour, Meshram *et al.* [1984] suggested that the transalkylation of TMB isomers, 1,3,5-TMB in particular, with toluene occurs mainly on the external surface of ZSM-5. This is even more likely in the disproportionation of 1,2,4-TMB due to larger products and / or transition states.

In the case that the biphenylmethane transition states could not be accommodated in the

channel system, there is still the possibility that the disproportionation of 1,2,4-TMB takes place via the dissociative dealkylation-alkylation mechanism. This mechanism may be favoured by high temperatures and involves no bulky transition states. The reaction would thus be limited by product diffusion.

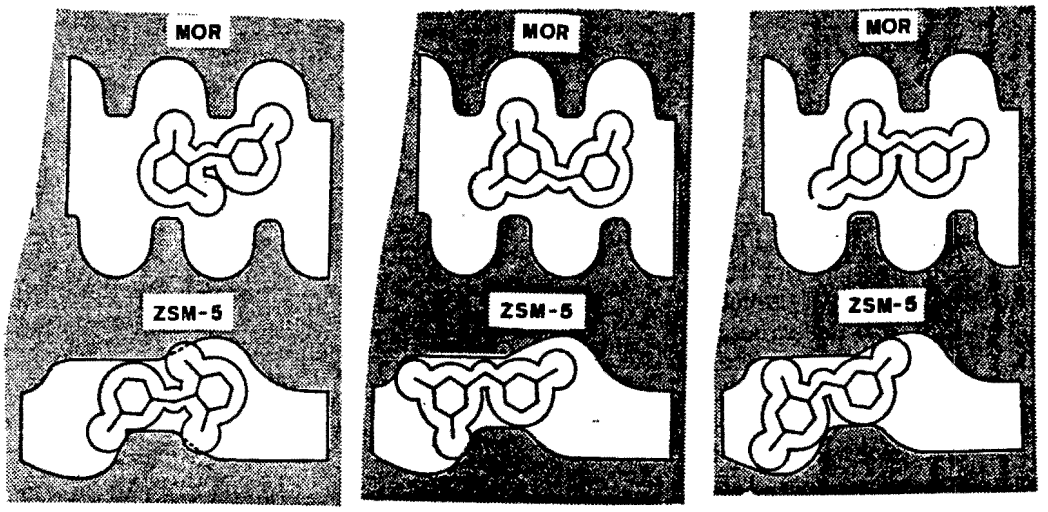

Figure 1.18: Accommodation of transition state complex for the disproportionation of m-xylene [Martens *et al.*, 1988]

In both mechanisms the disproportionation product 1,2,4,5-TeMB is favoured against the other TeMB isomers with respect to its formation inside the micropores, since it has the best fitting transition states and it is the smallest TeMB isomer. 1,2,4,5-TeMB is therefore expected to be selectively formed amongst the TeMB isomers over ZSM-5 if its formation inside the zeolite channels is possible although 1,2,3,5-TeMB is the thermodynamically favoured isomer (Table 1.6).

1.6.9 Summary

The relative contributions of the intracrystalline surface and the external surface to the global rate of a particular reaction depend mainly on the degree to which this reaction is inhibited inside the channels. At a first glance, the reactions of 1,2,4-TMB seems to

require larger pores than those of ZSM-5 and may therefore be restricted to the external surface. It is, however, not clear if mass transfer and/or transition state shape selectivity inside the ZSM-5 channels totally prevent observable product formation by the various reactions of 1,2,4-TMB and observations in literature are contradictory. Nevertheless, the pore effectiveness factor is expected to be low and therefore the transformation of 1,2,4-TMB is likely to occur mainly at acid sites near or on the external surface of the zeolite crystal. Thus the transformation of 1,2,4-TMB is expected to be a sensitive test reaction to probe the inertisation of the external surface and its effect on the shape selective properties of HZSM-5.

1.7 OBJECTIVES OF THIS RESEARCH

Based on the literature review the objectives of this study were:

1. To develop a chemical vapour deposition method which allows modification of the external surface of ZSM-5 in a controlled and uniform manner;

2. To evaluate the effect of this modification on the catalytic performance of the zeolite;

3. To develop suitable probe reactions with the aim of monitoring the effect of modifying the external surface of ZSM-5 on the:
   i) activity of the external surface;
   ii) intrinsic activity of the intracrystalline pore space;
   iii) accessibility of the intracrystalline pore space; and
   iv) the shape selectivity;

4. Of particular interest regarding (3) is the conversion of 1,2,4-TMB. Thus the final objective was to study the conversion of 1,2,4-TMB over HZSM-5 with particular focus on:
   i) the reaction network;
   ii) the catalytic role of the intracrystalline and the external surface;
   iii) and the use as probe reaction to monitor modifications of the external surface.

Chapter 2

Experimental

2.1 MATERIALS

2.1.1 Chemicals

The chemicals listed in Table 2.1 were used without further purification. Chromosorb was supplied by Supelco with a particle size of 60 to 80 mesh. Acid washed sand from Saarchem (100-500μm) was washed in deionised water until a pH of 7 was obtained.

Table 2.1: Properties and manufacturers of chemicals used

Chemical	Purity (%)	Density (g/m^3)	Molar mass (g/mol)	Boiling point (°C)	Manufacturer
cyclo-hexane	>99.5	0.78	84.16	79-81	Riedel-de Haën
n-hexane	99	0.66	86.18	68.7	Merck
toluene	>99.7	0.867	92.14	109-112	Saarchem
o-xylene	98	0.88	106.17	144	Riedel-de Haën
p-xylene	99	0.86	106.17	138	Saarchem
1,2,4-trimethylbenzene	98	0.889	120.2	168	Aldrich
1,3,5-triisopropylbenzene	97	0.845	204.36	232-236	Aldrich
tetraethoxysilane	98	0.933	208.33	163-167	Fluka Chemie

2.1.2 Catalysts

Both ZSM-5 samples used in this work, viz. ZSM-5 (B200) and ZSM-5* (B48), were synthesised according to the Argauer and Landolt patent [1972]. The synthesis conditions were the same as described by Weber *et al.* [1996], except that the synthesis time was 24 hours instead of 72 hours. The ZSM-5 sample was prepared in a larger autoclave using the threefold amounts of raw materials than for the sample ZSM-5*.

Silica-alumina pellets obtained from Kali-Chemie (BR2684) with an aluminium content of 4%, which is equivalent to a molar Si/Al ratio of approximately 10, were crushed and used as catalyst powder.

A fraction of the non-detemplated and non-ionexchanged sample ZSM-5* was coated according to the method described by Rollmann [1980] leading to sample Sil-ZSM-5* (B58). This procedure provides a crystalline zeolite having an aluminium free outer shell of crystalline SiO_2 which is isostructural to ZSM-5. To obtain this modification 4 g of the non-detemplated parent zeolite were subjected to a secondary synthesis treatment by resuspending the zeolite into a synthesis gel which contained no $Al(OH)_3$, but was otherwise of identical composition to the synthesis gel used in the primary synthesis. The secondary synthesis proceeded for 72 h at 160°C and the catalyst mass increased 4.5 times.

After the synthesis or modification the solid product was separated from the mother liquor and washed three times with deionised water. After drying at 100°C, all samples were detemplated at 500°C for 8 hours in 30cm^3/min nitrogen and 8 hours in 30cm^3/min air using not more than 10g of undetemplated zeolite per detemplation run. The sodium form thus obtained was ion-exchanged by refluxing the catalyst with stirring with an excess 2 molar solution of ammonium nitrate (NH_4NO_3) in deionised water at 100°C for 24 hours to obtain the ammonia form of ZSM-5 (NH_4-ZSM-5). The catalyst was separated from the solution by vacuum filtration and washed with deionised water before being dried at 100°C overnight.

The ZSM-5 structure was verified for all three samples via characteristic d-spaces by comparing the X-ray diffraction (XRD) patterns with simulated XRD patterns [Von Ballmoos, 1990] (Appendix I). Moreover no amorphous material was observed on the electron micrographs (Figure 2.1) and it was finally concluded that the samples were of high purity. Scanning electron microscopy (SEM) also showed that the morphology of all samples was spherical agglomerates and the particle size ranged from 1-3 μm for ZSM-5* and Sil-ZSM-5* and from 0.5 - 1.5 μm for ZSM-5. The Si/Al ratio as determined by Atomic Absorption Spectroscopy (AAS) and a gravimetric method (Appendix II) was 30, 26 and 100 for ZSM-5, ZSM-5* and Sil-ZSM-5* respectively. Table 2.2 summarises the physicochemical properties of the three samples.

Table 2.2: Physicochemical catalyst properties

Catalyst property	Characterisation tool	ZSM-5* (B48)	Sil-ZSM-5* (B58)	ZSM-5 (B200)
Number of acid sites [a] ($mmol_{NH3}/g_{Cat}$)[c]	TPD	0.61	0.18	0.36
Number of acid sites [b] ($mmol_{NH3}/g_{Cat}$)[c]	TPD	0.66	0.24	0.43
Si/AL	AAS	26	100	45
BET surface area (m^2/g)	BET	325	393	388
Meso + macropore volume [d] (cm^3/g)	BET	0.25	0.21	0.14
Micropore volume [e] (cm^3/g)	BET	0.09	0.11	0.12
Morphology [f]	SEM	S,A	S,A	S,A
Particle size (μm)	SEM	1.5-3.0	1.5-3.0	0.5-1.5

[a] Integration of the TCD signal between 200°C and 580°C.
[b] Titration
[c] The desorbed amount of ammonia is related to the mass of dry catalyst. The moisture as obtained by gravimetric analysis was between 2% and 3%
[d] BJH cumulative desorption pore volume of pores between 3000 and 17 Å in diameter
[e] Pore volume of pores less than 17 Å in diameter
[f] S=spherulitic, A=agglomerates

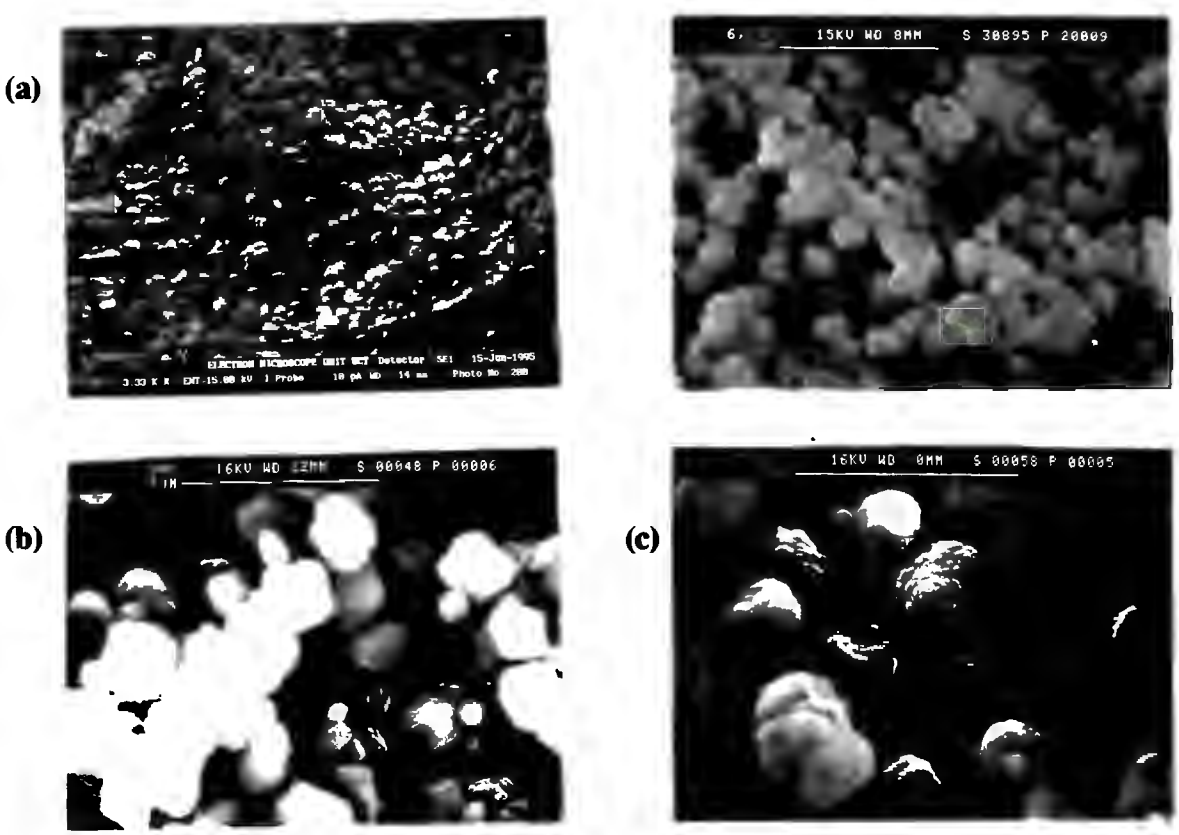

Figure 2.1: SEM micrographs for (a) ZSM-5, (b) ZSM-5* and (c) ZSM-5* coated with a Silicalite shell

2.1.3 Catalyst nomenclature

When referencing catalysts in this thesis, the terminology Sil-ZSM-5 is used for the ZSM-5 sample coated with a Silicalite shell and Si##-ZSM-5 for ZSM-5 samples treated by CVD of TEOS. ## refers to certain sequences of CVD experiments. The coding is described in Table 2.3. The two parent samples were termed ZSM-5 and ZSM-5*.

Table 2.3: Catalyst coding

Catalyst code	Sample description
ZSM-5*	B48, Parent I (Section 2.1.2)
ZSM-5	B200, Parent II (Section 2.1.2)
Sil-ZSM-5*	B58, ZSM-5* coated with a Silicalite shell (Section 2.1.2)
Si-75-ZSM-5 to Si-450-ZSM-5	ZSM-5 after CVD of TEOS at 75°C to 450°C (Section 2.3.2.5)
Si45-, Si90- and Si180-ZSM-5	ZSM-5 subjected to 45, 90 or 180 minutes of CVD respectively followed by a calcination step (Section 2.3.2.6)
Si45'-, Si90'- and Si180'-ZSM-5	ZSM-5 subjected to three CVD-calcination cycles with a deposition time of 15, 30 or 60 minutes respectively (Section 2.3.2.6)
Si01-ZSM-5 to Si16-ZSM-5	ZSM-5 modified by CVD of TEOS, the number indicates the number of CVD treatment cycles applied to the sample (Section 2.3.2.7)
SiV-, SiX- and SiXV-ZSM-5	ZSM-5 treated by 5, 10 or 15 CVD-calcination cycles for the purpose of sorption studies (Section 2.3.2.8)

2.2 CATALYST CHARACTERISATION

2.2.1 X-ray diffraction

Powder X-ray diffractograms (XRD) were obtained from a Phillips X-ray diffractometer using Cu-Kα radiation with a wavelength of 1.542Å at 40kV and 25mA with the ZSM-5 samples in their ammonia form. The scan range was $6<2\theta<48$ at a 2 θ step size of 0.1°, 1000 counts/s and a time constant of 1s.

2.2.2 Scanning electron microscopy

Electron micrographs were obtained using a Leica S440 and a Cambridge S200 Scanning Electron Microscope (SEM) with the accelerating voltage at 16 and 15 keV respectively. Samples were dusted on carbon coated aluminium stubs and subsequently sputter coated with an Au/Pd film.

2.2.3 Elemental analysis

The bulk Si/Al ratios of the ion-exchanged zeolite samples were determined using a gravimetric method in combination with atomic absorption spectroscopy (AAS) respectively. For the latter a Varian-1010 spectrometer was employed. 0.2 ± 0.05 g of each sample was digested in $15cm^3$ of hydrocloric acid at 150°C for 16 hours in Teflon Parr bombs. Thereafter the silica precipitation was filtered using ashless filter paper and dried at 1000°C overnight. The amount of SiO_2 was gravimetrically determined. To evaluate the aluminium, the filtrate was made up to $100cm^3$ with deionised water and compared to a standard solution of aluminium. The standard solution was made in the range 33.33 to 100 ppm. The calculation of the Si/Al ratio is described in Appendix II.

2.2.4 Temperature programmed desorption of ammonia

NH_3-TPD was performed in a quartz sample cell containing approximately 250 mg of catalyst. The sample was calcined in-situ in air ($45cm^3$/min, NTP) at 500°C for 240 minutes and then cooled to 150°C. Ammonia was adsorbed from a 5% NH_3 in He gas mixture which was passed over the catalyst for 60 minutes ($70cm^3$/min, NTP). Physisorbed NH_3 was flushed off the catalyst for 24 hours in a pure He stream at the same temperature. TPD spectra were recorded by heating the sample in flowing helium ($70cm^3$/min, NTP) at 10 deg/min from 150°C to 700°C while maintaining the final desorption temperature for 1 minute. The desorbed NH_3 was continually detected by a Thermal Conductivity Detector (TCD). A baseline subtraction was carried out to account for the desorbing water at high temperatures. The baseline was obtained by running a

TPD without adsorbing NH_3. The desorbed NH_3 was also titrated with 0.1N NaOH solution after bubbling through a saturator containing a 0.1N H_2SO_4 solution to confirm the total amount of NH_3 desorbed as measured by integration of the TCD signal.

2.2.5 Gravimetric sorption experiments

Sorption experiments were carried out using the heatable micro-balance of a Stanton Redcroft 780 TG-DTA-instrument under flow conditions. The TG-DTA-instrument consisted of a microbalance, DC-amplifier, balance control unit, universal temperature programmer and a PC to record the experimental data. The resolution of the balance was 0.1mg

1,2,4-TMB, o-xylene, p-xylene and n-hexane were adsorbed onto ZSM-5, SiV-ZSM-5, SiX-ZSM-5 and SiXV-ZSM-5 (preparation of these samples see Section 2.3.2.8). 50 ± 0.4 mg of the respective sample were loaded onto the micro-balance. Before each sorption experiment the sample was calcined for 4 hours at 500°C in air ($30cm^3$/min, NTP). 1,2,4-TMB, o-xylene and p-xylene were adsorbed for 11 hours at 150°C with a data sampling interval of 2 minutes, while n-hexane was adsorbed for 1 hour at 80°C with a data sampling interval of 10 seconds. The partial pressures of 1,2,4-TMB, o-xylene, p-xylene and n-hexane were 0.5, 1.7, 2.4 and 6.0 kPa respectively. The adsorbate delivery system consisted of a mass flow controller and a saturator using nitrogen as carrier gas ($30cm^3$/min, NTP). The saturator was thermostated using an ice bath.

2.2.6 BET surface area analysis

Nitrogen adsorption was carried out to characterise the pore volumes and surface areas of ZSM-5, ZSM-5* and Sil-ZSM-5* using a Micromeritics ASAP 2000. 0.5g of zeolite sample was dried for 120 minutes in situ at 150°C at vacuum conditions (p=0.65Pa). Nitrogen was then adsorbed at the boiling temperature of liquid nitrogen (77K) using an extended pressure table with 150 pressure points ranging from 0.65kPa to ambient pressure.

2.3 EXPERIMENTS USING A FIXED BED REACTOR

2.3.1 Experimental apparatus

All reactions and the chemical vapour deposition of TEOS were carried out in the apparatus as shown in Figure 2.2 and 2.3. Depending on whether a calcination/regeneration gas or carrier gas was needed air or nitrogen (99.99%) could be optionally fed. The feed line was equipped with two feed dosing systems, which could be operated in parallel or independently of each other. Each dosing system consisted of a Unit mass flow controller followed by a one way check valve and a thermostated saturator. Both saturators could be bypassed. The various saturators used are described in more detail in Section 2.3.1.2. The total pressure in the saturator was controlled by a needle valve (N1, Figure 2.2) and monitored by a pressure sensor. The saturator temperature was controlled by a water jacket or electrical heating tape. The actual gas temperature at the saturator outlet was monitored using a thermocouple.

The feed gas proceeded through an axial mixer followed by a radial mixer before it entered the reactor. The reactor bypass line was equipped with a needle valve (N2, Figure 2.2) which allowed equal pressure drops of bypass and reactor to be obtained in order to avoid pressure alterations in the saturator when switching from reactor to bypass. The reactor inlet pressure could be controlled via the needle valve (N3, Figure 2.2) in the product line in combination with the first pressure sensor upstream of the reactor. The reactor was situated inside a kiln thus minimising temperature gradients. The details of the reactor are documented in Section 2.3.1.1. The actual temperature of the catalyst bed was monitored by a thermocouple housed in a 1/8" closed stainless steel sleeve which was welded into the reactor head and protruded into the catalyst packing.

To facilitate product analysis an internal standard was fed into the product gas stream using a mass flow controller in combination with a thermostated saturator at atmospheric pressure. After passing through a radial mixer the final gas stream flowed through the ampoule sampler [Schulz *et al.*, 1986] (Section 2.3.1.3). The product gas stream passed

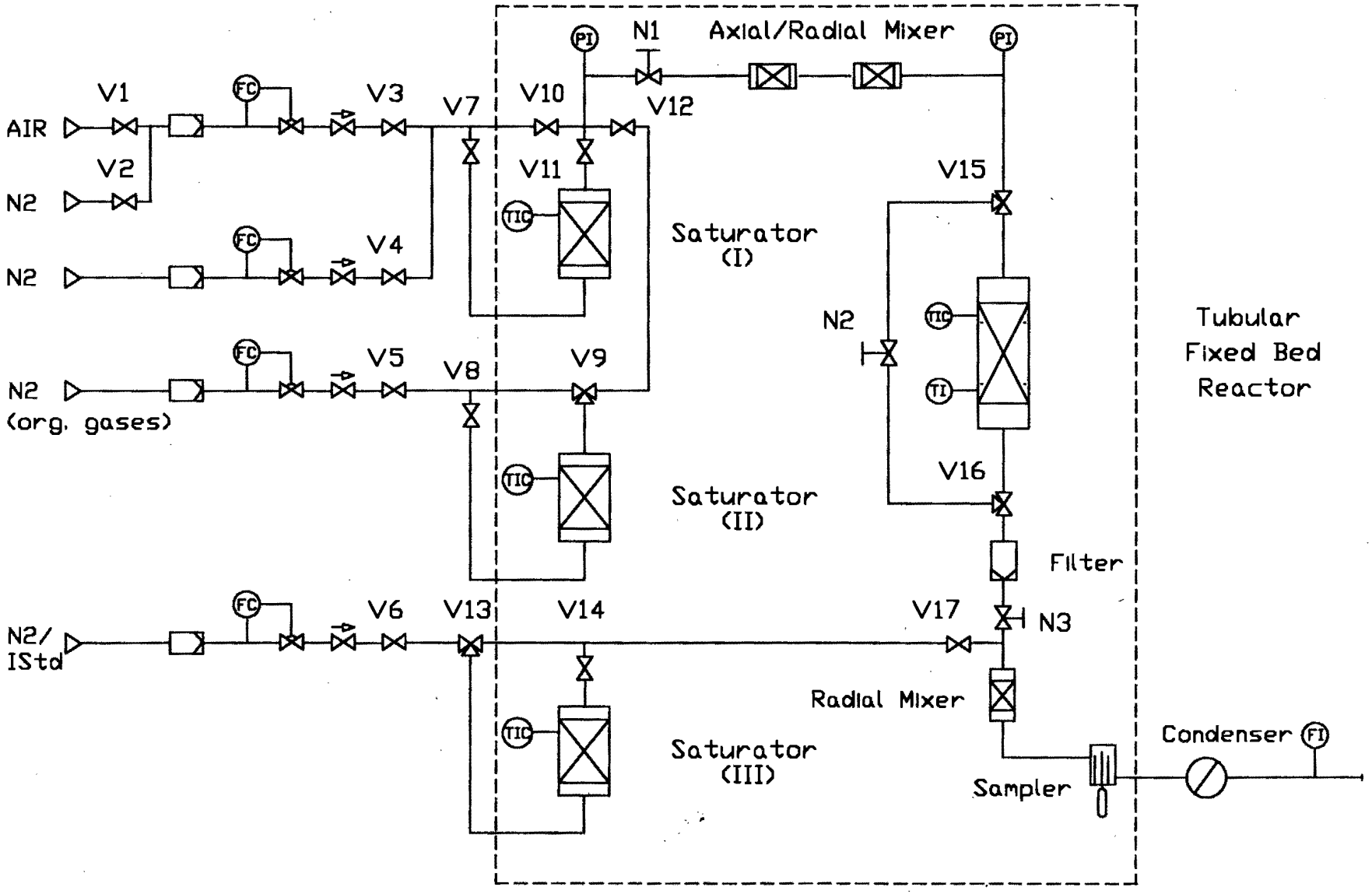

Figure 2.2: **Flowsheet of the experimental apparatus used for reaction work and CVD of TEOS**

Figure 2.3: Photograph of the experimental apparatus used for the reaction work and the CVD of TEOS

through a condenser which was kept at 10°C and a bubble meter before it was vented. Feed-, product- and the internal standard line were heated.

2.3.1.1 Reactor

Figure 2.4 shows a sketch of the fixed bed reactor, which consisted of a stainless steel tube with an internal diameter of 10 mm, an outer diameter of 12.5 and a length of 80 mm. The reactor volume was 7cm^3. The reactor was connected via VCR fittings to a head- and a bottom piece which were welded to the feed- and product line respectively and was operated in down flow mode. To measure the temperature in the packing, a thermowell with an outer diameter of 3.1 mm was welded to the head piece.

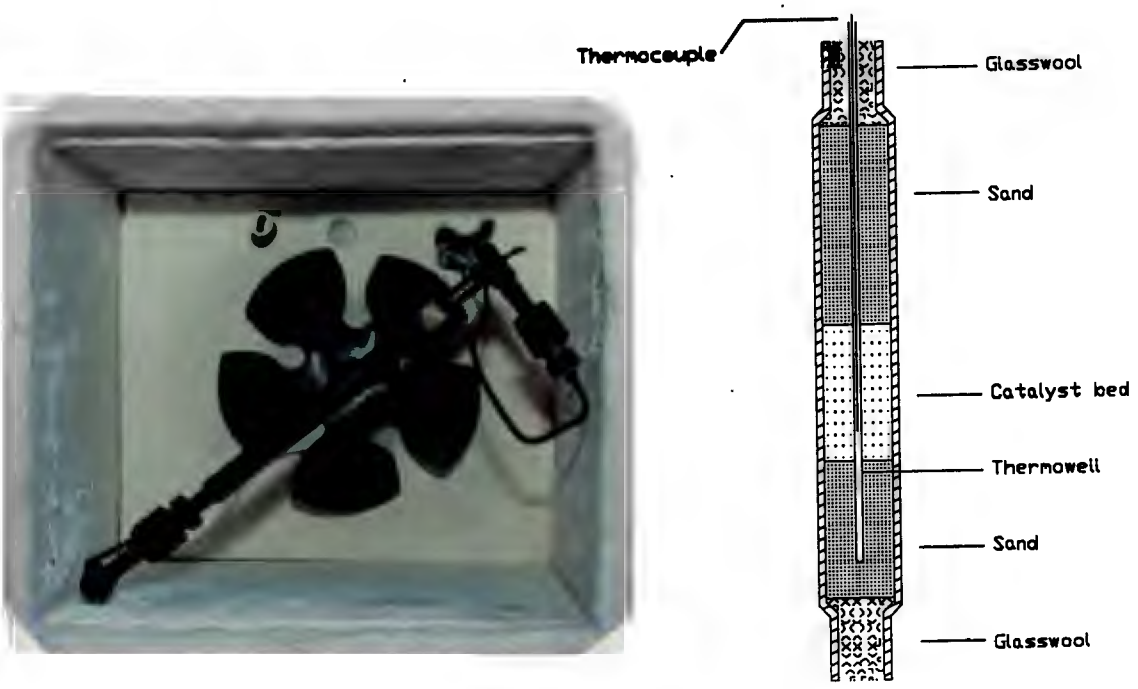

Figure 2.4: Photograph and sketch of reactor

2.3.1.2 Saturators

Three types of single stage saturators were used which all showed good performance (accuracy: ±2%) when temperature, pressure and the carrier gas flow rate were accurately controlled. Substances which were fed with a high rate were dosed using a bubble single stage saturator (Type I) made from glass. To minimise pulsation and to increase the contact between gas and liquid a saturator type was used where a steel tube was filled with Chromosorb (Type II). The Chromosorb packing was saturated with the substance to be dosed. The saturator was operated in up-flow mode to avoid increasing pressure drops due to compression of the Chromosorb bed. The disadvantage of this type of saturator is that it can only be used for short times on stream or for low evaporation rates.

To combine the advantages and to eliminate the disadvantages of these two saturator types a saturator was developed as shown in Figure 2.5 (Type III). The Chromosorb packing is in contact with liquid feed reserve in the lower compartment. Due to capillary forces

the liquid is transported into the Chromosorb bed thus maintaining a constant loading. To avoid pressure build up the lower compartment has to be pressure equilibrated with the upper compartment.

Type I saturator was used to feed TEOS and toluene, type II saturator was used to feed 1,2,4-TMB and 1,3,5-TiPB and type III saturator was employed to dose n-hexane and the internal standard (cyclo-hexane).

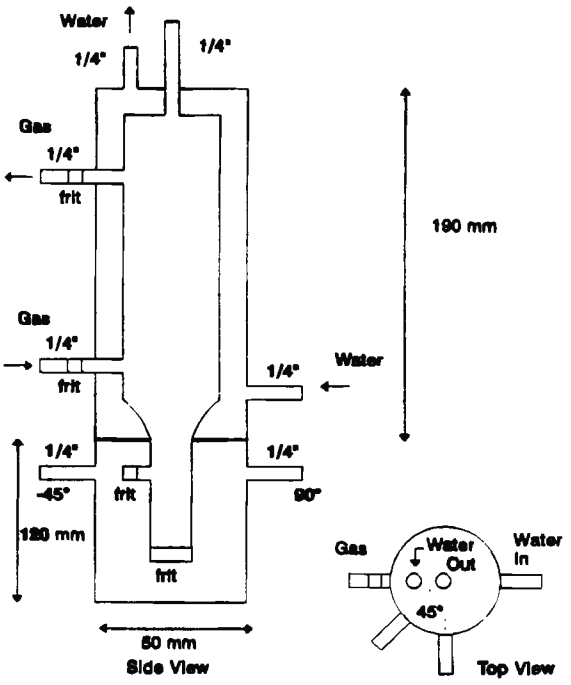

Figure 2.5: Sketch of saturator type III developed in this work

2.3.1.3 Ampoule sampler

A sketch of the ampoule sampler is shown in Figure 2.6. This method of capturing and analysing gas samples was developed by Schulz *et al.* [1986] and is described in detail in this reference.

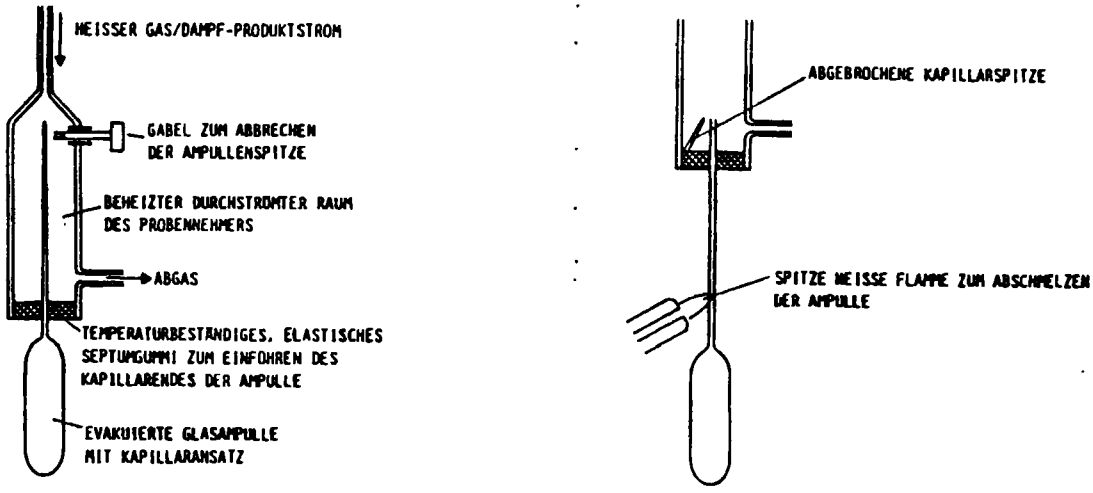

Figure 2.6: The ampoule sampler [Schulz *et al.*, 1986]

2.3.2 Experimental procedure

2.3.2.1 Preparation and packing of catalyst

Acid washed sand (100-500 μm) was washed with distilled water and it was confirmed a priori that the treated sand was catalytically inert Appendix VI, IX and Figure 2.8.

ZSM-5 powder in the ammonia form and sand were wetted with ionexchanged water, intensely mixed and dried at 50°C. The electron micrographs in Figure 2.7 show that the catalyst particles were homogeneously deposited onto the sand grains. The ZSM-5 catalyst was deposited onto sand particles for the purpose of avoiding channelling effects, maintaining isothermal condition as well as decreasing the dispersion and enhancing the plug flow behaviour of the bed. The mass ratios of catalyst to sand are specified in Table 2.4 and Appendix V.

The catalyst bed (e.g. L~23mm) was packed into the reactor described in Section 2.3.1.1 between beds of washed sand upstream (e.g. m=4 gram, L~30mm) and downstream (e.g. m=3 gram, L~23mm) respectively. The packing was stabilised by plugs of silane

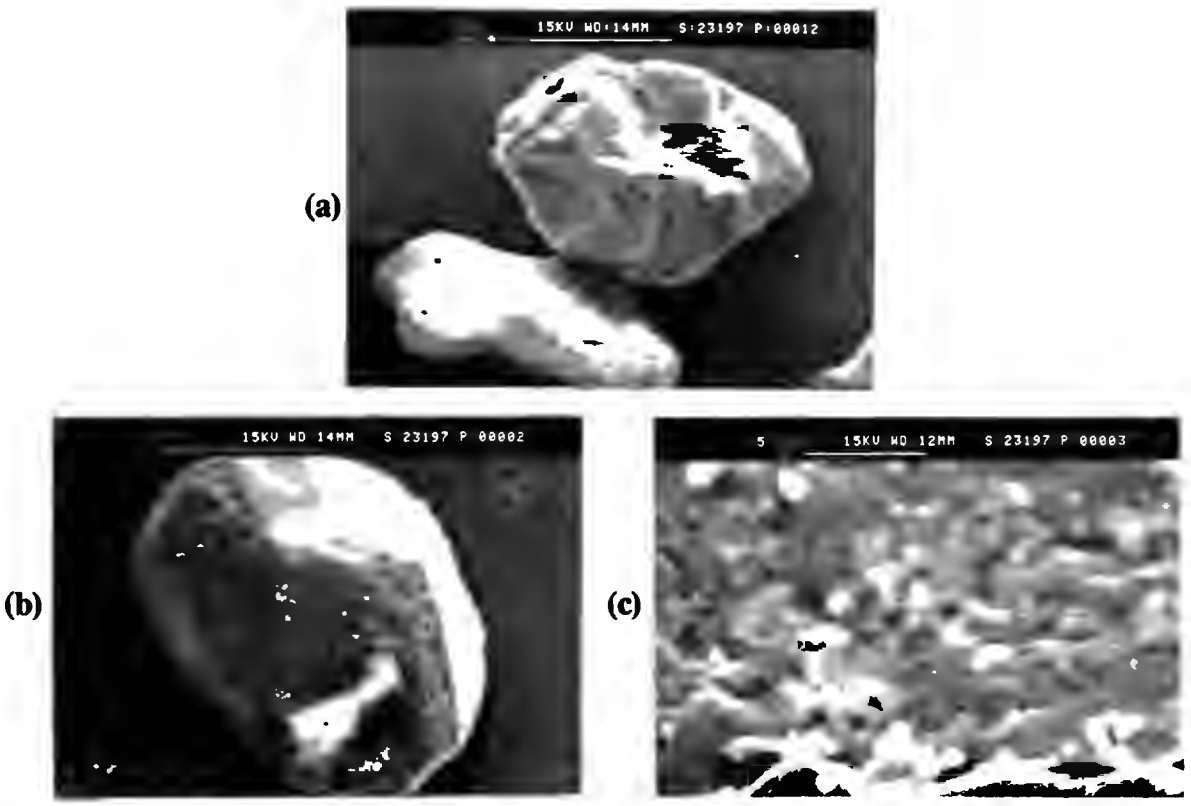

Figure 2.7: SEM micrographs of: a) Sand particle; b) and c) ZSM-5 deposited onto sand;

treated quartz wool at both the reactor top and bottom (Figure 2.4). Deviations from this standard packing will be mentioned in the specific description of the respective experimental procedure in the following sections. After each loading procedure the reactor was leak tested and before each reaction experiment the catalyst was calcined or regenerated for at least five hours at 500°C in air.

2.3.2.2 Setting of reactor conditions

After calcination / regeneration the reactor was set to the reaction temperature and flowing air was replaced with nitrogen. Once the reactor was at reaction temperature, the nitrogen flow was set and the pressure drop over the bypass, the head pressure of the reactor as well as of the feed saturator were adjusted (the experiments in Section 2.3.2.4 were carried out at atmospheric pressure and no pressure adjustment was performed). The saturator head pressure was kept 10 kPa above the reactor head pressure. The latter are

given in Table 2.6. Thereafter the thermostated feed and the internal standard saturator were switched in line and the flows were stabilised for 4 hours while bypassing the reactor. The moment when the reactor was switched in line is defined as zero time on stream. The dead time does not need to be accounted for since the reaction data were evaluated when the system reached steady state. An overview of the reaction conditions for all experiments using the fixed bed reactor is given in Table 2.5 while the reaction conditions for each single experiment are listed in Appendix V.

2.3.2.3 Reaction network in the conversion of 1,2,4-TMB

1,2,4-TMB was converted at T=450°C and a 1,2,4-TMB partial pressure of 3.5 kPa over ZSM-5 and amorphous silica-alumina. The WHSV was varied from 0.009 to 36 h^{-1} by changing both the catalyst mass and the volumetric flowrate thus achieving modified space times ranging from 1.7 to 7000 minutes in the case of ZSM-5. The pressures at the reactor head and in the saturator were kept constant at 150 and 160 kPa respectively. Product samples obtained at 240 minutes time on stream were used for the analysis of this experimental sequence. The WHSVs and the masses of catalyst and sand used for each experiment are specified in Table 2.5 and Appendix V.

2.3.2.4 Studies on the catalytic effects of a Silicalite I shell

In preliminary studies the catalytic effect of coating ZSM-5 with a Silicalite shell was investigated for cracking of 1,3,5-triisopropylbenzene, the cracking of n-hexane and the conversion of 1,2,4-trimethylbenzene at atmospheric pressure. Two sequences of reaction runs were carried out using 137 mg of ZSM-5* and 500 mg of Sil-ZSM-5* respectively. Each catalyst was diluted with 5 g sand. This ratio of catalyst masses was based on AAS results to keep the number of aluminium atoms in the catalyst bed, and therefore the WHSV relative to Al constant. The reactions conditions are listed in Table 2.4.

Table 2.4: Reaction conditions

Reactant	n-hexane	1,3,5-TIPB	1,2,4-TMB
T (°C)	538	270	450
$P_{Reactor-outlet}$	atm	atm	atm
$p_{Reactant}$ (kPa)	10	0.17	1.3
WHSV[a)] (h^{-1})	5.4	0.35	0.6
Time on stream (min)	100	150	300

[a)] The WHSVs are based on the mass of parent catalyst for all experiments, i.e. constant Al content

2.3.2.5 Effect of the CVD temperature

100mg of ZSM-5 were diluted with 2.9g sand and loaded into the reactor as described in Section 2.3.2.1. Figure 2.8 shows that sand was inert during the CVD of TEOS at 450°C and below. Calcination was then carried out at 500°C in air for at least 5 hours. The TEOS partial pressure during the CVD treatment was approximately 0.4kPa while the WHSV was $1.5h^{-1}$. The deposition time was 40 minutes. After 40 minutes the saturator

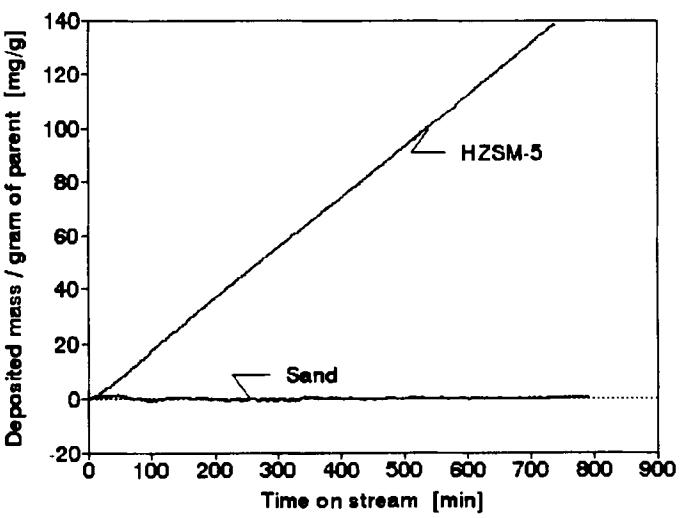

Figure 2.8: The reactivity of sand during the CVD of TEOS in a micro-balance at 450°C relative to ZSM-5

containing TEOS was bypassed. The system and the catalyst were then flushed for 90 minutes with nitrogen. At this stage the reactor temperature was set to 500°C and the catalyst was calcined in flowing air. Thereafter the reactor temperature was set to 270°C, flushed with nitrogen and TiPB cracking was carried out. The CVD-treatment was carried out at 75°C, 100°C, 150°C, 200°C, 270°C, 350°C and 450°C using a fresh catalyst for each temperature.

2.3.2.6 *Effect of calcination and CVD time*

The effect of calcination and CVD time was studied by varying the calcination frequency. This was done by subjecting ZSM-5 to a CVD time of, for example, 45 minutes followed by a calcination step. In a second experiment the calcination frequency was increased by calcining the modified samples after CVD periods of 15 minutes, thus keeping the total CVD time at 45 minutes by repeating the CVD-calcination sequence 3 times. The same experiments were carried out for a total CVD time of 90 and 180 minutes respectively, thus varying the CVD time. The CVD was carried out at T=100°C, $p_{TEOS} \approx 0.4$kPa, WHSV=1.5h^{-1}, m_{cat}=100mg. The conversion of 1,3,5-TiPB was employed as probe reaction at the conditions shown in Table 2.6.

2.3.2.7 *Effect of consecutive CVD-calcination cycles*

100mg of ZSM-5 were diluted with 2.9g sand and loaded into the reactor as described in Section 2.3.2.1. Calcination was then carried out at 500°C in flowing air for at least 5 hours. N-hexane, 1,3,5-TiPB, toluene and 1,2,4-TMB were sequentially converted at the conditions shown in Table 2.6. The catalyst was regenerated at 500°C in air for 5 hours after each reaction run. Using the same apparatus as for reactions, CVD was carried out operating the reactor differentially at 100°C, thus ensuring that the TEOS conversion was less than 5%. TEOS was fed via a saturator with a partial pressure of approximately 0.4 kPa and a WHSV of 1.5 h^{-1}. After the CVD treatment, the catalyst was flushed with nitrogen at 100°C for 10 minutes. The reactor was then heated to 500°C at which temperature (achieved after ca. 40 minutes) the nitrogen was replaced by air for

Table 2.5: Summary of the reaction conditions in the fixed bed reactor

Type of experiment	Section	Catalyst	Feed	T (°C)	$P_{Feed,\ in}$ (kPa)	WHSV (h^{-1})	m_{Cat} (g)	m_{Sand} (g)	Linear velocity (cm/s)
Reaction network	2.3.2.3	ZSM-5	1,2,4-TMB	300-450	3.5	36 - 0.009[b]	0.02 - 4[b]	0 - 14.6[b]	0.2 - 4.4
of 1,2,4-TMB		silica-alumina	1,2,4-TMB	450	3.5	17.4 - 0.08[b]	0.04 - 0.8[b]	2.2 - 2.96[b]	0.3 - 3.6
Effect of Silicalite I	2.3.2.4	ZSM-5*	n-hexane	538	10	5.4	0.137[a]	2.9	1.6
shell		and	1,2,4-TMB	450	1.3	0.6	0.137[a]	2.9	0.1
		Sil-ZSM-5*	1,3,5-TiPB	270	0.17	0.35	0.137[a]	2.9	2.4
Effect of the CVD[c]	2.3.2.5	ZSM-5	TEOS	75-450	~0.4	~1.5	0.1	2.9	2.0
temperature			1,3,5-TiPB	270	0.17	1.1	0.1	2.9	5.1
Effect of calcination on	2.3.2.6	ZSM-5	TEOS	100	~0.4	~1.5	0.1	2.9	2.0
CVD[d]		ZSM-5, Si45-, Si90-, Si180-, Si45'-, Si90'-Si180'-ZSM-5	1,3,5-TiPB	270	0.17	0.6	0.1	2.9	2.9
Effect of consecutive	2.3.2.7	ZSM-5	TEOS	100	~0.4	~1.5	0.1	2.9	2.0
CVD[c]-calcination		to	n-hexane	500	3.9	1.7 and 1.0	0.1	2.9	1.1 and 0.8
cycles		Si16-ZSM-5	toluene	450	13.4	4 and 2	0.1	2.9	0.7 and 0.3
			1,2,4-TMB	450	3.5	17.1 - 0.3	0.1	2.9	4 - 0.2
			1,3,5-TiPB	270	0.17	0.6	0.1	2.9	2.9
CVD samples for	2.3.2.8	ZSM-5	TEOS	100	~0.4	~1.5	0.1	2.9	2.0
sorption studies		ZSM-5, SiV-, SiX-, SiXV-ZSM-5	1,3,5-TiPB	270	0.17	0.6	0.1	2.9	2.9
Standard deviation	-	-	-	±2°C	±10%	±10%	±1%	-	-

a) The WHSVs are based on the mass of parent catalyst for all experiments, i.e. constant Al content
b) The WHSVs and the masses of catalyst and sand used for each experiment are given in Appendix V
c) CVD times: see Section 2.3.2.5 and 2.3.2.7
d) CVD times: 3x15, 3x30, 3x60, 1x45, 1x90 and 1x180 minutes; see Section 2.3.2.6

calcination. The above reaction-regeneration sequence was then repeated. This CVD-reaction sequence was carried out 16 times in-situ. The first five CVD treatments were continued for 15, 45, 30, 60 and 160 minutes respectively. Thereafter a constant deposition time of 90 minutes was used in each cycle. The catalyst stayed in the reactor from the first to the last CVD-reaction cycle.

In the reaction of toluene and especially 1,2,4-TMB the WHSV was varied to keep the conversion between 1.5 - 3.5% and 2 - 12% respectively. The reaction data were evaluated using the average value of samples taken in the time on stream interval given in Table 2.6.

Table 2.6: Reaction conditions

Reactant	n-C6	Toluene	1,2,4-TMB	1,3,5-TiPB
T (°C)	500	450	450	270
$P_{Reactor-head}$ (kPa)	130	140	150	140
$P_{Reactant}$ (kPa)	3.9	13.4	3.5	0.17
WHSV[a] (h^{-1})	1.7 and 1.0	4 and 2	17.1-0.3	0.6
X (mol%)	46-34	3.5-1.5	12-2	81-3
Time on stream[b] (min)	20-60	30-60	120-240	6-60

[a] The WHSVs are based on the mass of parent catalyst for all experiments
[b] Time on stream interval in which reaction data were averaged with the reaction being at pseudo steady state

2.3.2.8 Preparation of CVD samples for sorption studies

CVD treatment

Three samples of 100mg of ZSM-5 were subjected to 5, 10 and 15 CVD treatment-calcination cycles respectively at the same CVD conditions and times as described in Section 2.3.2.7. Only one 1,3,5-TiPB cracking experiment was carried out after the last treatment to monitor the success of the procedure.

Catalyst recovery

For the purpose of post-reactor characterisation ZSM-5 samples which had been modified

by CVD treatment were recovered from the catalyst-sand mixture by suspending the mixture in water and decanting the catalyst suspension from the settled fraction. Electron micrographs (Figure 2.9), however, showed that the sand/catalyst separation was not totally effective and the recovered samples still contained some sand and quartz wool.

(a) (b)

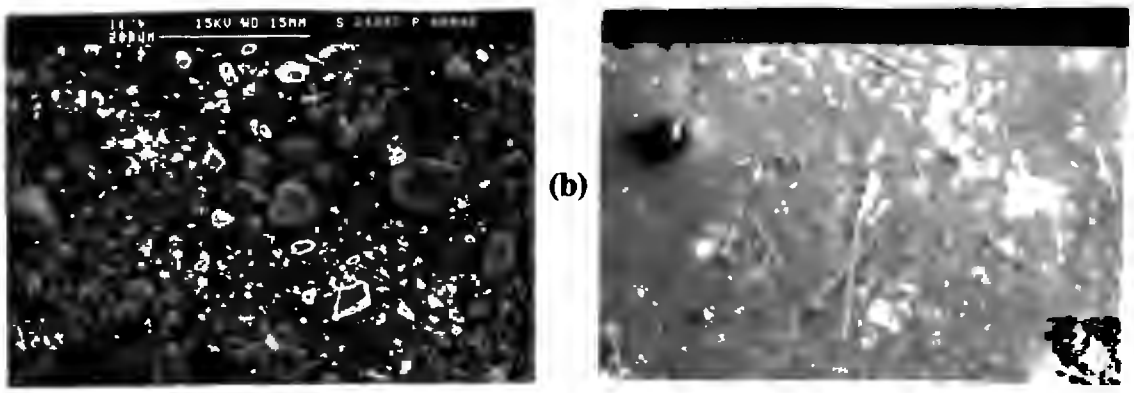

Figure 2.9: SEM micrographs of a) Sand and b)Quartz wool found in a ZSM-5 sample which was recovered from the catalyst bed

2.3.3 Product analysis

2.3.3.1 Ampoule sampling technique

Off gas sampling was carried out using the ampoule sampling technique developed by Schulz *et al.* [1986]. It is very important to avoid product separation due to condensation on the walls of the capillary or the ampoule during the sampling of the product. Therefore the ampoule and the capillary was preheated in the flame of a butane gas torch. The capillary of the ampoule was pushed through the septum of the ampoule sampler (Figure 2.6) until it was fully accommodated. The tip of the capillary was broken and the product gas filled the pre-evacuated ampoule within a fraction of a second. Thereafter the ampoule was sealed off immediately using a spot flame. The ampoule sampling technique completely decouples the sampling from analysis and thus samples can be stored over long time periods and data points with a frequency of up to one sample every 15 seconds can be achieved.

2.3.3.2 *Gas chromatographic analysis*

The samples contained in the glass ampoules were analysed by breaking them in a heated ampoule breaking device, which was connected to the gas chromatograph via a six port sampling valve. The GC carrier gas could thus either bypass the ampoule breaker or transport the product sample to the column when both were switched in-line (Figure 2.10).

The analysis of the product from the conversion of toluene, 1,2,4-TMB and 1,3,5-TiPB was performed using a Supelcowax™ 10 fused silica capillary column (30 m x 0.2 mm, film thickness 0.2 μm) fitted into a Varian 3300 gas chromatograph. The C_1-C_6 fraction in the 1,2,4-TMB product and the n-hexane cracking product was analysed using a Hewlett-Packard HP 5890A gas chromatograph equipped with a PONA column (50m x 0.2 mm, filmthickness 0.5 μm). Both GCs were equipped with a flame ionisation detector. Further specifications, temperature programmes and representative chromatograms are given in Appendix IV. To achieve good separation of the light hydrocarbons the temperature program had to be started at -25°C using liquid nitrogen as coolant.

When the ampoule technique is used carbon balances can only be determined with the help of an internal standard. For that purpose cyclo-hexane of 99.5% purity was dosed to the product stream via a single stage saturator of the type depicted in Figure 2.5 (Section 2.3.1.2) , giving an accuracy of the flow rate of $\pm$2%. Cyclo-hexane was not formed in any of the reactions carried out in this work and did not interfere with product peaks in the gas-chromatogram. Unless coke formation was significant, carbon balances better than 95% were achieved with only a few exceptions.

The product stream in the CVD of TEOS could not be monitored quantitatively due to a large scatter, which is suspected to be caused by reaction of TEOS with the walls of the glass ampoule and/or heated parts of the GC.

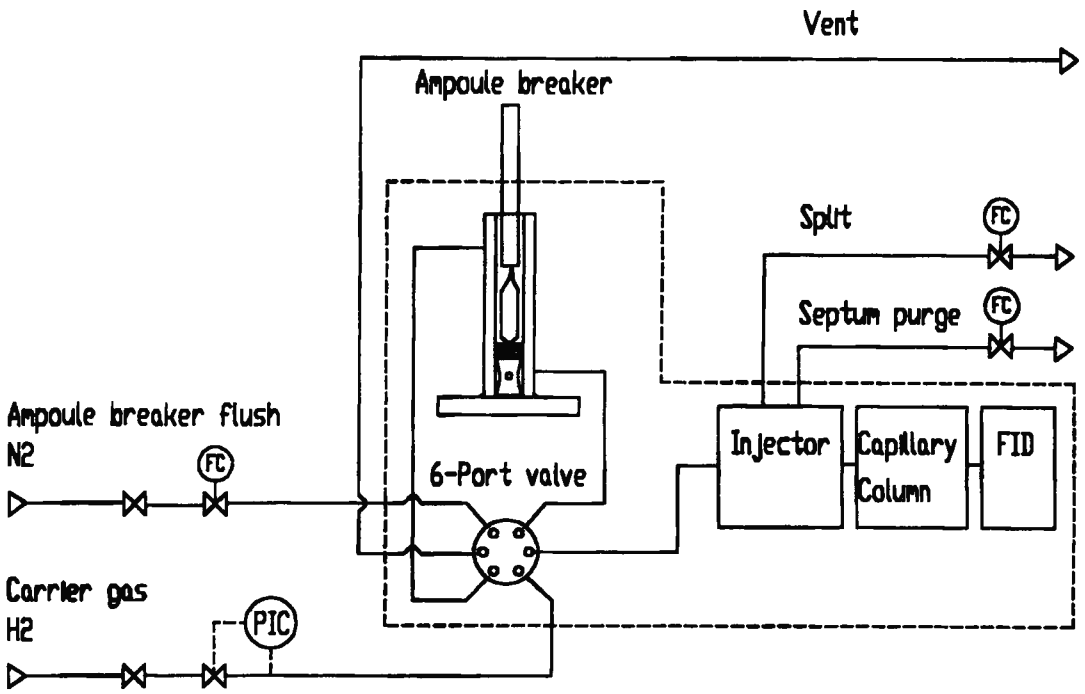

Figure 2.10: Flow sheet of ampoule breaking device and gas chromatograph

2.3.4 Evaluation of catalytic reaction data

2.3.4.1 Calibration of the internal standard flow rate

For the quantitative evaluation of a gas-chromatographical analysis a reference gas (cyclo-hexane) was continuously added to the gas stream in the product line as an internal standard. The molar flow of cyclo-hexane was calibrated by dosing methane with a purity of 99.5% as secondary reference gas using a mass flow controller. Knowing the molar flowrate of methane (F_{CH4}) the flowrate of cyclo-hexane (F_{is}) can be determined from the peak areas obtained in the GC-analysis.

$$F_{IStd} = F_{CH_4} \frac{N_{C,CH_4} A_{IStd} RF_{IStd}}{N_{C,IStd} A_{CH_4} RF_{CH_4}} \qquad (2.1)$$

The relative response factor RF_i on molar carbon basis can be assumed to be equal to one for hydrocarbons containing no hetero atoms [Dietz, 1967].

2.3.4.2 *Calculation of molar flow rates of feed and products*

The molar feed and product flowrates F_i were calculated based on the known flowrate of cyclo-hexane F_{IStd} and the peak areas A_i obtained by GC-analysis.

$$F_i = F_{IStd} \frac{N_{C,IStd} A_i RF_i}{N_{C,i} A_{IStd} RF_{IStd}} \tag{2.2}$$

2.3.4.3 *Calculation of concentrations*

The molar concentration c of a component i at reactor conditions was calculated as follows assuming ideal gas behaviour:

$$c_i = \frac{F_i \; p_{in}}{(F_{feed,out} + \sum_i F_i + F_{N_2}) \; R \; T} \tag{2.3}$$

Where p_{in} is the reactor head pressure, T the absolute reactor temperature and F_{N2} the molar flowrate of nitrogen as fed by the mass flow controller in the feed line.

2.3.4.4 *Calculation of conversion and carbon balance*

Carbon balances around the reactor were performed by comparing the flow of carbon in the feed to the flow of carbon in the product stream. The feed carbon flow was determined by analysis of the feed stream through the bypass before the reactor was switched inline.

$$C\text{-}balance = \frac{\sum_i F_{i,out} N_{C,i} + F_{feed,out} N_{C,feed}}{F_{feed,in} N_{C,feed}} \times 100\% \tag{2.4}$$

Using the peak areas on the gas chromatogram:

$$C\text{-}balance = \frac{\sum_i \frac{A_{i,out}\, RF_i}{A_{IStd}\, RF_{IStd}}}{\frac{A_{feed,in}\, RF_{feed}}{A_{IStd}\, RF_{IStd}}} \times 100\% \qquad (2.5)$$

The conversion of a reactant is defined by:

$$X = \frac{F_{feed,in} - F_{feed,out}}{F_{feed,in}} \qquad (2.6)$$

The conversion for each analysis was determined by:

$$X = 1 - \frac{\frac{A_{feed,out}\, RF_{feed}}{A_{IStd}\, RF_{IStd}}}{\frac{A_{feed,in}\, RF_{feed}}{A_{IStd}\, RF_{IStd}}} \qquad (2.7)$$

2.3.4.5 Calculation of first order rate constants

Apparent first order rate constants were determined for the integral conversion of n-hexane and 1,3,5-TiPB using the following equation:

$$k = -\frac{\dot{V}}{m_{cat}} \ln(1-X) \qquad (2.8)$$

where $\dot{V}$ is the total volumetric gas flow rate in cm^3/s at the reaction temperature in a constant density system, m_{cat} is the weight of catalyst in grams and X is the fractional conversion. Thus the unit of k is $cm^3g^{-1}s^{-1}$.

2.3.4.6 Calculation of reaction rates

If the reactor is operated differentially (viz. below 5% conversion) the rate of reactant consumption can simply be obtained by subtracting the molar flow of reactant at the reactor outlet $F_{feed,out}$ from the molar flow of reactant at the reactor inlet $F_{feed,in}$.

$$r = -\frac{1}{m_{cat}}\frac{dN_{feed}}{dt} = \frac{1}{m_{cat}}(F_{feed,in} - F_{feed,out}) \tag{2.9}$$

To determine the initial reaction rate for a first order reaction in an integral reactor the following equation can be used:

$$r = kc_{feed,in} \tag{2.10}$$

The rate of the isomerisation-, disproportionation- and dealkylation-reaction which occur during the transformation of 1,2,4-TMB (Chapter 3) were estimated using molar product flow rates F at the reactor outlet at low conversions ($< 10\%$).

$$r_{Is} = \frac{1}{m_{cat}}(F_{1,2,3\text{-}TMB,out} + F_{1,3,5\text{-}TMB,out}) \tag{2.11}$$

$$r_{Dis} = \frac{1}{m_{cat}}(\sum F_{xylenes,out} + \sum F_{TeMBs,out}) \tag{2.12}$$

$$r_{De} = \frac{1}{m_{cat}}(F_{benzene,out} + F_{toluene,out}) \tag{2.13}$$

The isomerisation, disproportionation and paring reaction rate are expressed in mmol of 1,2,4-TMB consumed in the respective reaction per gram of catalyst and time. The

stoichiometric formulae for these reactions are:

$$1,2,4\text{-}TMB \rightleftharpoons 1,2,3\text{-}TMB \tag{2.14}$$

$$1,2,4\text{-}TMB \rightleftharpoons 1,3,5\text{-}TMB \tag{2.15}$$

$$2 * 1,2,4\text{-}TMB \rightleftharpoons xylene + TeMB \tag{2.16}$$

$$1,2,4\text{-}TMB \rightleftharpoons toluene + ethene \tag{2.17}$$

$$1,2,4\text{-}TMB \rightleftharpoons benzene + propene \tag{2.18}$$

The evidence showing that reaction 2.18 occurs is discussed in Section 3.2.3.2.

2.3.5 Quantification of reactor conditions

2.3.5.1 Feed inlet partial pressure

The partial pressure of the feed at the reactor inlet was obtained by:

$$p_{feed,in} = p_{in} \frac{F_{feed,in}}{(F_{feed,in} + F_{N_2})} \tag{2.19}$$

The molar flow rate of the feed into the reactor $F_{feed,in}$ was determined by analysing the feed gas stream bypassing the reactor and the carrier gas flow F_{N2} was determined using a mass flow controller.

2.3.5.2 *Weight hourly space velocity and modified space time*

The weight hourly space velocity is defined as mass flow of feed reactant per mass of catalyst per hour:

$$WHSV = \frac{\dot{m}}{m_{cat}} \tag{2.20}$$

The reciprocal value was termed as modified space time:

$$ST = \frac{1}{WHSV} \tag{2.21}$$

2.3.5.3 *Linear velocity*

The linear velocity as defined is the gas velocity at reactor conditions in an empty reactor and was quantified assuming an constant density system:

$$u = (F_{N_2} + F_{feed,in}) \frac{RT_{reactor}}{p_{in} \frac{\Pi}{4}(d^2_{reactor} - d^2_{T\text{-}couple})} \tag{2.22}$$

2.3.5.4 *Film diffusion*

Since the zeolite powder was deposited onto sand particles reactant molecules have to diffuse from the bulk gas phase to the surface of the sand particle where the catalyst is deposited (Figure 2.7). The highest probability for film diffusion limitation occurs at the lowest linear velocity and the highest catalyst loading per sand particle (i.e. the highest catalyst to sand ratio). Run R090 (Appendix V), with a linear velocity of u=0.2 cm/s in the empty reactor and 4g of catalyst per 18.6g of catalyst-sand mixture, showed the highest potential for film diffusion limitation in the experiments where 1,2,4-TMB was converted.

The maximum rate of 1,2,4-TMB consumption occurs at the top of the catalyst bed and can be approximated using the rate at the lowest conversion of 3.6% (R076). The maximum rate of consumption per kg of pure ZSM-5 was $r_{max,ZSM-5}=2.95x10^{-3}$ mol kg^{-1} s^{-1}. In the criteria for film diffusion the diffusion rate is compared to the rate of consumption, which in this case has to be related to the mass of sand plus catalyst. Thus $r_{max,'pellet'}=6.33x10^{-4}$ mol kg^{-1} s^{-1}.

In steady state the rate of diffusion equals the observed rate of reactant consumption:

$$r_{Diff} = - r_{React} \tag{2.23}$$

The concentration drop of reactant over the gas film can thus be calculated as follows:

$$c_{TMB,bulk} - c_{TMB,surface} = \frac{r_{TMB,max,'pellet'}}{k_f a_m} \tag{2.24}$$

with k_f being the gas film mass transfer coefficient and a_m the specific surface area of the sand. The surface area for spherical particles with an average particle size of $d_p=300\mu m$ is 20000 m^2/m^3. With the density of sand $\rho=2500$ kgm^{-3} the specific surface area is $a_m=8m^2kg^{-1}$.

The gas film mass transfer coefficient k_f was estimated using the correlation of Wakao and Funazkri [1978]:

$$Sh = 2 + 1.1Sc^{1/3}Re^{0.6} \tag{2.25}$$

With the particle Reynolds number:

$$Re_p = \frac{d_p \mu \rho_{gas}}{\mu_{gas}} = 0.013 \tag{2.26}$$

with d_p=300μm, u=0.2cms^{-1} the linear gas velocity of run R090, $\mu_{N2}(450°C)$=0.033gs^{-1} m^{-1} [Perry *et al.*, 1984] and

$$\rho_{gas} = \frac{p_{reactor} M_{N_2}}{RT_{reactor}} = \frac{150kPa\ 28g/mol}{8.3147J/mol\ 723K} = 699gm^{-3} \qquad (2.27)$$

The Schmidt number at reactor conditions is:

$$Sc = \frac{\mu_{N_2}}{\rho_{gas} D_{1,2,4TMB,m}} = 1.33 \qquad (2.28)$$

with the mean diffusivity of 1,2,4-TMB in nitrogen at 450°C $D_{1,2,4\text{-}TMB,m}$=3.56x10^{-5}m^{2}s^{-1} as obtained using the equation of Fuller *et al.* [Reid *et al.*, 1987] assuming ideal gas and ideal mixture behaviour.

With Equation (2.25), (2.26) and (2.28) the Sherwood number can now be calculate:

$$Sh = \frac{k_f d_p}{D_{1,2,4TMB,m}} = 2.09 \qquad (2.29)$$

Knowing the Sherwood number the gas film mass transfer coefficient was estimated to be k_f=0.248 ms^{-1}. Using Equation (2.24) the difference between the concentration of 1,2,4-TMB in the bulk gas phase and the concentration on the particle surface was estimated to be smaller than 3.19x10^{-4}mol/m^3, which is less than 0.06% of the bulk concentration of 1,2,4-TMB for all experiments. This shows that gas film diffusion limitations are negligible for all reaction experiments when 1;2,4-TMB is converted. It should, however, be noted that Equation (2.25) was extrapolated below its fitted range of Reynolds numbers.

For the reaction of n-hexane and toluene it can be shown that gas film diffusion limitations are negligible using Equation 2.24. The maximum rate of consumption as related to the

mass of sand plus ZSM-5 for the experiments described in Section 2.3.2.7 was $r_{max,'pellet'}$(n-hexane)=1.07×10^{-4} mol kg^{-1} s^{-1} (R019) and $r_{max,'pellet'}$(toluene)=7.41×10^{-6} mol kg^{-1} s^{-1} (R004) respectively. These rates are lower than the maximum rate of 1,2,4-TMB consumption ($r_{max,'pellet'}$(1,2,4-TMB)=6.33×10^{-4} mol kg^{-1} s^{-1}. At the same time the gas film mass transfer coefficient is expected to be higher than during the conversion of 1,2,4-TMB, because the linear velocity was higher than the lowest linear velocity during the conversion of 1,2,4-TMB and the diffusivities of n-hexane and toluene are higher than for 1,2,4-TMB. Therefore the concentration difference (Equation 2.24) between the bulk gas phase and the sand particle surface should be even smaller than during the conversion of 1,2,4-TMB.

2.3.5.5 Plug flow

The ratio of reactor to particle diameter was 33 and thus exceeded a ratio of 15 which is sufficient to obtain a homogeneous radial gas velocity profile and thus plug flow [Chu *et al.*, 1989]. The following criterion for axial dispersion was used [Moulijn *et al.*, 1991]:

$$\frac{L}{d_p} > \frac{20n}{Pe_p} \ln \frac{1}{1-X} \tag{2.30}$$

where L is the bed length (~3cm), d_p is the average particle diameter (300μm) and the reaction order n was assumed to be one. For particle Reynolds numbers smaller than 1, a particle Peclet number of 0.5 has been suggested to be used in Equation (2.30) [Gierman, 1988]. The linear velocities in the transformation of 1,2,4-TMB ranged from u=0.2 cms^{-1} to u=3.6cms^{-1}, thus yielding particle Reynolds numbers between 0.013 and 0.229. For the maximum 1,2,4-TMB conversion in this work (X=0.9) the above criterion yields:

$$\frac{L}{d_p} = 100 > 92 = \frac{20n}{Pe_p} \ln \frac{1}{1-X} \tag{2.31}$$

All other experiments showed lower 1,2,4-TMB conversion levels and thus fulfill the

above criterion. In summary the criteria indicate that all reaction experiments using 1,2,4-TMB as reactant were carried out at plug flow conditions. Effects on the product distribution due to backmixing are therefore insignificant.

2.3.5.6 Time on stream

The moment when the reactor was switched in line is defined as zero time on stream thus including the dead time. The dead time does not need to be accounted for since the reaction data were evaluated when the system reached steady state.

2.4 CVD-EXPERIMENTS USING A MICRO-BALANCE

ZSM-5 was loaded in its ammonium-form into the platinum trays and placed in the micro-balance of the TG-DTA instrument described in Section 2.2.5. Before TEOS was adsorbed the catalyst was calcined at 500°C for 6 hours in flowing air (30cm^3/min, NTP). Tetraethoxysilane (TEOS) was adsorbed on ZSM-5 for at least 13 hours at 100°C, 270°C and at 450°C respectively. The saturator, containing TEOS, was kept at room temperature (p_s(18°C)=0.13kPa). For the data evaluation the mass increase was related to the mass of parent catalyst as measured after the initial calcination step, viz. $\Delta m/m_d$. After the CVD of TEOS the samples were flushed in nitrogen for 30 minutes at the respective deposition temperature. Then the temperature was ramped to 270°C at a rate of 20°C per minute while the flushing was continued for another 120 minutes. Thereafter the sample was calcined in flowing air for 400 minutes at 500°C. The mass change measured during the flushing and the calcination period was related to the total mass deposited during the CVD of TEOS. The data were recorded in time intervals of 10 seconds.

Chapter 3

The Transformation of 1,2,4-Trimethylbenzene over ZSM-5

3.1 INTRODUCTION

In order to analyse and understand the effects of a modification on the properties of a catalytic system it is essential to first determine and understand the characteristics of the reaction over the parent catalyst. This section investigates the time on stream behaviour, the dependence of product distributions on the conversion, the reaction network and activation energies occurring when 1,2,4-TMB is converted over ZSM-5. The role of the ZSM-5 micropore system and specific activity will be discussed by comparing the reaction data of ZSM-5 with amorphous silica-alumina.

3.2 RESULTS AND DISCUSSION

3.2.1 Products

The first step in the characterisation of a catalytic system and the investigation of a reaction network is the identification of the reaction products. Figure IV.4 (Appendix IV) shows the GC-trace of the light products obtained at 450°C, which consisted mostly of methane, ethane, ethene and propane. Small quantities of propene and C_4 were also observed. Benzene, toluene, p-, m-, o-xylene, 1,2,3,4-TeMB, 1,2,3,5-TeMB, 1,2,4,5-TeMB, in the C_9 fraction mainly 1,3,5-TMB and 1,2,3-TMB, and small quantities of C_2^+-alkyl-substituted benzenes, particularly methyl-ethyl-benzenes were observed in the aromatic product (Figure IV.5, Appendix IV). The formation of heavier products than TeMBs was negligible. The mentioned products were identified by comparison of the GC retention times of a known component and of the particular product.

The majority of the observed products can be formed by typical reactions of 1,2,4-TMB such as 1,2-methyl-shift-isomerisation and transalkylation and were also reported by Kojima *et al.* [1991] and Ko and Kuo [1994] who converted 1,2,4-TMB over pillared clays and zeolite HY respectively in a nitrogen atmosphere.

3.2.2 Time on stream behaviour

The evaluation of reaction data is simpler, when the catalytic system of interest is in steady state. Thus, it is essential to know its time on stream behaviour and to identify the time on stream interval in which steady state is approximated. The time on stream behaviour was studied at reaction temperatures of 300°C and 450°C and various WHSVs.

3.2.2.1 Effect on activity

Figure 3.1 shows that the conversion of 1,2,4-TMB was almost stable after 120 minutes of time on stream independent of temperature and weight hourly space velocity (WHSV). The highest standard deviations in this time on stream interval were ± 15 % and ± 8 % of the average conversion at 300°C and 450°C respectively. The highest deviations occurred at the WHSVs which correspond to the lowest conversions and are due to catalyst deactivation. This indicates that deactivation was slow and steady state can be assumed with respect to conversion after 120 minutes of time on stream.

The initial decrease of the conversion at low WHSVs (0.01 h^{-1}, 0.08 h^{-1}, Figure 3.1.a; 0.02 h^{-1}, Figure 3.1.b) was due to adsorption and dead-time phenomena as the respective carbon balances which are clearly below 100% at short times on stream show (Figure 3.2). The high, initial apparent conversions can thus be ascribed to feed being adsorbed by the zeolite and possibly dead time effects due to very low linear velocities at these extremely low WHSVs. After 120 minutes of time on stream the carbon balances are close to 100% at all WHSVs and temperatures.

A more detailed analysis of the time on stream behaviour at 450°C and a conversion level of 10% is represented in Figure 3.3 using rates of product formation. The initial decrease of these rates is most likely due to rapid initial catalyst deactivation. The high, initial activity may be ascribed to non-regular, highly active sites, e.g. extra-framework aluminium. Such sites are deactivated rapidly. The deactivation may occur via coking, however, because of the small number of sites there was no effect on the carbon balance.

(a)

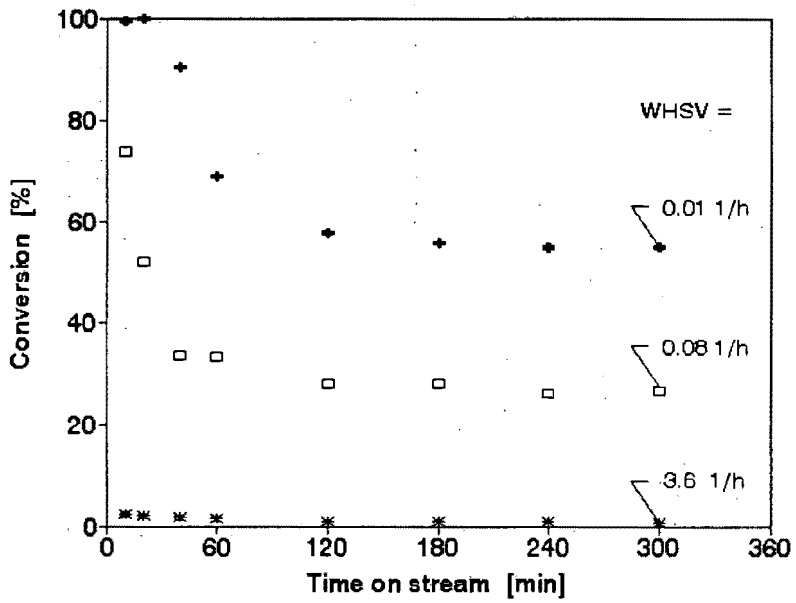

(b)

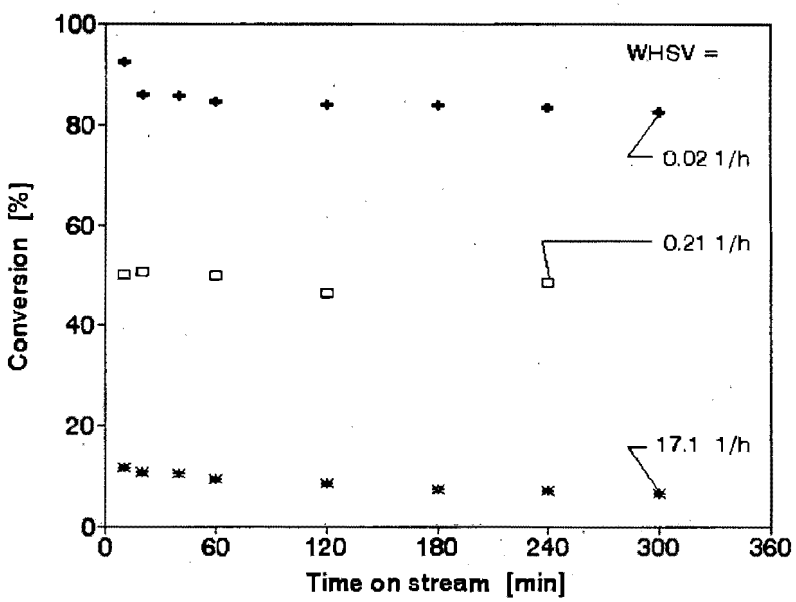

Figure 3.1: **The time on stream behaviour of the 1,2,4-TMB conversion over ZSM-5 at various WHSVs at (a) T=300°C and (b) T=450°C; $p_{1,2,4TMB,in}$=3.5kPa**

(a)

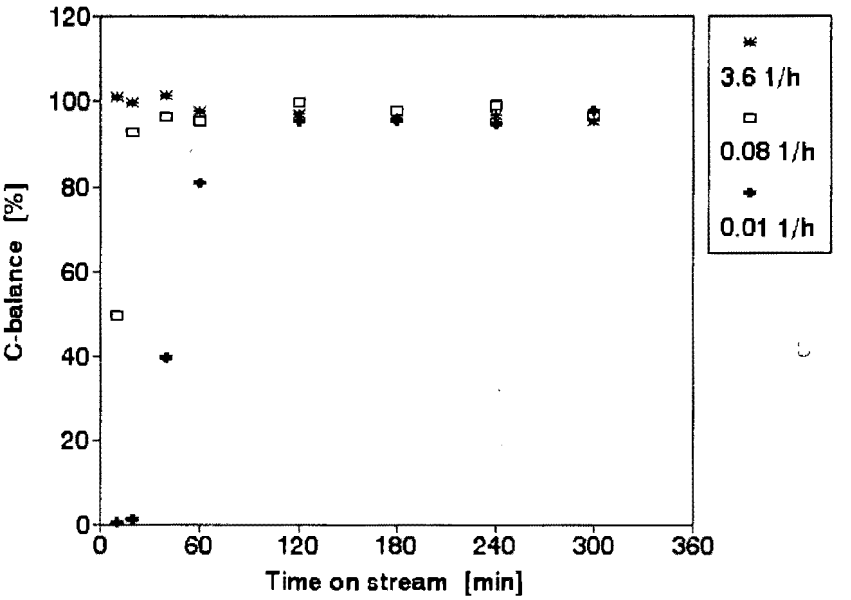

(b)

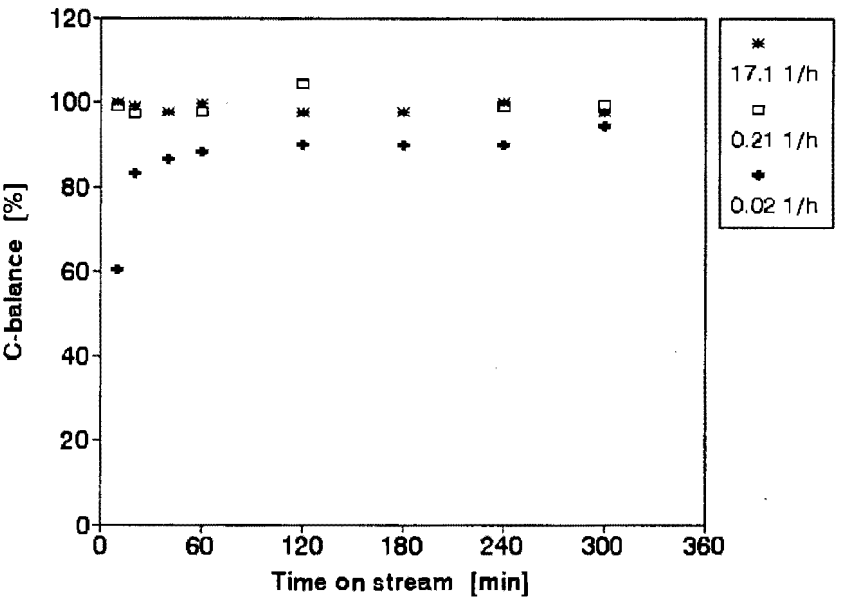

Figure 3.2: **The time on stream behaviour of the carbon balance during the conversion of 1,2,4-TMB over ZSM-5 at various WHSVs at (a) T=300°C and (b) T=450°C; $p_{1,2,4TMB,in}$=3.5kPa**

(a)

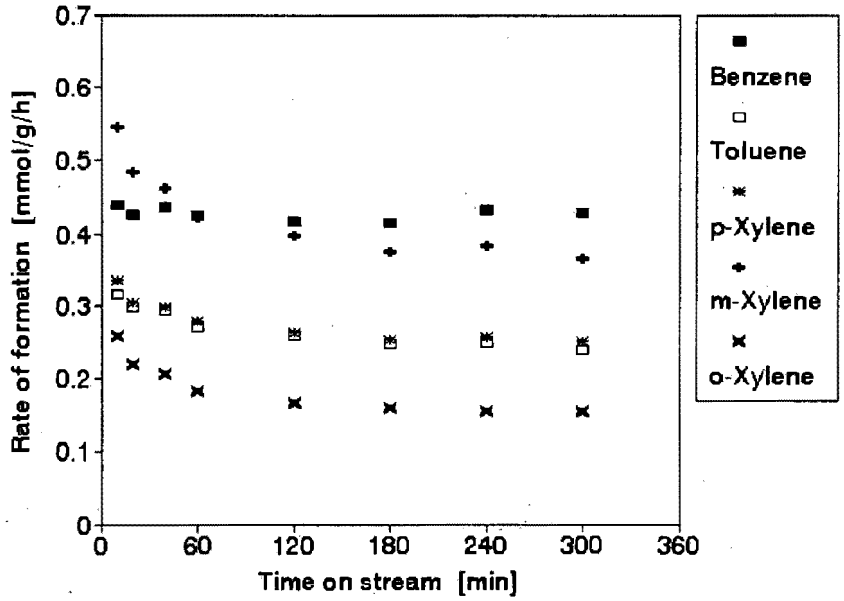

(b)

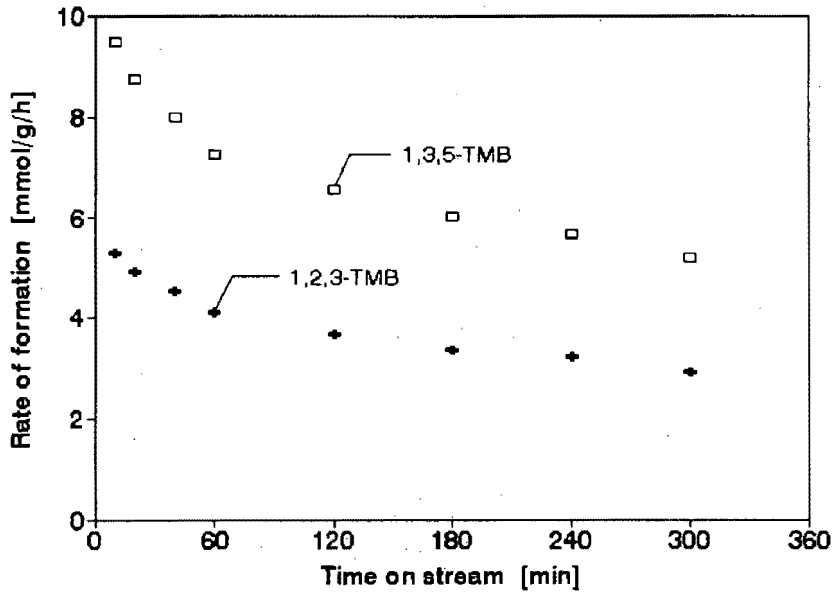

To Figure 3.3

(c)

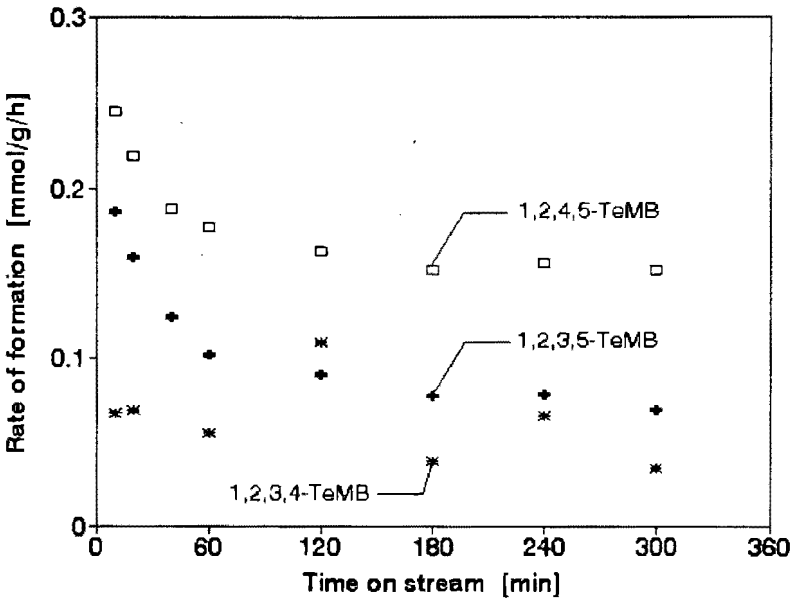

Figure 3.3: The effect of time on stream on rates of product formation during 1,2,4-TMB conversion over ZSM-5 at T=450°C, WHSV=17h^{-1} and $p_{1,2,4\text{-TMB, in}}$=3.5kPa

Initial adsorption and dead time effects can be ruled out since the carbon balance has reached 100% at the shortest time on stream studied (Figure 3.2).

The rates of formation of small product molecules, i.e. benzene, toluene, all xylene isomers and 1,2,4,5-TeMB were constant after 120 minutes of time on stream, whereas the rate of formation of 1,2,3-TMB, 1,3,5-TMB and 1,2,3,5-TeMB still decreased showing that the catalytic system only reached an apparent steady state within the studied time on stream interval with respect to the conversion. For 1,2,3,4-TeMB the scatter was too high to make a conclusive statement on the time on stream behaviour.

3.2.2.2 Effect on selectivity

Figure 3.4 shows the effect of time on stream on the selectivity as represented by selected concentration ratios at 450°C and a conversion level of about 10%. Some of the concentration ratios such as 1,3,5-TMB]/1,2,4,5-TeMB and 1,2,4,5-TeMB/1,2,3,5-TeMB

clearly changed with time on stream, thus confirming that the system did not reach steady state in the studied time on stream interval. Other concentration ratios, such as 1,2,3-TMB/1,3,5-TMB remained constant.

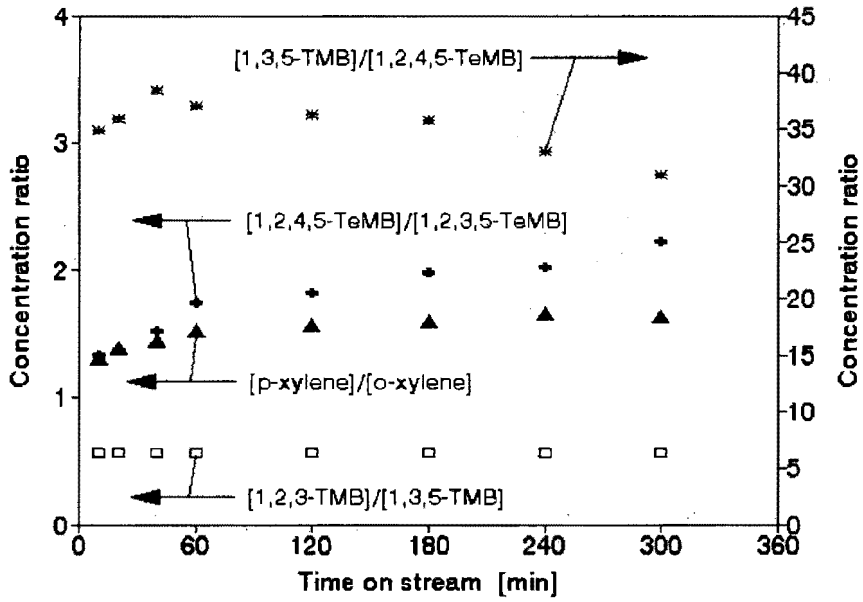

Figure 3.4: The effect of time on stream on the selectivity of ZSM-5 during 1,2,4-TMB conversion at T=450°C, WHSV = 17 h^{-1} and $p_{1,2,4\text{-TMB, in}}$=3.5kPa

Figure 3.5 shows the concentration ratios 1,2,4,5-TeMB/1,2,3,5-TeMB, 1,2,3-TMB/1,3,5-TMB, p-xylene/o-xylene and 1,3,5-TMB/1,2,4,5-TeMB which were obtained at 60 and 240 minutes of time on stream as a function of the conversion. The conversion was changed by variation of the WHSV. The effects of catalyst deactivation on selectivity may be due to the decreasing conversion and / or an increasing degree of coking. Figure 3.5 shows that the effect of coking is clearly smaller than the scatter and can therefore be neglected when compared to the effect of conversion. Catalyst selectivities can thus be compared at any time on stream between 60 and 240 minutes as long as this is done at the same conversion. Chapter 4 and 6 will show that this approximation between 120 and 240 minutes of time on stream at 450°C is sufficient to allow a sensitive observation of catalytic effects.

(a)

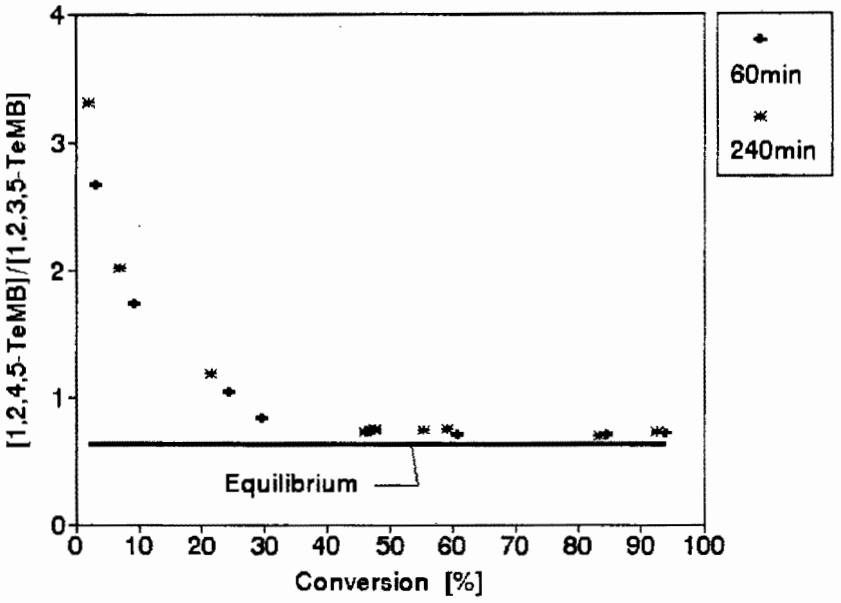

(b)

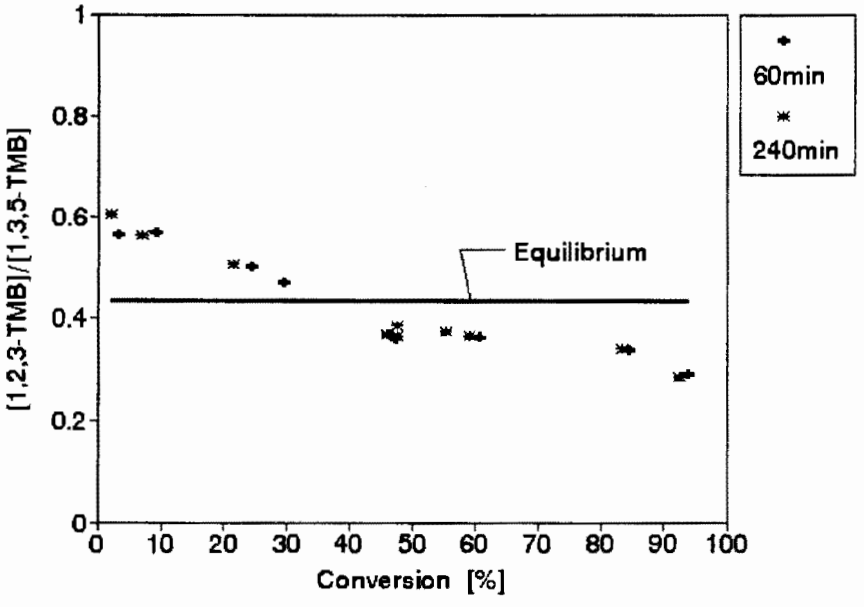

Figure 3.5: **Effect of time on stream on the concentration ratios: (a) [1,2,4,5-TeMB]/[1,2,3,5-TeMB] (b) [1,2,3-TMB]/[1,3,5-TMB] during the conversion of 1,2,4-TMB at T=450°C, $p_{1,2,4\text{-TMB,in}}$=3.5kPa** ***Solid lines: Thermodynamic equilibrium [Stull et al., 1969]***

(c)

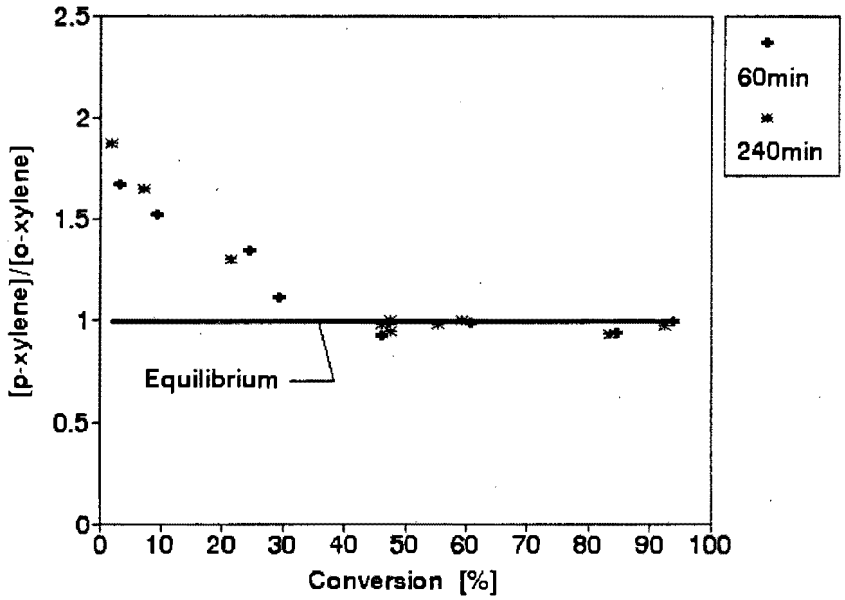

(d)

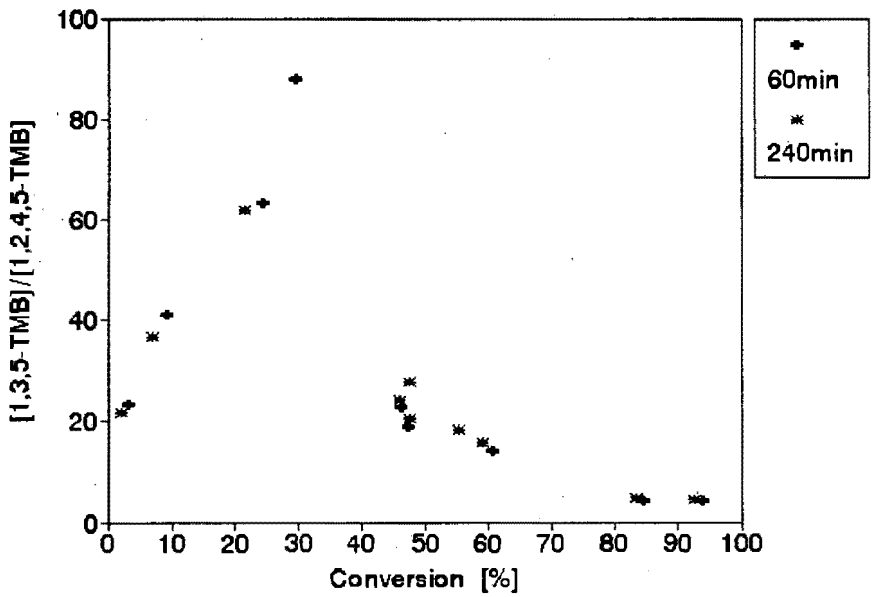

Figure 3.5: **Effect of time on stream on the concentration ratios:**
(c) [p-xylene]/[o-xylene] (d) [1,3,5-TMB]/[1,2,4,5-TeMB]
during the conversion of 1,2,4-TMB at T=450°C, $p_{1,2,4\text{-TMB,in}}$=3.5kPa
Solid lines: Thermodynamic equilibrium [Stull et al., 1969]

3.2.3 Reaction network

This section investigates the reaction network which describes the conversion of 1,2,4-TMB over ZSM-5. This was done by using concentration versus space time data and analysing the product distributions of samples taken at 240 minutes of time on stream. The experiments were carried out as described in Section 2.3.2.3 and the calculation of product concentrations is shown in Section 2.3.4.3. The reaction conditions of each experiment are given in Appendix V.

3.2.3.1 Primary reactions

The relation between the conversion, the concentration of 1,2,4-TMB at the reactor outlet and the modified space time (reciprocal WHSV) is shown in Figure 3.6.

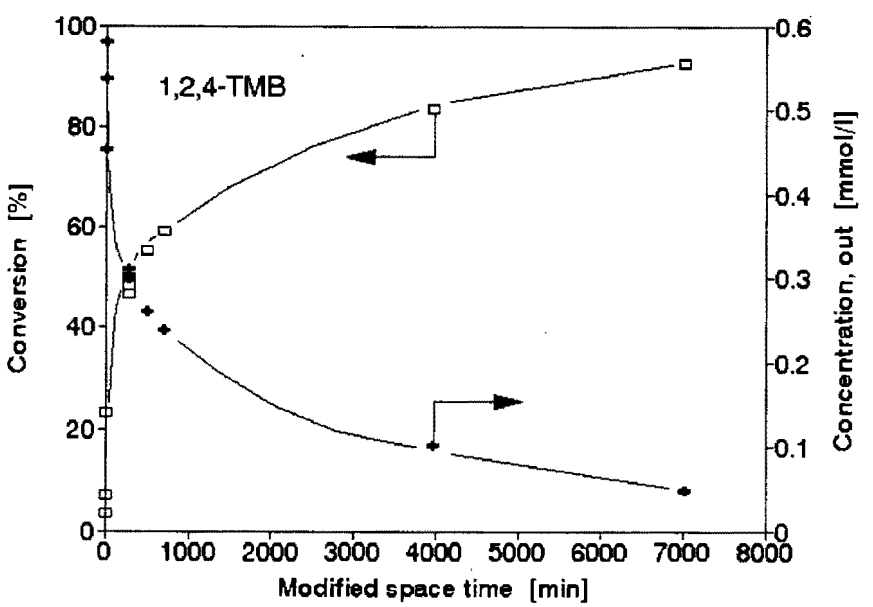

Figure 3.6: Conversion and concentration of 1,2,4-TMB at the reactor outlet versus modified space time for ZSM-5 at T=450°C and $p_{1,2,4\text{-TMB,in}}$ =3.5kPa

Figures 3.7 to 3.10 show product concentrations of the C_1 to C_4 aliphatics, benzene, toluene, xylenes, TMBs and TeMBs as a function of modified space time. While Figures

3.9 and 3.10 show the entire modified space time range investigated, Figures 3.7 and 3.8 magnify the profiles between zero and 500 min. The shapes of the curves for the individual isomers within the xylene, TMB and TeMB fraction were qualitatively identical to the shape of the lumped curve representing the respective aromatic fraction and are not expanded.

Figures 3.7 and 3.8 focus on the slopes at the origin. According to the mass balance for a plug flow reactor and a constant density system, the rates of product formation equal the slopes of curves in concentration versus space time plots [Levenspiel, 1972]. For consecutive reactions the time-concentration curve for the secondary and all following products has a zero slope at low contact times, whereas for products which are formed in primary reactions the slope is greater than zero [Levenspiel, 1972]. According to this criterion the following appear to be primary products in this reacting system: methane (Figure 3.9), ethene, propene, toluene, xylenes, 1,2,3-TMB, 1,3,5-TMB and the TeMB isomers. The initial rates of product formation were determined in the modified space time interval between 0 and 4 minutes and are listed in Table 3.1. It should be noted that these rates were determined at low conversion levels and were subject to a relatively high scatter. The initial rates in Table 3.1 should therefore be considered as semi-quantitative.

The presence of benzene and C_4-aliphatics at even very short modified space times in combination with a zero slope (Figure 3.11) shows that these compounds were not formed from 1,2,4-TMB. At short modified space times the formation of these compounds is attributed to the fast and complete dealkylation of butyl-benzene isomers which occur as impurities in the 1,2,4-TMB feed. Peaks which indicate such impurities appear in the vicinity of the 1,2,4-TMB peak in the GC-trace of the feed (Figure IV.3, Appendix IV). However, due to insufficient GC-separation and lack of reference compounds only some of these impurities could be identified. Both the concentration of benzene and of the C_4-aliphatics were therefore corrected by subtracting the concentration of the latter (0.0011 mmol/l) at space times close to zero (Figure 3.11). The corrected data are shown in Figures 3.7 to 3.10. These corrected concentration versus modified space time plots clearly indicate that the non-initial benzene and C4-aliphatics originate from 1,2,4-TMB

and that they are formed via a series of consecutive reactions. The dealkylation of butyl-benzenes accounts for approximately 75% of the initial formation of benzene (Figure 3.12). The residual 25% may be assigned to the dealkylation of propyl-benzene feed impurities. This is supported by the equimolar formation of propene and the corrected amount of benzene at conversions close to zero (Figure 3.13).

In a similar way the concentration versus modified space time curves of ethene and toluene should suffer from an initial offset from the x-axis due to the dealkylation of methyl-ethyl-benzenes which also occur as impurities in the 1,2,4-TMB feed. This would be consistent with the equimolar formation of ethene and toluene at conversions close to zero (Figure 3.13).

The initial slopes of the concentration versus modified space time plots for ethene, propene (Figure 3.7) and toluene (Figure 3.8) were greater than zero indicating that these compounds are also formed from 1,2,4-TMB even at modified space time close to zero. The effect of feed impurities was considered negligible regarding the scatter and no further corrections were made.

It might be argued that the C_2- to C_4-aliphatics are formed via dealkylation from feed impurities only. However, their formation with a concentration of approximately 0.17 mmol/l at 7000 minutes modified space time (Figure 3.9) as compared to the feed inlet concentration of approximately 0.6 mmol/l (=: $p_{1,2,4\text{-TMB,in}}$=3.5kPa at 450°C) would require a feed impurity of approximately 25 mol-% as compared to an actual impurity of about 2 mol-% only.

The only primary reaction yielding 1,2,3-TMB and 1,3,5-TMB is the isomerisation of 1,2,4-TMB, whereas transalkylation is the only reaction of a pure methyl-aromatic feed which yields higher substituted rings as a primary product.

Lower substituted methyl-aromatics can be formed via two reaction pathways, viz. transalkylation and possibly dealkylation. At a glance the formation of the observed

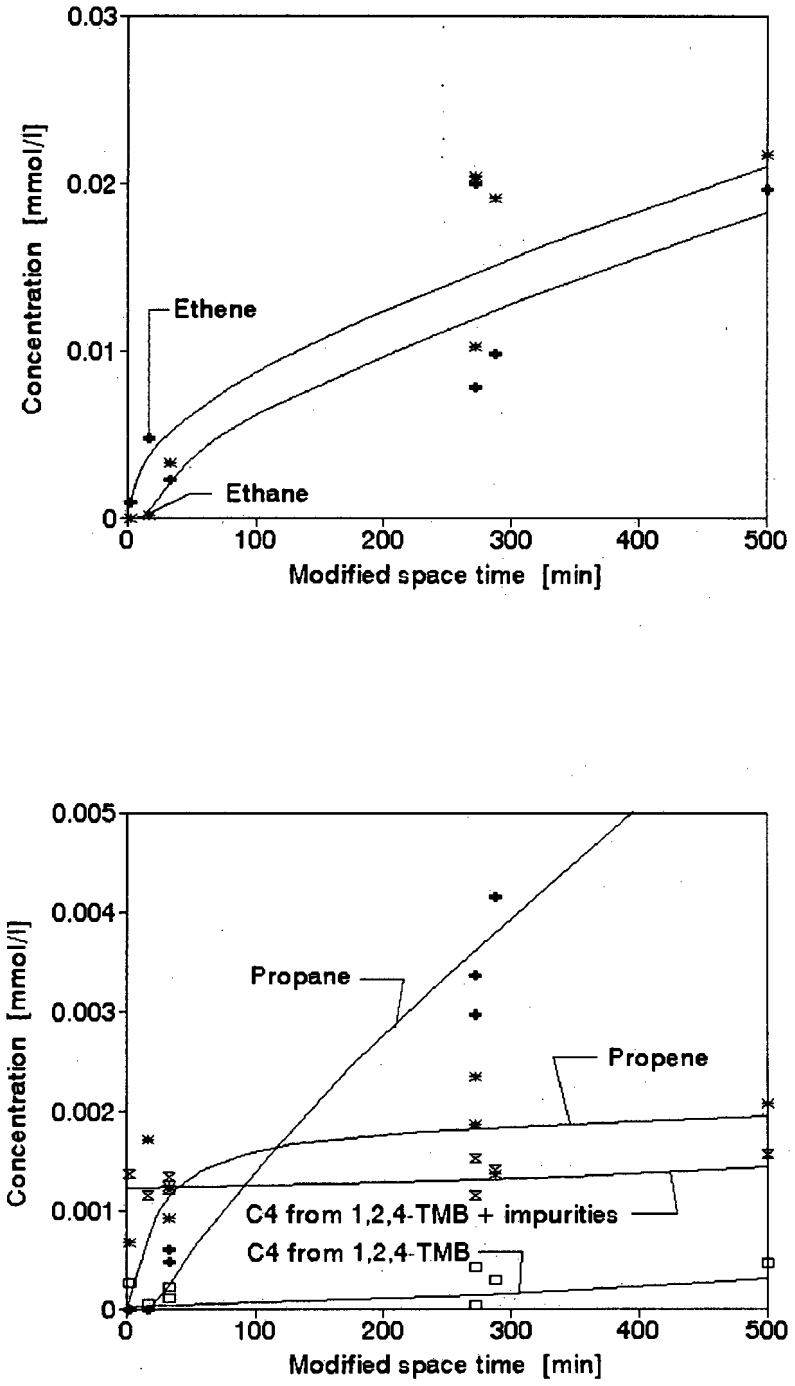

Figure 3.7: **Product concentrations of the C_2-C_4 aliphatics during the conversion of 1,2,4-TMB over ZSM-5 for short modified space times at T=450°C, $p_{1,2,4\text{-TMB, in}}$ = 3.5kPa (Total studied space time range see Figure 3.9)**

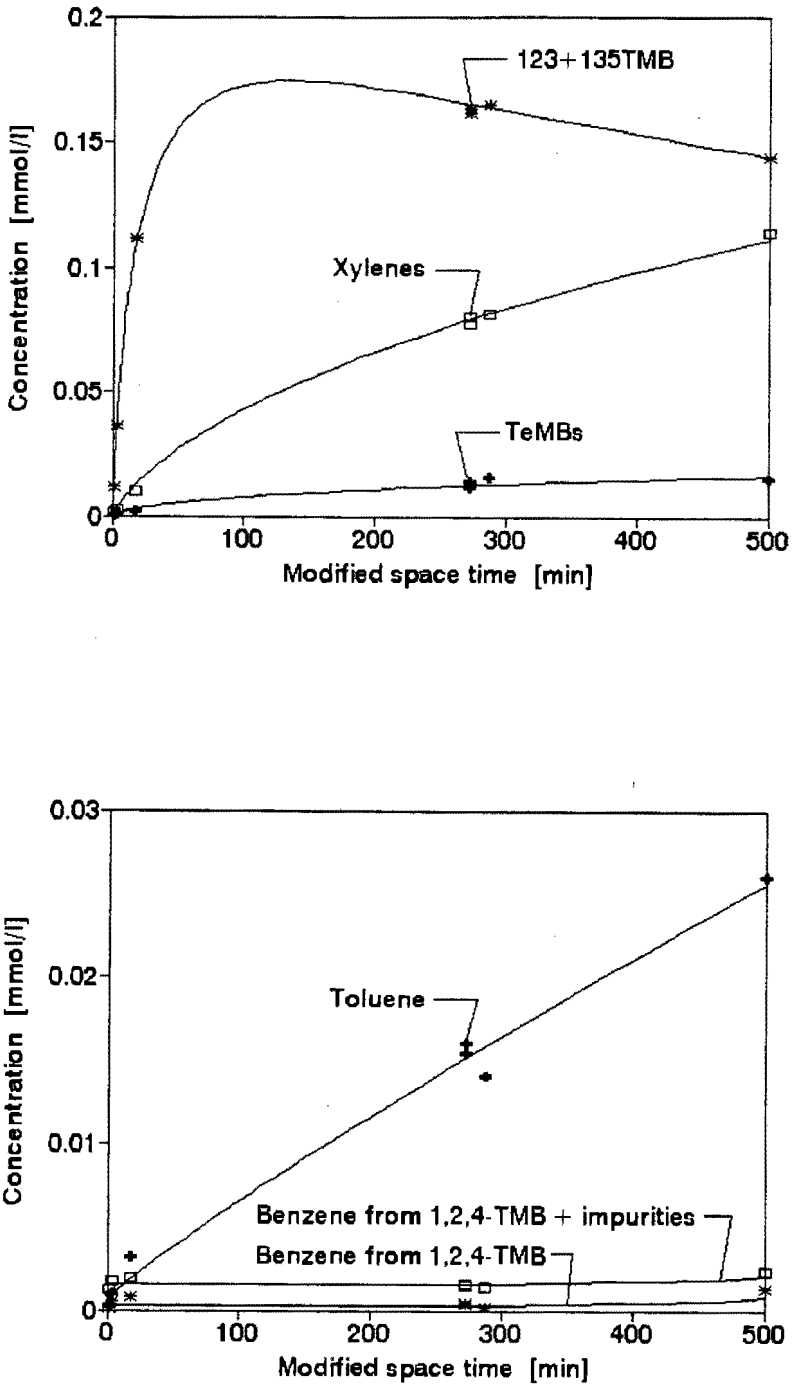

Figure 3.8: **Product concentrations during the conversion of 1,2,4-TMB over ZSM-5 for short modified space times at T=450°C, $p_{1,2,4\text{-TMB, in}}$= 3.5kPa (Total studied space time range see Figure 3.10)**

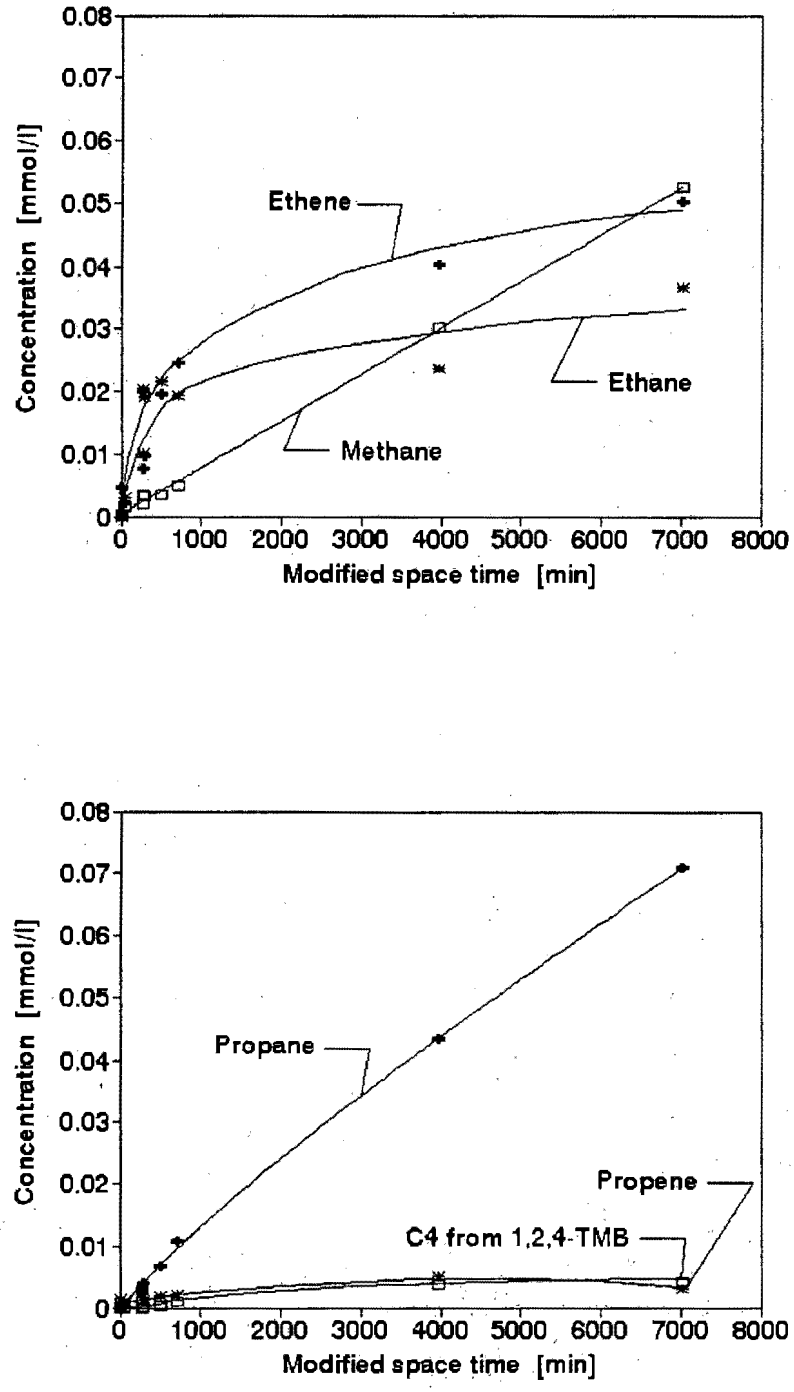

Figure 3.9: **Product concentrations of the C_1-C_4 aliphatics during the conversion of 1,2,4-TMB over ZSM-5 as a function of modified space time at T=450°C, $p_{1,2,4\text{-TMB, in}}$= 3.5kPa (Magnification of short space times see Figure 3.7)**

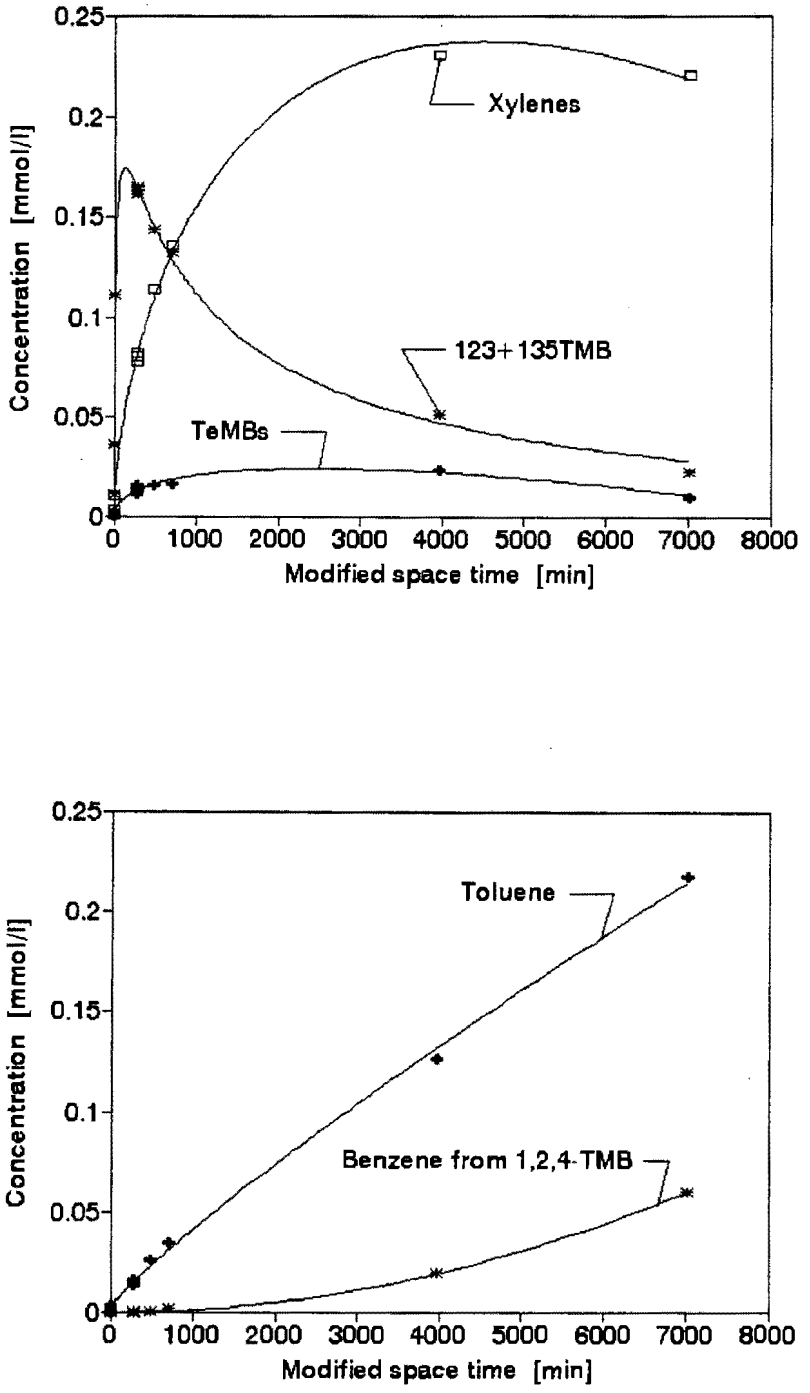

Figure 3.10: **Product concentrations during the conversion of 1,2,4-TMB over ZSM-5 as a function of modified space time at T=450°C, $p_{1,2,4\text{-TMB},\ in}$= 3.5kPa (Magnification of short space times see Figure 3.8)**

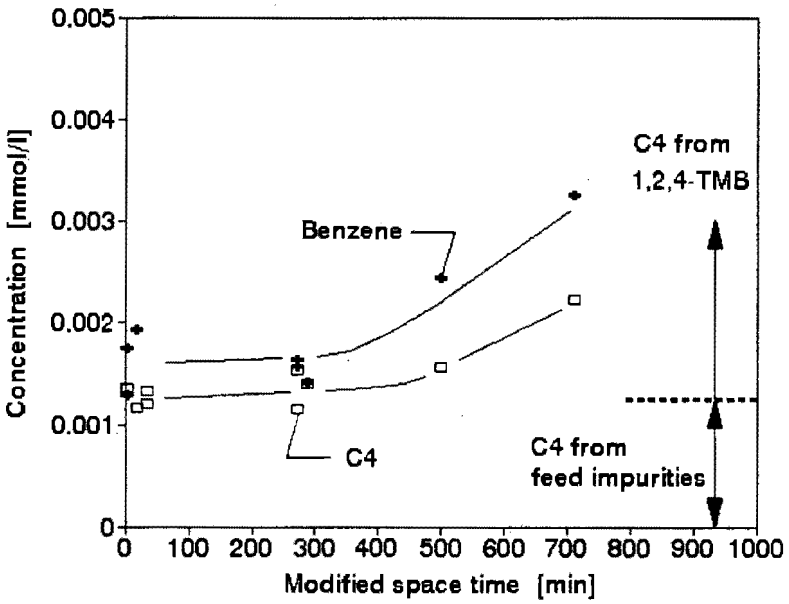

Figure 3.11: **Product concentrations of the C_4 aliphatics in comparison to benzene during the conversion of 1,2,4-TMB over ZSM-5 for short modified space times at T=450°C, $p_{1,2,4\text{-TMB, in}}$= 3.5kPa**

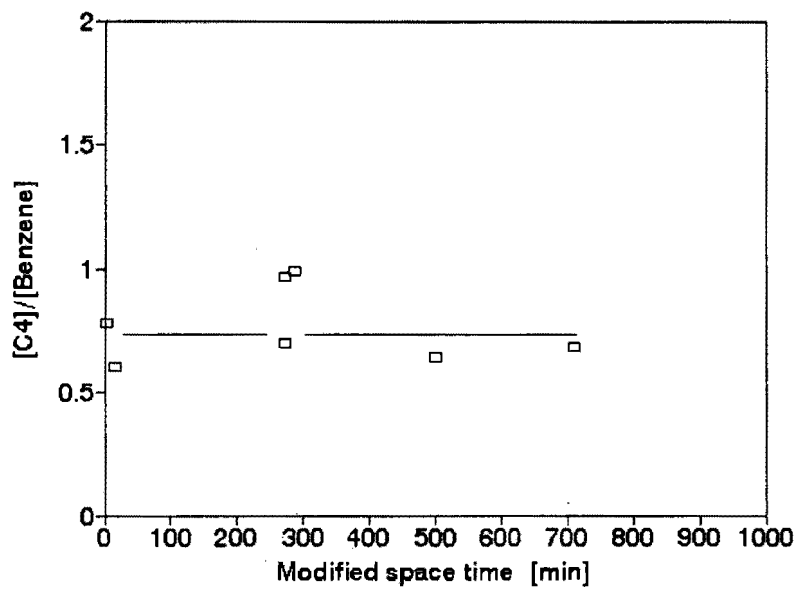

Figure 3.12: **The concentration ratio [C_4]/[Benzene] for short modified space times during the conversion of 1,2,4-TMB over ZSM-5 at T=450°C, $p_{1,2,4\text{-TMB, in}}$=3.5kPa**

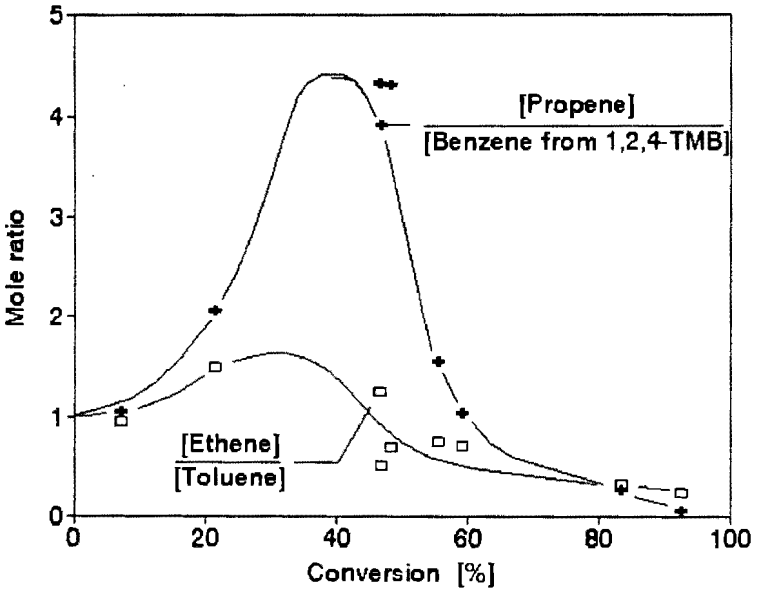

Figure 3.13: **The concentration ratios [Ethene]/[Toluene] and [Propene]/[Benzene] as a function of the 1,2,4-TMB conversion over ZSM-5 at T=450°C and $p_{1,2,4\text{-TMB, in}}$=3.5kPa**

aromatic products could be ascribed to well known, acid catalysed reactions as follows [(1)=primary, (2)=secondary; Is=Isomerisation, T=Transalkylation]:

i)	1,2,3-TMB and 1,3,5-TMB:	Is (1)
ii)	TeMBs	T (1)
iii)	Xylenes	T (1)
iv)	Toluene, Benzene	Repeated T (2)

However, none of these reactions yields CH_4 and C_2 to C_4 aliphatics. Thus the reactions forming these products still need to be identified. Methane is a typical by-product of coke formation during methanol conversion and may be formed by thermal demethylation of coke precursors [Schulz *et al.*, 1987]. The methane observed during the transformation of 1,2,4-TMB may thus also be attributed to the formation of coke. Nevertheless the concentration versus modified space time plot indicates methane as a primary product.

This presupposes that methane might be formed from 1,2,4-TMB via demethylation. This is very unlikely and therefore CH_4 is classified as a pseudo-primary product.

Table 3.1: Product types and semi-quantitative initial rates of product formation during the conversion of 1,2,4-TMB over ZSM-5 as determined from concentration versus modified space time plots; (1)=primary product; (2)=product of consecutive reactions

Product	Product Type	Maximum in the observed space time range (0-7000min)	initial rate (μmol/h/l)	initial specific rate (μmol/h/g_{cat})
methane	1[a]	No	3	45
ethene	1[a]	No	4	60
ethane	2[d]	No	0[d]	0[d]
propene	1[a]	Yes	1	15
propane	2[d]	No	0[d]	0[d]
C_4	2[d]	No	0[d]	0[d]
benzene	(1[a] and 2)[e]	No	0	0
toluene	1[a]	No	15	200
xylenes	1	Yes	55	800
1,2,3-TMB+1,3,5-TMB [b]	1	Yes	600	8500
TeMBs [c]	1	Yes	20	300

[a] pseudo-primary product (Def.: a product which is formed in consecutive reactions but appears at conversions close to zero indicating the last reaction to be much faster than the preceding ones)
[b] Trimethylbenzenes
[c] Tetramethylbenzenes
[d] Vide the first data points in Figure 3.7
[e] From mechanistic context. Not that important as to be visible in the respective plots. See zero initial rate in Figure 3.8

3.2.3.2 Evidence for the paring reaction

The C_2 to C_4 aliphatics indicate cracking. However, cracking of the aromatic ring is known to be kinetically highly restricted even at 450°C [Weitkamp, 1998] and additionally could be ruled out by an aromatic ring balance which was always equal or above the carbon balance (Figure 3.14).

Figure 3.15 shows that the average carbon number of aromatics decreased from 9 to approximately 7.5 at 7000 minutes modified space time therefore indicating that a kind of dealkylation takes place and / or that higher substituted aromatics e.g. TeMBs are consumed in the formation of coke. The latter is supported by the aromatic ring-balance decreasing in correspondence to the carbon balance (Figure 3.14). The coke yield of 10% at 90% conversion, however, is not high enough to justify the shift of the average carbon number per aromatic compound from 9 to 8.

Figure 3.16 shows that the average number of methylgroups per aromatic ring in the transalkylation product (benzene, toluene, xylenes and TeMBs) was clearly below the value of 3 for the 1,2,4-TMB feed even at conversions approaching zero. If only transalkylation and isomerisation would take place this ratio would equal 3.

When the carbon in the C_2 to C_4 aliphatics was added to the carbon in the aromatic methyl-groups, this ratio did indeed approach a value of 3 at zero conversion. If cracking of aromatic rings would occur this ratio would be expected to be larger than 3. The ratio approaching 3 at conversions close to zero thus confirms that the possibility of aromatic ring cracking could be ruled out. This and the aromatic ring balance show that the C_2 to C_4 aliphatics originate from methyl-groups and that a kind of secondary (or pseudo-primary, see below) dealkylation reactions do occur.

Figure 3.16 shows that this dealkylation type reaction was responsible for the disappearance of a third of the methyl-groups which should have been in the transalkylation product at conversions close to zero. More than 20% of the methyl groups contained in the 1,2,4-TMB feed were converted to C_2-C_4 aliphatics at 90% conversion as shown in Figure 3.17. Therefore this reaction is relevant.

The decrease of both ratios in Figure 3.16 with increasing conversion may be assigned to consecutive aromatisation of the olefins and/or the consumption of aromatics which are higher substituted than the 1,2,4-TMB feed during the formation of coke. The formation of coke from TeMBs is consistent with the decreasing aromatic ring balance (Figure 3.14)

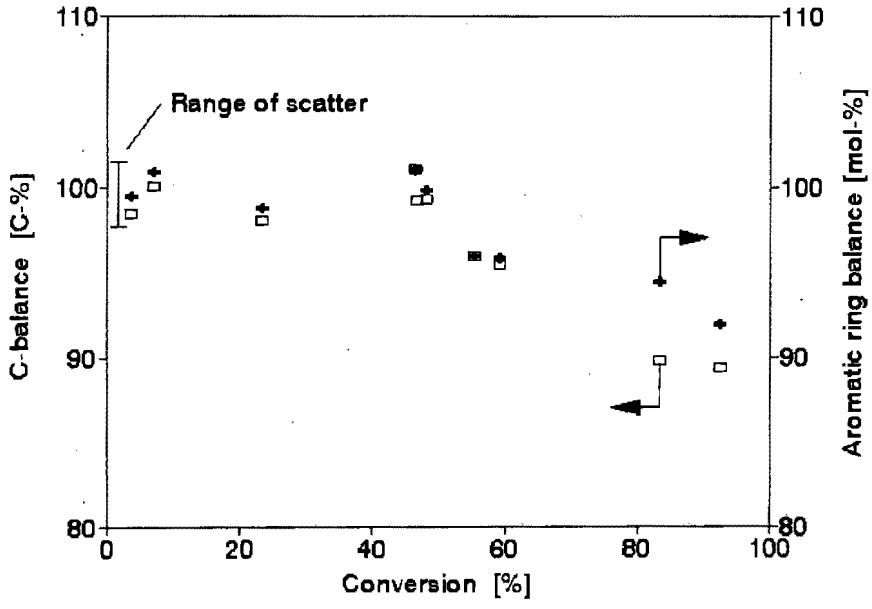

Figure 3.14: Carbon- and aromatic-ring-balance during the conversion of 1,2,4-TMB over ZSM-5 as a function of modified space time at T=450°C, $p_{1,2,4\text{-TMB, in}}$=3.5kPa

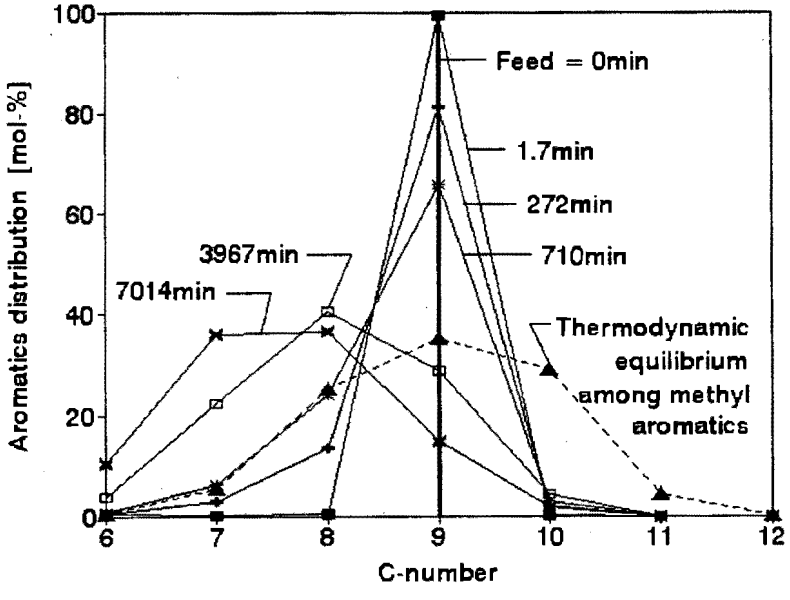

Figure 3.15: The aromatic carbon number distribution as a function of the modified space time during the conversion of 1,2,4-TMB over ZSM-5 at T=450°C, $p_{1,2,4\text{-TMB, in}}$=3.5kPa

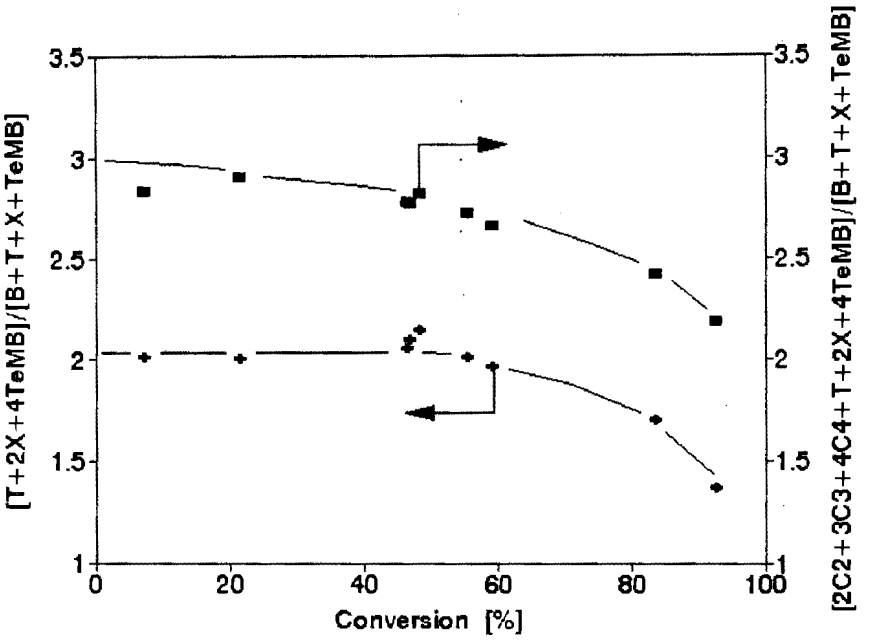

Figure 3.16: The ratio of methylgroups to aromatic rings in the transalkylation product versus 1,2,4-TMB conversion over ZSM-5 at T=450°C, $p_{1,2,4\text{-TMB, in}}$=3.5kPa

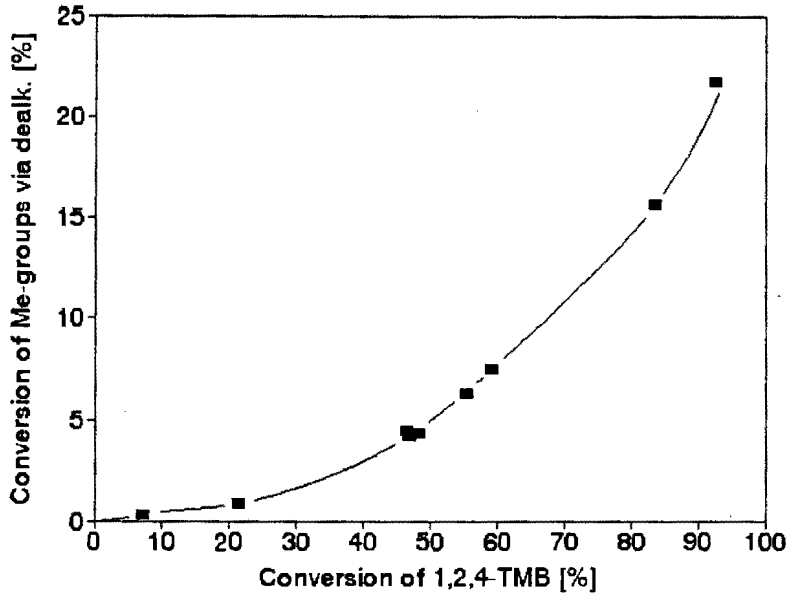

Figure 3.17: The conversion of methyl groups via dealkylation to C_2- to C_4-aliphatics, i.e. $\{2x[C_2]+3x[C_3]+4x[C_4]\}/\{3x[1,2,4\text{-TMB}_{in}]\}$ x 100%, versus the conversion of 1,2,4-TMB over ZSM-5 at T=450°C, $p_{1,2,4\text{-TMB, in}}$=3.5kPa

and the formation of methane (Figure 3.9) at increasing conversion. The aromatisation of olefins (which can include coke) is indicated by the formation of paraffins (Figure 3.9) which would be the hydrogen-rich co-product.

The dealkylation of alkylaromatics over solid acid cracking catalysts to form olefins is a known reaction [Greensfelder et al., 1945, 1949; Rase and Kirk, 1954]. However, only alkylgroups with 2 and more carbon atoms dealkylate readily without the need of hydrogen. Figure 3.7 shows that mainly ethene and propene were formed at short modified space times, thus being primary or better to say pseudo-primary products, whereas ethane and propane are indicated as secondary products.

As a hypothetical reaction path it is therefore proposed that 1,2,4-TMB isomerises to methyl-ethyl-benzenes, and propylbenzene. The former of which was observed in minor amounts in the product as shown in Figure IV.5 (Appendix IV). The dealkylation of these intermediates would then yield ethene plus toluene and propene plus benzene respectively. This reaction path is supported by the equimolar formation of ethene and toluene, and propene and benzene at conversions close to zero (Figure 3.13).

Sullivan *et al.* [1960] reported a similar reaction when hexamethylbenzene was converted over a nickel sulphide on silica-alumina catalyst in the presence of hydrogen and termed it the paring reaction. The observation of lower molecular weight methylbenzenes and light isoparaffins, particularly isobutane as products led to the proposal of this reaction, which in its apparent effect, peels or pares methyl groups from the aromatic ring forming iso-paraffins with essentially no loss of aromatic rings.

The paring reaction was also shown to occur on the silica-alumina support in the absence of nickel sulphide and hydrogen. This showed that the paring reaction also occurs on strongly acidic monofunctional catalysts [Sullivan *et al.*, 1960].

The mechanism proposed by Sullivan *et al.* [1960] involves a repeated contraction to a five-membered ring followed by expansion to a six-membered ring to produce side chain

growth by isomerisation. The cyclopentadienyl cationic intermediates postulated in this mechanism were derived from a similar intermediate proposed by Condon [1958] to occur during the formation of ethylbenzene from xylene. The discussion of mechanisms which involve contractions and expansions of aromatic rings is still actual. The contraction of the aromatic ring is for example part of the monomolecular 1,2-methyl-shift-isomerisation mechanism (Figure 1.16, Section 1.6.2) [Corma *et al.*, 1979, Martens *et al.*, 1988].

Sullivan *et al.*, [1960] reported an absence of large amounts of intermediate product aromatics having ethyl and propyl side chains during the paring reaction, which also applies for the present work. This was interpreted in terms of adsorbed species which do not desorb from the catalyst before the side chain is eliminated by cracking.

Sullivan *et al.* [1960] reported that the yield of methane and ethane in the paring reaction was low because of the difficulty of cleaving a methyl or ethyl group from the ring. Propyl groups are dealkylated somewhat more readily. However, an alkyl group containing four or more carbons cleaves rapidly. Correspondingly the paring reaction of C9-aromatics, which can form propyl side chains at the most, was found to occur to a smaller extent than with hexamethylbenzene.

In conclusion the corresponding reaction path which occurs during the transformation of 1,2,4-TMB over ZSM-5 will be referred to as paring reaction in the following.

3.2.3.3 Secondary reactions

Figure 3.32 shows that within the range of scatter the molar ratio [xylenes]/[TeMB] approaches 1 at zero conversion which is also observed when silica-alumina was used as catalyst. However, this ratio increases with increasing conversion. If only transalkylation took place, the molar ratio of xylenes to TeMBs would have been one. The surplus of xylenes observed thus indicates one or both of the following possibilities:

i) TeMBs may be trapped in the channel intersections as coke precursors and consumed in consecutive reactions. The formation of coke was indicated by a grey

colour of the catalyst after reaction, the formation of methane (Figure 3.9) and a decreasing carbon balance with increasing conversion from near to 100% to 90% (Figure 3.14). The missing carbon given by the deviation from 100%, may be interpreted as coke or coke precursors retained on the catalyst surface or trapped in the channel intersections.

ii) Xylenes may be formed via another reaction path occurring parallel to the transalkylation of 1,2,4-TMB. Similar to 1,2,4-TMB the TeMBs are also expected to undergo the paring reaction with di-methyl-ethyl-benzenes, di-ethyl-benzenes, methyl-propyl-benzenes and butyl-benzenes as non-desorbing intermediates. Dealkylation of these intermediates would yield amongst others xylenes at the same time consuming TeMBs. Similarly xylene is expected to form ethyl-benzene (Figure IV.5, Appendix IV).

The curves representing (1,2,3-TMB + 1,3,5-TMB), TeMBs and xylenes each show a maximum (Figure 3.10), indicating that these primary products are intermediates which are consumed in secondary reactions [Levenspiel, 1972]. 1,2-Methyl-shift-isomerisation, transalkylation and the paring reaction as discussed above are likely to occur not only as primary reactions of 1,2,4-TMB, but also as secondary reactions of all aromatic products. Transalkylation between benzene, toluene, xylenes, TMBs and TeMBs are further possible secondary reactions. The concentration versus modified space time plots for benzene, toluene and the C_1-C_4 aliphatics did not show maxima within the investigated range of space time (Figures 3.9 and 3.10). The respective classification of the various products is summarised in Table 3.1 (Section 3.2.3.1).

Mechanistically secondary products, such as CH_4, ethene, propene and toluene, which are indicated as primary products by concentration versus modified space time plots are termed as pseudo-primary products in this work. Pseudo-primary product kinetics in a plug flow reactor can result from two types of consecutive reactions:

i) the secondary reaction is very fast relative to the primary reaction

ii) once adsorbed the molecule undergoes several reaction steps in the adsorbed state without desorption/readsorption in between. This especially applies to molecules

with a low diffusivity in the micropores of ZSM-5, such as poly-alkyl-aromatics.

The mechanistic classification of the pseudo-primary product toluene as a secondary product is supported by the work of Ko and Kuo [1994]. Converting 1,2,4-TMB over zeolite HY, they proposed toluene to be a secondary product, formed by transalkylation of xylene. Although their lowest conversion was 10% and the curve had to be extrapolated in order to determine the slope at zero conversion their proposal should be mechanistically correct. In the present work modified space times yielding conversions down to 2% were investigated clearly indicating toluene as a pseudo-primary product.

Toluene may be formed via two parallel reaction pathways:

i) consecutive transalkylation with xylenes as intermediates and

ii) the earlier discussed paring reaction of 1,2,4-TMB yielding toluene and ethene via intermediate methyl-ethyl-benzenes.

The equilibrium constant for the paring reaction assuming an ideal gas is Kp=0.14 while the stoichiometry indicates that the products are favoured at low partial pressures. The formation of toluene via this reaction path would be accompanied by an equimolar formation of ethene. Figure 3.13 shows that this was the case when extrapolating to zero conversion.

In a similar way benzene may be formed via consecutive transalkylation reactions with xylene and toluene as intermediates and the paring reaction of 1,2,4-TMB with propyl- and iso-propyl-benzene as intermediates.

3.2.3.4 Reaction network models

The reaction network as illustrated in Figure 3.18 summarises the mechanistic pathways proposed above. At low conversion levels most secondary and reverse reactions are negligible. The reaction may then be described by a network model as simple as the one illustrated in Figure 3.19 which is more suited for the application of this reaction as probe reaction as will be discussed in Chapter 6.

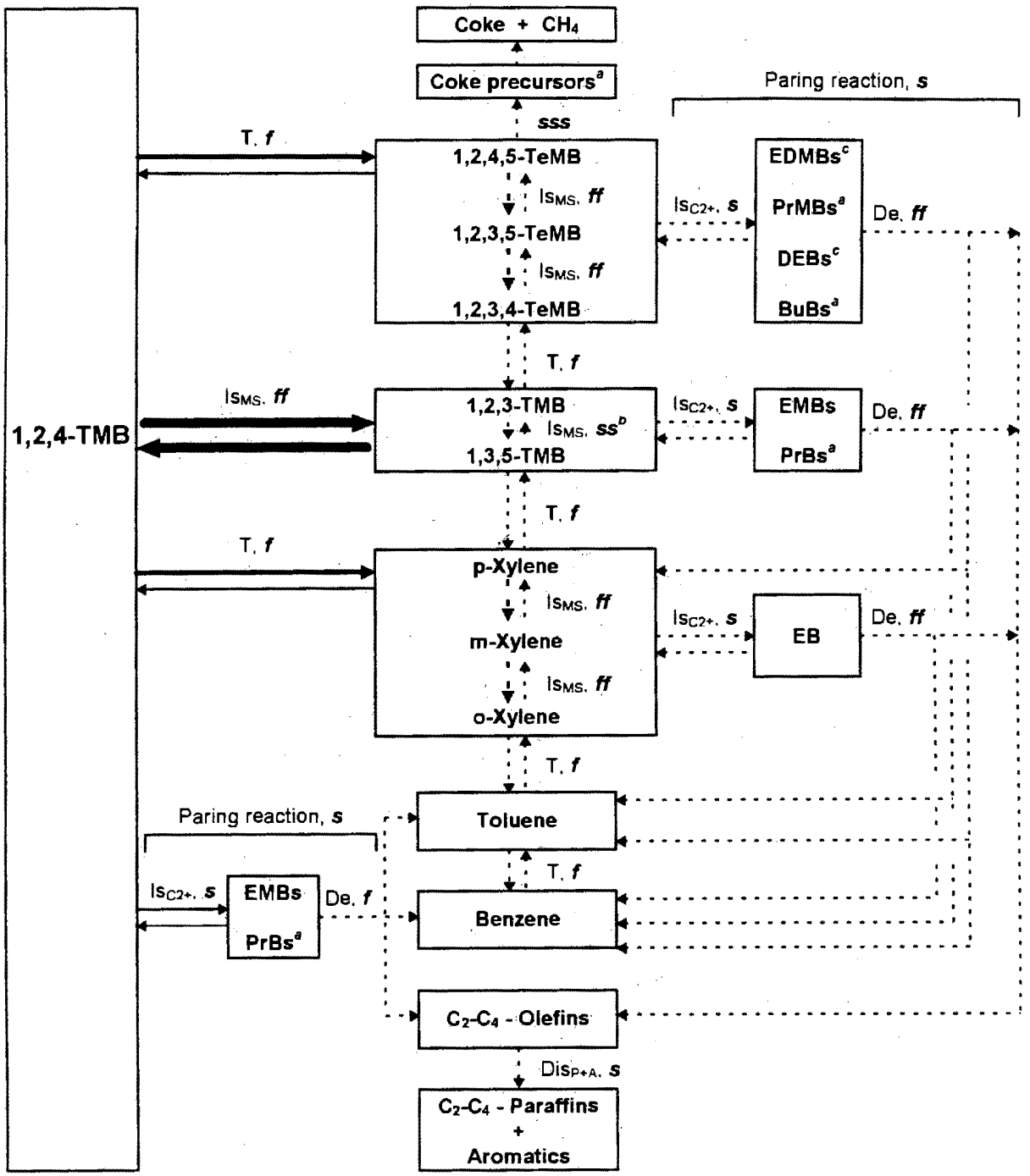

Figure 3.18: **Reaction network model for the conversion of 1,2,4-TMB over ZSM-5 at T=450°C and $p_{1,2,4\text{-TMB, in}}$=3.5kPa**

i) **Is_{MS}:** Isomerisation via 1,2-methyl-shift
T: Transalkylation
Is_{C2+}: Rearrangement of methyl-groups to form C_2^+-alkyl-groups
De: Dealkylation of C_2^+-alkyl-groups
Dis_{P+A}: Olefin conversion to paraffins and aromatics

ii) **f:** fast; **s:** slow

iii) **solid lines:** primary reactions; **dashed lines:** secondary reactions

[a] *product not observed* [b] *isomerisation via 1,2,4-TMB*

[c] *peaks observed in the expected range, but not identified (Figure IV.5)*

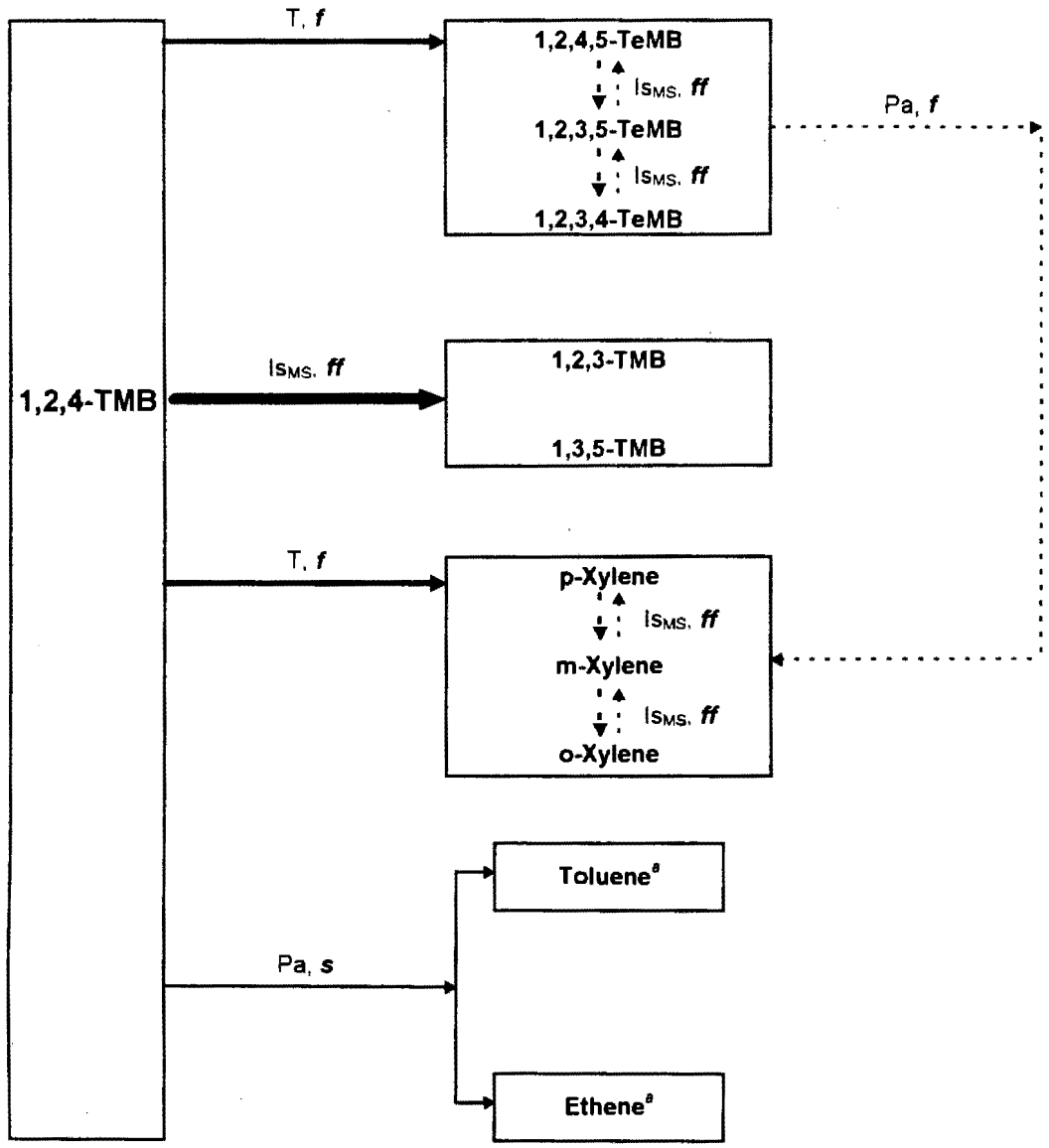

Figure 3.19: **Simplified reaction network model for the transformation of 1,2,4-TMB over ZSM-5 at conversions close to zero, T=450°C and $p_{1,2,4\text{-TMB},\,in}$=3.5kPa**

i) **Is_{MS}:** Isomerisation via 1,2-methyl-shift
T: Transalkylation
Pa: Paring reaction: Rearrangement of methyl-groups to form C_2^+-alkyl-groups followed by dealkylation

ii) **f:** fast; **s:** slow

iii) **solid lines:** primary reactions; **dashed lines:** secondary reactions

[a] *Pseudo-primary product*

The transalkylation and isomerisation reactions in the reaction network shown in Figure 3.18 are consistent with the findings of Ko and Kuo [1994] for the conversion of 1,2,4-TMB over HY zeolite. However, since their reaction temperatures were between 200°C and 300°C, compared to 450°C in the present work, only negligible amounts of light products were observed. In contrast to the observations in this work they found the transalkylation reaction to be faster than the isomerisation reaction. This may be due to various factors, such as the different reaction temperatures, feed partial pressure and the zeolite type (pore size, Si/Al).

Ko and Kuo [1994] found toluene to be a secondary product formed via consecutive transalkylation reactions only. This suggests that the paring reaction observed in this work is promoted by higher reaction temperatures and possibly by the ZSM-5 structure. Ko and Kuo observed only traces of benzene without considering it in their proposed reaction network. They also reported a significant amount of pentamethylbenzene, which was not observed in the present work, due to the pores of ZSM-5 being smaller than those of zeolite HY.

3.2.3.5 Selectivities

The primary reactions in Figure 3.19, i.e. isomerisation, transalkylation and the paring reaction were ranked with respect to their initial rates using the initial rates of product formation listed in Table 3.1 and Equations 2.11 to 2.13 (Section 2.3.4.6.). Figure 3.20 shows that the selectivities on ZSM-5 towards these reactions are constant up to a conversion of at least 25%. This shows that at conversions below 25% the primary reactions of 1,2,4-TMB occur in parallel to each other and that the corresponding rates of product formation are not affected by secondary and reverse reactions. At higher conversions the consumption and / or formation of products in secondary and / or reverse reactions becomes significant and the observed rates of product formation do not correlate with the respective reaction rates in the simple manner as described by Equations 2.11 to 2.13. Figure 3.20 shows therefore only the data obtained at conversions up to 50%.

Figure 3.20 and Table 3.1 show that the isomerisation of 1,2,4-TMB to 1,2,3-TMB and 1,3,5-TMB via methylgroup shifts was approximately an order of magnitude faster than the transalkylation which itself was an order of magnitude faster than the paring reaction. It should be noted that the transalkylation of 1,2,4-TMB is most likely a second order reaction while the isomerisation probably follows first order kinetics. The observed relation between the reaction rates thus depends on the partial pressure of 1,2,4-TMB. In summary the ranking of the reactions with respect to their rates is as follows:

1,2,-methyl-shift-isomerisation > transalkylation > paring reaction

The absence of C_2^+-alkyl-aromatics which are intermediates in the paring reaction indicates that the cleavage C_2^+-alkyl-groups from the aromatic ring is probably faster than their formation. The same ranking can be assumed for the secondary reactions of xylenes and TeMBs.

Figure 3.21 shows that the isomerisation of 1,2,4-TMB to 1,2,3-TMB and to 1,3,5-TMB reaches equilibrium at approximately 35% conversion. Figures 3.22 (a) and (b) show that the isomer distributions in the xylene and TeMB fractions depended on the extent of conversion. At conversions lower than 25% 1,2,4,5-TeMB showed the highest mole fraction amongst the TeMB isomers and the proportion of p-xylene in the xylene fraction was above the thermodynamic equilibrium value (Figure 3.22.a). Reasons for the selective formation of these products at low conversion will be discussed in Section 3.2.4.4 based on better evidence.

The thermodynamic equilibrium composition of the xylene and TeMB fraction was reached at conversions between 20% and 50% due to secondary isomerisation reactions. The isomerisation of o-xylene to p-xylene and the reverse occurs in two consecutive 1,2-methyl-shifts via m-xylene as intermediate rather than in a single step which would involve the simultaneous shift of two methyl groups or the migration of a methyl group via several positions on the aromatic ring (Section 1.6.2). The same can be said for the isomerisation of 1,2,3-TMB to 1,3,5-TMB or 1,2,4,5-TeMB to 1,2,3,4-TeMB.

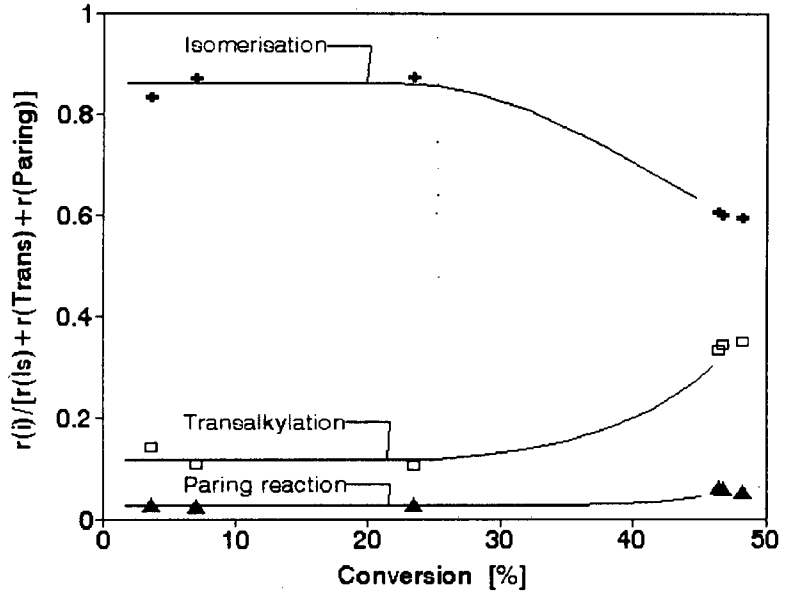

Figure 3.20: **The effect of conversion on the selectivity towards the primary reactions of 1,2,4-TMB over ZSM-5 at T=450°C, $p_{1,2,4\text{-TMB, in}}$=3.5kPa**

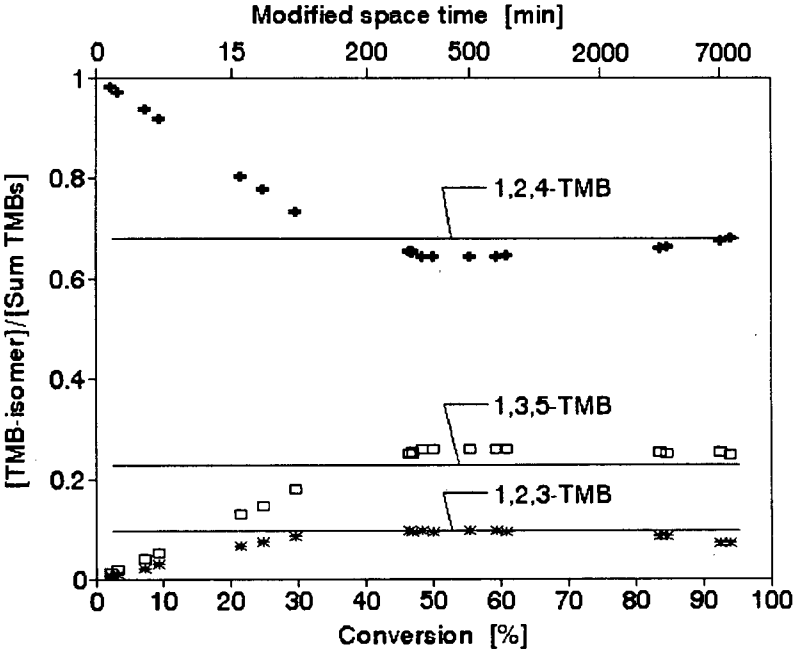

Figure 3.21: **Influence of the 1,2,4-TMB conversion on the isomer distribution in the TMB fraction over ZSM-5 at T=450°C, $p_{1,2,4\text{-TMB, in}}$=3.5kPa**
Solid lines: ***Equilibrium fractions [Stull et al., 1969]***

(a)

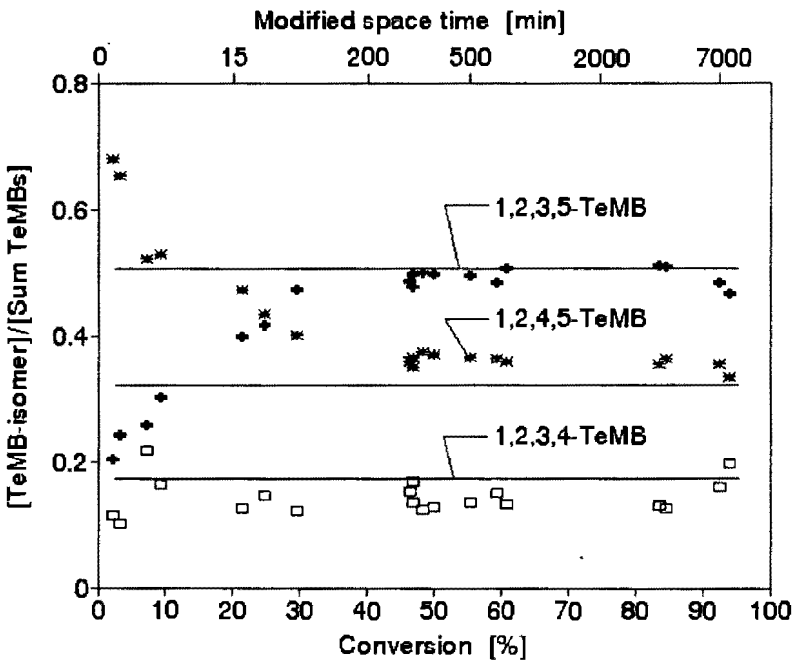

(b)

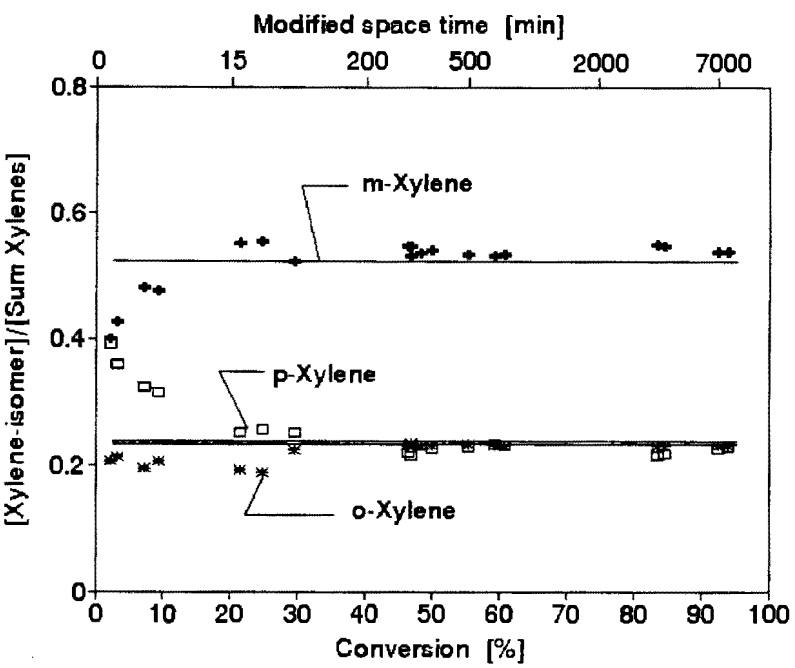

Figure 3.22: **Influence of the 1,2,4-TMB conversion on the isomer distribution in the a) TeMB and b) xylene fraction over ZSM-5 at T=450°C, $p_{1,2,4\text{-TMB, in}}$=3.5kPa**
Solid lines: ***Equilibrium fractions [Stull et al., 1969]***

3.2.4 Comparison of ZSM-5 and silica-alumina

Experiments using amorphous silica-alumina were carried out to simulate the non-shape-selective external surface of ZSM-5 in the absence of the intracrystalline micropore space. Thus the selectivity of silica-alumina should be dominated by intrinsic reaction kinetics. It should be noted that the two catalysts had different Si/Al ratios and that also the acid site strength and the activity of the two catalysts are different. Although the interpretation of certain effects may therefore be ambiguous, these experiments are expected to shed light on the role of the micropore space and shape selectivity in the transformation of 1,2,4-TMB over ZSM-5. The catalysts were compared at equal reaction conditions (T=450°C, p=3.5kPa) (Appendix V.3).

3.2.4.1 Activity

Figure 3.23 shows the conversion of 1,2,4-TMB over ZSM-5 and silica-alumina as a function of modified space time. The conversion of 1,2,4-TMB is higher for ZSM-5 showing that this catalyst was more active despite its 4.5 times higher Si/Al ratio. The higher activity of ZSM-5 is confirmed by the higher conversion level of the TMB-pool (i.e. the lump of 1,2,3-TMB, 1,2,4-TMB + 1,3,5-TMB) (Figure 3.24) and the higher individual semi-quantitative reaction rates listed in Table 3.2.

The initial rates of the 1,2-methyl-shift-isomerisation, the transalkylation and the paring dealkylation of 1,2,4-TMB over ZSM-5 and silica-alumina listed in Table 3.2 were obtained using Equations 2.11 to 2.13 (Section 2.3.4.6) and rates of product formation as obtained from the initial slopes in concentration versus modified space time plots. It should be noted that these rates are only semi-quantitative due to insufficient data at low conversion levels, i.e. low modified space times. The purpose of Table 3.2 is to give an idea of the order of magnitudes of the reaction rates relative to each other.

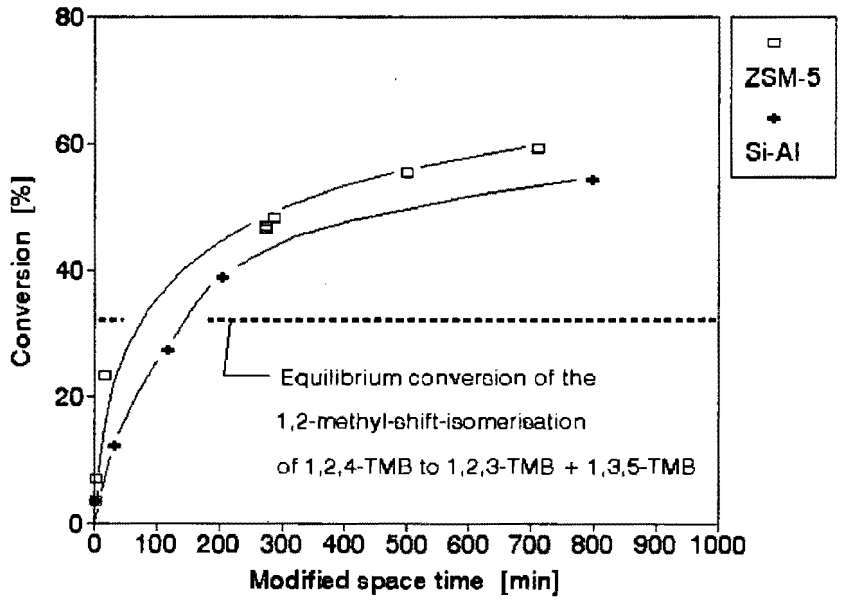

Figure 3.23: **Conversion of 1,2,4-TMB versus modified space time for ZSM-5 (Si/Al=45) and silica-alumina (Si/Al=10) at $p_{1,2,4\text{-TMB,in}}$ =3.5kPa, T=450°C**

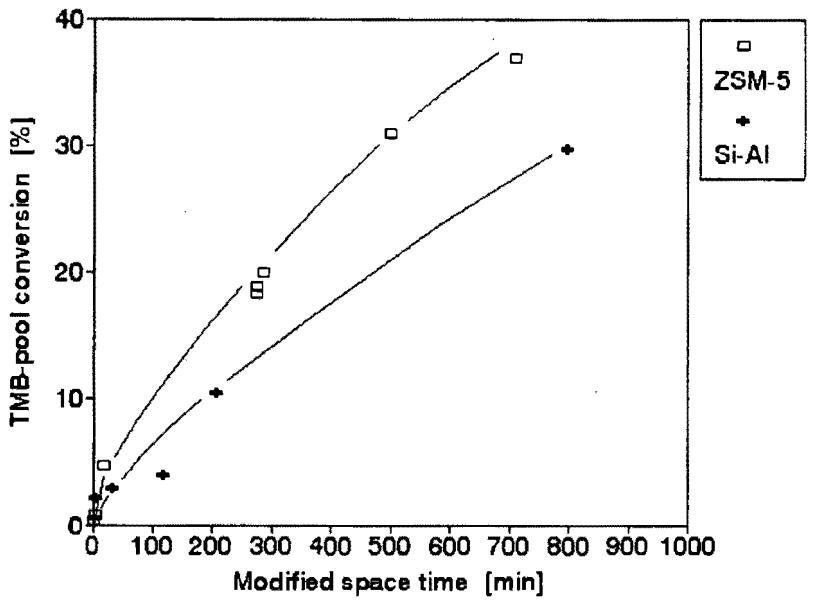

Figure 3.24: **Conversion of the TMB-pool versus modified space time for ZSM-5 (Si/Al=45) and silica-alumina (Si/Al=10) at $p_{1,2,4\text{-TMB,in}}$ =3.5kPa, T=450°C**

Table 3.2: Semi-quantitative initial reaction rates during the conversion of 1,2,4-TMB over ZSM-5 and silica-alumina as determined from concentration versus modified space time plots and Equations 2.11 to 2.13 (Section 2.3.4.6)

Reaction of 1,2,4-TMB	Rate over ZSM-5[d] (μmol/h/l)	Rate over silica-alumina[e] (μmol/h/l)
Isomerisation via 1,2-methyl-shift[a]	600	100
Transalkylation[b]	75	25
Paring reaction[c]	15	1

[a] Equ. 2.11: $r_{isomerisation} = r_{1,2,3\text{-TMB}} + r_{1,3,5\text{-TMB}}$
[b] Equ. 2.12: $r_{transalkylation} = r_{xylenes} + r_{TeMBs}$
[c] Equ. 2.13: $r_{paring\ reaction} = r_{benzene} + r_{toluene}$
[d] Si/Al=45
[e] Si/Al=10

3.2.4.2 The role of conversion in the comparison of selectivities

The effect of the catalyst on the product distribution and selectivity has to be studied at equal conversion. The product distributions obtained over ZSM-5 and silica-alumina have thus to be compared using concentration versus conversion plots. However, the nature of the 1,2,4-TMB transformation requires a special treatment as discussed in the following.

The 1,2-methyl-shift-isomerisation is the most rapid reaction of 1,2,4-TMB over both ZSM-5 and amorphous silica-alumina (Table 3.2). The maximum conversion of 1,2,4-TMB via 1,2-methyl-shift-isomerisation is determined by the isomer composition at thermodynamic equilibrium and amounts to 32% [thermodynamic data from Stull *et al.*, 1969]. Over both catalysts the equilibrium composition of the TMB fraction was reached at only slightly higher conversions between approximately 35% and 40% (Figure 3.19.b and 3.34.b) indicating that other reactions of 1,2,4-TMB than the isomerisation are initially negligible.

Figure 3.25 shows the conversion of the TMB pool as a function of the 1,2,4-TMB conversion. While 1,2,4-TMB is converted via 1,2-methyl-shift-isomerisation, transalkylation and paring reactions the TMB-pool is subject only to the two latter

reactions. Up to a 1,2,4-TMB conversion of 32% which corresponds to the 1,2,4-TMB isomerisation equilibrium the conversion of the TMB-pool is small compared to the conversion of 1,2,4-TMB. The conversion of the TMB-pool and therefore the conversion of 1,2,4-TMB via transalkylation and paring reactions occurs mainly at higher conversion levels at which the 1,2,4-TMB isomerisation to 1,2,3-TMB and 1,3,5-TMB is already at equilibrium.

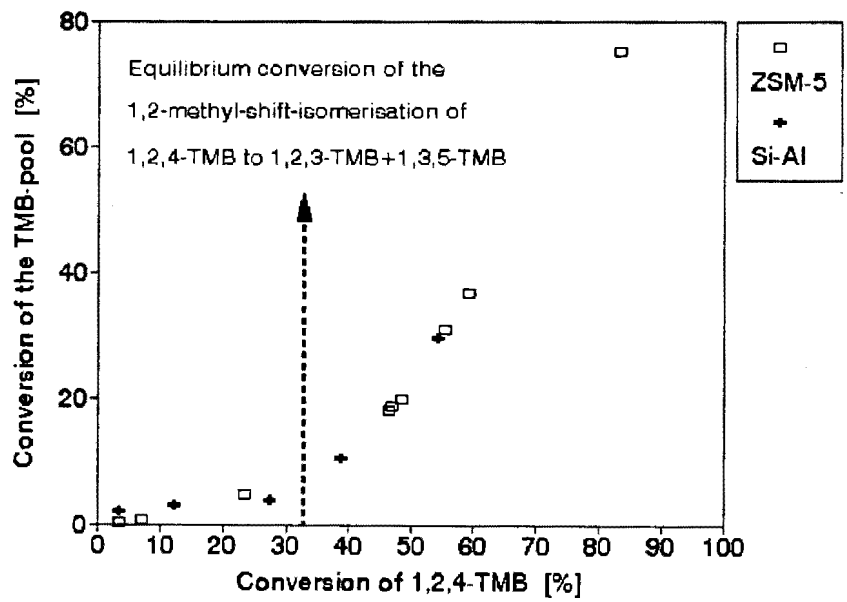

Figure 3.25: Conversion of the TMB-pool (i.e. 1,2,3-TMB+1,2,4-TMB+1,3,5-TMB) as a function of the 1,2,4-TMB conversion at $p_{1,2,4\text{-TMB,in}}$ =3.5kPa, T=450°C

The fact that 1,2,4-TMB is at equilibrium with 1,2,3-TMB and 1,3,5-TMB for most of the conversion of 1,2,4-TMB via transalkylation and paring reaction requires to treat the TMB-pool as the apparent feed and consequently to compare selectivities during the transalkylation and paring dealkylation at equal TMB-pool conversions. The distribution of the 1,2-methyl-shift-isomerisation product, i.e. 1,2,3-TMB and 1,3,5-TMB, however, has still to be compared at equal conversions of 1,2,4-TMB.

3.2.4.3 *Concentration versus conversion plots*

Figures 3.26 to 3.30 compare the concentration versus conversion plots obtained for silica-alumina and ZSM-5. The gradients in the origin obtained for the C_1-C_4-aliphatics, toluene, xylenes, 1,2,3-TMB + 1,3,5-TMB and TeMBs were greater than zero, showing that these products are primary or pseudo-primary products, just as found over ZSM-5.

As it was the case with ZSM-5, benzene produced at low conversions over silica-alumina plateaued at a concentration of approximately 0.0015 mmol/l at approximately 5% TMB-pool conversion (Figure 3.31). The formation of benzene over silica-alumina can be attributed to the dealkylation of butyl-benzene impurities in the feed.

Figures 3.26 and 3.27 show that the concentrations of C_1-C_4 aliphatics and toluene obtained over ZSM-5 were clearly higher than over silica-alumina. C_1-C_4 aliphatics and toluene are products of the paring reaction. This shows that the paring dealkylation of 1,2,4-TMB is selectively promoted by ZSM-5.

Analogously ZSM-5 should promote the consumption of TeMBs in secondary paring reactions. As expected Figure 3.30 shows that lower TeMB concentrations were obtained over ZSM-5 than over silica-alumina. At the same time the xylene concentrations were higher over ZSM-5.

Figure 3.32 shows the molar ratio of xylenes/TeMBs obtained over silica-alumina and ZSM-5. The almost equimolar formation of xylenes and TeMBs over silica-alumina shows that these molecules are mainly formed via transalkylation of TMBs and indicates that secondary reactions are negligible. The ratio being clearly greater than 1 over ZSM-5 shows that TeMBs are consumed and/or xylenes are formed via secondary reactions. Interestingly the lumped concentrations of xylenes and TeMBs obtained over ZSM-5 and silica-alumina are equal (Figure 3.33) and thus indicate that the total amount of xylenes and TeMBs obtained over ZSM-5 is determined by the primary transalkylation of TMBs mainly. Consequently the surplus of xylenes has to be formed from TeMBs. The

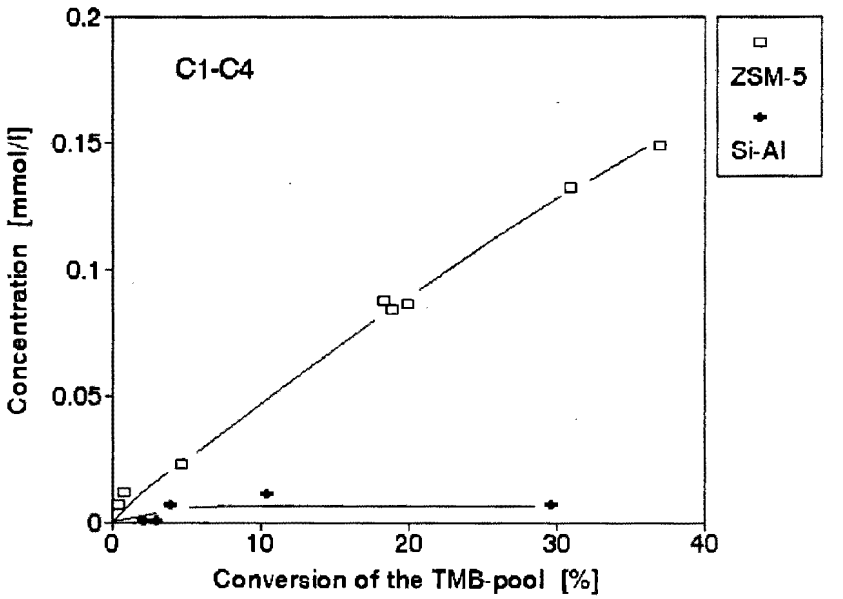

Figure 3.26: Concentration of C_1-C_4 in mmol of carbon atoms per litre versus the conversion of the TMB-pool over ZSM-5 and silica-alumina at $p_{1,2,4\text{-TMB,in}}$ =3.5kPa, T=450°C

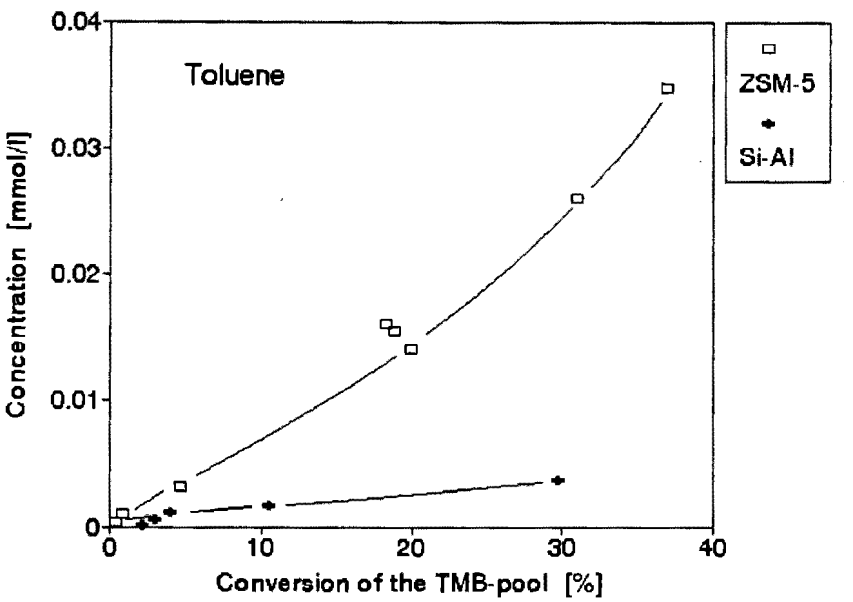

Figure 3.27: Concentration of toluene versus the conversion of the TMB-pool over ZSM-5 and silica-alumina at $p_{1,2,4\text{-TMB,in}}$=3.5kPa, T=450°C

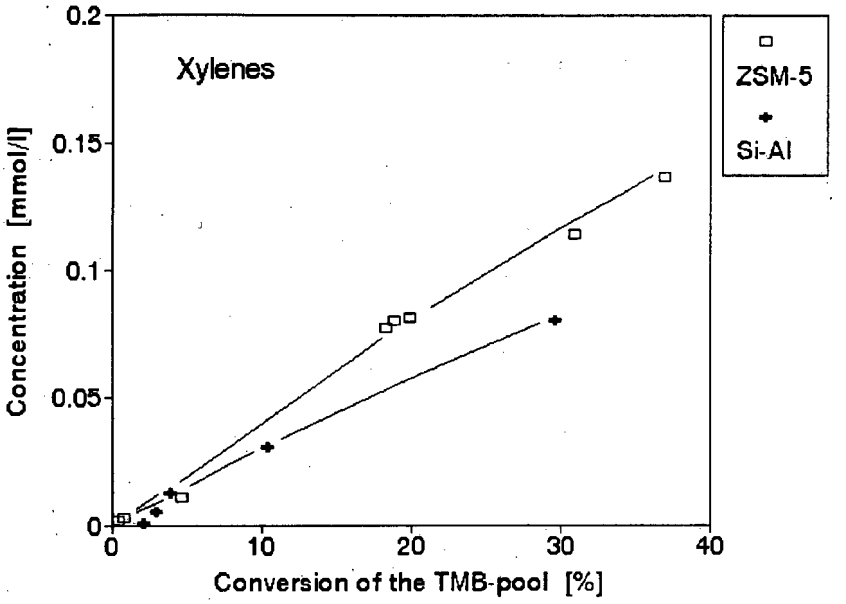

Figure 3.28: **Concentration of xylenes versus the conversion of the TMB-pool over ZSM-5 and silica-alumina at $p_{1,2,4\text{-TMB,in}}$=3.5kPa, T=450°C**

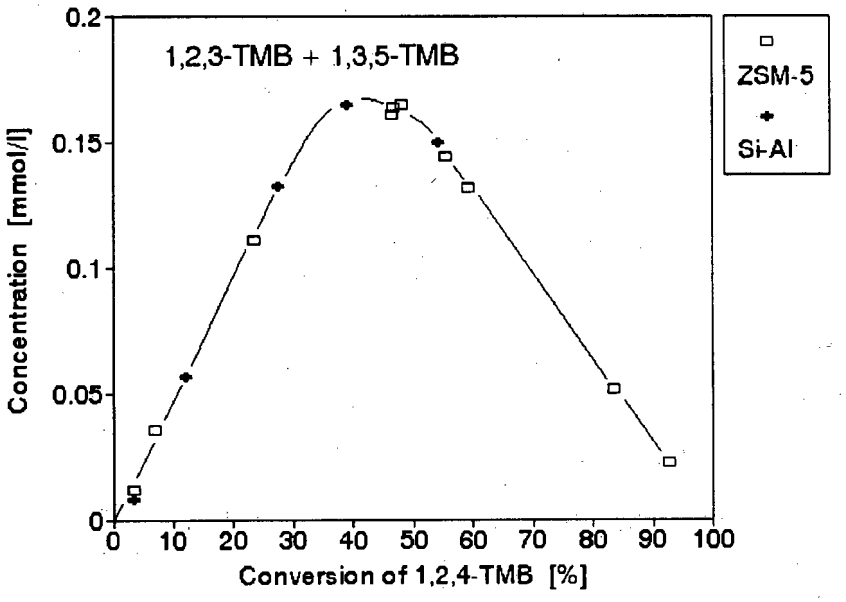

Figure 3.29: **Concentration of 1,2,3-TMB+1,3,5-TMB versus the conversion of 1,2,4-TMB over ZSM-5 and silica-alumina at $p_{1,2,4\text{-TMB,in}}$=3.5kPa, T=450°C**

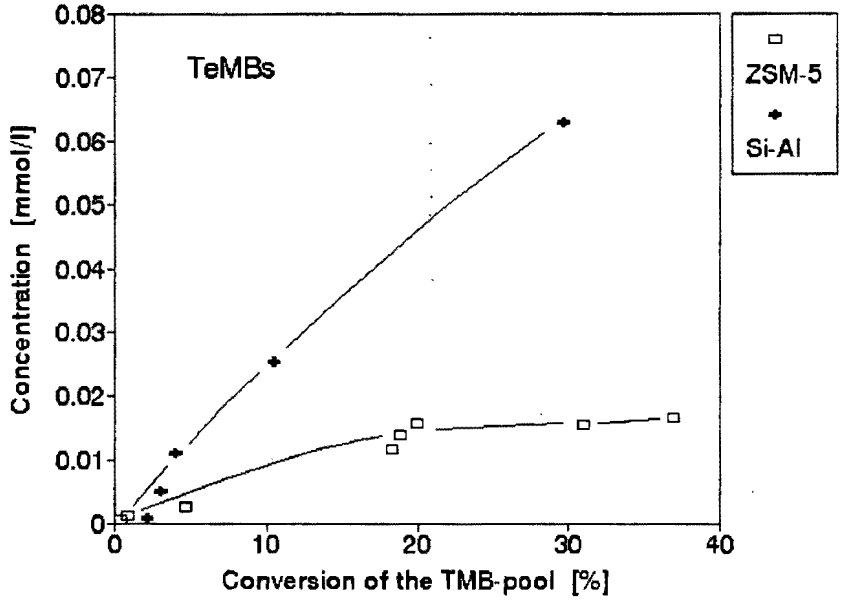

Figure 3.30: **Concentration of TeMBs versus the conversion of the TMB-pool over ZSM-5 and silica-alumina at $p_{1,2,4\text{-}TMB,in}$=3.5kPa, T=450°C**

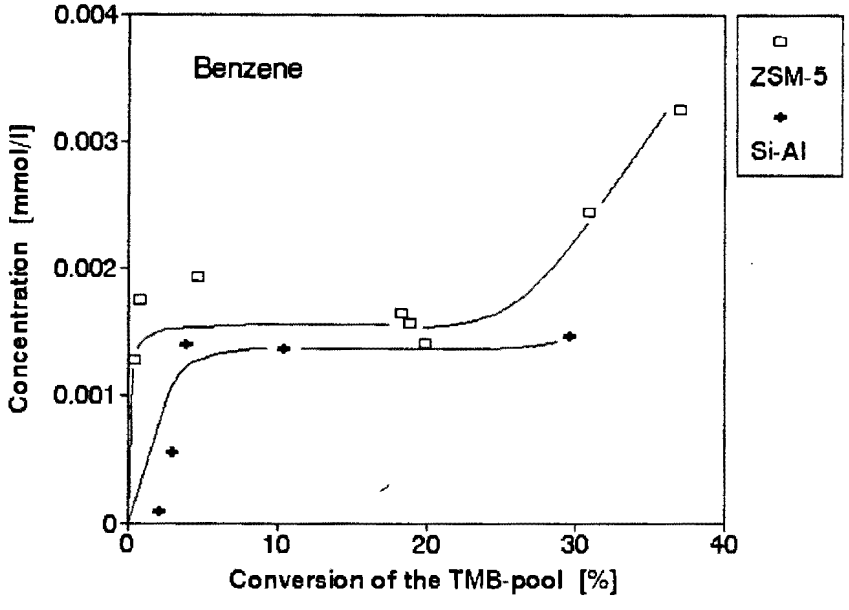

Figure 3.31: **Concentration of benzene versus the conversion of the TMB-pool over ZSM-5 and silica-alumina at $p_{1,2,4\text{-}TMB,in}$=3.5kPa, T=450°C**

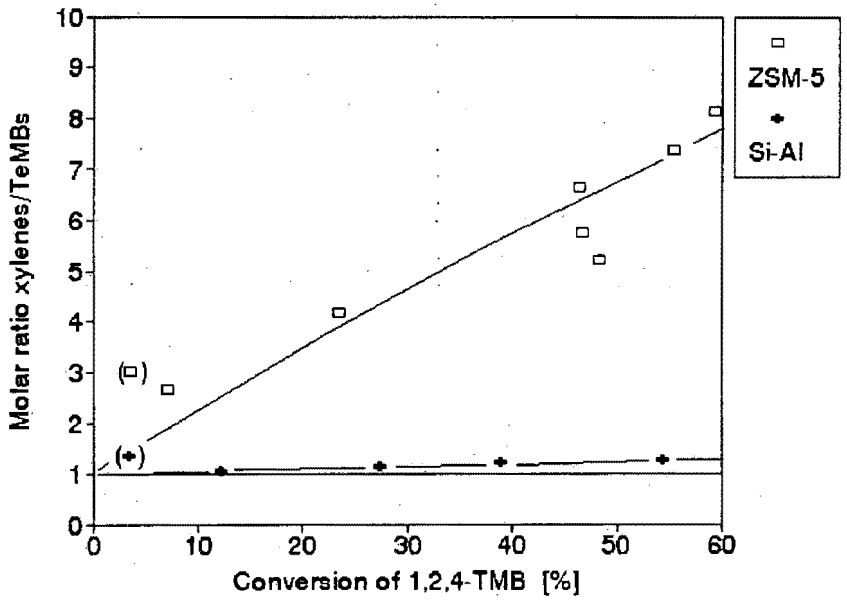

Figure 3.32: **The molar concentration ratio [xylenes]/[TeMBs] versus conversion of 1,2,4-TMB for ZSM-5 and silica-alumina at $p_{1,2,4\text{-TMB,in}}$ =3.5kPa, T=450°C**

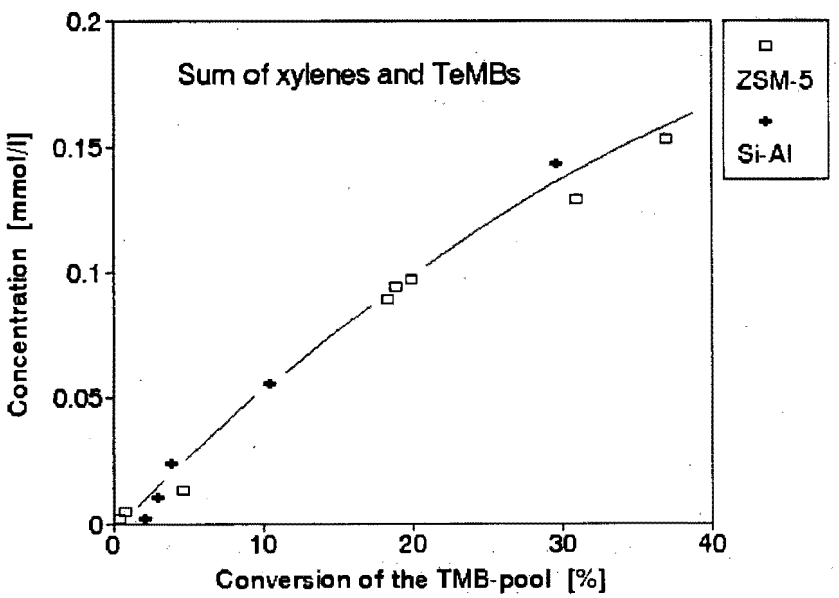

Figure 3.33: **The sum of xylene and TeMB concentration as a measure for the transalkylation activity versus the conversion of the TMB-pool for ZSM-5 and silica-alumina at $p_{1,2,4\text{-TMB,in}}$=3.5kPa, T=450°C**

secondary reactions of TeMBs are transalkylation and the paring reaction (Figure 3.18, Section 3.2.3). However, a direct formation of xylenes from TeMBs can occur only via the paring reaction yielding ethylene as co-product.

Figures 3.29 and 3.33 show that ZSM-5 and silica alumina yield identical concentration versus conversion plots for both the isomerisation product 1,2,3-TMB+1,3,5-TMB and the transalkylation product xylenes+TeMBs. This shows that influence of the ZSM-5 structure on the selectivity for these reactions is negligible.

However, although the paring reaction occurs to a higher extent over ZSM-5 no effect on the lumped product concentration of both the 1,2-methyl-shift-isomerisation and the transalkylation could be observed (Figures 3.29 and 3.33). This is due to the relatively slow rate of the paring reaction (Table 3.2).

For both ZSM-5 and silica-alumina the consumption of TMBs occurs mainly via transalkylation and only to a minor extent via the paring reaction (Table 3.2). The ZSM-5 structure appears to promote the paring reaction of TMBs and especially of TeMBs, however, with the available data it cannot be distinguished if this was due to stronger acid sites or to adsorption effects in the micropores.

3.2.4.4 The role of the micropores

Figure 3.34 shows the composition of the TeMB, the TMB and the xylene fraction as a function of 1,2,4-TMB conversion over silica-alumina. The isomer distributions obtained at 60 and 240 minutes of time on stream and for different space velocities were plotted in the same graph and fell onto the same curve, thus showing that the isomer distributions depended on the conversion but not on time on stream. 1,2,4,5-TeMB and o-xylene were initially formed above their equilibrium proportion and declined towards the equilibrium with increasing conversion due to secondary isomerisation reactions. This shows the selective transalkylation of 1,2,4-TMB to these products. This initially selective formation of 1,2,4,5-TeMB and o-xylene over silica-alumina was also observed by Kojima *et al.*

[1991] and was also obtained with other non-shape selective, acid catalysts, such as pillared clays [Kojima *et al.*, 1991] or zeolite HY [Ko and Kuo, 1994].

A generally accepted transalkylation mechanism of alkylaromatics involves a bi-phenylic transition state as proposed by Csicsery for the transalkylation of alkylbenzenes over mordenite catalysts [Csicsery, 1970; 1971]. Without spatial constraints, the selective formation of o-xylene and 1,2,4,5-TeMB is determined by intrinsic kinetics (e.g. stabilising electronic effects on the transition state) and it may be suggested that pore systems of wide pore, acid catalysts such as amorphous silica-alumina, pillared clays or zeolite Y are too spacious to either inflict any constraints on the transition states of transalkylation reactions between monocyclic, aromatic hydrocarbons or to cause any product selectivity due to diffusional limitations [Weitkamp, 1998].

However, amongst the possible transition states (Figure 1.15, Section 1.6.2) in the transalkylation of 1,2,4-TMB the first and most linear one would be sterically favoured inside micropores. The decomposition of this particular transition state yields 1,2,4,5-TeMB and o-xylene. The observation of the simultaneously occurring selective formation of these products over zeolite HY lead Ko and Kuo [1994] to the conclusion that the transalkylation of 1,2,4-TMB would be controlled by transition state shape selectivity even in the spacious micropore system of zeolite HY.

Over zeolite ZSM-5 matters are somewhat different. At low 1,2,4-TMB conversions the molar ratio [1,2,4,5-TeMB]/[1,2,3,5-TeMB] shows that 1,2,4,5-TeMB is still dominating the TeMB fraction, apparently to a higher extent than over silica-alumina (Figure 3.35.a). However, this only holds, if compared as a function of the 1,2,4-TMB conversion. When the 1,2,4,5-TeMB proportion is plotted against the conversion of the TMB-pool the differences have almost disappeared (Figure 3.35.b). The selective formation of 1,2,4,5-TeMB over ZSM-5 is thus not necessarily a shape selective effect.

(a)

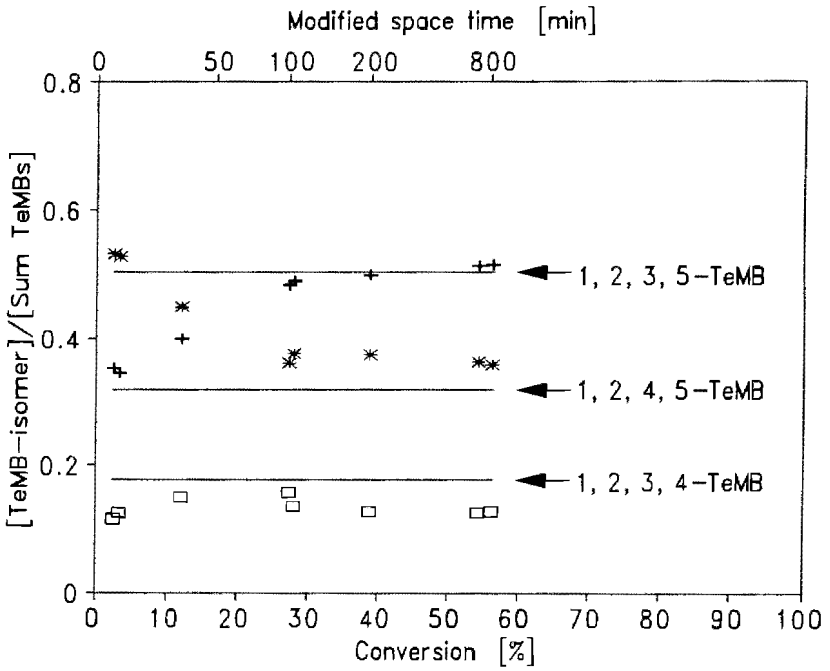

(b)

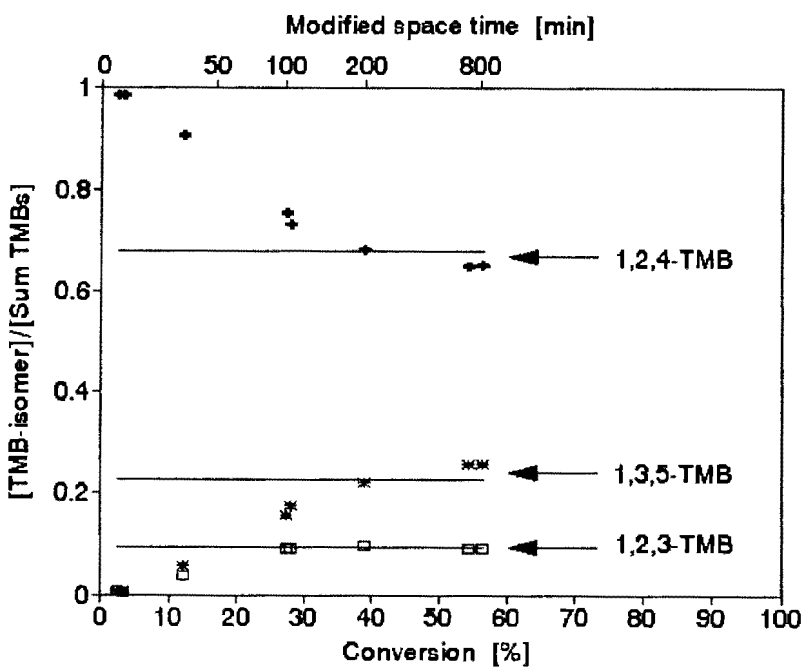

To Figure 3.34

(c)

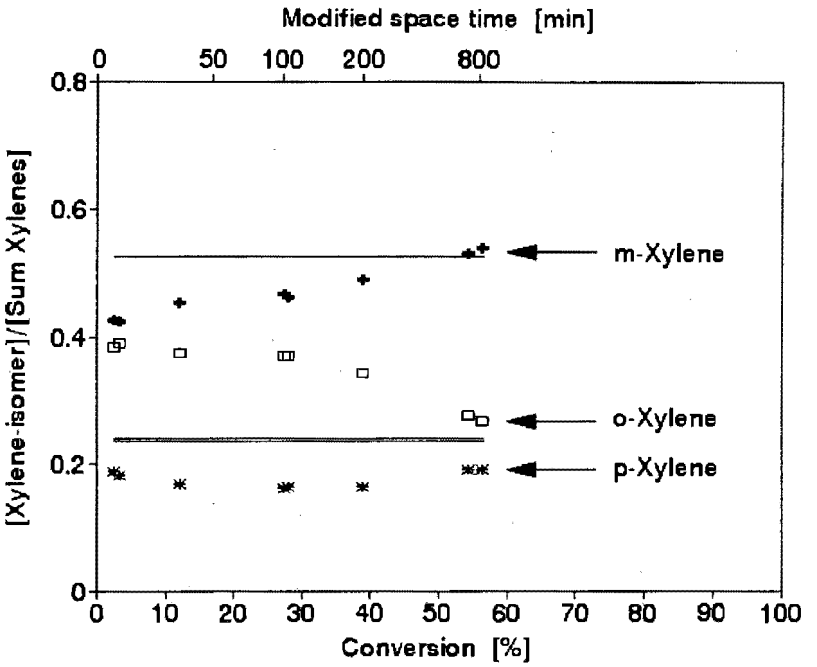

Figure 3.34: **Effect of conversion on the isomer distribution in the**
(a) TeMB fraction
(b) TMB fraction
(c) xylene fraction
during the transformation of 1,2,4-TMB over silica-alumina at $p_{1,2,4\text{-TMB,in}}$ =3.5kPa, T=450°C
Solid lines: Thermodynamic equilibrium fractions [Stull et al., 1969]

Figures 3.36 and 3.37 show that in contrast to silica-alumina which was selective towards the formation of o-xylene, ZSM-5 was selective towards the formation of p-xylene at low conversions. This shows that over ZSM-5 the xylene distribution is dominated by shape selective constraints as opposed to the control by intrinsic kinetics over Si-Al. Corresponding to the intrinsic kinetics o-xylene may initially still form preferentially inside the micropores but subsequently isomerises rapidly and preferably p-xylene elutes from the micropore system due to strong diffusional discrimination, i.e. product shape selectivity.

The shape selective formation of p-xylene over ZSM-5 shows that the xylenes are formed inside the micropores. The reaction network model in Figure 3.17 illustrates that the formation of xylenes as primary products necessarily involves the transalkylation of

(a)

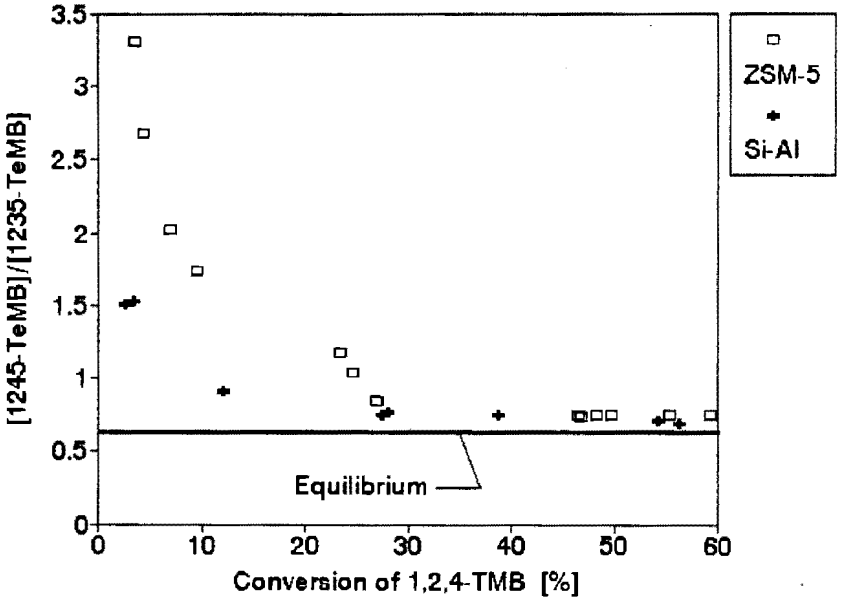

(b)

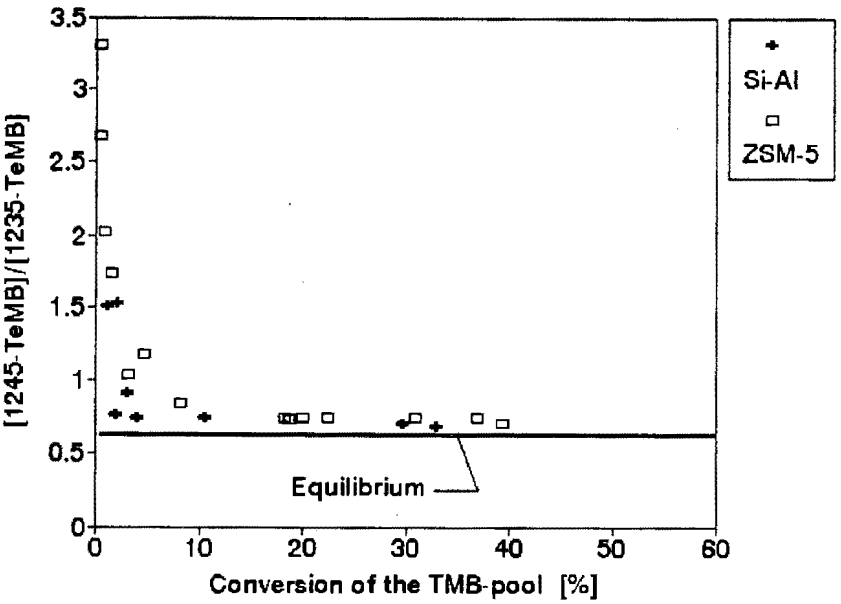

Figure 3.35: **Comparison of the molar ratio [1,2,4,5-TeMB]/[1,2,3,5-TeMB] during the transformation of 1,2,4-TMB over silica-alumina and ZSM-5 at $p_{1,2,4\text{-TMB,in}}$=3.5kPa, T=450°C as a function of the:**
(a) 1,2,4-TMB conversion
(b) TMB-pool conversion
Solid lines: Thermodynamic equilibrium [Stull et al., 1969]

(a)

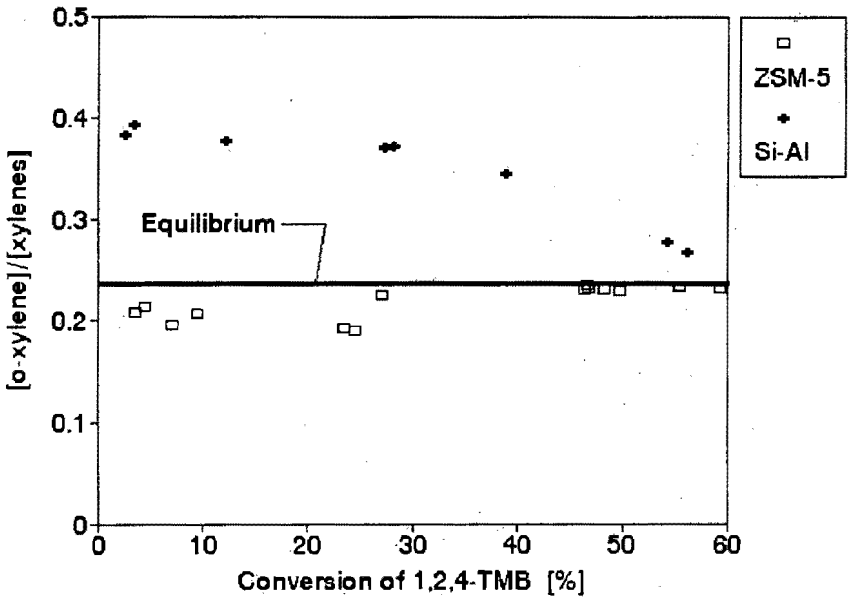

(b)

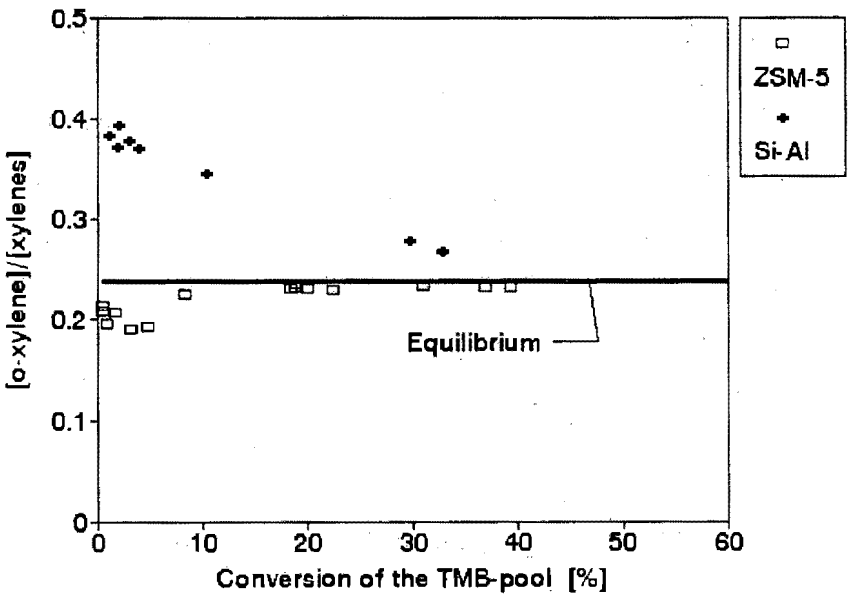

Figure 3.36: **Comparison of the o-xylene proportions in the xylene fraction during the transformation of 1,2,4-TMB over silica-alumina and ZSM-5 at $p_{1,2,4\text{-TMB,in}}$ =3.5kPa, T=450°C as a function of the:**
(a) 1,2,4-TMB conversion
(b) TMB-pool conversion
Solid lines: Thermodynamic equilibrium [Stull et al., 1969]

(a)

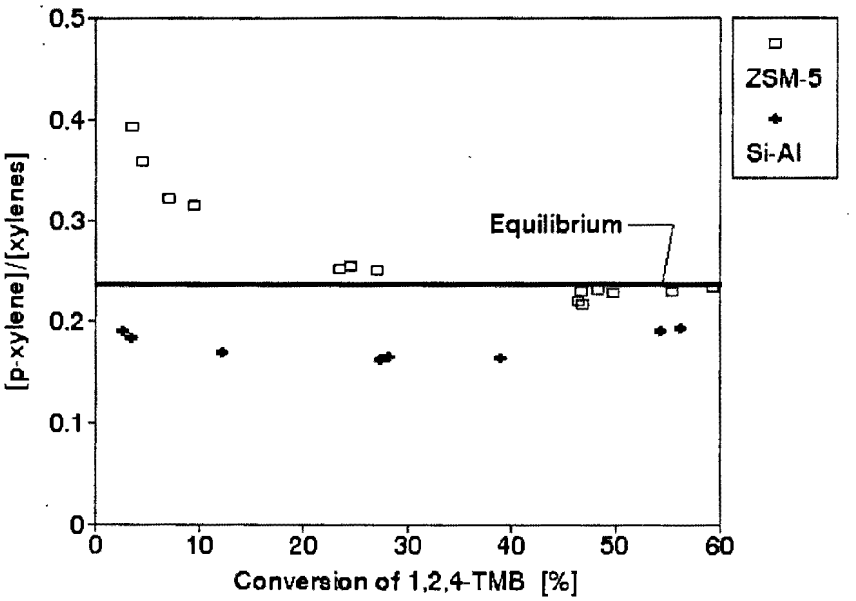

(b)

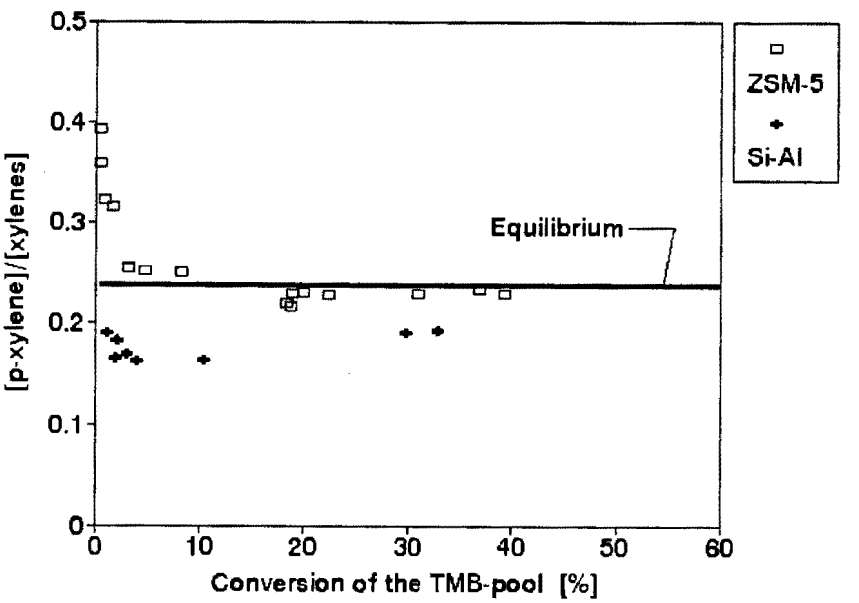

Figure 3.37: **Comparison of the p-xylene proportions in the xylene fraction during the transformation of 1,2,4-TMB over silica-alumina and ZSM-5 at $p_{1,2,4\text{-TMB,in}}$ =3.5kPa, T=450°C as a function of the:**
(a) 1,2,4-TMB conversion
(b) TMB-pool conversion
Solid lines: Thermodynamic equilibrium [Stull et al., 1969]

TMBs. It is therefore concluded that the transalkylation of 1,2,4-TMB to at least the 1,2,4,5-TeMB isomer occurs to a significant extent inside the micropores of ZSM-5. The absence of significant shape selectivity in the TeMB fraction, however, indicates that TeMB isomers hardly elute from the micropore system, although TeMBs have to be formed inside the micropores as co-products of xylenes. It is proposed that these trapped TeMBs are converted to xylene and ethylene via the paring reaction. This is supported by the surplus of xylenes compared to TeMBs (Figure 3.32) and the sums of xylenes and TeMBs obtained over ZSM-5 and silica alumina being equal (Figure 3.33). The TeMBs observed in the product stream are thus proposed to originate mainly from transalkylation reactions on the external surface of ZSM-5. The small shape selectivity towards 1,2,4,5-TeMB (Figure 3.), however, indicates that some 1,2,4,5-TeMB additionally elutes from the micropores.

This is supported by Yashima et al. [1985], who concluded that 1,2,4,5-TeMB is formed in the micropores and that 1,2,3,4-TeMB and 1,2,3,5-TeMB are restricted to the external surface. This was based on the selective formation of 1,2,4,5-TeMB during the methylation of 1,2,4-TMB over ZSM-5 at temperatures between 250°C and 400°C. Using single crystal X-ray diffraction analysis van Koningsveld and Jansen [1996] showed that naphthalene can be adsorbed into the micropores of H-ZSM-5. The molecular geometry of naphthalene and 1,2,4,5-TeMB is very similar, indicating the latter to be able to desorb from the micropore system once it is formed. During the methanol to gasoline reaction, Anderson and Klinowski [1989] observed 1,2,3-TMB, 1,3,5-TMB and all three TeMB isomers in the adsorbed phase using NMR-studies. They concluded that these molecules were adsorbed in the micropores of ZSM-5. Based on the observation of these molecules in the product stream they suggested that at high temperatures ($T \geq 370°C$) these relatively large species, amongst them 1,2,4,5-TeMB, are able to leave the crystallite because of the increased effective channel diameter. The possibility that these products may have been formed at the external surface, however, was not considered.

Figure 3.38 shows that the concentration ratio [1,2,3-TMB]/[1,3,5-TMB] obtained for silica-alumina was well above the equilibrium value at low conversions, thus showing that

intrinsic kinetics favour the isomerisation of 1,2,4-TMB to 1,2,3-TMB. With increasing conversion the ratio decreased reaching the equilibrium at 40% conversion. Extracting data for the isomerisation of 1,2,4-TMB over spacious materials such as silica-alumina, pillared clays or zeolite Y from literature, 1,2,3-TMB/1,3,5-TMB ratios can be derived which are also higher than the thermodynamic equilibrium value [Kojima *et al.*, 1991, Ko and Kuo, 1994]. There is also a decrease of this ratio with increasing conversion [Kojima *et al.*, 1991] and temperature [Ko and Kuo, 1994] almost independent of the catalyst.

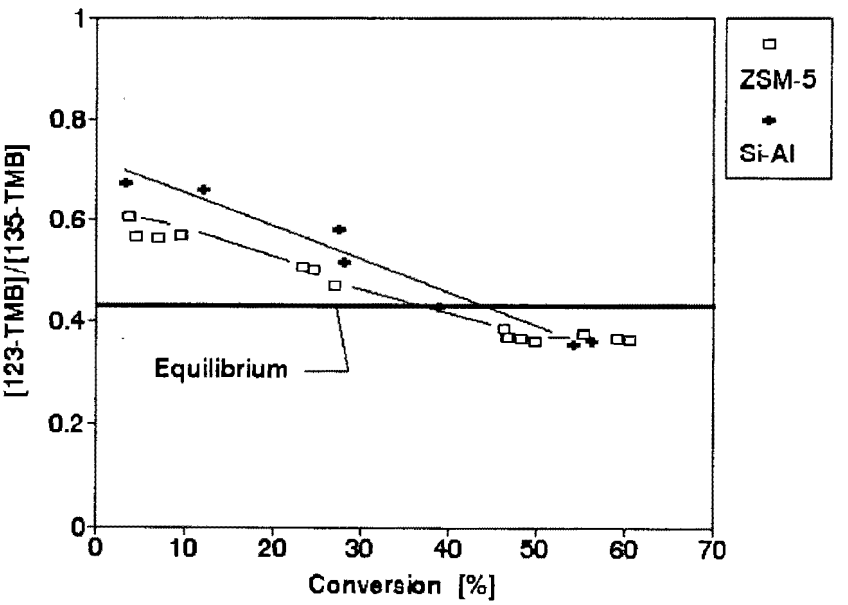

Figure 3.38: **The 1,2,3-TMB/1,3,5-TMB distribution during the transformation of 1,2,4-TMB over silica-alumina and ZSM-5 at $p_{1,2,4\text{-TMB,in}}$=3.5kPa, T=450°C**
Solid line: Thermodynamic equilibrium [Stull et al., 1969]

If the 1,2-methyl-shift-isomerisation of 1,2,4-TMB over ZSM-5 takes place inside the micropores, product shape selectivity as in the case of xylene isomerisation would be expected to rule the product distribution rather than intrinsic kinetics. Both reactions are fast and yield critically sized product molecules. Therefore, if the isomerisation of 1,2,4-TMB occurs inside the micropores this reaction should be diffusion controlled. The increased selective formation of p-xylene over ZSM-5 was based on a difference in molecular diameters of 0.8 Å (Table 1.7) between p-xylene and the two competing

isomers o- and m-xylene. The difference between 1,2,3-TMB and 1,3,5-TMB is 0.7 Å. Thus, in favour of the slimmer 1,2,3-TMB the ratio 1,2,3-TMB/1,3,5-TMB should be increased over ZSM-5 as compared to silica-alumina. However, this was not observed (Figure 3.38) and it is concluded that the 1,2-methyl-shift-isomerisation of 1,2,4-TMB takes place mainly on the external surface of ZSM-5.

This is supported by Yashima et al. [1985] who concluded from product distributions obtained during the methylation of 1,2,4-TMB over ZSM-5 at temperatures between 250°C and 400°C that 1,2,3-TMB and 1,3,5-TMB were formed primarily on the external surface.

3.2.5 Effect of reaction temperature

To study the effect of temperature on the significance of primary and secondary reactions and the behaviour of toluene as a primary product in the reaction network of the 1,2,4-TMB transformation, experiments were carried out where the space time was varied at 300°C, 350°C, 400°C and 450°C. The reaction conditions for each experiment are given in Appendix V.

If the relative significance of primary or secondary reactions shifts with temperature, the product distribution and consequently the product concentration as compared at constant conversion will be affected. The formation of the C_1-C_4-fraction, benzene, toluene, xylene and TeMB is relatively slow and occurs mainly at conversion levels at which the 1,2,4-TMB isomerisation to 1,2,3-TMB and 1,3,5-TMB is already at equilibrium (vide Section 3.2.4.2). Figures 3.39 to 3.41 therefore show the concentrations of these products as a function of the TMB-pool conversion whereas Figure 3.42 shows the concentration of 1,2,3-TMB + 1,3,5-TMB as a function of the 1,2,4-TMB conversion. Samples were taken at 240 minutes of time on stream.

The inlet partial pressure of the feed and the total reactor pressure were kept constant, however the concentrations changed due to thermal expansion with increasing temperature.

Therefore all concentrations in the Figures 3.39 to 3.42 were referred to 450°C.

Except for the TeMB fraction there is no significant effect of temperature on the concentration versus conversion plots to be observed.

Figures 3.39.b and 3.40.a show that there was no significant effect of temperature on the benzene nor the toluene concentration which suggests that the paring dealkylation of TMBs hardly gains in significance with increasing temperature.

In contrast the concentration of TeMBs decreased with increasing temperature as shown in Figure 3.41. This shows that the consumption of TeMB in secondary paring reactions (and / or coke formation) was faster at high temperatures. Correspondingly the concentration of the C_1-C_4-fraction which contains products of the paring reaction and coke formation (CH_4) was slightly lower at 300°C (Figure 3.39.a) (The C_1-C_4-fraction was not analysed in detail for reaction temperatures lower than 450°C, but even at 450°C and 90% conversion, methane which correlates with the rate of coke formation amounts to not more than 10% of the total C_1-C_4 carbon). The highly paraffinic character of the C_1-C_4 fraction (vide Figure 3.8), however, indicates the formation of aromatics from the C_2-C_4 olefins, a reaction which is particularly favoured at high temperatures. This reaction decreases the concentration of the C_1-C_4 fraction. The competing formation and consumption reactions therefore cause the C_1-C_4 fraction to appear rather independent of temperature.

Figure 3.40.b shows that no effect of temperature on the xylene concentration could be observed. Similar to the TMBs it would be expected that the consumption of xylenes in secondary paring reactions hardly increases in significance with temperature. However, xylenes are also formed via paring dealkylation of TeMBs as shown earlier. This is reflected by the amount of xylenes formed being higher than the theoretical amount if only transalkylation would occur (Figure 3.40.b) and the inverse observation for the TeMB concentration (Figure 3.41). Since the significance of the paring dealkylation of TeMB

(a)

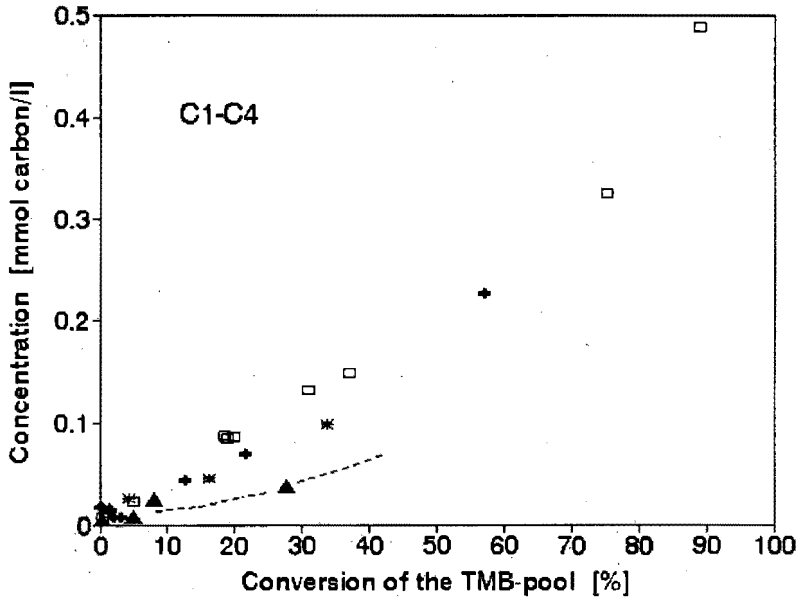

(b)

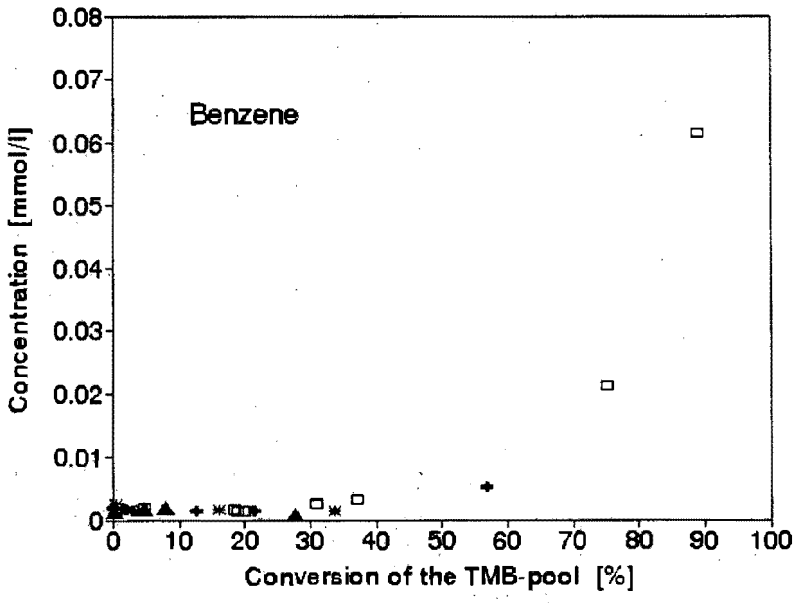

Figure 3.39: **Influence of temperature on product concentration versus conversion plots in the transformation of 1,2,4-TMB over ZSM-5 at $p_{1,2,4\text{-TMB,in}}$=3.5kPa**
Legend: ▲ 300°C; ∗ 350°C; + 400°C; □ 450°C

(a)

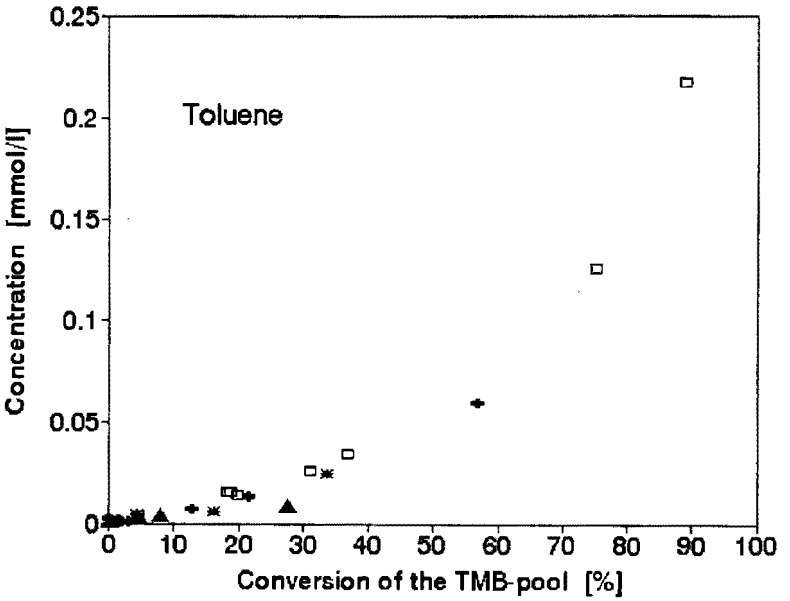

(b)

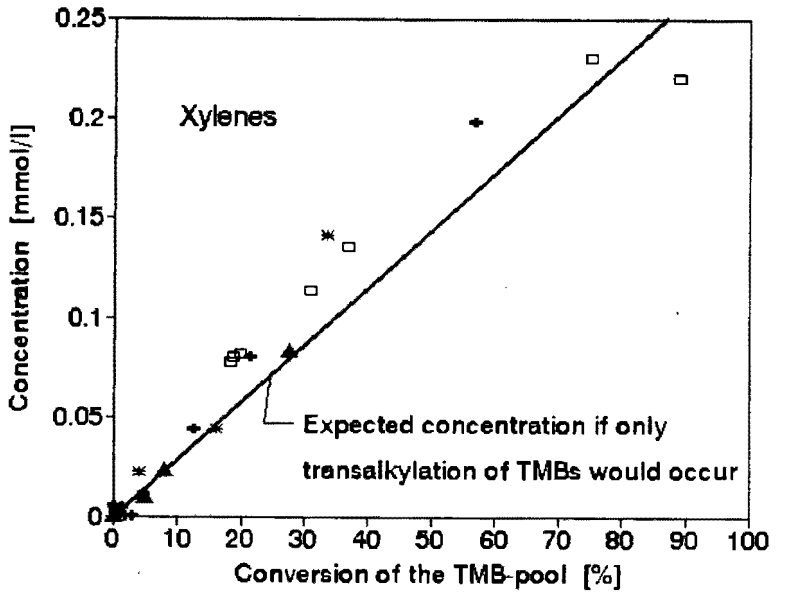

Figure 3.40: **Influence of temperature on product concentration versus conversion plots in the transformation of 1,2,4-TMB over ZSM-5 at $p_{1,2,4\text{-TMB,in}}$=3.5kPa**
Legend: ▲ 300°C; ∗ 350°C; + 400°C; □ 450°C

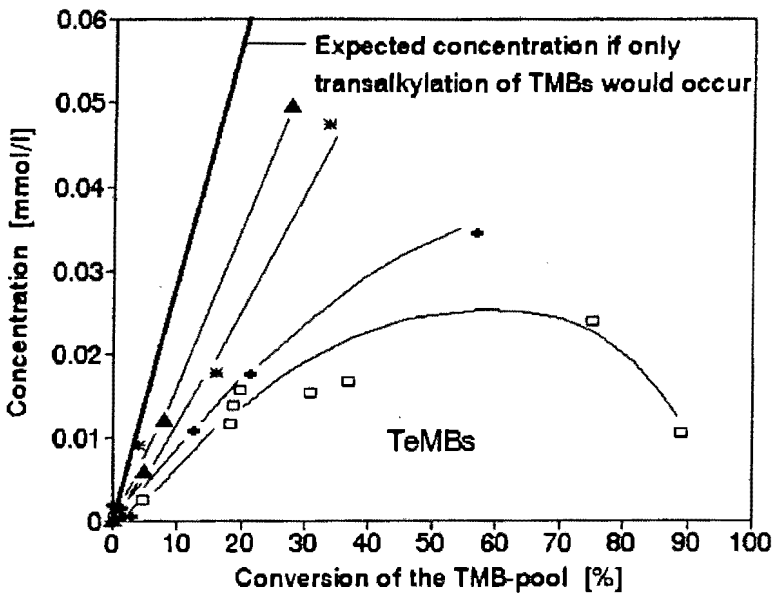

Figure 3.41: **Influence of temperature on product concentration versus conversion plots in the transformation of 1,2,4-TMB over ZSM-5 at $p_{1,2,4\text{-TMB,in}}$=3.5kPa**
Legend: ▲ 300°C; * 350°C; + 400°C; □ 450°C

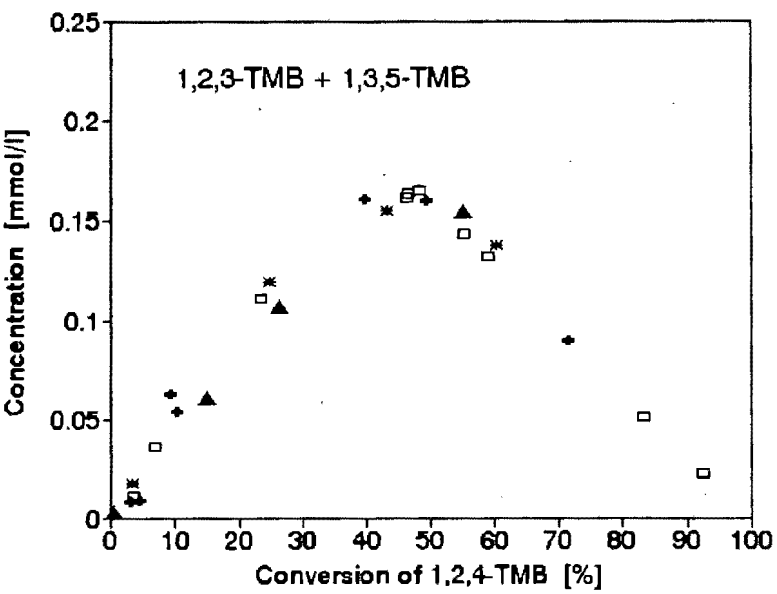

Figure 3.42: **Influence of temperature on product concentration versus conversion plots in the transformation of 1,2,4-TMB over ZSM-5 at $p_{1,2,4\text{-TMB,in}}$=3.5kPa**
Legend: ▲ 300°C; * 350°C; + 400°C; □ 450°C

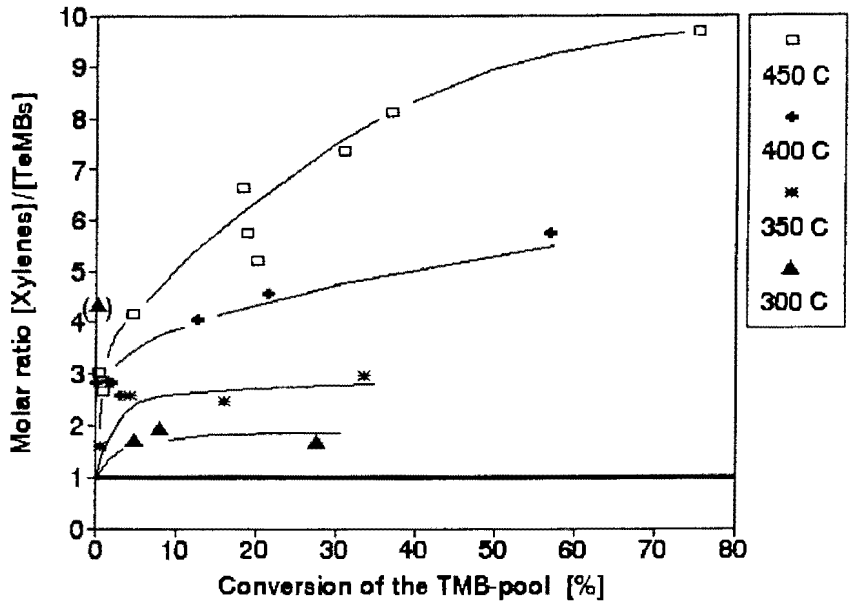

Figure 3.43: Influence of temperature on the concentration ratio [xylenes]/[TeMBs] in the transformation of 1,2,4-TMB over ZSM-5 at $p_{1,2,4\text{-TMB,in}}$=3.5kPa

increases with temperature it would be expected that the concentration of the xylene co-product also increases with temperature. This may be reflected by the concentration ratio of [xylenes]/[TeMBs] which increased as the temperature increased (Figure 3.43). The absence of a temperature effect on the xylene concentration would thus be contradictory. It is concluded that the possibly occurring temperature effects are not visible due to scatter and partly to compensation due to the formation and consumption of xylenes via paring reactions.

Figure 3.42 shows that the 1,2,3-TMB+1,3,5-TMB concentration versus 1,2,4-TMB conversion plot did not depend on temperature. This shows that the 1,2,-methyl-shift-isomerisation of 1,2,4-TMB did not change in significance relative to the transalkylation and paring reactions. The 1,2,-methyl-shift-isomerisation thus remains the fastest reaction of 1,2,4-TMB throughout the studied temperature range.

It is proposed that due to the relatively slow formation of TeMBs and the larger number of methyl-groups secondary paring reactions play a more significant role than for TMBs

(a)

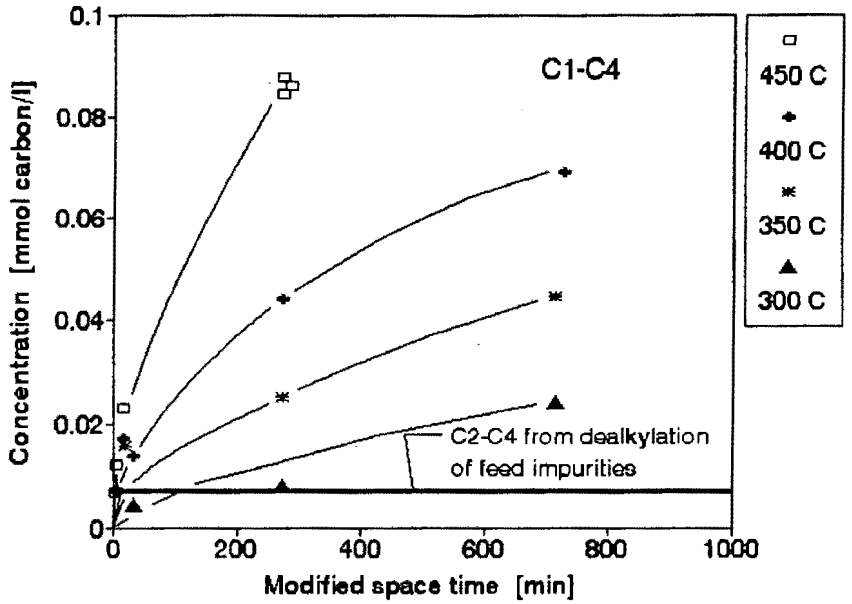

(b)

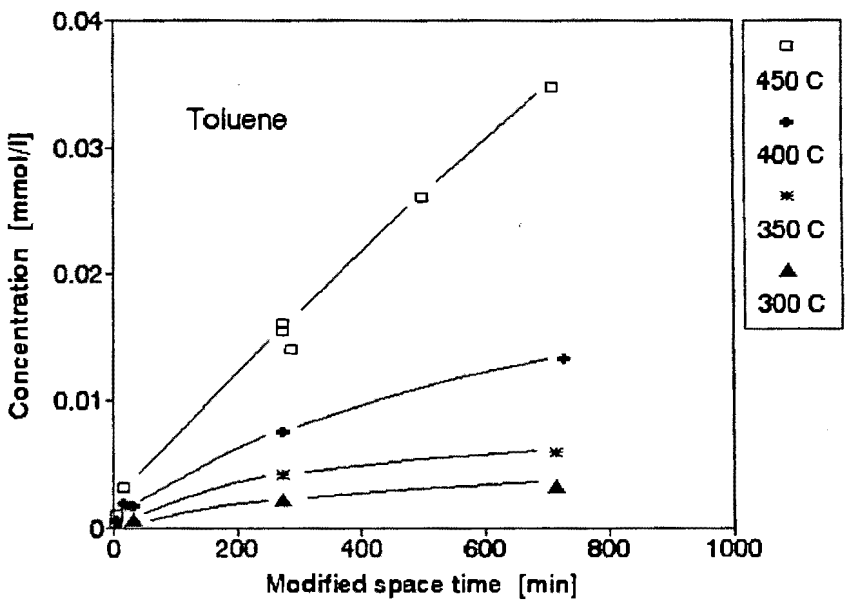

Figure 3.44: **Influence of temperature on the concentration versus modified space time plots for**
(a) the C1-C4 fraction (b) Toluene
in the transformation of 1,2,4-TMB over ZSM-5 at $p_{1,2,4\text{-TMB,in}}$=3.5kPa.
(the concentrations were calculated for T=450°C)

and xylenes. However, the corresponding effects on the concentrations of the other products are too small to be observed.

Figure 3.44 shows the effect of temperature on concentration versus modified space time plots for the lumped C_1-C_4 fraction and toluene for space times shorter than 1000 minutes. At all applied reaction temperatures the gradients in the origin were greater than zero confirming that both the lumped C_1-C_4 fraction and toluene are pseudo-primary products independent of temperature.

3.2.5.1 Apparent activation energies

The Arrhenius plot in Figure 3.45 was obtained using the reaction rates of the 1,2-methyl-shift-isomerisation, transalkylation and paring reaction measured at 240 minutes of time on stream at conversions of 1,2,4-TMB between 3% and 8% over ZSM-5. The reaction rates were calculated as described in Section 2.3.4.6 by Equations 2.11 to 2.13.

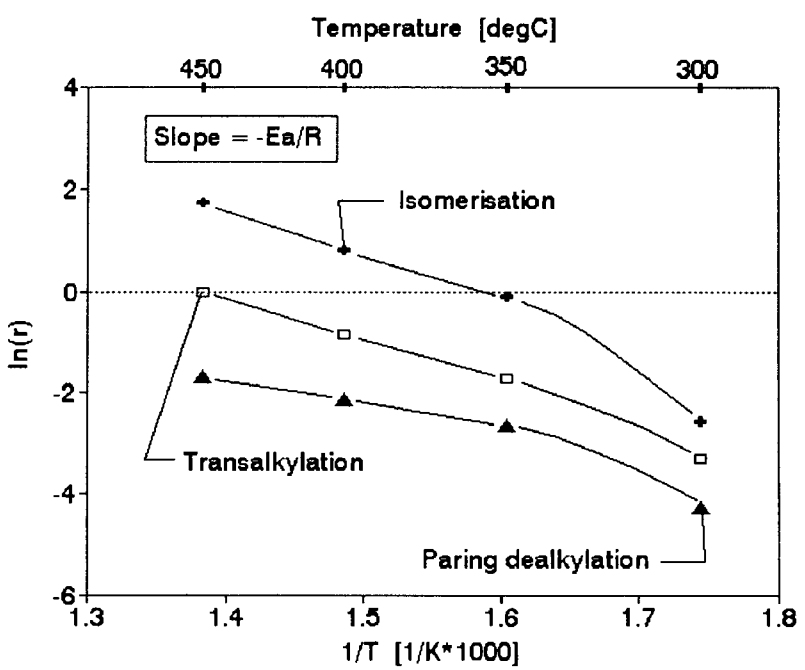

Figure 3.45: Arrhenius plot for the 1,2-methyl-shift-isomerisation, transalkylation and paring reaction of 1,2,4-TMB over ZSM-5 at $p_{1,2,4\text{-TMB,in}}$=3.5kPa

For the calculation of reaction rates it was assumed that the consumption of toluene, xylenes, 1,2,3-TMB, 1,3,5-TMB and TeMB in secondary reactions was negligible at such low conversion.

While the 1,2-methyl-shift-isomerisation of 1,2,4-TMB occurs mainly at the external surface the activation energies obtained for the transalkylation and paring reaction may be affected by intracrystalline diffusion, adsorption and the reaction itself and are therefore termed apparent activation energies. The apparent activation energies were approximately constant between 450°C and 350°C and amounted to 70kJ/mol, 70kJ/mol and 40kJ/mol for the 1,2-methyl-shift-isomerisation, transalkylation and paring reaction of 1,2,4-TMB respectively. There appears to be an increase in the apparent activation energy at lower temperature which indicates either a shift in the reaction mechanism or mass transfer limitation at high temperatures.

It is emphasised that the Arrhenius plot and the obtained apparent activation energies have to be treated as semi-quantitative, indicative data due to insufficient reaction data at low conversion levels.

3.3 CONCLUSIONS

In the temperature range 300°C to 450°C it was found that pseudo steady state can be assumed for times on stream longer than 120 minutes.

A reaction network model for the transformation of 1,2,4-TMB over ZSM-5 has been proposed (Figure 3.18). The 1,2-methyl-shift-isomerisation to 1,2,3-TMB and 1,3,5-TMB is the most rapid reaction of 1,2,4-TMB. The thermodynamic equilibrium of the TMB isomers accounts for approximately 32% conversion of the feed compound before any appreciable extent of other reactions has occurred. At low conversions up to 5-10% reverse reactions and other transformations of the TMBs are negligible relative to the main reaction. Under these conditions it is reasonable to assume that the rates of formation of

1,2,3-TMB and 1,3,5-TMB are equal to the rate of the respective isomerisation reactions of 1,2,4-TMB and thus reflect the isomerisation activity of the catalyst.

The composition of the xylene and TeMB fraction are not thermodynamically controlled at 1,2,4-TMB conversions below 30% and thus represent valuable information on the selectivity of ZSM-5.

There are further reactions occurring in parallel or consecutively to the initial 1,2-methyl-shift-isomerisation of 1,2,4-TMB. With regard to their kinetics and selectivities the rapid isomerisation of 1,2,4-TMB to 1,2,3-TMB and 1,3,5-TMB had to be treated as a pre-equilibration of the feed. The base of comparison for these reactions was therefore the conversion of the TMB-pool, i.e. the lumped TMB isomers.

Two primary reactions of 1,2,4-TMB or the TMB-pool were identified:

i) transalkylation yielding xylenes and TeMBs and

ii) the paring reaction leading to a pseudo-primary formation of toluene, benzene, ethene and propene.

The acid catalysed paring reaction and a corresponding reaction mechanism have been first reported by Sullivan *et al.* [1961]. However, this reaction is usually not considered in publications dealing with the transformation of methyl-aromatics over acid catalysts. This is mainly due to the very slow rate of this reaction relative to the main reactions, i.e. isomerisation and transalkylation, of frequently studied methyl-aromatics such as xylenes and toluene. The kinetics observed in this work and the presence of C_2^+-alkyl substituted benzenes which are required as intermediates, however, support that pathway.

Methane also was formed with primary or pseudo-primary kinetics and was assigned a co-product of coke formation which consequently behaves as a primary or pseudo primary product as well.

Xylenes and TeMBs are further converted in secondary reactions which are of the same type as the primary reactions of the TMB-pool:

i) 1,2-methyl-shift-isomerisation, which shifts the initially, kinetically controlled composition of the transalkylation product towards the thermodynamic equilibrium composition at higher conversions

ii) transalkylation yielding toluene as secondary and subsequently benzene as tertiary product

iii) the paring reaction leading to a secondary formation of xylene, toluene, benzene and C_2-C_4 olefins. This reaction path particularly affected the TeMB fraction.

The formation of paraffins in the C_2-C_4-fraction is attributed to olefin disproportionation yielding paraffins and aromatics.

A similar reaction network was found for the conversion of 1,2,4-TMB over amorphous silica-alumina with a Si/Al-ratio of 10 which was approximately 5 times less active than ZSM-5 with a Si/Al-ratio of 45.

A comparison of the obtained product distributions using concentration versus space time plots showed that the zeolite structure particularly promoted the paring reaction.

The isomer distribution in the TMB fraction at conversions lower than 30% was controlled by intrinsic kinetics over both ZSM-5 and silica-alumina. In the case of the 1,2,4-TMB transformation over ZSM-5 the absence of a shape selective effect over ZSM-5 was shown to indicate that the isomerisation of 1,2,4-TMB to 1,2,3-TMB and 1,3,5-TMB occurs primarily on the external surface of ZSM-5.

In contrast to amorphous silica-alumina, ZSM-5 showed a high product shape selectivity towards p-xylene. This showed that the formation of xylenes and thus transalkylation reactions of 1,2,4-TMB occur to a significant extent in the micropores of ZSM-5.

The selective formation of 1,2,4,5-TeMB accompanied by the selective formation of o-xylene over silica-alumina showed that this selectivity, can be caused by intrinsic kinetics and is therefore not necessarily due to transition state selectivity as often suggested in

literature. However, comparing silica-alumina and ZSM-5 a small shape selective effect favouring 1,2,4,5-TeMB was observed. It is concluded that the TeMBs observed in the product stream originate mainly from the external surface. However, 1,2,4,5-TeMB elutes to a small extent from the micropores. Most of the TeMBs which are formed in the micropores via transalkylation of 1,2,4-TMB are converted to xylene and ethene via the paring reaction before they can diffuse out of the crystal.

4.1 INTRODUCTION

The objective in this work was to study the transformation of 1,2,4-trimethylbenzene and its usefulness to probe external surface modifications of ZSM-5 crystals. This chapter describes preliminary experiments which were carried out in order to understand to what extent the 1,2-methyl-shift-isomerisation and transalkylation reactions of 1,2,4-TMB are restricted to the external surface. In order to decouple the catalytic effect of the external surface and the intracrystalline pore space the external surface of the parent sample coded ZSM-5* (Catalyst code vide Table 2.3) was coated with an inert Silicalite I shell using the secondary synthesis method described in Section 2.1.2.

4.2 RESULTS AND DISCUSSION

4.2.1 Characterisation of the modification

The parent ZSM-5* and the modified sample Sil-ZSM-5* were characterised by AAS, SEM, XRD, BET, NH_3-TPD, 1,3,5-TiPB cracking and n-hexane cracking.

4.2.1.1 Effect on physicochemical properties

The characteristic physicochemical data of ZSM-5* and Sil-ZSM-5* are listed in Table 2.2. The Si/Al ratio as measured by AAS increased from 26 to 100 when ZSM-5* was subjected to a secondary synthesis treatment. The increase of the Si/Al ratio by a factor of ~4 was roughly in agreement with the mass increase factor of $m_{Sil\text{-}ZSM\text{-}5*}/m_{ZSM\text{-}5*}=4.5$.

X-ray diffractograms verified that the crystals observed were iso-structural to ZSM-5 (Table I.1, Appendix I) and that no other crystal structure was formed. The absence of amorphous material was indicated by SEM micrographs (Figure 2.1). It can therefore be concluded that both materials had MFI-structure. The material formed during the secondary synthesis was expected to be aluminium free (Silicalite I). However, it should be noted that aluminium of the parent ZSM-5 may redissolve during the secondary

synthesis and incorporate into the forming Silicalite.

The BET meso- and macro-pore volume decreased while the micropore volume increased (Table 2.2) indicating an increase in the crystal size.

The SEM micrographs showed that the apparent crystal size of both the parent and the modified sample ranged from 1-3 μm thus not showing a change in apparent crystal size due to the formation of a Silicalite shell. A theoretical increase of 60% of the crystal diameter was calculated, assuming that all the material was deposited on the parent crystals, all crystals had grown with the same mass ratio and all crystals had an initial diameter of 2 μm. The data obtained in the physicochemical characterisation, however, are not sufficient to show that the Silicalite has formed as a shell around the parent ZSM-5 crystals.

4.2.1.2 Effect on the external surface activity

The amounts of ZSM-5* and Sil-ZSM-5* loaded into the reactor were chosen with the intention to keep the number of aluminium atoms in the catalyst bed constant. It was assumed that by loading the same amounts of aluminium the same amount of parent seeds were loaded, and thus the WHSV with respect to the mass of ZSM-5* was kept constant (Section 2.3.2.4). In this way changes in conversion can then clearly be ascribed to changes in activity caused by structural modifications (e.g. a Silicalite shell).

The conversion of 1,3,5-TiPB over the parent ZSM-5 decreased from 90% to 80% within 2 hours of time on stream as shown in Figure 4.1. Over Sil-ZSM-5* the conversion decreased from 10% to 6%. To account for the change of activity with time on stream conversions measured after 10 minutes were considered to be representative for the fresh catalyst in pseudo steady state. Thus the modification procedure caused the conversion to decrease from 90% to 10% (Table 4.1). Since 1,3,5-TiPB cracking is limited to the external surface of ZSM-5 crystals (Section 1.5.3) the difference in activity can be ascribed to inactivation thereof. The inactivation of the external surface may be due either

Chapter 4

Investigation on the Role of the External Surface during the Transformation of 1,2,4-Trimethylbenzene over ZSM-5 using a Silicalite I Shell

to the formation of a catalytically inert Silicalite shell on the external surface of the ZSM-5* crystals or aluminium leached from the crystal surface during the secondary synthesis.

A 1,3,5-TiPB conversion of 10% over Sil-ZSM-5* showed that the expected 100% inactivation of the external surface was not achieved. A blank run where the reactor was packed with pure sand showed that this residual conversion was not due to thermal cracking (Appendix V.4). Alternatively, trace quantities of aluminium may have either incorporated into the inert Silicalite shell or migrated from ZSM-5* seeds during or after the secondary synthesis. It is also possible that dissolution of the ZSM-5* seeds during the secondary synthesis could provide aluminium for incorporation into the Silicalite layer. It may also be possible that fractions of the external surface were not coated. Nevertheless, a significant change was observed in the activity. If a first order rate equation can be assumed for this reaction, the rate constant can be calculated using Equation 2.8 (Section 2.3.4.5) with m_{cat} being the mass of ZSM-5* in the evaluation of both constants (i.e. on Al-basis). The first order rate constant decreased by a factor of 22 from $k_{ZSM\text{-}5*}=33$ $cm^3g^{-1}s^{-1}$ to $k_{Sil\text{-}ZSM\text{-}5*}=1.5$ $cm^3g^{-1}_{parent}s^{-1}$. This is to say that there is 22 times less active external surface on Sil-ZSM-5* when compared to ZSM-5*.

4.2.1.3 Effect on the bulk activity

Hexane cracking is widely used to measure relative activities of cracking catalysts [Haag *et al.*, 1990] (Section 1.5.1). For ZSM-5 it has been shown that intracrystalline diffusional limitations are negligible for crystal sizes smaller than 40 μm at 500°C [Haag *et al.* 1981; Post *et al.*, 1983; Voogd and van Bekkum, 1990]. Thus hexane cracking represents a reaction which fully utilises the intracrystalline pore space.

Plotting the conversion versus time on stream as in Figure 4.2 showed that changes in activity due to catalyst deactivation were within the experimental scatter. Thus the average conversion was used to compare activities. The conversion of hexane was reduced from 23% over ZSM-5* to 12% over Sil-ZSM-5*. This represented a decrease in the first order rate constant as related to the mass of ZSM-5* by a factor of 2. It is,

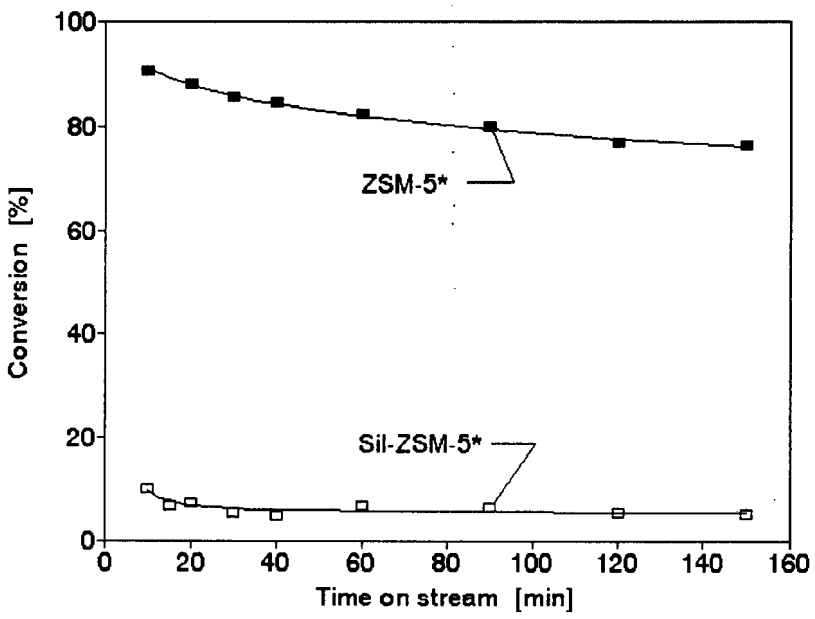

Figure 4.1: **Effect of coating ZSM-5* with a Silicalite I shell on the conversion of 1,3,5-TiPB as a function of time on stream [T=270°C, $p_{1,3,5\text{-TiPB}}$=0.15kPa and WHSV=0.35h^{-1}]**

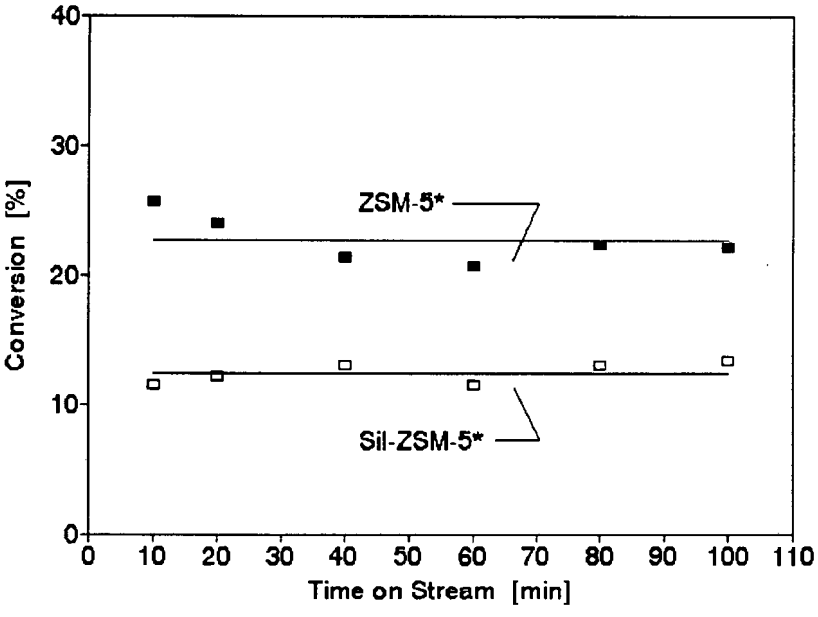

Figure 4.2: **Effect of coating ZSM-5* with a Silicalite I shell on the conversion of n-hexane as a function of time on stream [T=538°C, $p_{n\text{-hexane}}$=10kPa and WHSV = 5.5h^{-1}]**

however, highly unlikely that the external surface could contribute 50% to the observed reaction rate over ZSM-5*.

The decrease in activity due to a lower number of aluminium atoms or Brønsted acid sites in the catalyst bed can be ruled out, since both were kept the same (Section 2.3.2.4). Considering the data obtained from NH_3-TPD, the total number of Brønsted acid sites in the catalysts bed was even slightly larger for Sil-ZSM-5* (0.09 mmol) than for ZSM-5* (0.084 mmol) (Specific NH_3-TPD values are given in Table 2.2).

Aluminium dissolution during secondary synthesis and incorporation into the formed Si rich material may have decreased the acid site density and possibly reduce the intrinsic n-hexane cracking activity of an acid site. However, Olson *et al.* [1980] and Wielers *et al.* [1991] showed that at 538°C the cracking constant varies linearly with the aluminium content. Since the intrinsic activity of an acid site in ZSM-5 is represented by the slope of this correlation, it is independent of the acid site density.

This high loss of n-hexane cracking activity therefore suggests that the modification created significant diffusion resistances. It is of course possible that the growth of a Silicalite layer over the ZSM-5* seeds may not be as defect free and crystalline as would be expected. Thus it is possible that the Silicalite layer partially blocks pore openings and increases the tortuosity of the diffusion path. These diffusional resistances may influence the accessibility of the acid sites and consequently the activity of Sil-ZSM-5*. The creation of diffusion resistances and the simultaneous inactivation of the external surface strongly indicates that the material formed during the secondary synthesis was deposited on the external surface of the parent seeds.

4.2.2 Effects of Silicalite I coating on the transformation of 1,2,4-TMB

The effect of the inactivation of the external surface on the conversion, rates of formation and selectivity is expected to shed light on the role of the intracrystalline pore space and the external surface in the transformation of 1,2,4-TMB over ZSM-5.

4.2.2.1 Conversion

The conversion of 1,2,4-TMB decreased with time on stream (Figures 4.3). After 120 minutes of time on stream, however, stable conversions were achieved over both catalysts. The conversions as shown in Table 4.1 are the average of the values measured between 120 and 300 minutes of time on stream.

Table 4.1 shows that Silicalite coating reduced the conversion of 1,2,4-TMB from 23% to 5% notwithstanding that the number of aluminium atoms in the catalyst bed was kept constant. The decreased activity may be ascribed to the reduced accessibility of the micropore space and / or the inactivation of the external surface.

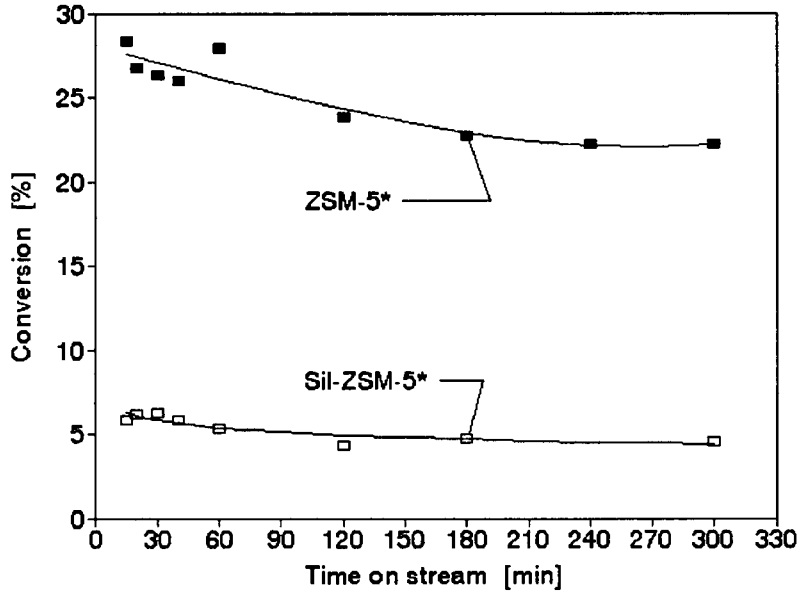

Figure 4.3: Effect of coating ZSM-5* with a Silicalite I shell on the conversion of 1,2,4-TMB as a function of time on stream [T=450°C, $p_{1,2,4\text{-TMB}}$=1.3kPa and WHSV=0.6h^{-1}]

The activity of Sil-ZSM-5* during the conversion of n-hexane, 1,2,4-TMB and 1,3,5-TiPB was 48%, 20% and 5% of the activity of ZSM-5* respectively (Table 4.1). Comparing these activity ratios shows that the sensitivity of the 1,2,4-TMB reaction

towards a loss of activity was between the two extreme cases of 1,3,5-TiPB and n-hexane. If the transformation of 1,2,4-TMB over ZSM-5 was not subjected to any significant diffusion or external surface effects, a decrease in conversion similar to that of n-hexane cracking might have been expected. On the other hand, if the conversion of 1,2,4-TMB takes place exclusively on external acid sites the decrease in conversion might have been expected to be similar to the decrease of the first order rate constant for 1,3,5-TiPB cracking. For the latter deduction it is assumed that reactions which are limited to the external surface would experience similar reductions in activity. The catalytic activity data indicate that the consumption of 1,2,4-TMB takes place to a certain degree inside the micropores. A quantitative analysis of these data is not possible since the reaction kinetics of 1,3,5-TiPB cracking and the conversion of 1,2,4-TMB are not known.

Table 4.1: Activities of ZSM-5* and Sil-ZSM-5* as measured by conversion at T=450°C, $p_{1,2,4\text{-TMB}}$=1.3kPa and WHSV=0.6h^{-1} (i.e. equivalent number of aluminium atoms in the catalyst bed)

Reactant	X over ZSM-5* (mol%)	X over Sil-ZSM-5* (mol%)	Ratio Sil-ZSM-5*/ZSM-5*
n-hexane[a)]	25	12	0.48
1,3,5-TiPB[b)]	90	10	0.05[d]
1,2,4-TMB[c)]	23	5	0.22

[a)] Average of data obtained between 10 and 100 minutes of time on stream
[b)] Conversion after 10 minutes of time on stream
[c)] Average of data obtained between 120 and 300 minutes of time on stream
[d)] Ratio of first order rate constants

4.2.2.2 Individual reaction rates

1,2,4-TMB is converted via several parallel occurring reaction paths, i.e. isomerisation, transalkylation and the paring reaction (Figure 3.18, Section 3.2.3.4), involving product molecules and possibly transition states of different sizes (Section 1.6 and 3.2.3). The catalyst activity for each reaction path is reflected by the respective reaction rate.

In Section 3.2.3.5 it was shown that at conversions up to 25% (Figure 3.20) secondary and reverse reactions are negligible. The effect of the Silicalite shell on the rates of the 1,2-methyl-shift-isomerisation, the transalkylation and the paring reaction can therefore be monitored using the rates of formation of 1,2,3-TMB+1,3,5-TMB, xylenes+TeMBs and toluene respectively (Equations 2.11 to 2.13, Section 2.3.4.6). The rates of product formation (mmol/g_{parent}/h) used in Equations 2.11 to 2.13 are the average of the integral rates measured between 120 and 300 minutes of time on stream, at 23% and 5% conversion for ZSM-5* and Sil-ZSM-5* respectively. The rates were related to the mass of the parent catalyst in both cases and are listed in Table 4.2

The effect of the Silicalite shell on a particular reaction rate is quantified in the fourth column of Table 4.2 as a rate ratio:

$$R_i = \frac{r_{i,Sil\text{-}ZSM\text{-}5*}}{r_{i,ZSM\text{-}5*}} \qquad (4.1)$$

where $r_{i,x}$ is the average, integral rate of the reaction i over the respective zeolite x.

The reaction rate ratios show that the Silicalite shell reduced the 1,2-methyl-shift-isomerisation to 10% of the parents activity as compared to 48% and 60% for the transalkylation and paring reaction respectively thus increasing the selectivity towards the two latter reactions. In Section 3.2.3.5 (Figure 3.20), however, it was shown that the selectivity towards the primary reactions of 1,2,4-TMB does not change when the conversion is decreased from 23% to 5%. It can therefore be concluded that the different degrees of reduction for the various reaction rates is a shape selective effect of the Silicalite shell and not a conversion effect.

From the fact that the reaction rates are reduced in a selective way it can be concluded that the intracrystalline pore space does play a significant role in the transformation of 1,2,4-TMB. If all reactions of 1,2,4-TMB would be totally restricted to the external surface an indiscriminative reduction of the reaction rates would have been expected.

Table 4.2: **Effect of Silicalite coating on the integral rates of product formation and reaction rates during the transformation of 1,2,4-TMB over ZSM-5* and Sil-ZSM-5* at T=450°C, $p_{1,2,4\text{-TMB}}$=1.3kPa and WHSV=0.6h^{-1} (i.e. constant number of aluminium atoms in the catalyst bed)**

Product	$r_{formation}$ over ZSM5*[a] at 23% conversion (mmol/g_{parent}h)	$r_{formation}$ over Sil-ZSM5*[a] at 5% conversion (mmol/g_{parent}h)[b]	Rate ratio R_i Sil-ZSM5*$_{5\%}$/ ZSM5*$_{23\%}$
toluene	0.020	0.012	0.13
o-xylene	0.013	0.007	0.15
m-xylene	0.029	0.015	0.10
p-xylene	0.014	0.010	0.22
1,2,3-TMB	0.35	0.03	0.12
1,3,5-TMB	0.64	0.07	0.10
1,2,3,4-TeMB	0.0025	0.0003	0.12
1,2,3,5-TeMB	0.0091	0.0009	0.10
1,2,4,5-TeMB	0.0080	0.0034	0.25
$r_{Isomerisation}$[c]	0.99	0.10	0.10
$r_{Transalkylation}$[d]	0.076	0.036	0.48
$r_{Paring\text{-}reaction}$[e]	0.020	0.012	0.60

[a] Average of data obtained between 120 and 300 minutes of time on stream

[b] the same mass of parent is based on equal aluminium contents in the catalyst bed

[c] $r_{Isomerisation} = r_{1,2,3\text{-TMB}} + r_{1,3,5\text{-TMB}}$

[d] $r_{Transalkylation} = r_{xylenes} + r_{TeMBs}$

[d] $r_{Paring\text{-}reaction} = r_{toluene}$

As discussed for the decreased 1,2,4-TMB conversion in the previous section the reduction of the individual reaction rates may be caused by the inactivation of the external surface and / or the introduction of diffusion resistances caused by the Silicalite shell.

For example the selective reduction of the 1,2-methyl-shift-isomerisation by the Silicalite shell could be explained bothways:

i) due to their larger molecular diameter 1,2,3-TMB and 1,3,5-TMB are more sensitive towards increased diffusion limitations than transalkylation and paring reaction products such as 1,2,4,5-TeMB, xylenes and toluene. If 1,2,3-TMB+1,3,5-TMB are primarily formed inside the micropores the introduction of

diffusion resistances would selectively inhibit the 1,2-methyl-shift-isomerisation;

ii) if the 1,2-methyl-shift-isomerisation would be restricted to the external surface of ZSM-5, while the transalkylation and paring reaction of 1,2,4-TMB also occurs in the micropores, the inactivation of the external surface would also lead to a selective inhibition of the 1,2-methyl-shift-isomerisation.

Therefore it is not possible to relate the effect of the Silicalite shell on the reaction rates to the inactivation of the external surface in a straightforward manner and the data on their own do not clearly rank the reactions of 1,2,4-TMB according to the degree to which they are limited to the external surface.

However, over ZSM-5* the observed rate of 1,2-methyl-shift-isomerisation is one order of magnitude greater than the transalkylation or paring reaction rate (Table 4.2). All the 1,2,4-TMB reaction molecules are large enough to undergo diffusion restriction within the ZSM-5 pores. Thus fast 1,2-methyl-shift-isomerisation reactions occurring within the pores will be severely diffusion limited and thus it is more likely that the 1,2-methyl-shift-isomerisation products originate mainly from the external surface (vide Section 3.2.4.4). Within the pores the 1,2-methyl-shift-isomerisation could still be faster than the transalkylation and paring reaction, but the contribution of the micropores to the overall reaction may be negligible.

For a qualitative approximation the inactivation of the external surface and the introduction of diffusion resistances by the Silicalite shell may be decoupled by comparing the 1,2,4-TMB data to n-hexane and 1,3,5-TiPB cracking data. The reduction in the rate of formation for both 1,2,3-TMB and 1,3,5-TMB and consequently the isomerisation rate, as expressed by $R_i = 0.10$ (Table 4.2) is similar to the reduction in the first order rate constant observed in the reaction of 1,3,5-TiPB ($R_i = 0.05$, Table 4.1) which occurs only at the external surface. This suggests that 1,2,3-TMB and 1,3,5-TMB originate mainly from the external surface.

On the other hand the paring reaction as well as the transalkylation of 1,2,4-TeMB seem to occur to a significant proportion inside the zeolite channels since these reaction rates

were clearly less reduced by the Silicalite shell analogous to the case of n-hexane cracking.

The effect of the Silicalite shell showed that the extent to which a reaction of 1,2,4-TMB occurs in the micropores of ZSM-5 increases according to the following sequence:

1,2-methyl-shift-isomerisation < transalkylation < paring reaction

thus confirming the findings when ZSM-5 was compared with amorphous silica-alumina.

4.2.2.3 Selectivity

Since only minor amounts of the samples ZSM-5* and Sil-ZSM-5* were available it was most practical to study the effect of the Silicalite shell on catalytic properties while keeping the WHSV constant. ZSM-5* and Sil-ZSM-5*, however, showed different activities and thus yielded different conversions of 24% and 5% respectively. In this conversion range the distributions of isomers in the xylene, the TMB and the TeMB fractions are not at equilibrium and changes significantly with conversion (Figures 4.5 - 4.7). Since the distribution of these isomers is affected by the conversion level, the effect of the Silicalite shell on selectivity cannot be studied by comparing Sil-ZSM-5* with ZSM-5*.

Figures 4.5 to 4.7 show that the respective isomer distributions obtained over ZSM-5* at 1.3 kPa were identical with the isomer distributions obtained over the sample coded ZSM-5 at 3.5 kPa. Although, the distributions were very close to thermodynamic equilibrium, this indicates that the two ZSM-5 samples yielded similar selectivities and that the variation of the 1,2,4-TMB partial pressure from 1.3 kPa to 3.5 kPa had no significant effect. With this in mind the selectivity over Sil-ZSM-5* may be compared with the selectivity over the sample ZSM-5 at the same 1,2,4-TMB conversion level. The data for the sample ZSM-5 were already discussed in Chapter 3.

Figure 4.4 shows that Silicalite coating decreased the ratio [1,2,3-TMB]/[1,3,5-TMB] by approximately 25% at a conversion level of 5%. In a reaction which is limited to the external surface, neither the inactivation of the external surface nor of the intracrystalline pore space is expected to affect the product distribution. The fact that a change in the composition of the isomerisation product occurred at all thus indicates that the intracrystalline pore space does play a role in the 1,2-methyl-shift-isomerisation of 1,2,4-TMB to a certain extent.

To discuss this effect on the [1,2,3-TMB]/[1,3,5-TMB] ratio it is assumed a priori that the formation of 1,3,5-TMB (σ=7.7Å) is limited to the external surface while 1,2,3-TMB (σ=7.0Å) which has a smaller kinetic diameter can also be formed by the intracrystalline pore space. Based on this assumption it would be expected that inactivating the external surface would inhibit the formation of both isomers on the external surface to the same degree without inhibiting the formation of 1,2,3-TMB by the micropore space. The net effect would thus be an increase in the selectivity towards 1,2,3-TMB. However, the opposite was observed.

Hexane cracking showed that the Silicalite coating reduced not only the external surface activity but also the accessibility of the intracrystalline pore space. The inactivation of the intracrystalline pore space would selectively inhibit the formation of 1,2,3-TMB. With the inactivation of the external surface affecting the formation of 1,2,3-TMB and 1,3,5-TMB on the external surface to the same degree the expected net effect would be a decreased selectivity towards the formation of 1,2,3-TMB. This was indeed observed, thus indicating that 1,2,3-TMB is formed by the micropores to a higher degree than 1,3,5-TMB.

In apparent contradiction to the shape selective formation of 1,2,3-TMB by the micropore space, Section 3.2.4.4 showed that the concentration ratio [1,2,3-TMB]/[1,3,5-TMB] was similar for both the unmodified ZSM-5 and amorphous silica-alumina. Thus the 1,2-methyl-shift-isomerisation of 1,2,4-TMB over unmodified ZSM-5 is controlled by intrinsic reaction kinetics as opposed to shape selectivity. However, this is in contrast to what

would be expected if fast primary reactions yielding critically sized product molecules would take place predominantly in the micropores. This indicates that the isomerisation of 1,2,4-TMB takes place to a large proportion on the external surface.

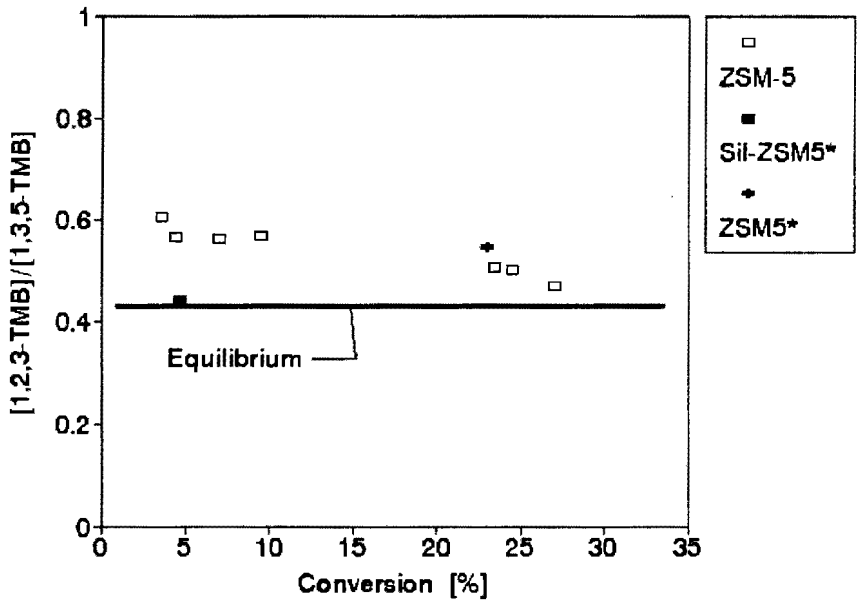

Figure 4.4: **The effect of the Silicalite shell on the ratio [1,2,3-TMB] / [1,3,5-TMB] at T=450°C and 5% conversion. ZSM-5 and ZSM-5* are different samples (vide Table 2.3).**

Figure 4.5 and 4.6 show that the Silicalite coating affected the product distributions in the TeMB fraction thus confirming that the micropores play a role in the transalkylation of 1,2,4-TMB. The selectivity of ZSM-5 for the various transalkylation reactions is therefore subject to transition state and / or product shape selectivity. The bi-phenylic transition states leading to the formation of 1,2,4,5-TeMB and the product molecule itself are smaller than 1,2,3,4-TeMB, 1,2,3,5-TeMB (Table 1.7) and their transition states (Figure 1.15) with respect to their critical molecular diameters. Thus it can be concluded that 1,2,4,5-TeMB is formed to a larger proportion by the micropore space than 1,2,3,4-TeMB and 1,2,3,5-TeMB. This is confirmed by the increased concentration ratios [1,2,4,5-TeMB]/[1,2,3,5-TeMB] and [1,2,4,5-TeMB]/[1,2,3,4-TeMB] by approximately 35% and 100% respectively. Both, the inactivation of the external surface and the

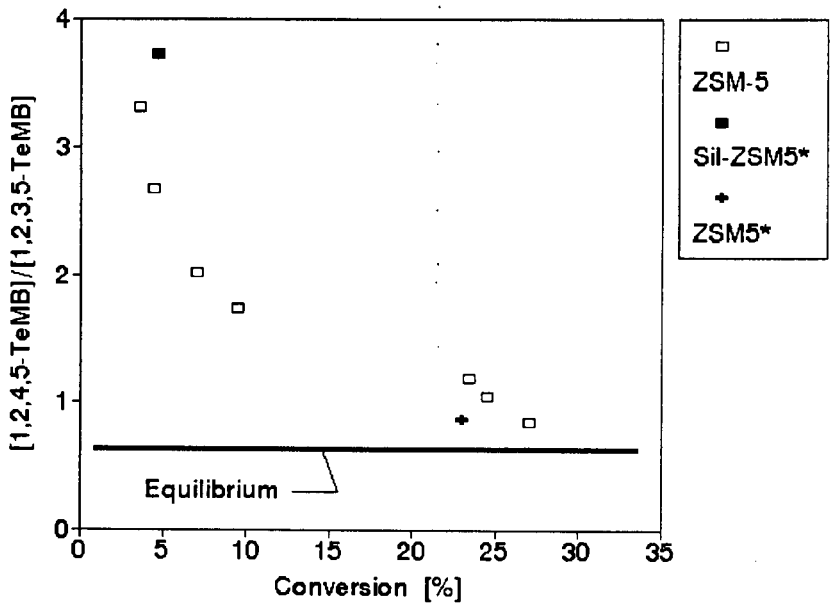

Figure 4.5: **The effect of the Silicalite shell on the ratio [1,2,4,5-TeMB] / [1,2,3,5-TeMB] at T=450°C and 5% conversion. ZSM-5 and ZSM-5* are different samples (vide Table 2.3).**

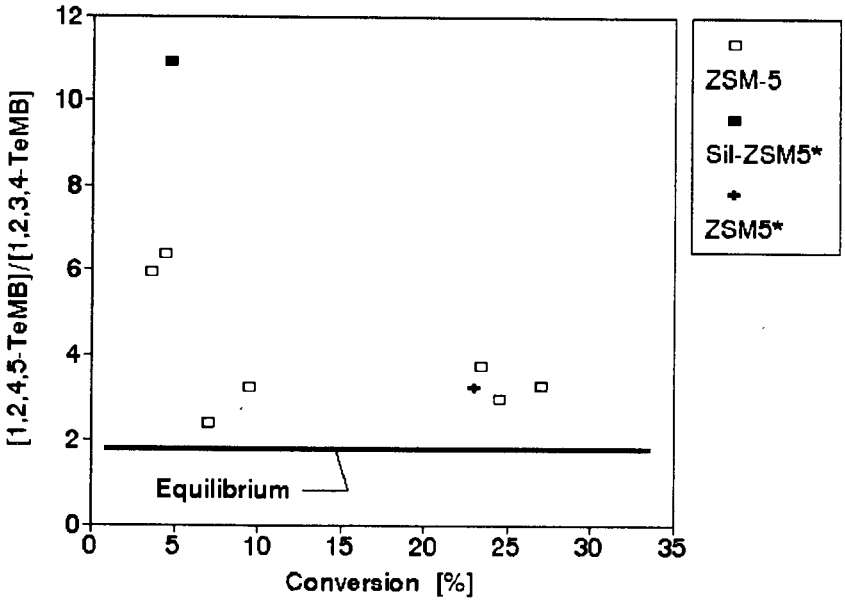

Figure 4.6: **The effect of the Silicalite shell on the ratio [1,2,4,5-TeMB] / [1,2,3,4-TeMB] at T=450°C and 5% conversion. ZSM-5 and ZSM-5* are different samples (vide Table 2.3).**

reduced accessibility of the micropore space may selectively inhibit the formation of the bulkier 1,2,3,5-TeMB and 1,2,3,4-TeMB.

The xylene distribution was not significantly affected by the Silicalite shell (Figure 4.7). The composition of this fraction, however, was close to the thermodynamic equilibrium composition. It may, therefore, be concluded that fast secondary 1,2-methyl-shift-isomerisation reactions of the xylene isomers take place and mask the effects of the Silicalite shell on the selectivity towards primary transalkylation reactions. From a product shape selective aspect all xylenes can be formed in the micropores with p-xylene as the favoured product.

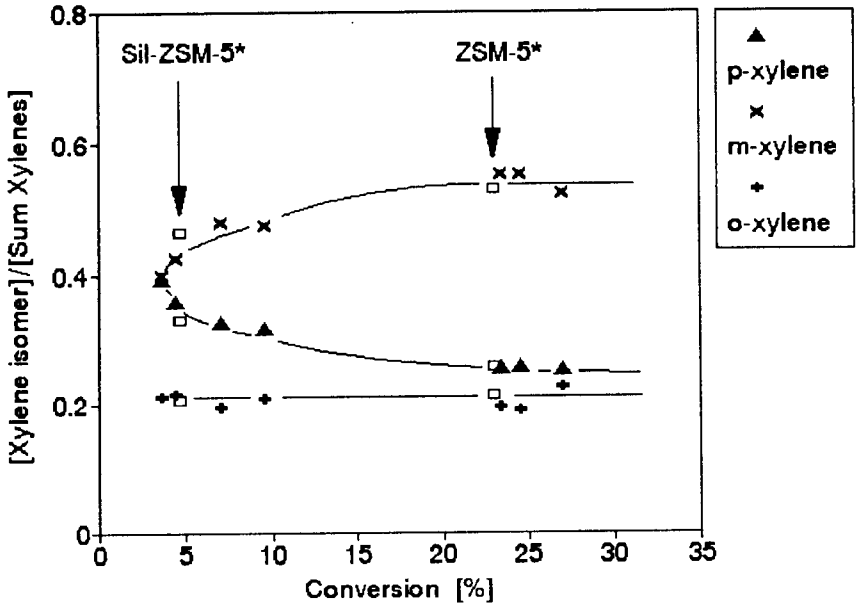

Figure 4.7: **The effect of the Silicalite shell on the distribution of xylene isomers at T=450°C and 5% conversion. The data points representing the relation between the xylene distribution and the conversion were obtained over the sample with the code ZSM-5 (Table 2.3), whereas the symbols□ represent the distributions obtained over ZSM-5* and Sil-ZSM-5*.**

4.3 CONCLUSIONS

Coating ZSM-5 crystals with a Silicalite shell inactivated the external surface by a factor of 22 but simultaneously reduced the activity and / or the accessibility of the intracrystalline pore space by a factor of 2 as measured by n-hexane cracking. The latter factor is likely to be larger for the reactions of 1,2,4-TMB. This modification method is therefore insufficient to completely decouple the catalytic effects of the external surface and the intracrystalline pore space. This method can thus not be used to prove that a reaction is totally restricted to the external surface nor that the catalytic activity of the external surface is negligible.

However, the Silicalite shell selectively inhibited the 1,2-methyl-shift-isomerisation of 1,2,4-TMB and it is concluded that the transalkylation and paring reaction occur to a larger extent inside the micropores of ZSM-5 than the 1,2-methyl-shift-isomerisation.

Effects on product distributions in combination with the consideration of shape selective aspects indicated that 1,2,3-TMB is formed to a larger extent inside the micropores than 1,3,5-TMB, and 1,2,4,5-TeMB is formed to larger extent inside the micropores than 1,2,3,4-TeMB and 1,2,3,5-TeMB.

The 1,2-methyl-shift-isomerisation was the fastest reaction of 1,2,4-TMB. Considering the high diffusional demands of 1,2,3-TMB and 1,3,5-TMB and the non-shape selective product composition observed over unmodified ZSM-5 it is proposed that these products are primarily formed on the external surface.

For the purpose of using the transformation of 1,2,4-TMB as a probe reaction it is proposed that the concentration ratio [1,2,4,5-TeMB]/[1,2,3,5-TeMB] may be used to quantify the effect on the shape selective properties of ZSM-5, while the rate of formation of the isomerisation products 1,2,3-TMB and 1,3,5-TMB is suggested to monitor the activity of the external surface.

Chapter 5

Chemical Vapour Deposition of Tetraethoxysilane over ZSM-5

5.1 INTRODUCTION

It has been reported that the chemical vapour deposition (CVD) of tetra-alkoxysilanes over ZSM-5 inertises the external surface, reduces the pore mouth size while leaving the micropore space unaffected. These effects result in a modified shape selectivity. It would be desirable to identify a CVD procedure which allows a controlled, stepwise increase the degree of modification. This section investigates the effect of the deposition temperature, calcination, deposition time and the effect of repeated CVD-calcination cycles during the CVD of tetra-ethyl-ortho-silicate (tetraethoxysilane, TEOS) over ZSM-5. Characterisation is done using probe reactions which offer a more realistic measure of modifications by probing the bulk activity, the activity of the external surface and shape selectivity. The CVD of TEOS is also a promising method to study the effect of external surface modifications on the transformation of 1,2,4-TMB.

5.2 RESULTS AND DISCUSSION

5.2.1 Preliminary screening of important CVD parameters

It is adequate to monitor the sample weight and the external surface activity when screening CVD parameters. This was done using a micro-balance and 1,3,5-TiPB cracking in a fixed bed reactor.

5.2.1.1 Deposition temperature

Figure 5.1 shows the effect of the deposition temperature during the CVD of TEOS in a flow reactor on the external surface activity of ZSM-5 as measured by the conversion of 1,3,5-TiPB (Experimental see Section 2.3.2.5). The CVD treatment at 75°C reduced the external surface activity as measured by 1,3,5-TiPB conversion by 55% from a conversion of 33% over the parent to 18% over the modified catalyst. At CVD temperatures above 250°C the conversion was decreased to approximately 3%. Thus the external surface was deactivated to a higher degree at higher CVD temperatures. This may be due to a higher

amount of deposited material or a more uniform coating of the external surface.

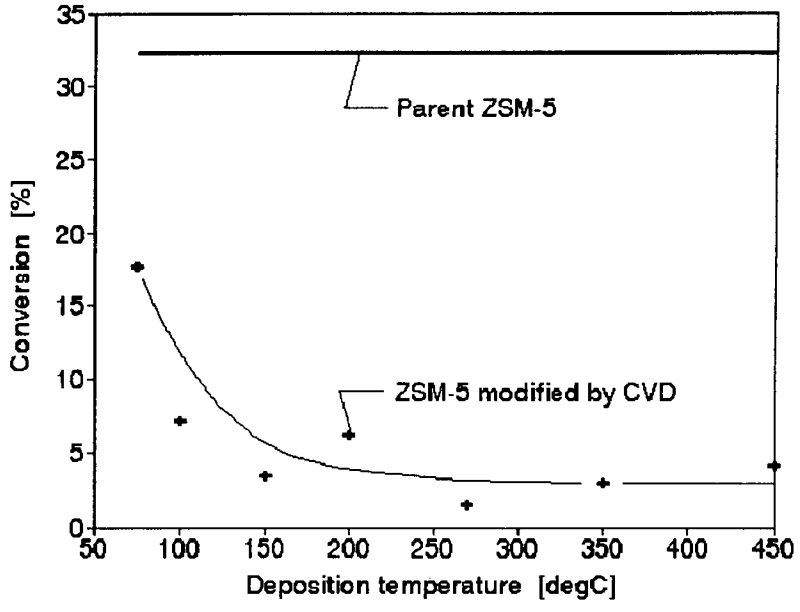

Figure 5.1: **The effect of deposition temperature during CVD of TEOS followed by calcination in air on the activity of ZSM-5 in the conversion of 1,3,5-TiPB.**
CVD of TEOS: $p_{TEOS}=0.4kPa$, **WHSV=1.5h^{-1}**
TiPB cracking: $p_{1,3,5\text{-}TiPB,\ in}=0.17kPa$, **WHSV=1.1h^{-1}, T=270°C**

Gravimetric experiments using a micro-balance showed a mass increase at the end of the CVD treatment of 35, 79 and 138mg per gram of dry catalyst for a deposition temperature of 100°C, 270°C and 450°C respectively (Figure 5.2). This shows that the increased amount of deposited material was mostly the cause of the higher degree of inactivation of the external surface at higher CVD temperatures (Figure 5.1).

At 100°C and 270°C the deposition rate of TEOS indicated by the slope of the uptake curves decreased with time on stream and thus with increasing coverage of the external surface (Figure 5.2). For example at 100°C the uptake rate decreased from an initial rate $r_{ads,\ 100°C}=4.2mg/g/h$ to a final rate $r_{ads,\ 100°C}=0.57mg/g/h$. When explaining this behaviour, it should be noted that in theory it is possible to distinguish between deposition sites on the fresh zeolite surface which may be termed as surface hydroxyls

(i.e. terminal silanol groups plus Brønsted acid sites) and the deposition sites on the surface of the deposited phase which are most probably ethoxy groups. The decreasing deposition rate at 100°C shows that the surface of the deposited phase is less reactive than the surface of the fresh zeolite. Wang *et al.* [1988] observed a similar behaviour at temperatures between 180°C and 230°C.

As the CVD temperature increased the deposition rate as measured at equal amounts of deposited mass increased, indicating an increased reactivity of the surface of the fresh zeolite and / or the surface of the deposited phase. An increased reactivity of the surface of the deposited phase, however, may enhance vertical growth of the deposited phase and may thus lead to a less uniform and less controlled deposition. Vertical growth may also be promoted by the presence of product water which may be more readily available at temperatures above 200°C [Chun *et al.*, 1994] due to the decomposition of ethanol which is a primary deposition product. Ethoxy groups of chemisorbed ethoxy-silanes may thus be hydrolysed to silanol groups which may be more reactive for further deposition of TEOS.

At a CVD temperature of 450°C the uptake rate was constant. The mass flow rate of TEOS was 2g/h, assuming that the carrier gas was saturated with TEOS. The rate of mass deposited, however, was only 0.6mg/h, thus ruling out the possibility that the mass flow rate of TEOS entering the micro-balance was the rate limiting step. However, it may be possible that the actual reaction rate of both the surface of the fresh zeolite and the surface of the deposited phase increased to such an extent due to the high temperature that diffusion into zeolite packing became the rate limiting step, thus disguising the time on stream behaviour of the actual reaction rate.

It may also be argued that the original surface of ZSM-5 was as reactive towards TEOS as the deposited phase (Figure 5.2), indicating that the chemisorption sites of both surfaces are of the same type. It may therefore be suggested that the growth of the deposited phase at high temperatures proceeds via the transformation of surface ethoxy groups into intermediate silanol groups, which also occur on the external surface of the unmodified

ZSM-5, followed by chemisorption of TEOS. The formation of intermediate silanol groups may occur either via decomposition of adsorbed ethoxy groups into a silanol group and ethylene or via hydrolysis of the surface ethoxy group by reaction water. The reaction water may be formed via dehydration of ethanol, which is a primary product in the deposition reaction of TEOS (Section 1.3.6).

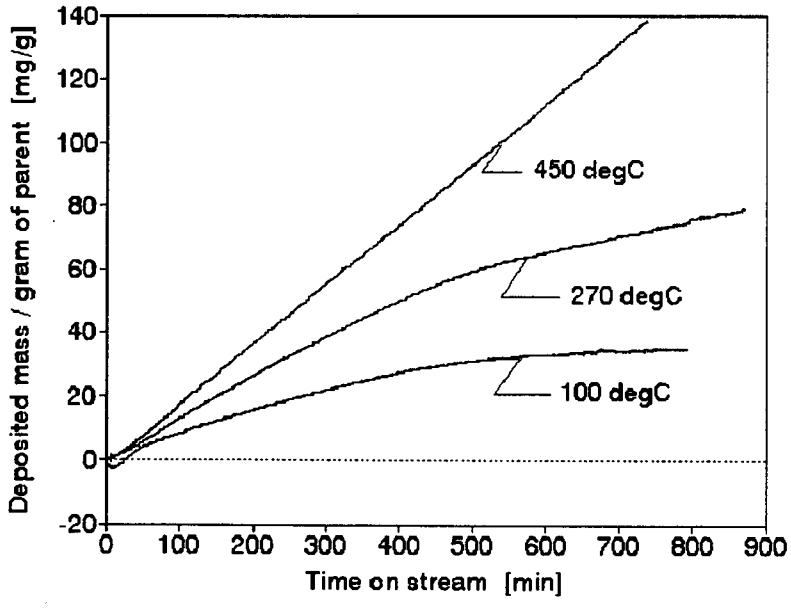

Figure 5.2: The effect of deposition temperature on the sorption behaviour of ZSM-5 during the CVD of TEOS, $m_{0,dry\ cat}$=47.3mg

It may be proposed that at low CVD temperatures TEOS is deposited primarily on the original zeolite surface while deposition onto the surface of deposited material is slow. With increasing temperature the significance of the latter and therefore the significance of vertical growth increases.

Figure 5.2 showed that the final deposition rate decreased with decreasing deposition temperature. At 100°C the CVD reaction showed a saturation effect and thus appeared to be self regulating. Hence the uniformity of the deposition throughout the catalyst bed and epitaxial growth is expected to be promoted best at low temperatures. Therefore from this point on CVD treatments were carried out at 100°C.

5.2.1.2 *Post-CVD flushing and calcination*

Figure 5.3 to 5.5 show the effects of flushing at deposition temperature, heating or cooling to 270°C during flushing and calcination after completion of the CVD period in the micro-balance at various deposition temperatures.

Figure 5.3 shows that at deposition temperatures between 100°C and 450°C the mass loss during 30 minutes of flushing at deposition temperature is smaller than 3% of the deposited mass and thus negligible.

Cooling from 450°C to 270°C (Figure 5.3.c) or isothermal flushing at 270°C (Figure 5.3.b) did not result in a significant mass loss. Whereas heating to 270°C resulted in a mass loss of 35wt% of the mass deposited at 100°C (Figure 5.3.a) due to the desorption and / or decomposition of TEOS surface species.

(a)

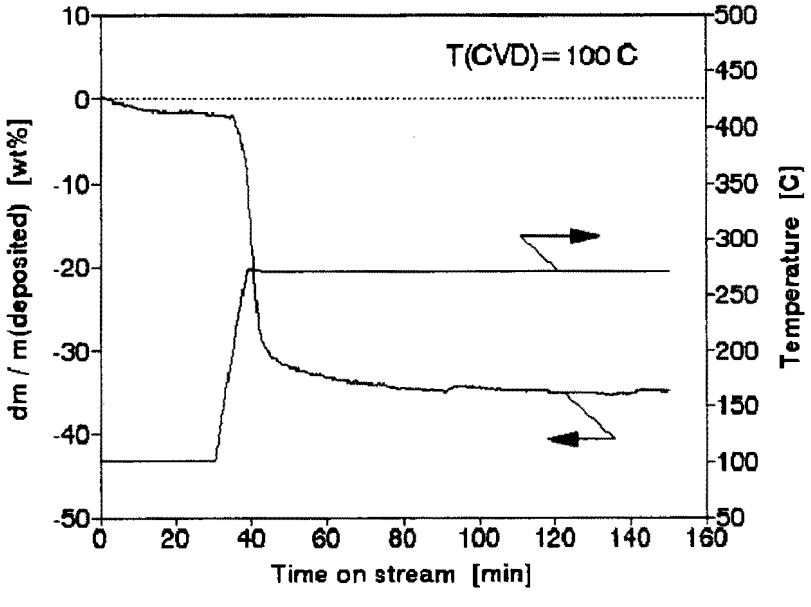

To Figure 5.3

(b)

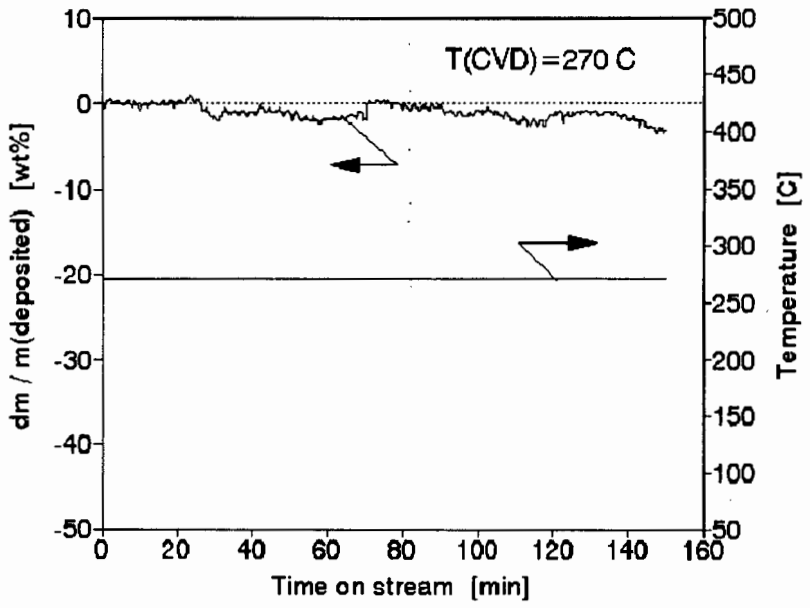

(c)

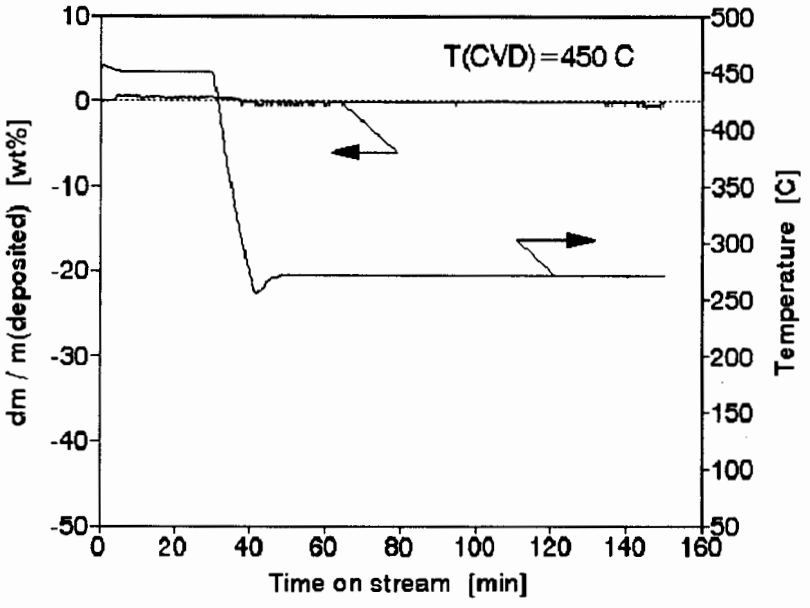

Figure 5.3: **The effect of the post-CVD flushing procedure on the amount of material adsorbed onto ZSM-5 at various CVD temperatures**
a) 100°C, b) 270°C, c) 450°C

The heating from 270°C to 500°C and calcination in air caused a mass loss of approximately 5wt% of the mass deposited at 100°C and 270°C (Figure 5.4). The sample mass was stable after one hour. For the deposition temperature of 450°C calcination had no effect on the sample mass. This indicates that the adsorbed phase obtained at 450°C consisted only of chemisorbed and not combustible species thus excluding ethoxy groups of TEOS surface species, adsorbed hydrocarbons and coke. In contrast to high temperatures these carbon containing species may be present at low deposition temperatures.

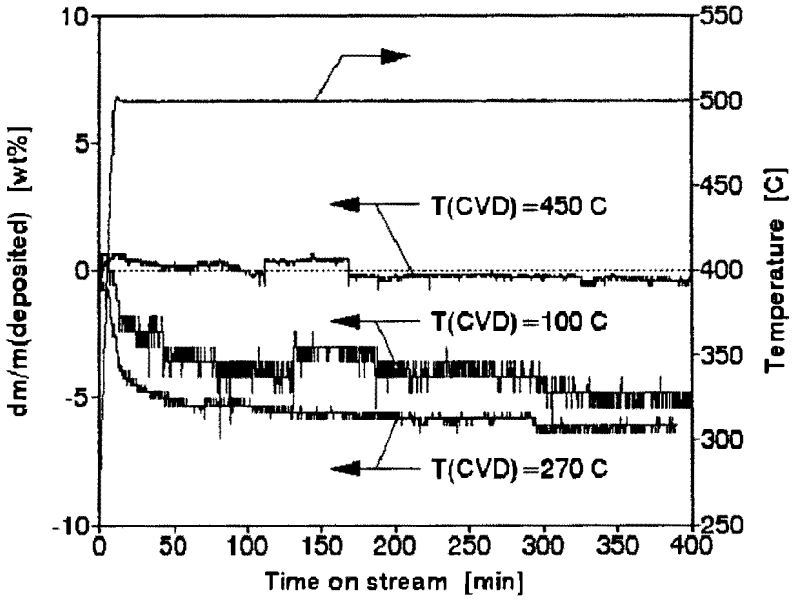

Figure 5.4: The effect of calcination on the amount of material adsorbed onto ZSM-5 at various CVD temperatures

After calcination the final structure is expected to consist of silanol groups and oxygen bridges between Si atoms independent of the CVD temperature. The mass proportion of the initially adsorbed material which is permanently deposited increased with deposition temperature and was approximately 100% at 450°C (Figure 5.5). This shows that surface ethoxy groups were not stable at 450°C and decomposed in situ. Thus it may be concluded that at high temperatures the phase formed during the CVD period is in its final stable form.

The saturation effect observed at 100°C (Figure 5.2) suggests that vertical growth and thus secondary reactions involving ethoxy groups of adsorbed TEOS species are highly inhibited. If it is assumed that at 100°C TEOS is chemisorbed as a triethoxysilane species linked via an oxygen bridge to the zeolite framework, the decomposition of this species into framework-O-Si$(OH)_3$ during calcination would necessarily lead to a minimum mass decrease of 51.5wt% of the mass originally deposited. However, the observed mass loss of the originally deposited material was only 40wt%. This indicated that not only triethoxysilane derivatives were formed during the TEOS reaction period but also interlinked TEOS surface species. It is not clear if the permanently deposited phase was immediately chemisorbed. It also may be possible that physisorbed material became chemisorbed by reaction with silanol groups or with ethoxygroups of other TEOS surface species while the temperature was ramped up.

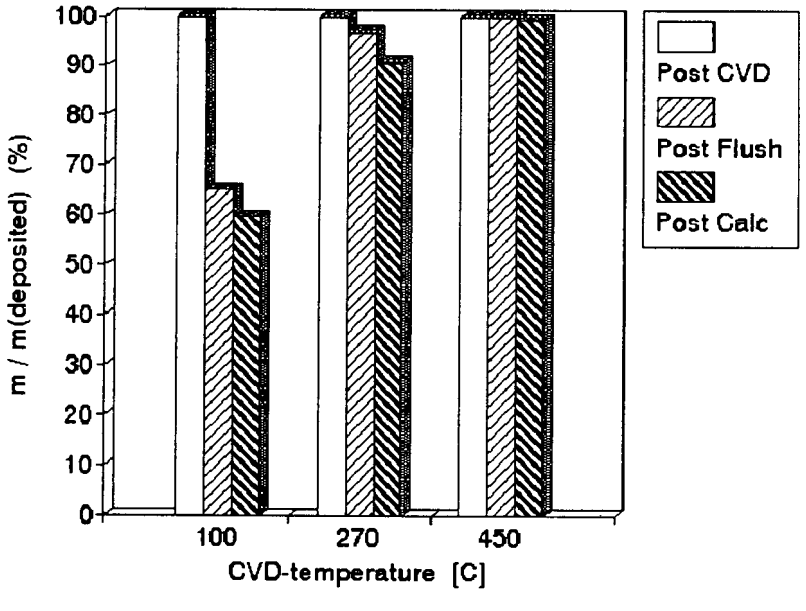

Figure 5.5: **The effect of flushing and calcination on the relative amount of material adsorbed onto ZSM-5 at a CVD temperature of 100°C, 270°C and 450°C**

5.2.1.3 *The role of calcination and deposition time in a series of CVD-calcination cycles*

From the saturation effect observed during gravimetric experiments (Figure 5.2) it was concluded that the CVD of TEOS at 100°C promotes epitaxial growth and uniform deposition (Section 5.2.1.1). The saturation effect, however, limits the surface loading and thus the degree of modification. To overcome this limitation the application of repeated CVD-calcination cycles was investigated.

The role of calcination in a series of CVD-calcination cycles was studied in a flow reactor by monitoring the activity of the external surface using the conversion of 1,3,5-TiPB and by comparing a series of three CVD-calcination cycles with one CVD-calcination cycle of equivalent cumulative total deposition times.

Figure 5.6 shows that the 1,3,5-TiPB conversions over the samples modified by 3 CVD-calcination cycles were 3.7 to 11 times lower than over the samples treated by an uninterrupted deposition and one subsequent calcination step. Thus the fragmentation of the cumulative deposition time by intermediate calcination steps resulted in an enhanced inactivation of the external surface.

The calcination step in a series of CVD-calcination cycles induced a reorganisation of the deposited phase yielding a more effective final surface coverage. This may be achieved via a higher dispersion and/or the deposition of more material. This implies that the calcination step activates the surface of the modified zeolite for further deposition of TEOS. This is proposed to occur via the conversion of surface ethoxy groups into surface silanol groups and the combustion of adsorbed carbonaceous material which is consistent with the weight loss observed during heating (Figure 5.3.a) and calcination (Figure 5.4) in the micro-balance. It is proposed that the regeneration of silanol groups is essential for an effective deposition technique which employs low deposition temperatures, e.g. 100°C. However, it should be noted that the structure and crystallinity of the final deposited phase has not been clarified.

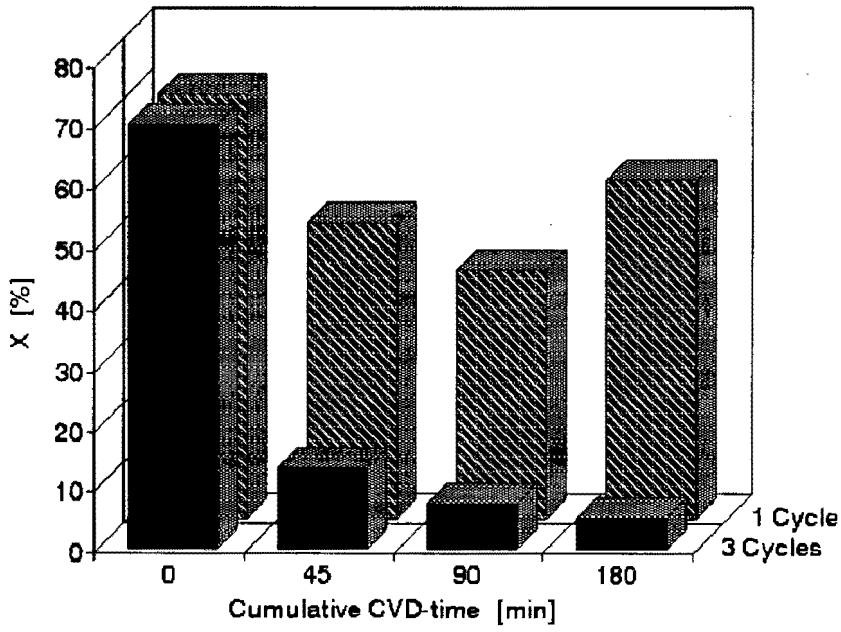

Figure 5.6: **The effect of deposition time in comparison to calcination in a series of CVD-calcination cycles on the activity of the external surface as measured by 1,3,5-TiPB cracking**
1,3,5-TiPB cracking: $T=270°C$, $p_{1,3,5\text{-TiPB, in}}=0.15kPa$, $WHSV=0.5h^{-1}$
CVD of TEOS: $T=100°C$, $p_{TEOS}\approx 0.4kPa$, $WHSV\approx 1.5h^{-1}$

Figure 5.6 shows that the 1,3,5-TiPB conversion continuously decreased when the deposition time per CVD-calcination cycle was increased from 15 to 60 minutes in the set of experiments which employed 3 subsequent cycles. The treatment with one cycle reduced the 1,3,5-TiPB conversion from 70% over the parent to an average of 50% over the modified samples. However, no clear trend of the external surface activity could be observed when the deposition time per cycle was increased from 45 to 180 minutes. This may be a consequence of the earlier observed saturation effect (Section 5.2.1.1) and suggests that the saturation of the external surface takes place within 45 to 60 minutes deposition time when a fixed bed flow reactor is used. In contrast saturation in the micro-balance was observed only after 400 minutes deposition time.

At this point it should be noted that the catalyst bed in the micro-balance was mounted in a cup (Section 5.2.1.1). Hence the observed deposition rates are likely to be affected by diffusion limitations and concentration gradients. The observed correlation between

deposition rates, the masses of deposited material and time on stream in the micro-balance are therefore not quantitatively applicable to a flow reactor. The mass increase measured with the micro-balance when the ZSM-5 surface was saturated cannot be applied to the ZSM-5 modified in the flow system because TEOS was fed at different partial pressures as determined by a saturator temperature of 0°C and 45°C respectively.

In summary the degree of modification can be more effectively controlled by the number of consecutive CVD-calcination cycles than by deposition time when the CVD of TEOS is carried out at 100°C.

5.2.2 The effect of repeated CVD-calcination cycles on structural and catalytic properties of ZSM-5

Using the cyclic CVD-calcination procedure suggested in the preceding section the relation between the number of consecutive CVD-calcination cycles and particular properties of ZSM-5 was investigated. Although the deposition of TEOS appears to be self limiting a uniform deposition throughout the catalyst bed was additionally promoted by operating the reactor differentially (viz. at a conversion of TEOS smaller than 5%).

The following methods were used to characterise the incrementally modified samples:

i)	n-hexane cracking:	micropore activity
ii)	toluene disproportionation:	shape selectivity
iii)	1,3,5-TiPB cracking:	external surface activity
iv)	sorption of n-hexane, o-xylene p-xylene and 1,2,4-TMB:	pore structure

The experimental procedures were described in Sections 2.3.2.7, 2.3.2.8 and 2.4.

Ideally the effects of CVD should be studied as a function of the deposited amount of TEOS. However, with the experimental set up used in this work the deposited amount

of TEOS could not be determined when the fixed bed flow reactor was used. Therefore the data were shown as a function of the CVD cycle number.

5.2.2.1 Pore mouth size

ZSM-5 was modified in the fixed bed flow reactor and thereafter recovered from the catalyst-sand mixture as described in Section 2.3.2.8. The separation of the modified ZSM-5 from the sand was not totally effective (Section 2.3.2.8), and the recovered catalyst still contained an unknown quantity of sand. The amount of catalyst in this mixture was determined using the measured sorption capacity of n-hexane assuming that the sorption capacity of ZSM-5 for this molecule was not affected by CVD. This assumption may be supported by the conservation of n-hexane cracking activity as shown in Figure 5.9. The sorption capacity of the sand was negligible. The apparent sorption capacities for n-hexane were 1.28, 0.43, 0.41 and 0.27 mmol/g for ZSM-5, SiV-ZSM-5, SiX-ZSM-5 and SiXV-ZSM-5 respectively (Nomenclature vide Section 2.1.3). With the mass of the parent sample loaded onto the micro-balance being 47.2 g the masses of SiV-ZSM-5, SiX-ZSM-5 and SiXV-ZSM-5 amount to 15.9, 15.1 and 9.9 mg respectively.

Figure 5.7 shows that the parent ZSM-5 adsorbed p-xylene and 1,2,4-TMB into its micropore system. 1,2,4-TMB and o-xylene were excluded from adsorption after 5 and 10 CVD cycles respectively. The sorption capacity of p-xylene showed no change even after 15 cycles. The reduction in sorption in a sequence according to the molecular size of the adsorbates confirms that CVD of TEOS onto ZSM-5 gradually reduces the pore mouth size with increasing number of CVD cycles. A reduction of the pore size throughout the crystal interior could be ruled out by the conservation of the n-hexane cracking activity (Section 5.2.2.3). A reduction of the pore mouth size was also reported for the CVD of TMOS over ZSM-5 [Niwa *et al.*, 1986; Hibino *et al.*, 1991].

The observed residual uptake of o-xylene and 1,2,4-TMB may be due to adsorption onto the external surface or to sorption into the micropores of non-uniformly modified crystals. The rather complete exclusion of an adsorbate due to reduction of the pore mouth size

(a)

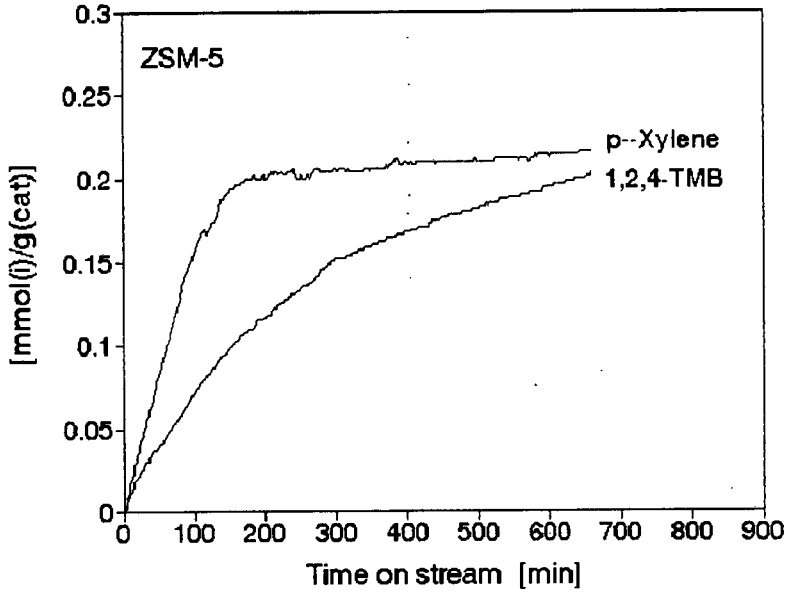

(b)

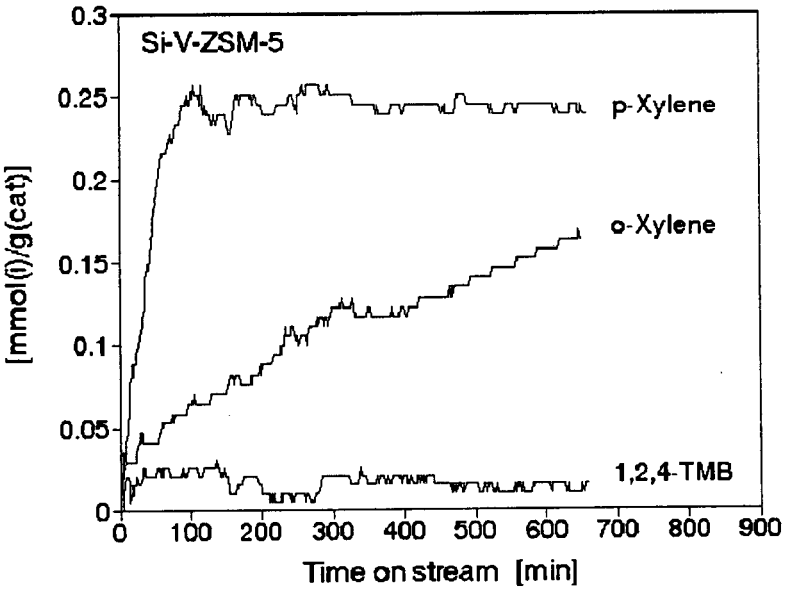

To Figure 5.7

(c)

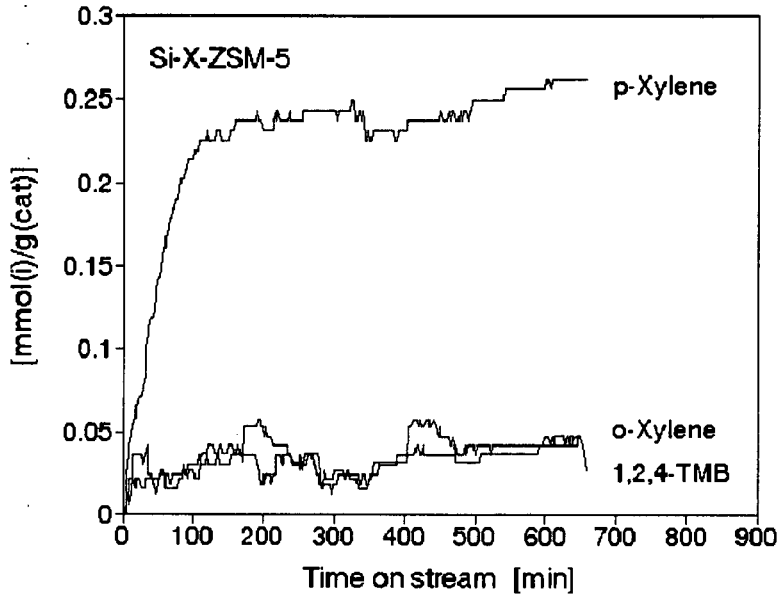

(d)

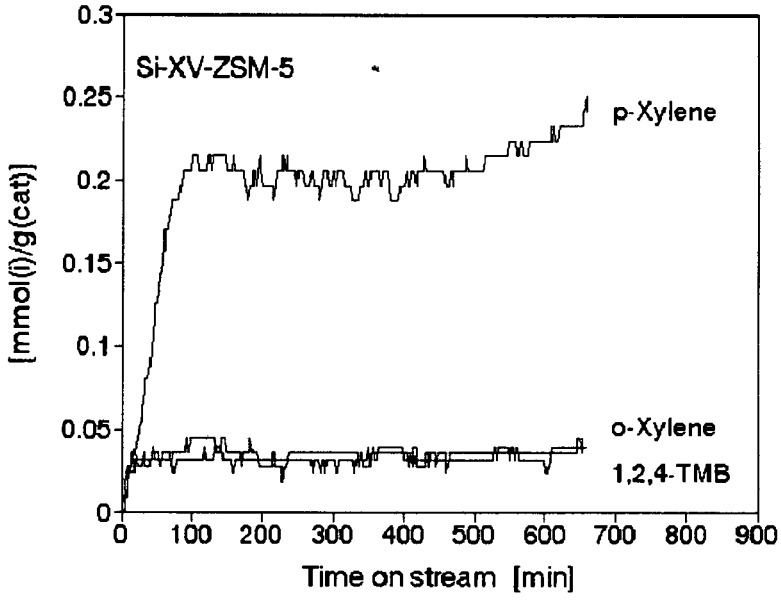

Figure 5.7: **Effect of repeated CVD treatment on the sieving properties of ZSM-5 in the adsorption of probe molecules of various size at $T_{ads}=150°C$, $p_{ads}=p_s(0°C)$ CVD at $T_{CVD}=100°C$, $p_{TEOS}\approx 0.4kPa$, $WHSV_{TEOS}\approx 1.5h^{-1}$**

indicates a highly uniform modification. In the case of a non-uniform reduction of the pore mouth size intermediate sorption capacities would be expected.

The effect of the pore mouth size on the sorption rate could not be determined reliably due to varying packing factors during the loading of the balance cups with zeolite.

5.2.2.2 *Activity of the external surface*

Figure 5.8 shows that the first five CVD treatment cycles stepwise decreased the conversion of 1,3,5-TiPB with increasing number of CVD treatments at a constant WHSV of $0.6h^{-1}$. After 5 CVD treatment cycles the conversion was reduced from 81% over the parent ZSM-5 to 3% over Si05-ZSM-5, indicating that the external surface was gradually inertised. If 1,3,5-TiPB cracking is assumed to follow first order kinetics, the first 5 CVD cycles deactivated the external surface by 98%. Hibino *et al.* [1993] have reported that the external surface was inertised after the deposition of 4-5 theoretical layers of

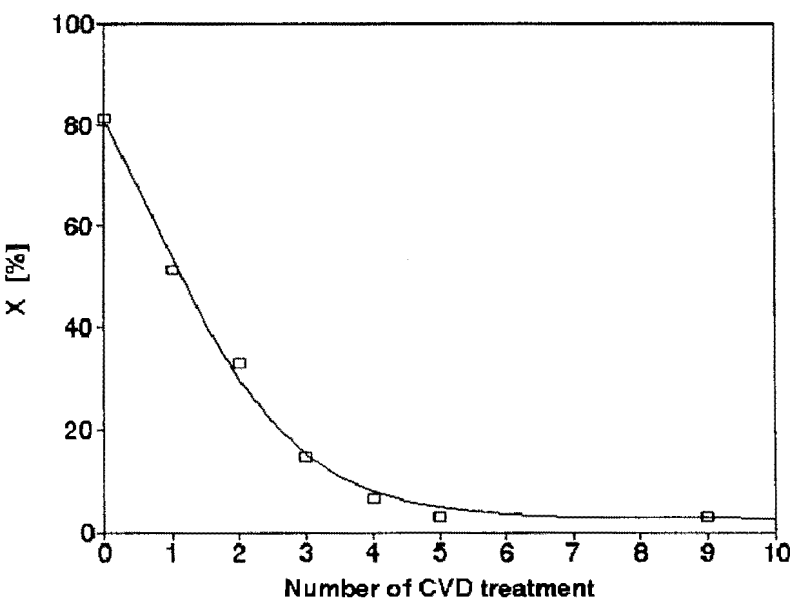

Figure 5.8: **Effect of repeated CVD treatments on the external surface activity of ZSM-5 as measured by the conversion of 1,3,5-TiPB**
1,3,5-TiPB cracking: $T=270°C$, $p_{1,3,5\text{-TiPB, in}}=0.16kPa$, $WHSV=0.6h^{-1}$
CVD of TEOS: $T=100°C$, $p_{TEOS}\approx 0.4kPa$, $WHSV\approx 1.5h^{-1}$

silica. This suggests that in the present work a monolayer is deposited per CVD cycle.

5.2.2.3 *Intrinsic activity of the micropore system*

The effect of CVD on the micropore activity of ZSM-5 was investigated using the first order rate constant for n-hexane cracking and the toluene disproportionation rate at differential conversions of $2.5 \pm 1\%$.

Figure 5.9 and 5.10 show that after about 12 CVD cycles the activity for n-hexane cracking and toluene disproportionation was hardly reduced. Therefore neither the inertisation of external acid sites during the first five CVD cycles, as shown by 1,3,5-TiPB cracking, nor pore mouth narrowing, as shown by sorption studies, caused any significant loss in activity of ZSM-5 for both reactions. At this point it should be noted that in contrast to 1,3,5-TiPB, n-hexane and toluene are reactants which easily enter the micropore system of ZSM-5. It can be concluded that the intrinsic activity of the intracrystalline pore space was not affected by the CVD treatment.

The conservation of the intrinsic micropore space activity indicates that the CVD of siliceous material is limited to the external surface when TEOS is used as CVD precursor. Only those samples which were exposed to more than 14 CVD cycles showed some loss of activity. The activity of Si16-ZSM-5 was reduced to 67% and 70% of the parent activity for n-hexane cracking and the toluene disproportionation respectively, which was most likely due to a continued pore mouth narrowing with increasing CVD cycle numbers.

From a commercial point of view a modification technique ideally enhances selectivity at no cost of activity and lifetime. While a deposition of TEOS onto the micropore walls can be excluded, the inertisation of the external surface and the creation of diffusional resistances caused by pore mouth narrowing are expected to reduce the activity of ZSM-5. The effect of these parameters on the activity, however, depends clearly on the reaction, or more explicitly on the effectiveness factor which again depends on transition states, the diffusivity of reactant or products and the intrinsic reaction kinetics.

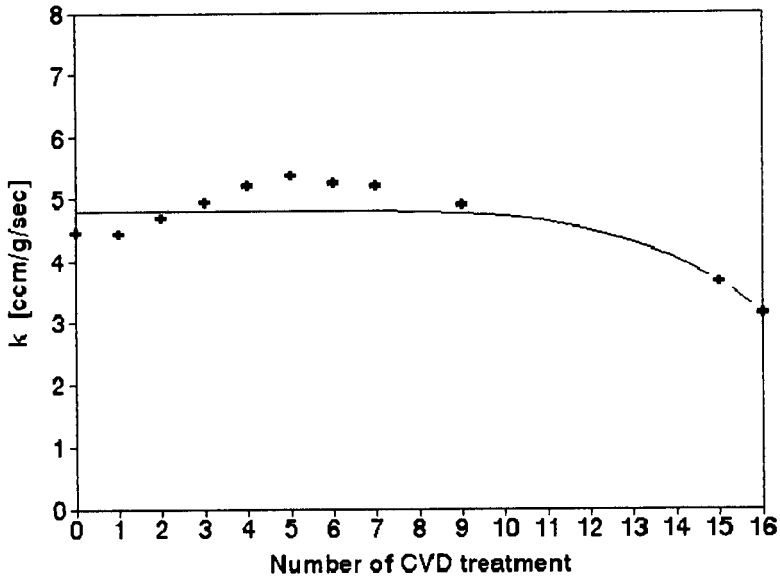

Figure 5.9: Effect of repeated CVD treatments on the micropore space activity of ZSM-5 as measured by the first order rate constant for n-hexane cracking
n-C_6 cracking: T=500°C, $p_{n\text{-}C6,\,in}$=3.9kPa, WHSV=1.7 and 1h^{-1}, X=34-46%
CVD of TEOS: T=100°C, p_{TEOS}≈0.4kPa, WHSV≈1.5h^{-1}

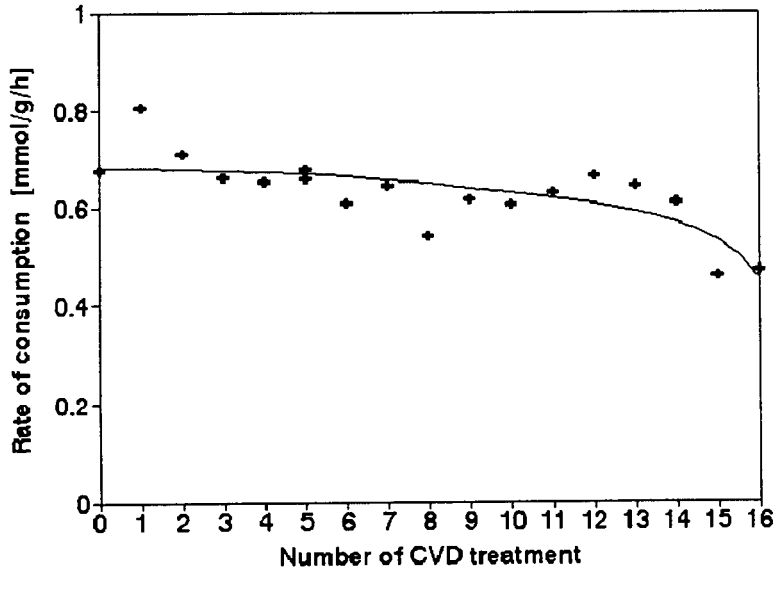

Figure 5.10: Effect of repeated CVD treatments on the micropore space activity of ZSM-5 as measured by the toluene disproportionation rate at 2.5±1% conversion
Toluene conversion: T=450°C, $p_{Toluene,\,in}$=12.5kPa, WHSV=4 and 2h^{-1}
CVD of TEOS: T=100°C, p_{TEOS}≈0.4kPa, WHSV≈1.5h^{-1}

5.2.2.4 *Micropore volume*

Since the catalyst sand mixture could not be completely separated after the CVD treatment in the flow reactor, the sorbent still contained sand (Section 2.3.2.8). It was thus not possible to determine the accurate mass of ZSM-5 loaded into the micro-balance which needs to be known to determine the adsorption capacity. Hence the micropore volume could not be monitored via the adsorption capacity of the respective zeolite sample.

A reduction of the micropore volume by deposition of TEOS on the micropore walls is expected to reduce the activity. However, the conservation of the activity of the micropore system (Section 5.2.2.3) indicated that the state of the intracrystalline pore space and therefore the micropore volume were retained. This was also reported for CVD of TMOS over ZSM-5 [Niwa *et al.*, 1986; Hibino *et al.*, 1991; Kim *et al.*, 1996]. Since the deposition of TMOS is restricted to the external surface of ZSM-5 and TEOS is clearly larger than TMOS, the same restriction is expected for TEOS.

5.2.2.5 *Shape selectivity*

Figure 5.11 shows that during the disproportionation of toluene the effect on shape selectivity is observed as an increase in the proportion of p-xylene in the xylene fraction with increasing number of CVD treatment cycles. Pore mouth narrowing may selectively suppress the diffusion of o- and m-xylene from the micropores into the bulk gas phase while the inertisation of the external surface may prevent the secondary isomerisation of p-xylene at non-shape-selective external acid sites after eluting from the micropore system. Both effects theoretically increase the selectivity to p-xylene.

The first 4 or 5 CVD cycles affected the xylene distribution only marginally by increasing the proportion of p-xylene from 25% to 33% at the expense of o-xylene. Since the external surface was inertised during these CVD cycles (Figure 5.8), it can be concluded that the external surface activity has little influence on the xylene distribution. It should be noted that the xylene distribution was close to equilibrium even at a toluene conversion

as low as 2% which is typical for crystal sizes smaller than 7.5μm [Kaeding *et al.*, 1981; Beltrame *et al.*, 1985; Hibino *et al.*, 1991]. The most significant effect was observed between the 5th and the 10th CVD cycle, when the content of p-xylene in the xylene fraction increased from 30% to 90%. After 15 CVD cycles the xylene fraction consisted to 98.5% of p-xylene.

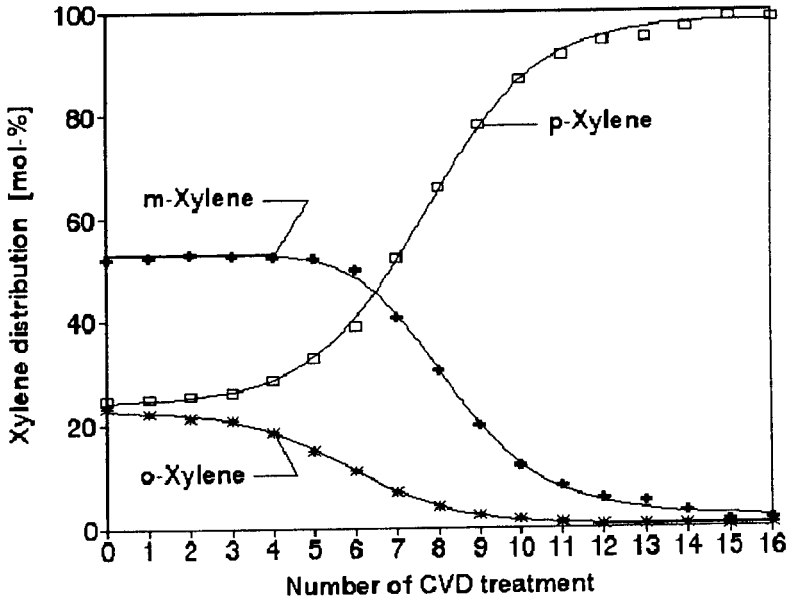

Figure 5.11: **Effect of repeated CVD treatments on the shape selectivity of ZSM-5 during toluene disproportionation as measured by the composition of the xylene fraction at 2.5±1% conversion**
Toluene conversion: T=450°C, $p_{Toluene,\ in}$=12.5kPa, WHSV=4 and 2h^{-1}
CVD of TEOS: T=100°C, p_{TEOS}≈0.4kPa, WHSV≈1.5h^{-1}

These results are consistent with the sorption of p-xylene and o-xylene. While o-xylene was still adsorbed after 5 CVD cycles no adsorption was observed after 10 and 15 CVD cycles. In the same manner o-xylene was still formed from toluene after 5 CVD cycles whereas after 10 and 15 cycles its formation was completely suppressed. P-xylene was adsorbed and formed after all CVD cycles. From the results of the sorption studies and since the inertisation of the external surface showed only a small effect it is concluded that significant improvements in the p-selectivity during toluene conversion are mainly due to pore mouth narrowing. This was also found by Kim *et al.* [1996] and Hibino *et al.*

[1991] for the methylation and disproportionation of toluene. The xylene distribution obtained during the conversion of toluene may thus be used to monitor the degree of pore mouth size reduction in a CVD procedure.

Similar enhancements of the para-selectivity up to 98% p-xylene in the xylene fraction during toluene disproportionation were reported when ZSM-5 was modified by CVD of TMOS [Hibino *et al.*, 1991] and TEOS [Wang *et al.*, 1988; Das *et al.*, 1994a], however, at CVD conditions different to those in this work.

The disproportionation of toluene showed that repeated CVD-calcination cycles at a deposition temperature of 100°C changed the shape selectivity of ZSM-5 in a highly controlled manner (see also Appendix XI, Figure XI.1).

5.2.2.6 Catalyst deactivation

No significant effect of the CVD treatment on the deactivation behaviour of ZSM-5 during the conversion of n-hexane, toluene and 1,3,5-TiPB could be observed in the studied time on stream interval as shown in Figures 5.12 to 5.14. It may be argued that the observed time on stream interval may have been too short to study the catalyst deactivation in a reliable manner. However, Das *et al.* [1994a] observed no deactivation of a CVD treated ZSM-5 during toluene disproportionation during 50 hours of time on stream. The respective ZSM-5 catalyst was modified to such a degree that the xylene fraction consisted to 90% of p-xylene.

Nevertheless Section 1.4.2.3 shows that the modification of the external surface by means of CVD of alkoxysilanes does increase the deactivation rate for certain catalytic systems. This would be expected since the reduction of the pore mouth size may lead to a trapping of large product molecules which may function as coke precursors.

For the evaluation of the catalytic experiments in the previous sections it is essential to know that the n-hexane, toluene and 1,3,5-TiPB conversions were at steady state after 5,

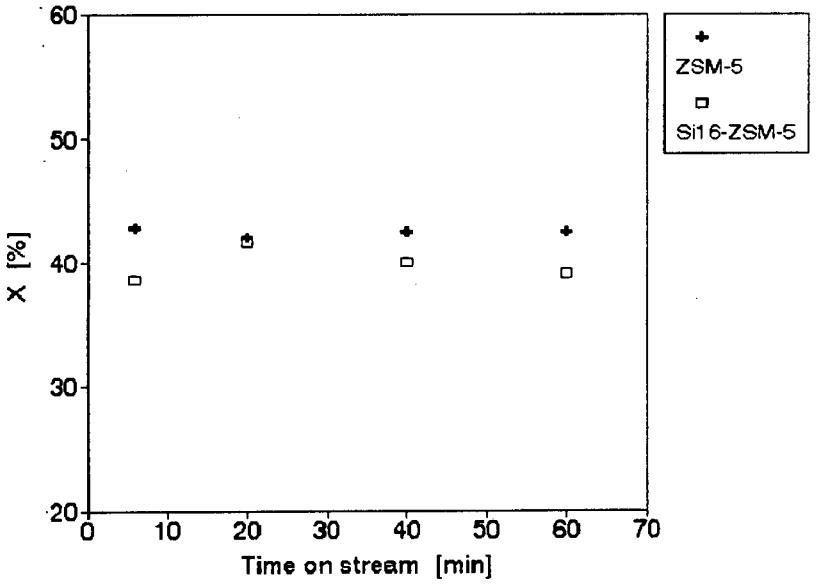

Figure 5.12: **Effect of 16 CVD treatments on the deactivation behaviour of ZSM-5 during n-hexane cracking**
n-hexane cracking: **$T=500°C$, $p_{n\text{-hexane, in}}=4kPa$, $WHSV=1.7h^{-1}$ and $1h^{-1}$**
CVD of TEOS: **$T=100°C$, $p_{TEOS}\approx 0.4kPa$, $WHSV\approx 1.5h^{-1}$**

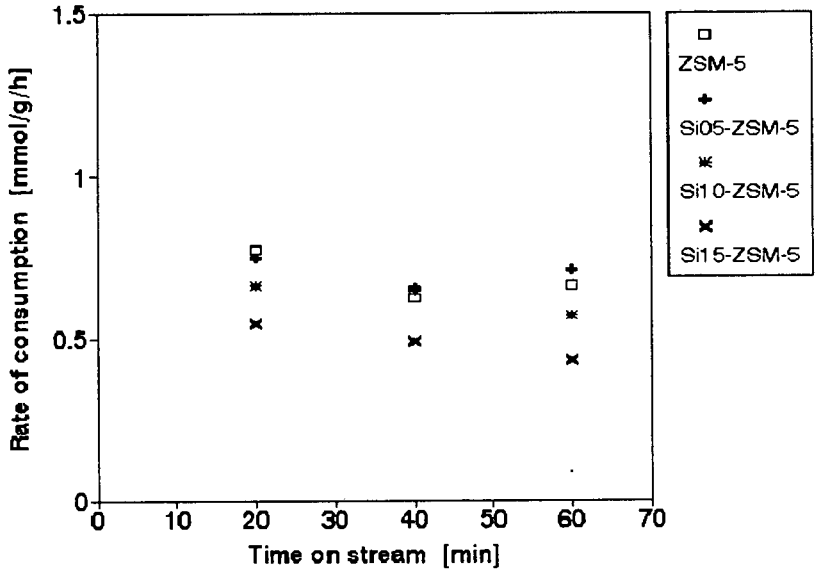

Figure 5.13: **Effect of repeated CVD treatments on the deactivation behaviour of ZSM-5 during toluene disproportionation at $2.5\pm1\%$ conversion**
Toluene conversion: **$T=450°C$, $p_{Toluene, in}=12.5kPa$, $WHSV=4$ and $2h^{-1}$**
CVD of TEOS: **$T=100°C$, $p_{TEOS}\approx 0.4kPa$, $WHSV\approx 1.5h^{-1}$**

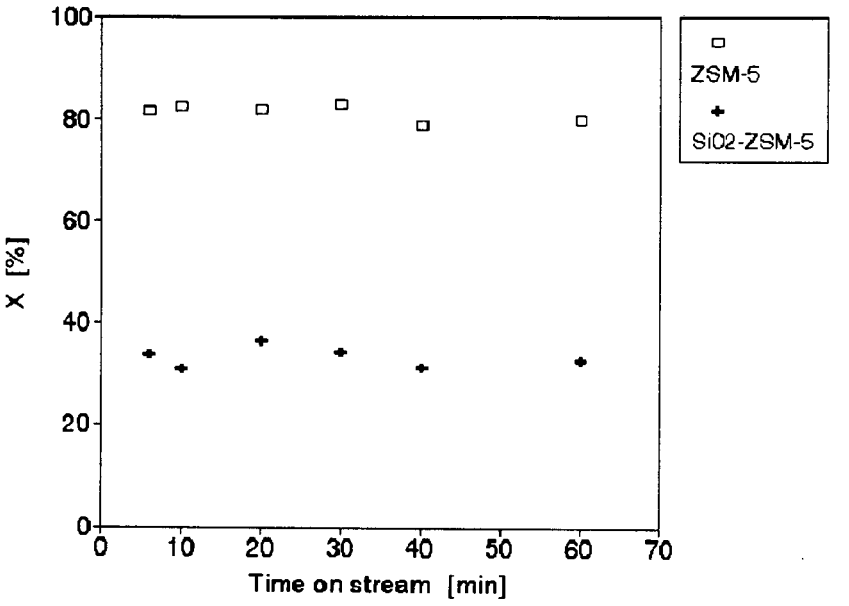

Figure 5.14: **Effect of two CVD treatments on the deactivation behaviour of ZSM-5 during 1,3,5-TiPB cracking**
1,3,5-TiPB cracking: $T=270°C$, $p_{1,3,5\text{-TiPB, in}}=0.16kPa$, $WHSV=0.6h^{-1}$
CVD of TEOS: $T=100°C$, $p_{TEOS}\approx 0.4kPa$, $WHSV\approx 1.5h^{-1}$

20 and 5 minutes of time on stream respectively. The activity could therefore be evaluated using the average of the respective measure of activity measured in the time on stream intervals listed in Table 2.6 (Section 2.3.2.7).

5.2.2.7 Comparison with previously reported methods

The majority of studies dealing with the CVD of alkoxysilanes employed deposition temperatures between 200°C and 400°C (Table 1.3 and 1.4). The CVD of silica onto the external surface of zeolite crystals in a conventional flow reactor, at low temperatures ($\leq 100°C$) using TEOS as a silica source, without additives has only been studied for zeolite β [Chun *et al.*, 1994] and zeolite Y [Murakami *et al.*, 1988a] (Table 1.4). For the CVD of TEOS over ZSM-5 only deposition temperatures higher than 180°C have been applied. The comparison in this section is limited to ZSM-5 and techniques which used TMOS and TEOS as CVD precursors. The quality of the modifications is compared using

the disproportionation of toluene thus limiting the comparison to the methods of Wang *et al.*, 1989], Hibino *et al.* [1991] and Das *et al.* [1994a] (Table 5.2).

Wang *et al.* [1988] reported a more effective modification when TEOS was used as compared to TMOS. Their CVD temperatures ranged from 180°C to 230°C and a mixture of 5% TEOS, 50% toluene and 45% methanol was fed using a flow system. The proportion of p-xylene in the xylene fraction was enhanced to 55% at 20% conversion

Table 5.1: Comparison of CVD-methods based on the disproportionation of toluene over ZSM-5

Method	This work	Wang *et al.* 1989	Hibino *et al.* 1991	Das *et al.* 1994
CATALYTIC EFFECTS				
Activity loss at 90% p-selectivity [%]	none	-	~50%	~50%
Number of samples in the range of rapid p-selectivity enhancement	5-6	-	2-3	1
Maximum p-xylene/xylene ratio [%]	98.5	55	98.5	94
Toluene conversion [%]	2.5	20	1.1	20
ZSM-5 CATALYST				
Si/Al	45	45	21	-
Crystal size [μm]	0.5-1.5	2	0.25	-
CVD-METHOD				
CVD-temperature [°C]	100	180-230	320	230
Control of modification degree	Number of CVD-calcination cycles	CVD-time	repeated deposition-evacuation cycles, m(cat), p(TMOS)	CVD-time
CVD feed	TEOS	5% TEOS, 50% toluene and 45% methanol	TMOS	TEOS in a 50:50 toluene-methanol solution
Apparatus	Flow reactor	Flow reactor	Vacuum balance	Flow reactor

[Wang *et al.*, 1989]. Hibino *et al.* [1991] have shown that the CVD of TMOS at 320°C in a static vacuum system could achieve an improvement in the p-xylene to xylene ratio up to 98.5% at 1.1% conversion, which has also been achieved in this work. However, they had only 2-3 samples in the range where rapid enhancement of p-selectivity occurs as the degree of modification increases as compared to 5-6 samples in this work (Figure 5.11). The method applied in this work thus appears to facilitate a higher degree of control. More recently, Das *et al.* [1994a] modified ZSM-5 at 230°C in a flow reactor using a mixture of TEOS in a 50:50 toluene-methanol solution and hydrogen as carrier gas. This method yielded p-xylene to xylene ratios up to 94% at 20% conversion. In their work only one sample was obtained in the range where the p-selectivity increases rapidly.

Das *et al.* [1994a] and Hibino *et al.* [1991] reported activity losses of ZSM-5 for the disproportionation of toluene of approximately 50% by the time the proportion of p-xylene in the xylene fraction was increased to 90%. Whereas in this work no significant activity loss could be observed when the same selectivity was reached after 11 CVD treatment cycles. These higher losses of activity at high deposition temperatures may be due to a less uniform deposition throughout the catalyst bed. A non-uniform deposition may for example block pore entrances of a certain fraction of crystals making them inactive while other crystals may have not been modified thus showing no improved selectivity. On average the catalyst sample will show lower selectivity or higher losses of activity than a uniformly modified sample.

The ZSM-5 samples used by Wang *et al.* [1989] and Hibino *et al.* [1991] had similar characteristics to the ZSM-5 sample used in this work. Their Si/Al ratio was 45 and 21 while the crystal size was 2μm and 0.25μm respectively. The results should therefore useful to compare these CVD-methods. Unfortunately no Si/Al ratio and crystal size was given by Das *et al.* [1994a].

The high controllability of the p-selectivity at no cost of activity in this work suggests that low CVD temperatures (100°C) and controlling the degree of modification via the number

of CVD-calcination cycles is desirable. This may be due to the self-regulating saturation effect which suppresses the formation of multilayers and thus promotes a uniform deposition throughout the catalyst bed. Other methods at higher deposition temperatures which used the deposition time [Wang *et al.*, 1989; Das *et al.*, 1994a], repeated deposition-evacuation cycles in a vacuum system, the catalyst mass or the alkoxysilane pressure [Niwa *et al.*, 1986; Hibino *et al.*, 1991] in order to control the degree of modification were not shown to achieve such a high degree of control over the p-selectivity as the method used in this work.

5.3 CONCLUSIONS

In contrast to 270°C and 450°C the CVD of TEOS at 100°C shows a saturation effect and therefore a self-limiting deposition behaviour which promotes a controlled and uniform modification of ZSM-5. At a deposition temperature of 100°C the degree of modification can be accurately controlled by the number of consecutive CVD-calcination cycles. The calcination step in such a cycle enhances the effectivity of the subsequent CVD treatment. This is proposed to be due to the activation of the surface of the modified sample due to the regeneration of silanol groups. At 100°C the degree of modification can thus be more effectively controlled via the number of consecutive CVD-calcination cycles than by the deposition time.

The CVD of TEOS allows to inactivate the external surface and adjust the pore mouth size without affecting the intrinsic properties of the micropore space. The method of repeated CVD-calcination cycles at a deposition temperature of 100°C is capable to fine tune the shape selective properties of ZSM-5 as measured by the p-selectivity during the disproportionation of toluene with a degree of control which has not been reported to date.

The proportion of p-xylene in the xylene fraction could be increased up to 98.5% with an activity loss of less than 10%. The activity for the conversion of toluene and n-hexane decreased only at high degrees of modification most probably due to the reduction of the

pore mouth size. The improvement of the p-selectivity in the disproportionation of toluene was primarily due to pore mouth narrowing as opposed to the inertisation of the external surface. No effect on the deactivation behaviour could be observed during one hour of time on stream.

The effect of the CVD treatment on the catalytic properties of ZSM-5 clearly depends on the reaction. For example the inertisation of the external surface had no effect on the activity for n-hexane cracking and toluene disproportionation, whereas ZSM-5 was almost completely inactivated for the conversion of 1,3,5-TiPB. Therefore the fine tuning of the shape selective properties of ZSM-5 for the application in an industrial reaction has to be studied using the particular feed or at least an appropriate model reactant.

Sorption studies, n-hexane cracking, toluene disproportionation and the conversion of 1,3,5-TiPB proved to be effective and sensitive tools to monitor the accessibility and the intrinsic activity of the intracrystalline pore space, shape selective properties and the activity of the external surface of ZSM-5 respectively.

Chapter 6

The Transformation of 1,2,4-Trimethylbenzene as Probe Reaction to monitor the Chemical Vapour Deposition over ZSM-5

6.1 INTRODUCTION

One of the objectives of this work was to establish the transformation of 1,2,4-TMB as a probe reaction which is capable to simultaneously monitor more than one property of ZSM-5 during external surface modifications. It has been shown that repeated CVD-calcination cycles gradually varied the shape selectivity, the activity of the external surface and the pore mouth size of ZSM-5 while the intracrystalline pore space remained unaffected. Monitoring more than one of these properties by one probe reaction is expected to be achieved by using the fact that 1,2,4-TMB is converted by more than one reaction pathway. This section discusses the role of the intracrystalline and external surface and investigates if the 1,2-methyl-shift-isomerisation-, transalkylation- and paring-dealkylation-activity of ZSM-5, and product distributions in the xylene- and TeMB-fraction can be correlated with one of the above catalyst properties.

6.2 RESULTS AND DISCUSSION

6.2.1 The role of the intracrystalline and the external surface of ZSM-5

Figures 6.1 and 6.2 illustrate the effect of the number of CVD-calcination cycles on the rates of consumption, 1,2-methyl-shift-isomerisation, transalkylation and paring reaction (vide Section 3.2.3.2 and Figures 3.18 and 3.19, Section 3.2.3.4) of 1,2,4-TMB over ZSM-5 at conversions scattering randomly between 2% and 12%. To keep the conversion approximately constant the WHSV was decreased with increasing number of CVD-calcination cycles. In Section 3.2.3 it was shown that at the low conversions used most secondary reactions are negligible and that the reaction network model as shown in Figure 3.19 applies. The rates of the mentioned primary reactions can therefore be determined from the rates of product formation using Equations 2.11 to 2.13 in Section 2.3.4.6.

Figure 6.3 compares the reactions of 1,2,4-TMB with toluene disproportionation and 1,3,5-TiPB cracking in terms of normalised activities as measured by normalised reaction rates. To account for the integral conversion during 1,3,5-TiPB cracking the differential

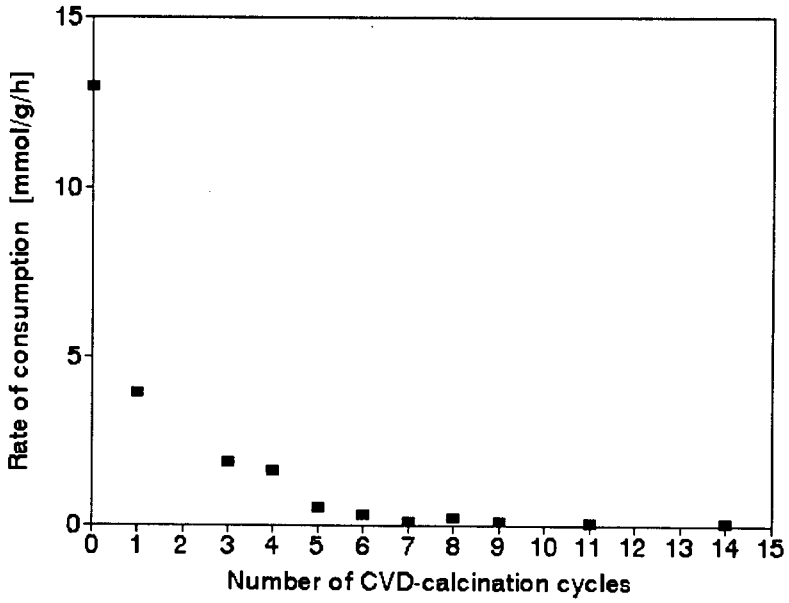

Figure 6.1: **Effect of repeated CVD-calcination cycles on the rate of 1,2,4-TMB consumption over ZSM-5 at T=450°C, $p_{1,2,4\text{-TMB}}$=3.5kPa and X scattering between 2% and 12% (WHSV=17 to 0.3 h^{-1})**

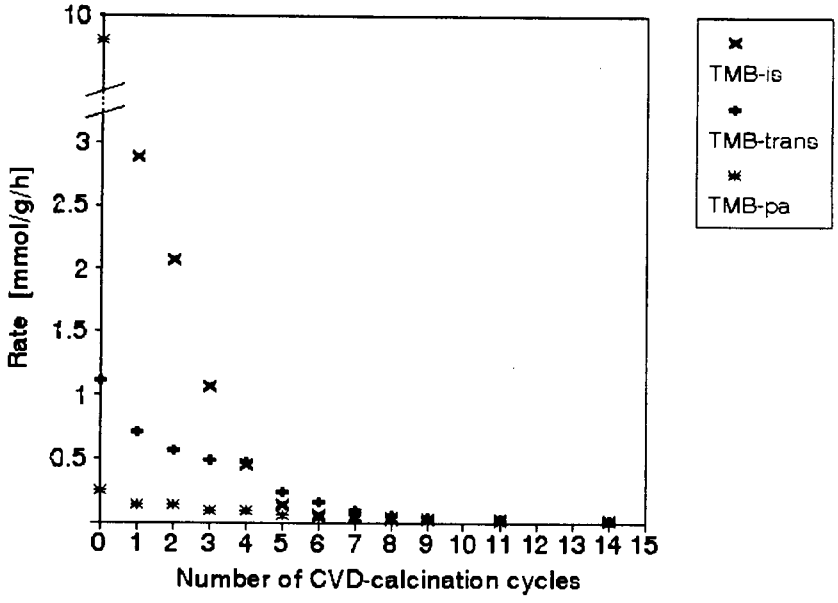

Figure 6.2: **Effect of repeated CVD-calcination cycles on the rate of 1,2-methyl-shift-isomerisation, transalkylation and paring reaction of 1,2,4-TMB over ZSM-5 at T=450°C, $p_{1,2,4\text{-TMB}}$=3.5kPa and X scattering between 2% and 12%**

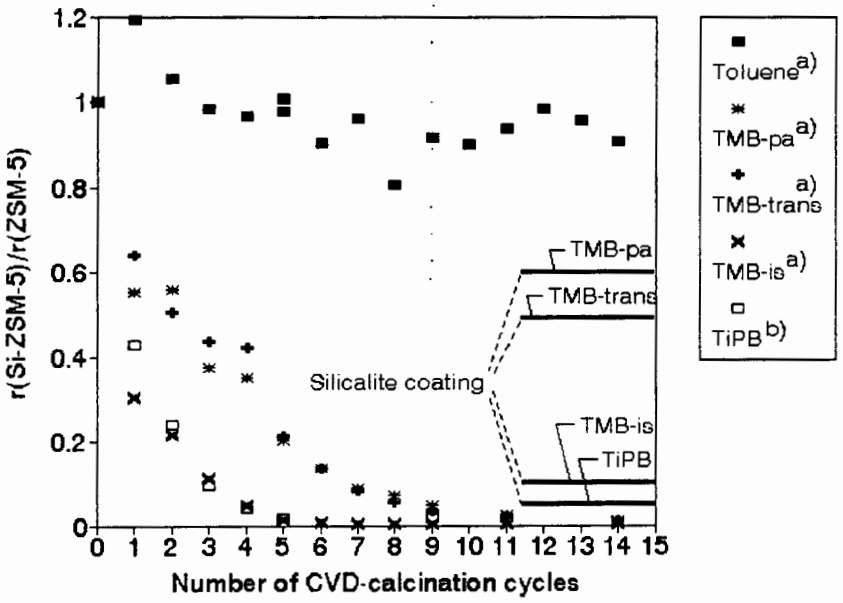

Figure 6.3: **Effect of repeated CVD-calcination cycles on normalised reaction rates during the conversion of toluene and 1,3,5-TiPB in comparison to the isomerisation, transalkylation and paring reaction of 1,2,4-TMB over ZSM-5**
a) Reaction rates measured in a differentially operated reactor
b) Reaction rates determined assuming first order kinetics (Equations 2.8 and 2.10)
Solid lines: Ratios for ZSM-5* coated with a Silicalite shell (Table 4.2, Section 4.2.2.2)

reaction rate was determined assuming first order reaction kinetics. The normalised activities during 1,3,5-TiPB cracking may be considered as lower boundary values representing a reaction which is limited to the external surface, while the normalised activities during toluene disproportionation are upper boundary values representing a reaction which easily takes place in the micropore system without diffusional constraints.

The normalised activities in all primary reactions of 1,2,4-TMB are clearly lower than the normalised activities in the conversion of toluene, showing that the conversion of 1,2,4-TMB is much more sensitive to the inactivation of the external surface and / or pore mouth narrowing. The normalised activities in the transalkylation and the paring reaction of 1,2,4-TMB, however, are higher than the normalised activities obtained for 1,3,5-TiPB cracking and are therefore less affected by the inactivation of the external surface. This shows that these reactions of 1,2,4-TMB occur inside the micropores of ZSM-5 which is

consistent with the findings when ZSM-5* (catalyst nomenclature see Section 2.1.3, Table 2.3) was coated with a Silicalite I shell (Section 4.2.2.2) and when ZSM-5 was compared with amorphous silica-alumina (Section 3.2.4.4).

While the reduction of the transalkylation- and paring-activity was intermediate to the activity reductions obtained in the conversion of toluene and 1,3,5-TiPB, the 1,2-methyl-shift-isomerisation was almost identical with the normalised activity in 1,3,5-TiPB cracking (Figure 6.3). This shows that the 1,2-methyl-shift-isomerisation of 1,2,4-TMB is largely restricted to the external surface.

As discussed in Section 4.2.2.2 the observed selective inhibition of the 1,2-methyl-shift-isomerisation of 1,2,4-TMB as compared to the transalkylation and paring reaction can also be explained by the reduction of the micropore space accessibility and is therefore not conclusive evidence to prove that the isomerisation of 1,2,4-TMB is restricted to the external surface of ZSM-5. If this reaction significantly takes place in the micropores, a reduction of the isomerisation activity could also be due to pore mouth narrowing. However, it is unlikely that a combined effect of pore mouth narrowing and external surface inactivation on the 1,2,4-TMB isomerisation would correlate that well with the effect of the external surface inactivation on the 1,3,5-TiPB cracking activity.

Hibino *et al.* [1991] modified ZSM-5 by CVD of tetramethoxysilane and concluded that in the modification range where the para-xylene selectivity during toluene disproportionation increases only slightly, viz. after fewer than five CVD cycles in the present work (Figure 5.11, Section 5.2.2.5), the pore mouth size was scarcely reduced. In the previous chapter it was shown that the intrinsic activity of the intracrystalline pore space remained unaffected. Any reduction of a reaction rate due to the first CVD-calcination cycle can therefore most likely be attributed to the inactivation of the external surface. If the latter is the only effect on the activity of ZSM-5 the effect of the first CVD cycle on the normalised reaction rates unambiguously ranks the various reactions according to the degree to which they are occurring in the micropores.

The first CVD-calcination cycle reduced the rates in the 1,2-methyl-shift-isomerisation, transalkylation and paring reactions of 1,2,4-TMB to 30%, 60% and 60% of the activity of the unmodified ZSM-5 respectively. This shows that the two latter reactions occur to a higher degree inside the micropores than the 1,2-methyl-shift-isomerisation. This was also found when ZSM-5* was coated with a Silicalite I shell (Section 4.2.2.2) and supports the above conclusion that the 1,2-methyl-shift-isomerisation of 1,2,4-TMB is largely restricted to the external surface.

Next, distributions of the xylene-, the TMB- and the TeMB-isomers of the respective fractions are compared for the various CVD treated ZSM-5 catalysts, ZSM-5 which was coated with a Silicalite I shell (data from Section 4.2.2.3) and amorphous silica-alumina (data from Section 3.2.4.4). The conversion for the CVD treated catalysts scattered between 2 and 12% while the conversion for the two latter catalysts was 4%. It should be noted that the 1,2,3,4-TeMB isomer was not further considered since its formation became highly suppressed after only a few CVD cycles so that reliable product analysis was not possible.

Figures 6.4 to 6.6 show the distribution of xylene isomers as a function of the number of CVD-calcination cycles. While the first 4 CVD cycles which mainly inactivate the external surface of ZSM-5 do not affect the xylene distribution the 5th to the 8th cycle increase the p-selectivity at the expense of o-xylene and m-xylene due to continued pore mouth narrowing. This was also observed during the disproportionation of toluene (Section 5.2.2.5, Figure 5.11). In contrast to the toluene disproportionation the shape selectivity during the transalkylation of 1,2,4-TMB deteriorates at high CVD cycle numbers and the xylene distribution approaches the non-shape selective, by intrinsic kinetics controlled distribution which was observed over amorphous silica-alumina (See also Appendix XI). It is concluded that the continued reduction of the pore mouth size increasingly prevents 1,2,4-TeMB from entering the micropores and restricts the reaction to the now modified, non-shape selective, external surface. The deposited material thus seems to show a very small activity which corresponds to approximately 2% of the original external surface activity of the ZSM-5 used as measured by 1,3,5-TiPB cracking.

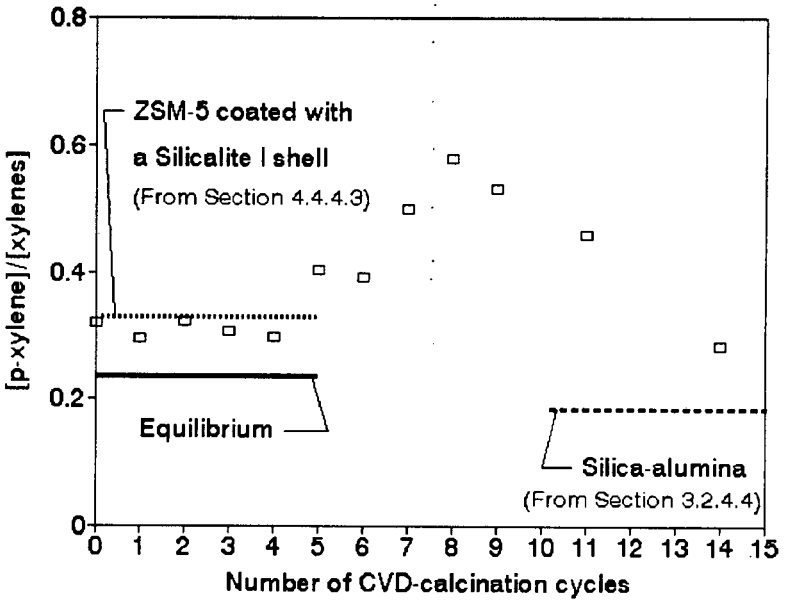

Figure 6.4: **Effect of repeated CVD-calcination cycles on the proportion of p-xylene in the xylene fraction during the transformation of 1,2,4-TMB over ZSM-5 at T=450°C, $p_{1,2,4\text{-TMB}}$=3.5kPa and X scattering between 2% and 12%**

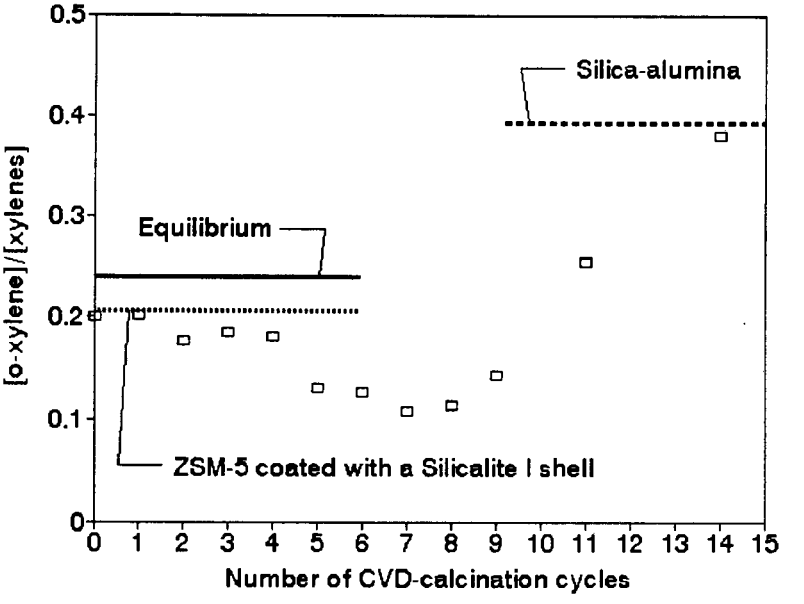

Figure 6.5: **Effect of repeated CVD-calcination cycles on the proportion of o-xylene in the xylene fraction during the transformation of 1,2,4-TMB over ZSM-5 at T=450°C, $p_{1,2,4\text{-TMB}}$=3.5kPa and X scattering between 2% and 12%**